

Research Project Number TPF-5(193) Supplement #62

SAFETY INVESTIGATION AND DESIGN GUIDANCE FOR CURBS NEAR ENERGY- ABSORBING END TERMINALS

Submitted by

Jennifer D. Schmidt, Ph.D., P.E.
Research Assistant Professor

Robert W. Bielenberg, M.S.M.E., E.I.T.
Research Engineer

Brock D. Schroder, B.S.M.E.
Graduate Research Assistant

Ronald K. Faller, Ph.D., P.E.
Director and Research Associate Professor

Karla A. Lechtenberg, M.S.M.E., E.I.T.
Research Engineer

MIDWEST ROADSIDE SAFETY FACILITY

Nebraska Transportation Center
University of Nebraska-Lincoln
130 Whittier Research Center
2200 Vine Street
Lincoln, Nebraska 68583-0853
(402) 472-0965

Submitted to

WISCONSIN DEPARTMENT OF TRANSPORTATION

4802 Sheboygan Avenue
Madison, Wisconsin 53707

MwRSF Research Report No. TRP-03-358-17

July 10, 2017

TECHNICAL REPORT DOCUMENTATION PAGE

1. Report No. TRP-03-358-17	2.	3. Recipient's Accession No.	
4. Title and Subtitle Safety Investigation and Design Guidance for Curbs Near Energy-Absorbing End Terminals		5. Report Date July 10, 2017	
		6.	
7. Author(s) Schmidt, J.D., Bielenberg, R.W., Schroder, B.D., Faller, R.K., and Lechtenberg, K.A.		8. Performing Organization Report No. TRP-03-358-17	
9. Performing Organization Name and Address Midwest Roadside Safety Facility (MwRSF) Nebraska Transportation Center University of Nebraska-Lincoln 130 Whittier Research Center 2200 Vine Street Lincoln, Nebraska 68583-0853		10. Project/Task/Work Unit No.	
		11. Contract © or Grant (G) No. TPF-5(193) Supplement #62	
12. Sponsoring Organization Name and Address Wisconsin Department of Transportation 4802 Sheboygan Avenue Madison, Wisconsin 53707		13. Type of Report and Period Covered Final Report: 2013 – 2017	
		14. Sponsoring Agency Code	
15. Supplementary Notes			
16. Abstract <p>Guardrail end terminals have been developed to shield the end of a longitudinal barrier and function as a redirective barrier when struck along the side. The use of curbs is often desired adjacent to guardrail and end terminals due to restricted right-of-way, drainage considerations, access control, and other functions. Curbs can adjacent to guardrail have resulted in some unsuccessful crash tests. However, the safety performance of energy-absorbing end terminals installed adjacent to curbs and gutters is unknown. Little guidance is available to State Departments of Transportation that desire installations with curbs adjacent to energy-absorbing guardrail end terminals. The objective of this research study was to investigate whether curb placement in advance of guardrail end terminals significantly degrades system performance. A generic, energy-absorbing, W-beam end terminal model was developed using LS-DYNA computer simulation software to represent existing, energy-absorbing, compression-based, end terminal systems. These systems include an impact head with a guide chute placed over the rail end, which dissipates an errant vehicle's kinetic energy when propelled downstream through changes to the rail shape. Impacts on the end of the terminal were evaluated according to NCHRP Report 350 and <i>Manual for Assessing Safety Hardware (MASH)</i> 2009 safety performance criteria. The simulations were compared to results from available crash tests to ensure that the energy-absorbing, end terminal model accurately represented the performance of end terminals. Curbs that were 2 to 6 in. high with a sloped or vertical shape were laterally offset 0 in., 6 in., and 6 ft away from the face of the Midwest Guardrail System model. Additionally, flared tangent end terminal performance was also evaluated. The safety performance of the system with and without curbs was compared, and general performance trends were identified.</p>			
17. Document Analysis/Descriptors Highway Safety, LS-DYNA FEA, Computer Simulation, NCHRP Report 350, MASH, TL-3, Energy-Absorbing End Terminals, Guardrail End Terminals, Curbs		18. Availability Statement No restrictions. Document available from: National Technical Information Services, Springfield, Virginia 22161	
19. Security Class (this report) Unclassified	20. Security Class (this page) Unclassified	21. No. of Pages 155	22. Price

DISCLAIMER STATEMENT

This report was completed with funding from the Wisconsin Department of Transportation. The contents of this report reflect the views and opinions of the authors who are responsible for the facts and the accuracy of the data presented herein. The contents do not necessarily reflect the official views or policies of the Wisconsin Department of Transportation. This report does not constitute a standard, specification, regulation, product endorsement, or an endorsement of manufacturers.

ACKNOWLEDGEMENTS

The authors wish to acknowledge several sources that made a contribution to this project: (1) Wisconsin Department of Transportation for sponsoring this project, (2) Livermore Software Technology Corporation (LSTC) for LS-DYNA support, and (3) the Holland Computing Center at the University of Nebraska for the high-performance computing resources.

Acknowledgement is also given to the following individuals who made a contribution to the completion of this research project.

Midwest Roadside Safety Facility

J.D. Reid, Ph.D., Professor
J.C. Holloway, M.S.C.E., E.I.T., Test Site Manager
S.K. Rosenbaugh, M.S.C.E., E.I.T., Research Engineer
C.S. Stolle, Ph.D., Research Assistant Professor
A.T. Russell, B.S.B.A., Shop Manager
S.M. Tighe, Laboratory Mechanic
D.S. Charroin, Laboratory Mechanic
M.A. Rasmussen, Laboratory Mechanic
E.W. Krier, Laboratory Mechanic
Undergraduate and Graduate Research Assistants

Wisconsin Department of Transportation

Jerry Zogg, P.E., Chief Roadway Standards Engineer
Erik Emerson, P.E., Standards Development Engineer
Rodney Taylor, P.E., Roadway Design Standards Unit Supervisor

TABLE OF CONTENTS

TECHNICAL REPORT DOCUMENTATION PAGE	i
DISCLAIMER STATEMENT	ii
ACKNOWLEDGEMENTS	iii
TABLE OF CONTENTS.....	iv
LIST OF FIGURES	vi
LIST OF TABLES	x
1 INTRODUCTION	1
1.1 Problem Statement	1
1.2 Research Objective	3
1.3 Scope.....	3
2 SURVEY.....	7
3 TEST REQUIREMENTS AND EVALUATION CRITERIA	11
3.1 Test Requirements	11
3.2 Evaluation Criteria.....	11
4 END TERMINAL DETAILS	13
5 LS-DYNA MODELS.....	18
5.1 Hardware Models.....	18
5.1.1 End Terminal System.....	20
5.1.1.1 Impact Head	20
5.1.1.2 W-beam Guardrail	22
5.1.1.3 Anchorage	23
5.1.1.4 CRT Post Assembly	23
5.1.2 Strong Post Guardrail Model	28
5.2 Vehicle Models	28
5.2.1 Geo Metro (820C).....	28
5.2.2 Chevrolet c2500 (2000P)	29
5.2.3 Toyota Yaris (1100C)	30
5.2.4 Chevrolet Silverado (2270P).....	30
6 SIMULATIONS ON LEVEL TERRAIN.....	31
6.1.1 NCHRP Report 350 Test No. 3-30	32
6.1.1.1 Shallow Quarter-Point Offset	33
6.1.1.2 Deep Quarter-Point Offset	36
6.1.2 NCHRP Report 350 Test No. 3-31	39
6.1.3 NCHRP Report 350 Test No. 3-32	40
6.1.4 NCHRP Report 350 Test No. 3-33	46
6.1.5 MASH 2009 Test No. 3-30.....	50

6.1.5.1 Shallow Quarter-Point Offset	50
6.1.5.2 Deep Quarter-Point Offset	54
6.1.6 MASH 2009 Test No. 3-31	57
6.1.7 MASH 2009 Test No. 3-32	61
6.1.7.1 5-Degree Impact Angle.....	61
6.1.7.2 15-Degree Impact Angle.....	66
6.1.8 MASH 2009 Test No. 3-33	69
6.1.8.1 5-Degree Impact Angle.....	69
6.1.8.2 15-Degree Impact Angle.....	73
7 COMPARISON OF THE END TERMINAL MODEL	76
7.1 NCHRP Report 350 Test No. 3-30	76
7.1.1 27¾-in. (706-mm) Tall W-Beam End Terminal Impacts	76
7.1.2 31-in. (787-mm) Tall W-Beam End Terminal Impacts	76
7.2 NCHRP Report 350 Test No. 3-31	83
7.2.1 27¾-in. (706-mm) Tall W-Beam End Terminal Impacts	83
7.2.2 31-in. (787-mm) Tall W-Beam End Terminal Impacts	87
7.3 NCHRP Report 350 Test No. 3-32	90
7.3.1 27¾-in. (706-mm) Tall W-Beam End Terminal Impacts	90
7.3.2 31-in. (787-mm) Tall W-Beam End Terminal Impacts	94
7.4 NCHRP Report 350 Test No. 3-33	96
7.4.1 27¾-in. (706-mm) Tall W-Beam End Terminal Impacts	96
7.4.2 31-in. (787-mm) Tall W-Beam End Terminal Impacts	96
7.5 Discussion	100
8 SIMULATIONS WITH CURBS	101
8.1 Results.....	103
8.1.1 Occupant Risk Measures.....	104
8.2 Vehicle Stability.....	109
8.3 Feed Lengths and Vehicle Interaction	116
8.4 0-in. and 6-in. (152-mm) Lateral Offset Curbs-Discussion.....	121
8.5 6-ft (1.8-m) Wide Curb Sidewalk Adjacent to End Terminal	121
9 END TERMINAL PERFORMANCE – TANGENT VS. FLARED SYSTEMS	123
10 FLARED END TERMINAL SIMULATIONS WITH CURBS	141
11 SUMMARY, CONCLUSIONS, AND RECOMMENDATIONS	149
12 REFERENCES	151

LIST OF FIGURES

Figure 1. Representative End Terminal System	15
Figure 2. Representative End Terminal Details	16
Figure 3. Representative Impact Head Details	17
Figure 4. 175-ft (53.3-m) Long Guardrail Model	18
Figure 5. Cross Sections Through End Terminal and Guardrail Model (a) Modified G4(1S) and (b) MGS	19
Figure 6. 50-ft (15.2-m) Long End Terminal System	19
Figure 7. Impact Head Model	21
Figure 8. End Terminal Anchorage Model	25
Figure 9. CRT Post Assembly Model	26
Figure 10. Post-to-Guardrail Bolt Model	26
Figure 11. Bolt Head Snagging and Deformation Around Guardrail Slot	27
Figure 12. Bolt Head Deformation with Distorted Element Deletion	28
Figure 13. Geo Metro Model	29
Figure 14. Chevrolet c2500 Model	29
Figure 15. Toyota Yaris Model	30
Figure 16. Chevrolet Silverado Reduced V3 Model	30
Figure 17. NCHRP Report 350 Test No. 3-30, Shallow Quarter-Point Offset Impact	32
Figure 18. NCHRP Report 350 Test No. 3-30, Deep Quarter-Point Offset Impact	32
Figure 19. NCHRP Report 350 Test No. 3-30, Shallow Quarter-Point Offset, Overhead View	34
Figure 20. NCHRP Report 350 Test No. 3-30, Shallow Quarter-Point Offset, Downstream View	35
Figure 21. NCHRP Report 350 Test No. 3-30, Deep Quarter-Point Offset, Overhead View	37
Figure 22. NCHRP Report 350 Test No. 3-30, Deep Quarter-Point Offset, Downstream View	38
Figure 23. NCHRP Report 350, Test No. 3-31 Impact	39
Figure 24. NCHRP Report 350 Test No. 3-31, Overhead View	41
Figure 25. NCHRP Report 350 Test No. 3-31, Downstream View	42
Figure 26. NCHRP Report 350 Test No. 3-32 Impact	43
Figure 27. NCHRP Report 350 Test No. 3-32, Overhead View	44
Figure 28. NCHRP Report 350 Test No. 3-32, Downstream View	45
Figure 29. NCHRP Report 350 Test No. 3-33 Impact	46
Figure 30. NCHRP Report 350 Test No. 3-33, Overhead View	48
Figure 31. NCHRP Report 350 Test No. 3-33, Downstream View	49
Figure 32. MASH 2009 Test No. 3-30, Shallow Quarter-Point Offset Impact	50
Figure 33. MASH 2009 Test No. 3-30, Deep Quarter-Point Offset Impact	50
Figure 34. MASH 2009 Test No. 3-30, Shallow Quarter-Point Offset, Overhead View	52
Figure 35. MASH 2009 Test No. 3-30, Shallow Quarter-Point Offset, Downstream View	53
Figure 36. MASH 2009 Test No. 3-30, Deep Quarter-Point Offset, Overhead View	55
Figure 37. MASH 2009 Test No. 3-30, Deep Quarter-Point Offset, Downstream View	56
Figure 38. MASH 2009 Test No. 3-31 Impact	57
Figure 39. MASH 2009 Test No. 3-31, Overhead View	59
Figure 40. MASH 2009 Test No. 3-31, Downstream View	60
Figure 41. MASH 2009 Test No. 3-32 at 5-Degree Impact	61

Figure 42. MASH 2009 Test No. 3-32 at 15-Degree Impact.....	61
Figure 43. Post-to-Rail Bolt Snag	63
Figure 44. MASH 2009 Test No. 3-32 at 5 Degrees, Overhead View	64
Figure 45. MASH 2009 Test No. 3-32 at 5 Degrees, Downstream View	65
Figure 46. MASH 2009 Test No. 3-32 at 15 Degrees, Overhead View	67
Figure 47. MASH 2009 Test No. 3-32 at 15 Degrees, Downstream View	68
Figure 48. MASH 2009 Test No. 3-33 at 5 Degrees Impact	69
Figure 49. MASH 2009 Test No. 3-33 at 15 Degrees Impact	69
Figure 50. MASH 2009 Test No. 3-33 at 5 degrees, Overhead View	71
Figure 51. MASH 2009 Test No. 3-33 at 5 degrees, Downstream View	72
Figure 52. MASH 2009 Test No. 3-33 at 15 degrees, Overhead View	74
Figure 53. MASH 2009 Test No. 3-33 at 15 degrees, Downstream View	75
Figure 54. NCHRP Report 350 Test No. 3-30, 27¾ in. (706 mm) Tall	78
Figure 55. NCHRP Report 350 Test No. 3-30, 27¾ in. (706 mm) Tall	79
Figure 56. NCHRP Report 350 Test No. 3-30, 27¾ in. (706 mm) Tall	80
Figure 57. NCHRP Report 350 Test No. 3-30, 31 in. (787 mm) Tall	81
Figure 58. NCHRP Report 350 Test No. 3-30, 31 in. (787 mm) Tall	82
Figure 59. NCHRP Report 350 Test No. 3-31, 27¾ in. (706 mm) Tall	84
Figure 60. NCHRP Report 350 Test No. 3-31, 27¾ in. (706 mm) Tall	85
Figure 61. NCHRP Report 350 Test No. 3-31, 27¾ in. (706 mm) Tall	86
Figure 62. NCHRP Report 350 Test No. 3-31, 31 in. (787 mm) Tall	88
Figure 63. NCHRP Report 350 Test No. 3-31, 31 in. (787 mm) Tall	89
Figure 64. NCHRP Report 350 Test No. 3-32, 27¾ in. (706 mm) Tall	91
Figure 65. NCHRP Report 350 Test No. 3-32, 27¾ in. (706 mm) Tall	92
Figure 66. NCHRP Report 350 Test No. 3-32, 27¾ in. (706 mm) Tall	93
Figure 67. NCHRP Report 350, Test No. 3-32, 31 in. (787 mm) Tall	95
Figure 68. NCHRP Report 350 Test No. 3-33, 27¾ in. (706 mm) Tall	97
Figure 69. NCHRP Report 350 Test No. 3-33, 27¾ in. (706 mm) Tall	98
Figure 70. NCHRP Report 350 Test No. 3-33, 31 in. (787 mm) Tall	99
Figure 71. Curb Shapes	101
Figure 72. Typical End Terminal Installation Adjacent to 6-in. (152-mm) Tall Curb	103
Figure 73. Typical Curb Mesh Model.....	104
Figure 74. End Terminal with Curb Simulation ORAs, MASH 2009 Test No. 3-30 with Shallow ¼-Point Offset.....	105
Figure 75. End Terminal with Curb Simulation ORAs, MASH 2009 Test No. 3-30 with Deep ¼-Point Offset	106
Figure 76. End Terminal with Curb Simulation ORAs, MASH 2009 Test No. 3-31	106
Figure 77. End Terminal with Curb Simulation ORAs, MASH 2009 Test No. 3-32 at 5-deg Impact Angle.....	107
Figure 78. End Terminal with Curb Simulation ORAs, MASH 2009 Test No. 3-32 at 15- deg Impact Angle	107
Figure 79. End Terminal with Curb Simulation ORAs, MASH 2009 Test No. 3-33 at 5-deg Impact Angle.....	108
Figure 80. End Terminal with Curb Simulation ORAs, MASH 2009 Test No. 3-33 at 15- deg Impact Angle	108
Figure 81. End Terminal with Curb Simulation Vehicle Stability, MASH 2009 Test No. 3- 30 with Shallow ¼-Point Offset.....	109

Figure 82. End Terminal with Curb Simulation Vehicle Stability, MASH 2009 Test No. 3-30 with Deep ¼-Point Offset	110
Figure 83. End Terminal with Curb Simulation Vehicle Stability, MASH 2009 Test No. 3-31	110
Figure 84. End Terminal with Curb Simulation Vehicle Stability, MASH 2009 Test No. 3-32 at 5-deg Impact Angle	111
Figure 85. End Terminal with Curb Simulation Vehicle Stability, MASH 2009 Test No. 3-32 at 15-deg Impact Angle	111
Figure 86. End Terminal with Curb Simulation Vehicle Stability, MASH 2009 Test No. 3-33 at 5-deg Impact Angle	112
Figure 87. End Terminal with Curb Simulation Vehicle Stability, MASH 2009 Test No. 3-33 at 15-deg Impact Angle	112
Figure 88. MASH 2009 Test No. 3-32 with Curbs, 5 Degrees, 0" Offset, Overhead View	113
Figure 89. MASH 2009 Test No. 3-32 with Curbs, 5 Degrees, 0" Offset, Downstream View	114
Figure 90. MASH 2009 Test No. 3-30 with Curbs, Deep Quarter-Point, 0" Offset	115
Figure 91. End Terminal with Curb Simulation Feed Length, MASH 2009 Test No. 3-30 with Shallow ¼-Point Offset	116
Figure 92. End Terminal with Curb Simulation Feed Length, MASH 2009 Test No. 3-30 with Deep ¼-Point Offset	117
Figure 93. End Terminal with Curb Simulation Feed Length, MASH 2009 Test No. 3-31	117
Figure 94. End Terminal with Curb Simulation Feed Length, MASH 2009 Test No. 3-32 at 5-deg Impact Angle	118
Figure 95. End Terminal with Curb Simulation Feed Length, MASH 2009 Test No. 3-32 at 15-deg Impact Angle	118
Figure 96. End Terminal with Curb Simulation Feed Length, MASH 2009 Test No. 3-33 at 5-deg Impact Angle	119
Figure 97. End Terminal with Curb Simulation Feed Length, MASH 2009 Test No. 3-33 at 15-deg Impact Angle	119
Figure 98. MASH 2009 Test No. 3-32 with Curbs, 5 Degrees, 6-ft Offset, Downstream View	122
Figure 99. MASH 2009 Test No. 3-30, Shallow Quarter-Point Offset, Overhead View	124
Figure 100. MASH 2009 Test No. 3-30, Shallow Quarter-Point Offset, Downstream View	125
Figure 101. MASH 2009 Test No. 3-30, Deep Quarter-Point Offset, Overhead View	126
Figure 102. MASH 2009 Test No. 3-30, Deep Quarter-Point Offset, Downstream View	127
Figure 103. MASH 2009 Test No. 3-31, Overhead View	128
Figure 104. MASH 2009 Test No. 3-31, Downstream View	129
Figure 105. MASH 2009 Test No. 3-32 at 5 Degrees, Overhead View	130
Figure 106. MASH 2009 Test No. 3-32 at 5 Degrees, Downstream View	131
Figure 107. MASH 2009 Test No. 3-32 at 15 Degrees, Overhead View	132
Figure 108. MASH 2009 Test No. 3-32 at 15 Degrees, Downstream View	133
Figure 109. MASH 2009 Test No. 3-33 at 5 degrees, Overhead View	134
Figure 110. MASH 2009 Test No. 3-33 at 5 degrees, Downstream View	135
Figure 111. MASH 2009 Test No. 3-33 at 15 degrees, Overhead View	136
Figure 112. MASH 2009 Test No. 3-33 at 15 degrees, Downstream View	137
Figure 113. Tangent vs. Flared End Terminal Simulations, Feed Lengths	138
Figure 114. Tangent vs. Flared End Terminal Simulations, Vehicle Roll	138
Figure 115. Tangent vs. Flared End Terminal Simulations, Vehicle Pitch	139

Figure 116. Tangent vs. Flared End Terminal Simulations, Vehicle Yaw	139
Figure 117. Tangent vs. Flared End Terminal Simulations, Longitudinal ORA	140
Figure 118. Tangent vs. Flared End Terminal Simulations, Lateral ORA	140
Figure 119. MASH 2009, Test No. 3-32 at 5 Degrees, Overhead View	142
Figure 120. MASH 2009, Test No. 3-32 at 5 Degrees, Overhead View	143
Figure 121. MASH 2009, Test No. 3-33 at 5 degrees, Overhead View	144
Figure 122. MASH 2009, Test No. 3-33 at 5 degrees, Overhead View	145
Figure 123. Flared End Terminal Simulations with Curbs, Feed Length	146
Figure 124. Flared End Terminal Simulations with Curbs, Vehicle Roll	146
Figure 125. Flared End Terminal Simulations with Curbs, Vehicle Pitch	147
Figure 126. Flared End Terminal Simulations with Curbs, Vehicle Yaw	147
Figure 127. Flared End Terminal Simulations with Curbs, Longitudinal ORA	148
Figure 128. Flared End Terminal Simulations with Curbs, Lateral ORA	148

LIST OF TABLES

Table 1. Energy-Absorbing Roadside Terminals [2].....	4
Table 2. Energy-Absorbing Roadside Terminals (cont'd) [2].....	5
Table 3. Energy-Absorbing Median Terminals [2].....	6
Table 4. MASH 2009 TL-3 Crash Test Conditions for Terminals and Crash Cushions [4]	11
Table 5. MASH 2009 Evaluation Criteria for End Terminal [4].....	12
Table 6. End Terminal Summary [20-21].....	14
Table 7. Impact Head Model Parts	20
Table 8. CRT Post Properties.....	24
Table 9. NCHRP Report 350 Test No. 3-30, Shallow Quarter-Point Offset.....	33
Table 10. NCHRP Report 350 Test No. 3-30, Deep Quarter-Point Offset.....	36
Table 11. NCHRP Report 350 Test No. 3-31	40
Table 12. NCHRP Report 350 Test No. 3-32	43
Table 13. NCHRP Report 350 Test No. 3-33	47
Table 14. MASH 2009 Test No. 3-30, Shallow Quarter-Point Offset.....	51
Table 15. MASH 2009 Test No. 3-30, Deep Quarter-Point Offset	54
Table 16. MASH 2009 Test No. 3-31	58
Table 17. MASH 2009 Test No. 3-32 at 5 Degrees.....	62
Table 18. MASH 2009 Test No. 3-32 at 15 Degrees.....	66
Table 19. MASH 2009 Test No. 3-33 at 5 Degrees.....	70
Table 20. MASH 2009 Test No. 3-33 at 15 Degrees.....	73
Table 21. NCHRP Report 350 Test No. 3-30, 27¾ in. (706 mm) Tall, Results Comparison	77
Table 22. NCHRP Report 350 Test No. 3-30, 31 in. (787 mm) Tall, Results Comparison	77
Table 23. NCHRP Report 350 Test No. 3-31, 27¾ in. (706 mm) Tall, Results Comparison	83
Table 24. NCHRP Report 350 Test No. 3-31, 31 in. (787 mm) Tall, Results Comparison	87
Table 25. NCHRP Report 350 Test No. 3-32, 27¾ in. (706 mm) Tall, Results Comparison	90
Table 26. NCHRP Report 350 Test No. 3-32, 31 in. (787 mm) Tall, Results Comparison	94
Table 27. NCHRP Report 350 Test No. 3-33, 27¾ in. (706 mm) Tall, Results Comparison	96
Table 28. NCHRP Report 350 Test No. 3-33, 31 in. (787 mm) Tall, Results Comparison	96
Table 29. Change in Vertical Bumper Height at Impact	120

1 INTRODUCTION

Guardrail end terminals have been developed to shield the end of a longitudinal barrier and function as a redirective barrier when struck along the side. Several guardrail end terminal systems utilize an energy-absorbing mechanism, such as cutting, kinking, flattening, or another mechanism to safely decelerate errant passenger vehicles that impact the end of the terminal. The Federal Highway Administration (FHWA) resource charts identified seven energy-absorbing roadside end terminals for W-beam guardrail systems [1]. Median configurations of energy-absorbing end terminals utilize similar components as roadside energy-absorbing end terminals. The FHWA resource charts identified five energy-absorbing median end terminals for W-beam guardrail systems [2]. These systems were installed on level terrain and tested at Test Level 3 (TL-3) of the National Cooperative Highway Research Program (NCHRP) Report 350 [3] or the 2009 edition of the *Manual for Assessing Safety Hardware* (MASH) [4]. A summary of the roadside and median end terminal systems is shown in Tables 1 through 3. However, the safety performance of these energy-absorbing, guardrail end terminals may change if a curb is installed adjacent to the terminal, and little guidance is available to State Departments of Transportation (DOTs) that have installations where a curb is required adjacent to energy-absorbing, guardrail end terminals.

1.1 Problem Statement

Highway design policy typically discourages the use of 6- to 8-in. (152- to 203-mm) tall vertical curbs on high-speed roadways due to their potential to cause drivers to lose control in a crash [5]. Curbs can also affect the interaction of errant vehicles with roadside barriers by affecting vehicle capture and barrier loading. However, the use of curbs is commonly required because of restricted right-of-way, drainage considerations, access control, and other functions. Often, there is a desire to laterally offset the guardrail away from the curb to reduce the propensity for snow plows to gouge and/or damage the W-beam rail sections or to allow for the placement of sidewalks between the road and a barrier or other roadside features.

When curbs are required, modeling and crash testing have shown that the lateral barrier offset from the curb is critical to W-beam guardrail performance. Previous work with 27¾-in. (705-mm) tall steel-post, nested W-beam guardrail has shown that a 4-in. (102-mm) high sloped curb with the toe of the curb placed at the front face of the guardrail was capable of meeting NCHRP Report 350 TL-3 safety requirements [6-7]. Further research with standard wood-post, W-beam guardrail (G4(2W)) has shown that a 4-in. (102-mm) high sloped curb with its toe 1 in. (25 mm) in front of the front face of the guardrail was also capable of meeting NCHRP Report 350 TL-3 requirements [8].

Investigation of curb-barrier combinations was reported in NCHRP Report No. 537, *Recommended Guidelines for Curbs and Curb-Barrier Combinations* and the *Roadside Design Guide* [9-10]. This study developed guidelines for the use of curbs and curb-barrier combinations on roadways with operating speeds greater than 37.3 mph (60 km/h). It was recommended that guardrail be installed flush with the face of a sloped curb or offset more than 8.2 ft (2.5 m) behind a curb for operating speeds in excess of 37.3 mph (60 km/h). In addition, the study recommended that guardrail not be offset behind sloped curbs for speeds greater than 62.1 mph (100 km/h).

Development and testing of the Midwest Guardrail System (MGS) demonstrated that a 6-in. (152-mm) tall, American Association of State Highway Transportation Officials (AASHTO) Type B curb positioned 6 in. (152 mm) in front of the face of the guardrail element resulted in successful barrier performance [11-12]. In 2008, a 6-in. (152-mm) high AASHTO Type B curb was impacted under MASH 2009 TL-3 conditions [13-14]. The main goal of the tests was to determine vehicle behavior following the impact, with particular attention focused on the pitch angles and the bumper trajectories of the vehicles. By comparing the critical bumper impact point trajectories against the MGS top/bottom corrugation heights, the critical override/underide offset for placing the MGS behind the curb was determined. Results of this analysis created potential offset guidelines for placement of the MGS with a 6-in. (152-mm) high curb.

To further investigate the critical offset distance for MGS placement behind an AASHTO Type B curb with MASH 2009 TL-3 impact conditions, finite element analysis was performed. The MGS was offset from a 6-in. (152-mm) high AASHTO Type B curb at various distances and impacted with a 4,409-lb (2,000-kg) test vehicle (designated 2000P) as a 2270P vehicle model was unavailable. Based on previous vehicle-curb simulation results and to ensure reliability of the model, the offset distance under investigation was limited to the range of 0.0 ft (0.0 m) to 7.35 ft (2.2 m) behind the curb. Simulation results indicated that the 2000P pickup model accurately predicted the vehicle trajectory within 7.35 ft (2.2 m) behind the curb. Details of this research effort are documented in prior MwRSF research reports [13-14].

Based on the simulation results, a MASH 2009 TL-3 full-scale crash test was performed on the MGS with a top mounting height of 37 in. (940 mm) above the roadway and offset 8 ft (2.4 m) behind a 6-in. (152-mm) high AASHTO Type B Curb [15]. In the test, the 2270P vehicle was contained by the guardrail but became unstable and rolled over. Analysis of the test revealed that the truck's right-front tire snagged on a post and detached. The right-rear tire overrode the detached tire, causing the rear of the vehicle to pitch upward. The vehicle subsequently became unstable and rolled over. Thus, the MGS offset 8 ft (2.4 m) behind a 6-in. (152-mm) high curb with a top mounting height of 37 in. (940 mm) relative to the roadway was deemed to be unacceptable according to TL-3 of MASH 2009.

The MGS was installed 6 ft (1.8 m) behind a 6-in. (152-mm) high, AASHTO Type B curb and was successfully evaluated according to MASH 2009 TL-2 conditions [16]. The MGS with a 37-in. (940-mm) top rail height relative to the roadway was recommended for MASH 2009 TL-2 applications for lateral offsets ranging between 4 and 12 ft (1.2 and 3.7 m) behind a 6-in. (152-mm) high, AASHTO Type B curb. Prior TL-3 curb testing indicated potential vehicle problems beyond a 12-ft (3.7-m) lateral offset. As discussed by Polivka et al. and Fallor et al. [11-12], the Type B curb is considered the worst-case geometry for sloped curbs. Thus, this recommendation is also valid for other sloped curbs with heights of 6 in. (152 mm) or less. For lower-height curbs, the rail height should be reduced in order to maintain the 31-in. (787-mm) top rail height relative to the ground behind the curb.

The *Roadside Design Guide* recommends that, for design speeds above 50 mph (80 km/h), guardrails should be used with 4 in. (102 mm) or shorter sloping curbs, and the face of the curbs should be flush with the face of the guardrail [10]. The performance of guardrail end terminals behind curbs has not been tested, and one transportation agency addressed this issue by transitioning the curb to a laydown curb along the length of the end terminal and extending typically 100 ft (30 m) in advance of the terminal. Additionally, the *Roadside Design Guide*

states that curbs should not be built in new construction where crash cushions are to be installed, and a curb no higher than 4 in. (102 mm) may be considered acceptable on existing crash cushion locations unless it has contributed to poor crash cushion performance in the past [10].

In 1979, the California Department of Transportation performed several curbed gore area vehicle jump tests and a full-scale crash test with a 2,790-lb (1,265-kg) passenger car impacting a sand barrel crash cushion on top of a 6-in. (152-mm) tall curbed gore area at a speed of 41 mph (66.0 km/h) [17]. The sand barrel crash cushion was 5 ft (1.5 m) behind the perpendicular curb, and the curb did not adversely affect the crash cushion performance. It was recommended to place a sand barrel crash cushion 0 to 5 ft (1.5 m) or over 50 ft (15.2 m) behind a perpendicular 6-in. (152-mm) tall curb (the front of the gore area) and 0 to 3 ft (0.9 m) behind a parallel curb (the side of the gore area) if a curb was necessary. No other known research has been conducted in relation to curbs and end treatments.

While much research has been conducted to determine the safe placement of curbs adjacent to W-beam guardrail, no guidance exists on the use of curbs adjacent to end terminals. Thus, a study was desired to evaluate curb configurations and placement adjacent to energy-absorbing end terminals.




1.2 Research Objective

The research objective was to investigate whether curb placement in advance of guardrail end terminals significantly degrades barrier performance on high-speed roadways. Design guidance and recommendations will be provided for the safe placement of curbs and gutters installed adjacent to energy-absorbing guardrail end terminals. Performance trends will be identified, and further research needs will be recommended.

1.3 Scope

The Wisconsin DOT and members of the Midwest States Pooled Fund Program were surveyed about their use of energy-absorbing end terminals and installations of guardrail and curbs adjacent to high-speed roadways to tailor the study to their needs. An energy-absorbing, W-beam end terminal model was developed using LS-DYNA computer simulation software. Simulated impacts on the end of the terminal (test nos. 3-30, 3-31, 3-32, and 3-33) were evaluated according to NCHRP Report 350 and MASH 2009 safety performance criteria. The simulations were compared to available crash test data to ensure that the energy-absorbing end terminal model accurately represented the performance of end terminals. Several curb configurations adjacent to the energy-absorbing end terminal, including variations in size, shape, and location, were evaluated using computer simulations with MASH 2009 TL-3 impacts on the end of the terminal. The performance of the system with and without curbs was compared, and general performance trends were identified. The simulation results were summarized, and recommendations and guidance were provided in regard to the safe placement of curbs and gutters installed adjacent to energy-absorbing end terminals. Performance trends and limitations of the research were identified, and further research needs were recommended.

Table 1. Energy-Absorbing Roadside Terminals [2]

NAME	MANUFACTURER	PERFORMANCE CHARACTERISTICS		TEST LEVEL		FLARED	TANGENT	31-inch Height (option)	DISTINGUISHING CHARACTERISTICS	LOCATIONS CAN BE USED
		Energy Absorbing	Non Energy Absorbing	NCHRP 350	MASH					
Flared Energy-Absorbing Terminal (FLEAT) http://roadsystems.com/fleat.html		Road Systems, Inc.	X		TL-2, TL-3		X	X	Rectangular impact front face, with steel tube on top. Rail has 5 slots (1/2"x4" long) on both the top and bottom corrugations of the w-beam section. There may also be 3 additional (1/2"x4" long) slots in the valley of the rail which makes it interchangeable with the first SKT section. Breakaway steel end posts #1 and #2, standard steel guardrail post #3 and beyond. Cable anchor bracket is fully seated on the shoulder portion of the cable anchor bolts. All hinge steel post, plug weld steel posts, or wood posts available.	End of W-beam rail with offset of 2'-6" to 4'-0".
TREND 350 Flared http://www.highwayguardrail.com/products/et.html		Trinity Highway Products, LLC	X		TL-3		X	X	Rectangular Impact Face All steel driven posts. Breakaway steel posts at #1 and #2, standard steel guardrail posts #3 and beyond. Steel Strut between posts #1 and #2. During head on impacts the system telescopes rearward, using friction between the guardrail panels and deformation of the rail sections to decelerate the vehicle.	End of W-Beam rail with offset of 1' to 4'0"
Sequential Kinking Terminal (SKT) http://roadsystems.com/skt.html		Road Systems, Inc.	X		TL-2, TL-3		X	X	Square Impact Face. Has a feeder chute (channel section that surrounds the rail) that gets wider at the downstream end. Breakaway steel end posts #1 and #2 and standard steel guardrail posts #3 and beyond. Rail has 3 (1/2"x4" long) slots in the valley of the rail. There may also be an additional 5 slots (1/2"x4" long) on both the top and bottom corrugations of the w-beam section, which makes it interchangeable with the FLEAT section. Cable anchor bracket is fully seated on the shoulder portion of the cable anchor bolts. All hinge steel post, plug weld steel posts, or wood posts available.	End of W-beam rail with offset of 0 to 2'-0".







U.S. Department of Transportation
Federal Highway Administration

The safety systems shown on this chart are eligible for reimbursement under the Federal-Aid Highway Program. This reference is for informational purposes only, and was created by KLS Engineering under FHWA Contract, DTFH61-10-D-00021, Roadside Safety Systems Installers and Designers Mentor Program. For further information on an individual system please refer to the manufacturers' website.



Table 2. Energy-Absorbing Roadside Terminals (cont'd) [2]

NAME	MANUFACTURER	PERFORMANCE CHARACTERISTICS		TEST LEVEL		FLARED	TANGENT	31-inch Height (option)	DISTINGUISHING CHARACTERISTICS	LOCATIONS CAN BE USED
		Energy Absorbing	Non Energy Absorbing	NCHRP 350	MASH					
Extruder Terminal (ET-Plus) http://www.highwayguardrail.com/products/etplus.html	 Trinity Highway Products, LLC	X		TL-2, TL-3			X	X	Rectangular Impact Front Face (Extruder Head). Rectangular holes in 1st rail support the tabs of the cable anchor bracket. Steel HBA and SYTP and wood post options are available. SYTP Retrofit in tube sleeve option available.	End of W-beam rail with offset of 0 to 2'-0".
SoftStop http://www.highwayguardrail.com/products/et.html	 Trinity Highway Products, LLC	X			TL-3		X	X (Only)	Rectangular Impact Face. Breakaway steel posts at #1 and #2, standard posts 3 and beyond.	End of W-Beam rail with offset of 0' to 2'-0"
X-Tension Guardrail End Terminal http://www.barriersystemsinc.com/#/x-tension	 Barrier Systems, Inc.	X		TL-3		X	X	X	Impact head with locking bar to lock cables into place. Strut between the first post and a front anchor post. Steel and wood post options available. Tension Cable Based Energy Absorber. Two cables attached to soil anchor extend the entire length of the terminal.	End of W-beam rail with offset of 0 to 4'-0".
X-Lite Terminal http://www.barriersystemsinc.com/#/x-lite-redirective-gating-end-treatment	 Barrier Systems, Inc./Formet, Inc.	X		TL-3		X	X	X	Only approved with steel post. Uses a slider mechanism between post 1 and 2 that gathers and retains the rail when hit. The anchor consists of posts #1 and #2 connected by tension struts and a soil plate below grade on post #2. Tangent systems uses 3 modified crimped posts and special shear bolts at second and third splice location. Flared layout uses 6 modified crimped posts and special shear bolts at second splice location. Flared layout uses blockout at post #2 where tangent does not.	End of W-Beam rail at tangent locations or at flared locations with a 4-ft offset








U.S. Department of Transportation
Federal Highway Administration

The safety systems shown on this chart are eligible for reimbursement under the Federal-Aid Highway Program. This reference is for informational purposes only, and was created by KLS Engineering under FHWA Contract, DTFH61-10-D-00021, Roadside Safety Systems Installers and Designers Mentor Program. For further information on an individual system please refer to the manufacturers' website.



Table 3. Energy-Absorbing Median Terminals [2]

NAME	MANUFACTURER	PERFORMANCE CHARACTERISTICS		TEST LEVEL		31-inch Height (option)	DISTINGUISHING CHARACTERISTICS	HOW IT WORKS	LOCATIONS CAN BE USED
		Energy Absorbing	Non-Energy Absorbing	NCHRP 350	MASH				
Brakemaster 350 http://www.energyabsorption.com/products/products_brakemaster350_crash.asp	 Energy Absorption Systems, Inc.	X		TL-3			Steel posts are not embedded. Break Tension System at post #1. Short W-Beam rail sections that translate over each other.	During head-on impacts, the system telescopes rearward, using friction technology to decelerate the vehicle.	Low frequency impact areas. In the median with 1-way or 2-way traffic.
Crash Cushion Attenuating Terminal (CAT-350) http://www.highwayguardrail.com/products/cat350.html	 Trinity Highway Products, LLC	X		TL-3			Breakaway wood posts and a cable anchorage system. The beam elements are slotted W-beam rail sections. Nose is 10 gauge And first set of rails are 12 gauge and second set of rails are heavier 10 gauge.	During head-on impacts, the system telescopes rearward, shearing out tabs between the slots to decelerate the vehicle.	Low frequency impact areas. Attached directly to a W-Beam median barrier, or to a Thrie-Beam median barrier using the standard W-Beam to Thrie-Beam transition section.
TREND 350 Median http://www.highwayguardrail.com/products/et.html	 Trinity Highway Products, LLC	X		TL-3		X	Square Impact Face. All steel driven posts. Breakaway steel posts at #1 and #2, standard steel guardrail posts #3 and beyond. Steel Strut between posts #1 and #2.	During head on impacts the system telescopes rearward, using between the system rails and the deformation of the rails to decelerate the vehicle.	Low Frequency impact areas. Attached directly to a W-Beam Median Barrier, or to a Thrie-Beam median barrier using the standard W-Beam to Thrie-Beam transition section.
FLEAT Median Terminal (FLEAT-MT) http://www.roadsystems.com/fleat-mt.html	 Road Systems, Inc.	X		TL-3		X	Two impact heads, two modified W-beam rails, standard W-beam rails, two breakaway cable anchor assemblies and weakened steel or wood posts. Uses many of the same components as the roadside FLEAT terminal.	During head-on impacts, the impact head translates down the rail kinking the rail to decelerate the vehicle.	Low frequency impact areas. Attached directly to a W-Beam median barrier, or to a Thrie-Beam median barrier using the standard W-Beam to Thrie-Beam transition section.
X-Tension Median Attenuator System (X-MAS) http://www.barriersystemsinc.com/#/x-tension-median	 Barrier Systems, Inc.	X		TL-3		X	Impact head with locking bar to lock cables into place. Two cables attached to soil anchor extend the entire length of the terminal. Only available with steel posts.	During head on impacts, X-Tension is energy absorbing with resistance at the impact head. As the head is pushed down the two cables, the cables are pulled through the cable friction plate in a twisting path which dissipates the energy.	Low frequency impact areas. Attached directly to a W-Beam median barrier, or to a Thrie-Beam median barrier using the standard W-Beam to Thrie-Beam transition section.



2 SURVEY

In 2014, the Wisconsin DOT and additional State DOTs in the Midwest States Pooled Fund Program were surveyed about their use of energy-absorbing, W-beam end terminals and installation practices, including if and when curbs were present on high-speed roadways. The list of end terminals provided in the survey was obtained from the FHWA resource charts [1-2]. Variations in end terminal post types and system lengths were not included in the survey. Other systems that were previously installed on the roadway, but are not listed on the FHWA resource charts, fall into the category of 'Other'. More than one answer could be selected for several of the questions. The survey questions and the number of responses for each answer are as follows:

1. Which of the following energy-absorbing roadside end terminals have you installed?

- 6 - FLEAT [Road Systems, Inc.]
- 0 - TREND 350 Flared [Trinity Highway Products, LLC]
- 8 - SKT [Road Systems, Inc.]
- 8 - ET-Plus [Trinity Highway Products, LLC]
- 0 - SoftStop [Trinity Highway Products, LLC]
- 2 - X-Tension Guardrail End Terminal [Barrier Systems, Inc.] (Noted experimental use only)
- 1 - X-Lite Terminal [Barrier Systems, Inc.] (Noted experimental use only)
- 0 - None
- 2 - Other: older systems that were previously installed

2. Which of the systems in Question#1 is installed most frequently?

ET-Plus (5 States), FLEAT (3 States), SKT (1 State), Unknown (2 States)

3. Which of the following energy-absorbing median end terminals have you installed?

- 2 - Brakemaster 350 [Energy Absorption Systems, Inc.]
- 6 - CAT-350 [Trinity Highway Products, LLC]
- 0 - TREND 350 Median [Trinity Highway Products, LLC]
- 3 - FLEAT-MT [Road Systems, Inc.]
- 1 - X-MAS [Barrier Systems, Inc.] (Noted experimental use only)
- 1 - None
- 1 - Other: Bullnose

4. What top of rail height are new installations of end terminals installed at?

- 0 - 27¾ in.
- 6 - 31 in.
- 2 - Other: 27 ¼ in. and 28 in.

5. Do you install more tangent or flared end terminal installations?

- 3 - Tangent
- 2 - Flared
- 3 - Both

6. Are tangent end terminals typically installed with a flare?

- 3 - Yes – 1:50 flare rate
- 3 - Yes – 1:25 flare rate
- 1 - Yes – Other flare rate: 1:15
- 1 - No

7. Have you installed curbs and gutters adjacent to energy-absorbing end terminals? If yes, please provide a drawing at an installed location, if available. Keep in mind this is only for high-speed roadways.

- 2 - Yes – at many locations
- 4 - Yes – at a few locations
- 1 - No – but may in the future
- 1 - No – and do not plan to

8. What is the typical lateral offset from the front of the curb to the face of the W-beam guardrail for guardrail-curb installations?

- 5 - 0" (flush)
- 2 - 6"
- 1 - Other: 10 ft
- 1 - Not used

9. Have you installed a curb perpendicular to an energy-absorbing end terminal (e.g. near an intersection or median cross-over)? Keep in mind this is only for high-speed roadways.

- 0 - Yes – at many locations
- 3 - Yes – at a few locations
- 3 - No – but may in the future
- 3 - No – and do not plan to

10. If you answered 'yes' in Question#9, how far was the curb offset from the nose of the end terminal?

50 to 100 ft or more, varies, or unsure

11. What curb shape is installed near guardrail and/or end terminals?

- 7 – Sloped (includes AASHTO Type G and other constant sloped curbs)
- 0 - Type B
- 0 - Type D
- 2 - Vertical
- 2 - None
- 0 - Other:

12. What curb height is installed near guardrail and/or end terminals?

- 3 - < 4 in.
- 6 - 4 in.
- 2 - 6 in.
- 1 - None
- 0 - Other:

13. Do end terminal manufacturers provide any installation guidance in relation to curbs and gutters?

- 1 - Yes, please describe: reference RDG
- 1 - Yes, please describe: if curb is taller than 4", replace with 4" curb for 75' in advance of nose and extend 50' beyond
- 5 - No

14. Do you plan on using any tension-based, energy-absorbing end terminals (e.g. Trinity Highway Products SoftStop, Barrier Systems X-Tension Guardrail End Terminal, and Barrier Systems X-Tension Median Attenuation System (X-MAS))?

- 0 - Yes – we currently are
- 2 - Yes – we are considering in the next year
- 3 - Yes – we are considering in the next two years
- 3 - No – not in the foreseeable future

15. What would be your desired use for curbs and gutters adjacent to energy-absorbing terminals (if the configuration was crashworthy)?

Most States need the curbs for drainage control.
Need to know how to safely start and terminate curbs near end terminals.
Some would like to be able to use with different shaped curbs (6" tall AASHTO Type B) with a minimal lateral offset.

16. Please provide any additional comments about the use of curbs near energy-absorbing end terminals

Tangent terminals must be flared if the guardrail is installed flush with the curb so the end anchorage doesn't interfere with the curb and to move the impact head farther from the edge of the road.

Based on the results of the survey, most State Departments of Transportation installed the ET-Plus, SKT, and FLEAT end terminal systems. These systems involve an end terminal head that translates longitudinally along the end terminal system upon impact and has an energy-absorbing mechanism that deflects guardrail laterally behind or in front of the guardrail system. Most State DOTs utilized 31-in. (787-mm) tall W-beam guardrail. Tangent and flared end terminal systems were commonly used, and many tangent end terminals were installed with a 1:25 or 1:50 flare. Several State DOTs had at least a few curb installations that were adjacent to energy-absorbing end terminal systems on high-speed roadways. The curbs were typically

installed flush with the face of the rail or laterally offset 6 in. (152 mm) away from the front face of the rail. Most State DOTs used a constant-sloped curb, and two State DOTs used a vertical curb. The curb height may be up to 6 in. (152 mm), although 4-in. (102-mm) tall curbs were used most frequently. Curbs perpendicular to energy-absorbing end terminals were used infrequently but may be utilized more in the future.

Needs were identified by this survey:

- 1) Curbs and gutters are necessary for drainage control, which may include placement adjacent to energy-absorbing end terminals
- 2) Guidance is not available on proper curb placement adjacent to end terminals
- 3) Tangent end terminals installed flush or with a small offset from a curb must be flared to properly install the anchorage posts and move the impact head farther from the roadway

3 TEST REQUIREMENTS AND EVALUATION CRITERIA

3.1 Test Requirements

End terminals and crash cushions, such as energy-absorbing, W-beam guardrail end terminals, must satisfy impact safety standards in order to be declared eligible for federal reimbursement by the FHWA for use on the National Highway System (NHS). For new hardware, these safety standards consist of the guidelines and procedures published in MASH 2009 [4]. According to TL-3 of MASH 2009, end terminals must be subjected to nine full-scale vehicle crash tests, as summarized in Table 4. MASH 2016 was published after this project was initiated and provides revisions to test no. 3-37, which was not conducted as part of this project [18]. Note that there is no difference between MASH 2009 and MASH 2016 for the tests performed herein.

Table 4. MASH 2009 TL-3 Crash Test Conditions for Terminals and Crash Cushions [4]

Test Article	Test No.	Test Vehicle	Vehicle Weight, lb (kg)	Impact Conditions		Evaluation Criteria ¹
				Speed, Mph (km/h)	Angle, deg.	
Terminals and Crash Cushions	3-30	1100C	2,425 (1,100)	62 (100)	0	C,D,F,H,I,N
	3-31	2270P	5,000 (2,270)	62 (100)	0	C,D,F,H,I,N
	3-32	1100C	2,425 (1,100)	62 (100)	5/15	C,D,F,H,I,N
	3-33	2270P	5,000 (2,270)	62 (100)	5/15	C,D,F,H,I,N
	3-34	1100C	2,425 (1,100)	62 (100)	15	C,D,F,H,I,N
	3-35	2270P	5,000 (2,270)	62 (100)	25	A,D,F,H,I
	3-36	2270P	5,000 (2,270)	62 (100)	25	A,D,F,H,I
	3-37	2270P	5,000 (2,270)	62 (100)	25	C,D,F,H,I,N
	3-38	1500A	3,300 (1,500)	62 (100)	0	C,D,F,H,I,N

¹ Evaluation criteria explained in Table 5.

3.2 Evaluation Criteria

Evaluation criteria for full-scale vehicle crash testing are based on three appraisal areas: (1) structural adequacy, (2) occupant risk, and (3) vehicle trajectory after collision. Criteria for structural adequacy are intended to evaluate the ability of the end terminal to contain, redirect, or control test article penetration and stopping of impacting vehicles. In addition, controlled lateral deflection of the test article is acceptable. Occupant risk evaluates the degree of hazard to occupants in the impacting vehicle. Post-impact vehicle trajectory is a measure of the potential of the vehicle to result in a secondary collision with other vehicles and/or fixed objects, thereby increasing the risk of injury to the occupants of the impacting vehicle and/or other vehicles. Vehicle trajectory behind the system is acceptable for gating end terminals under MASH 2009 test nos. 3-30 through 3-34, 3-37, and 3-38. Vehicle trajectory behind the system is not acceptable for MASH 2009 test nos. 3-35 and 3-36. These evaluation criteria are summarized in

Table 5 and defined in greater detail in MASH 2009. While all the end terminals listed in the FHWA resource charts have been tested to either NCHRP Report 350 or MASH 2009 safety performance criteria, the complete crash testing matrix has not been conducted on any terminal at both the 27³/₄-in. (705-mm) and 31-in. (787-mm) guardrail heights.

In lieu of conducting several full-scale crash tests to evaluate end terminal systems with curbs, a computer simulation effort was conducted, and the results were evaluated using the MASH 2009 evaluation criteria. Test nos. 3-30 through 3-33 involve impacts on the end of the system, while test nos. 3-34 through 3-37 involve impacts along the length of the system. Test nos. 3-34 through 3-37 were not evaluated as the results of impacts along the length of a terminal with a curb were expected to be similar to impacts along the length of W-beam guardrail with a curb, which was previously evaluated in NCHRP Report 537 [9] and other studies noted previously. Test no. 3-38 is only recommended if a force vs. deflection analysis predicts that the terminal will not meet occupant impact velocity and ridedown acceleration requirements, which was not expected, so this test was not evaluated with simulation.

Table 5. MASH 2009 Evaluation Criteria for End Terminal [4]

Structural Adequacy	A.	Test article should contain and redirect the vehicle or bring the vehicle to a controlled stop; the vehicle should not penetrate, underride, or override the installation although controlled lateral deflection of the test article is acceptable.		
	C.	Acceptable test article performance may be by redirection, controlled penetration, or controlled stopping of the vehicle.		
Occupant Risk	D.	Detached elements, fragments or other debris from the test article should not penetrate or show potential for penetrating the occupant compartment, or present an undue hazard to other traffic, pedestrians, or personnel in a work zone. Deformations of, or intrusions into, the occupant compartment should not exceed limits set forth in Section 5.3 and Appendix E of MASH 2009.		
	F.	The vehicle should remain upright during and after collision. The maximum roll and pitch angles are not to exceed 75 degrees.		
	H.	Occupant Impact Velocity (OIV) (see Appendix A, Section A5.3 of MASH 2009 for calculation procedure) should satisfy the following limits:		
		Occupant Impact Velocity Limits		
		Component	Preferred	Maximum
		Longitudinal and Lateral	30 ft/s (9.1 m/s)	40 ft/s (12.2 m/s)
	I.	The Occupant Ridedown Acceleration (ORA) (see Appendix A, Section A5.3 of MASH 2009 for calculation procedure) should satisfy the following limits:		
		Occupant Ridedown Acceleration Limits		
		Component	Preferred	Maximum
		Longitudinal and Lateral	15.0 g's	20.49 g's
Vehicle Trajectory	N.	Vehicle trajectory behind the test article is acceptable.		

4 END TERMINAL DETAILS

Based on the results of the survey and with sponsor direction, a plan was devised to evaluate energy-absorbing end terminal systems. Since several State DOTs install more than one type of end terminal system, a generic end terminal, which was representative of all of these systems, was developed. Several end terminal systems involve an impact head that translates longitudinally along the system upon impact and has an energy-absorbing mechanism that deflects guardrail laterally behind or in front of the guardrail system, including the ET-2000, BEST (Beam Eating Steel Terminal), SKT, FLEAT, and ET-Plus. The ET-2000 and BEST were not included in the FHWA resource chart. However, the ET-2000 and BEST, which are similar to the others, were crash tested and evaluated according to NCHRP Report 350.

The overall length of end terminal systems is typically 37.5 ft (11.4 m) or 50 ft (15.2 m). The ET-2000, BEST, SKT, and ET-Plus systems have an option for a 50-ft (15.2-m) system length. Thus, a 50-ft (15.2-m) system length was selected for the generic design. The dimensions of the five systems' impact head components varied and were averaged, resulting in a representative system, as shown in Figures 1 through 3.

These systems were tested at a 27 $\frac{3}{4}$ -in. (706-mm) rail height with wood posts spaced at 6 ft – 3 in. (1.9 m) installed in soil. Most systems also have steel post options, some of which are proprietary, for the anchorage (post nos. 1 and 2) and/or the line posts (post no. 3 and downstream). The steel and wood post options were designed to be similar, so the non-proprietary Breakaway Cable Terminal (BCT) wood posts and Controlled Release Terminal (CRT) wood posts were selected for the anchorage posts and the line posts, respectively.

End terminal system anchorages typically include a groundline strut to distribute loads between post nos. 1 and 2, steel soil tubes embedded in soil that contain the CRT posts, a cable anchor that spans between the bottom of post no. 1, and a cable anchor bracket attached to the W-beam. The cable anchor bracket disengages when impacted by the impact head, which releases tension in the guardrail. Many of the anchorage parts are unique to each energy-absorbing end terminal system; however, they perform similarly. Therefore, MGS downstream anchorage parts were utilized with modifications so the cable anchor bracket would disengage when impacted, similar to existing end terminal systems [19].

Each end terminal system also contains a post breaker to initiate fracture of post no. 1 and an impact head support bracket attached to post no. 1. For the purposes of this study, a solid rectangular support was utilized for each, which is described in Chapter 5.

All of the end terminal systems utilize the same AASHTO M-180 W-beam guardrail. However, the length of each section and the location of rail splices varies by system. In general, the rail splices for the 27 $\frac{3}{4}$ -in. (706-mm) tall system are located at post nos. 3, 5, 7, etc. For the 31-in. (787-mm) tall systems, rail splices are located typically at the midspan between posts, but the location of the first rail splice from the end of terminal varies by manufacturer. For example, some 31-in. (787-mm) tall systems have rail splices located at post no. 3, midspan between post nos. 5 and 6, midspan between post nos. 7 and 8, etc. Other 31-in. (787-mm) tall systems have rail splices located at midspan between post nos. 3 and 4, midspan between post nos. 5 and 6, midspan between post nos. 7 and 8, etc. The location of the rail splices may affect the

performance of end terminals. Guardrail has localized stiffness points when the rail splices are located at posts due to the overlapping rail plies and post bolts. When the splices are located at the midspan between posts, the localized stiffness points are distributed differently.

The energy-absorbing mechanism in each end terminal system varies greatly. Coon previously determined the average force exerted during an impact with energy-absorbing end terminals [20-21], as shown in Table 6. For each system, the average force range was determined by analyzing the rail deflection versus vehicle velocity and applying conservation of momentum during several full-scale crash tests.

Table 6. End Terminal Summary [20-21]

End Terminal System	Impact Head Weight lb (kg)	Average Force kips (kN)
BEST-350 [22-23]	275 (125)	18.7 to 22.5 (83.4 to 100)
ET-2000 [24-26]	268 (122)	12 to 21.3 (53.2 to 94.7)
ET-2000 Plus [27-30]	175 (79)	
FLEAT-350 [31-34]	120 (54.5)	13.5 to 16.7 (60.2 to 74.5)
SKT-350 [32-35]	172 (78)	10.5 to 15.2 (46.7 to 67.6)

Analyses were conducted on additional NCHRP Report 350 test no. 3-31 crash test results that were not included in Coon's force range derivation. The weight of the impact head was not explicitly given for each crash test, so the values listed in Table 6 were assumed. Test no. SMG-1 was conducted on the SKT-MGS (installed with 31-in. (787-mm) tall guardrail) and resulted in an approximate average force of 10.5 kips (46.8 kN) [32]. Test no. ET27-31 was conducted on the ET-Plus (installed with 27³/₄-in. (706-mm) tall guardrail) and resulted in an approximate average force of 15.0 kips (66.8 kN) [27]. Test no. ET31-31 was conducted on the ET-Plus (installed with 31-in. (787-mm) tall guardrail) and resulted in an approximate average force of 12.7 kips (56.4 kN) [28]. The average force for each of these tests fell into the force ranges previously established by Coon.

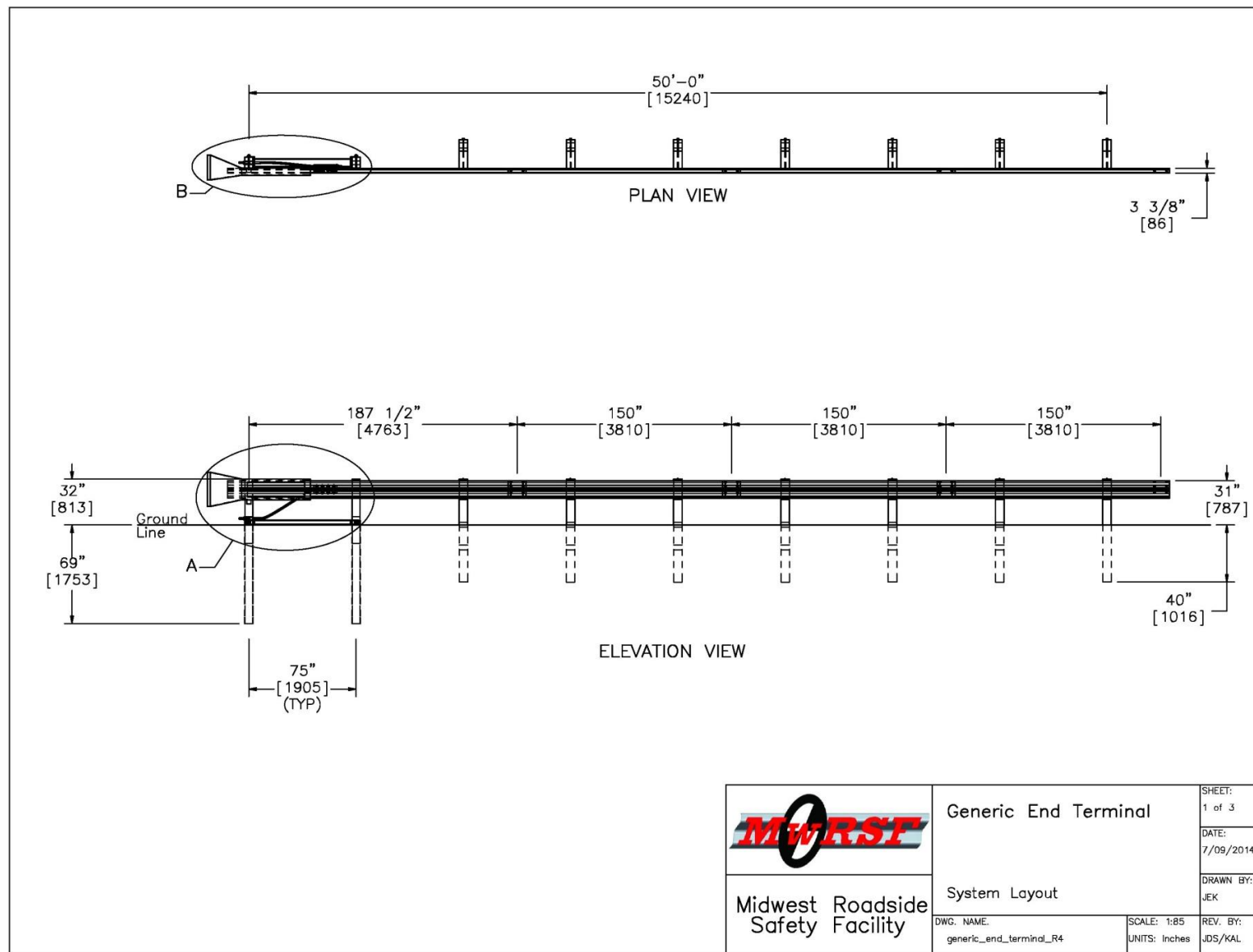


Figure 1. Representative End Terminal System

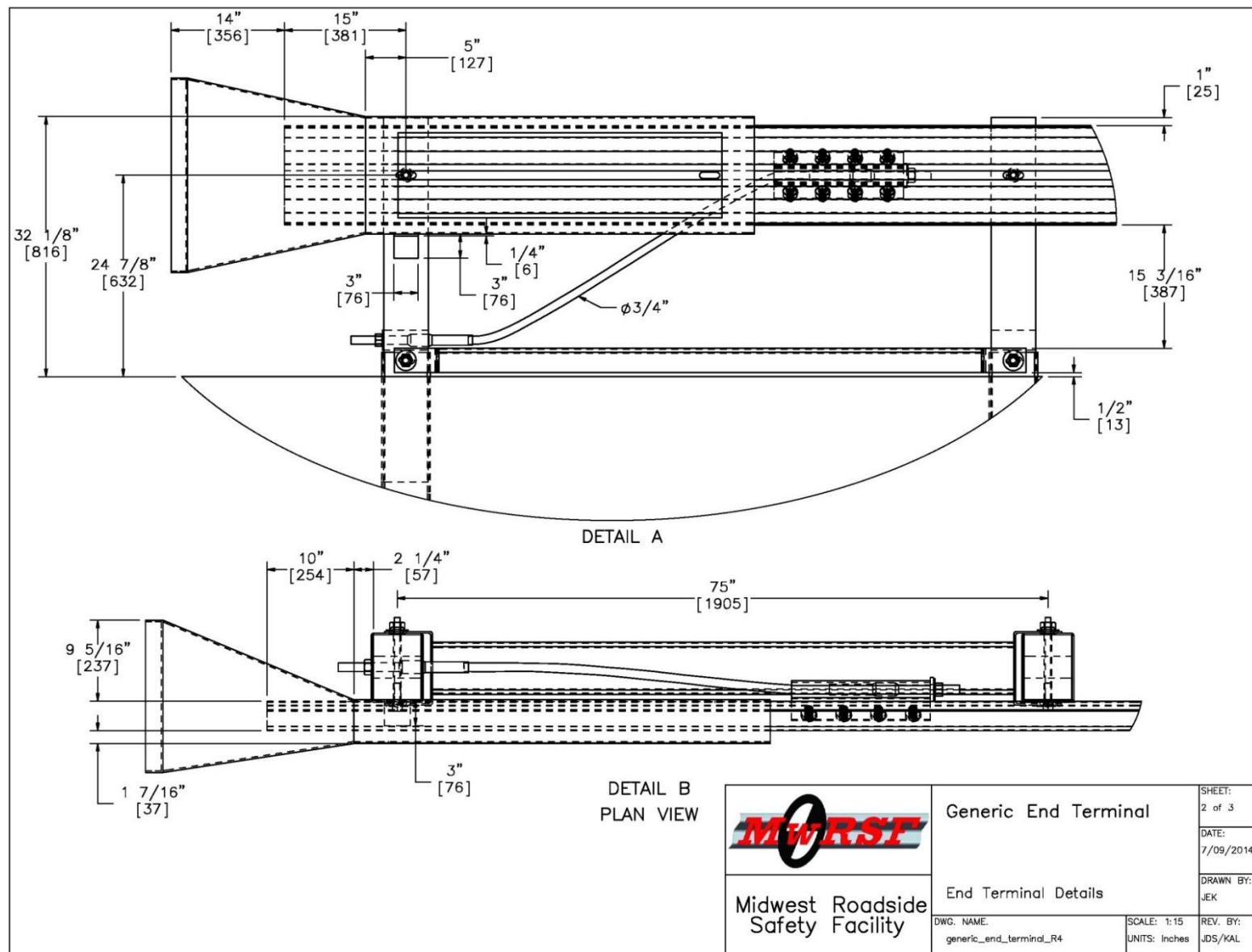


Figure 2. Representative End Terminal Details

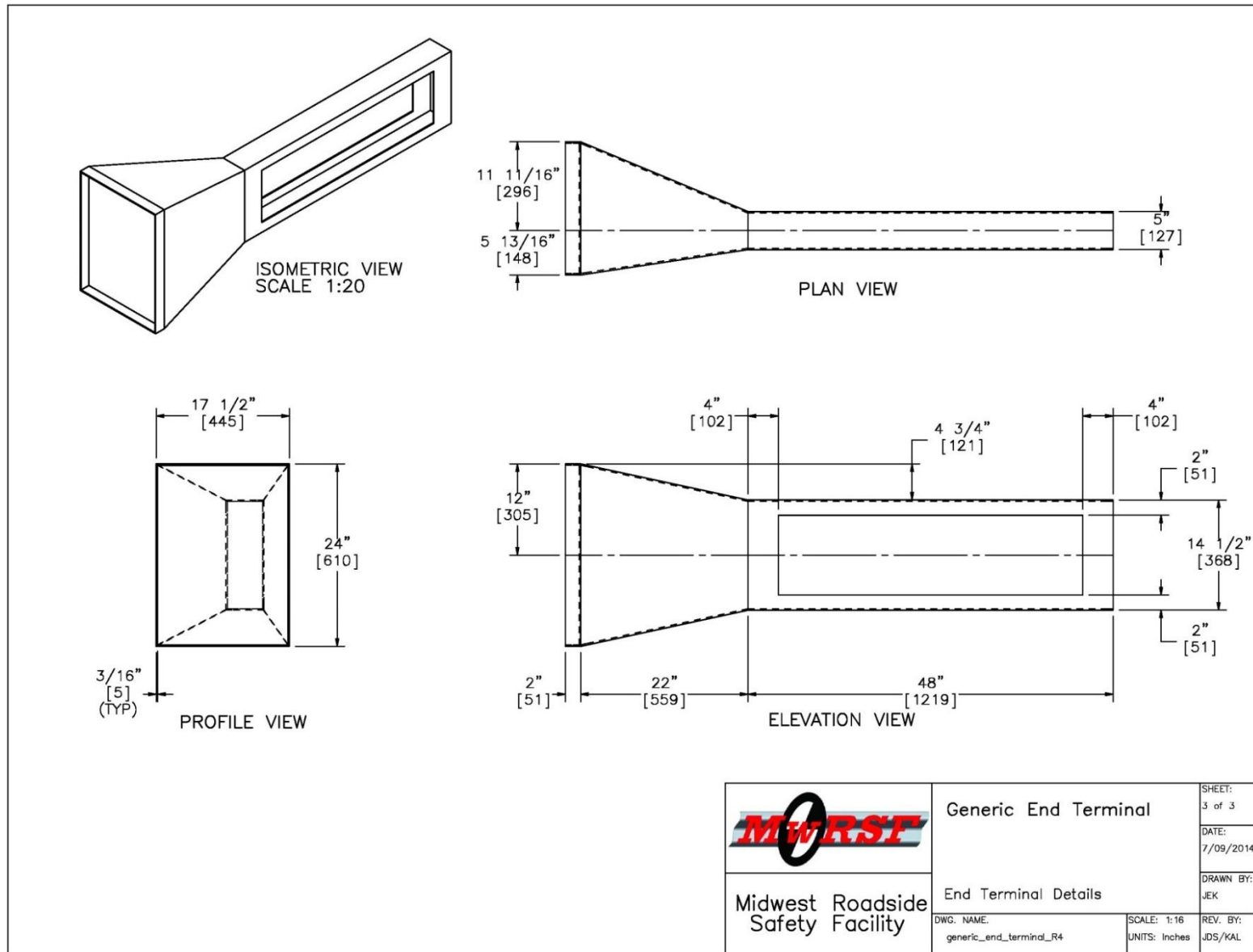


Figure 3. Representative Impact Head Details

5 LS-DYNA MODELS

5.1 Hardware Models

The 175-ft (53.3-m) long MGS LS-DYNA finite element analysis model previously developed and validated at MwRSF was modified to incorporate the end terminal system detailed in Figures 1 through 3. The models were developed using LS-DYNA Version 7.1.1 [36]. Two variations of a 29-post, 175-ft (53.3-m) long model, shown in Figures 4 and 5, were created:

- 1) 27¾-in. (705-mm) tall guardrail with posts with 8-in. (203-mm) blockouts representative of a modified G4(1S) with an end terminal; and
- 2) 31-in. (787-mm) tall guardrail with posts with 12-in. (305-mm) blockouts representative of MGS with an end terminal

Each model consisted of several components, which are described in detail in the following sections:

- 1) 50-ft (15.2-m) long end terminal system with 8 posts spaced at 6 ft – 3 in. (1.9-m), as shown in Figure 6, consisting of
 - a. 2 BCT posts and an anchorage system consistent with the MGS downstream anchorage;
 - b. 6 CRT posts with blockouts embedded 40 in. (1,020 mm);
 - c. 16-ft 10½-in. (5.1-m) long W-beam guardrail end section;
 - d. 13-ft 6½-in. (4.1-m) W-beam guardrail sections
 - e. W-beam guardrail splices located every 12 ft – 6 in. (3.8 m) at the midspans between post nos. 3 and 4, 5 and 6, and 7 and 8;
 - f. Impact head; and
 - g. Impact head support bracket attached to post no. 1;
- 2) 19 W6x9 steel posts with blockouts spaced at 6 ft – 3 in. (1.9-m) embedded 40 in. (1,020 mm) for MGS, and 43¼ in. (1,100 mm) for G4(1S);
- 3) 2 BCT posts with the MGS downstream anchorage spaced at 6 ft – 3 in. (1.9-m);
- 4) 13-ft 6½-in. (4.1-m) W-beam guardrail sections; and
- 5) W-beam guardrail splices located every 12 ft – 6 in. (3.8 m) at the midspans between posts.

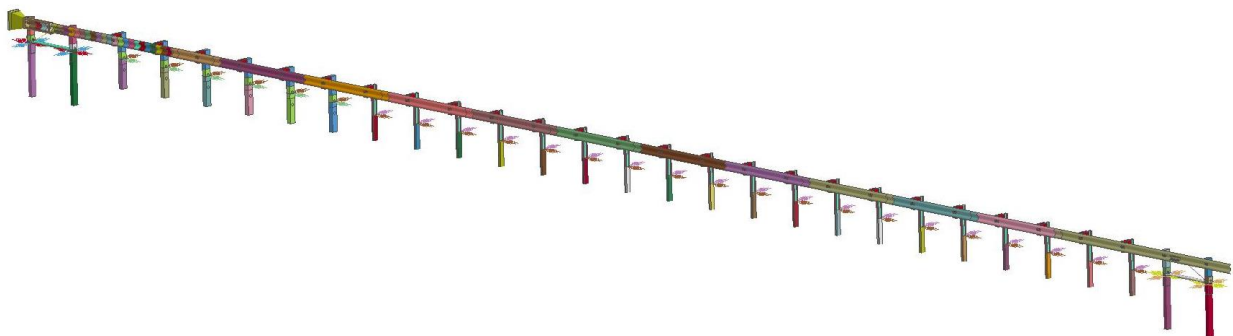


Figure 4. 175-ft (53.3-m) Long Guardrail Model

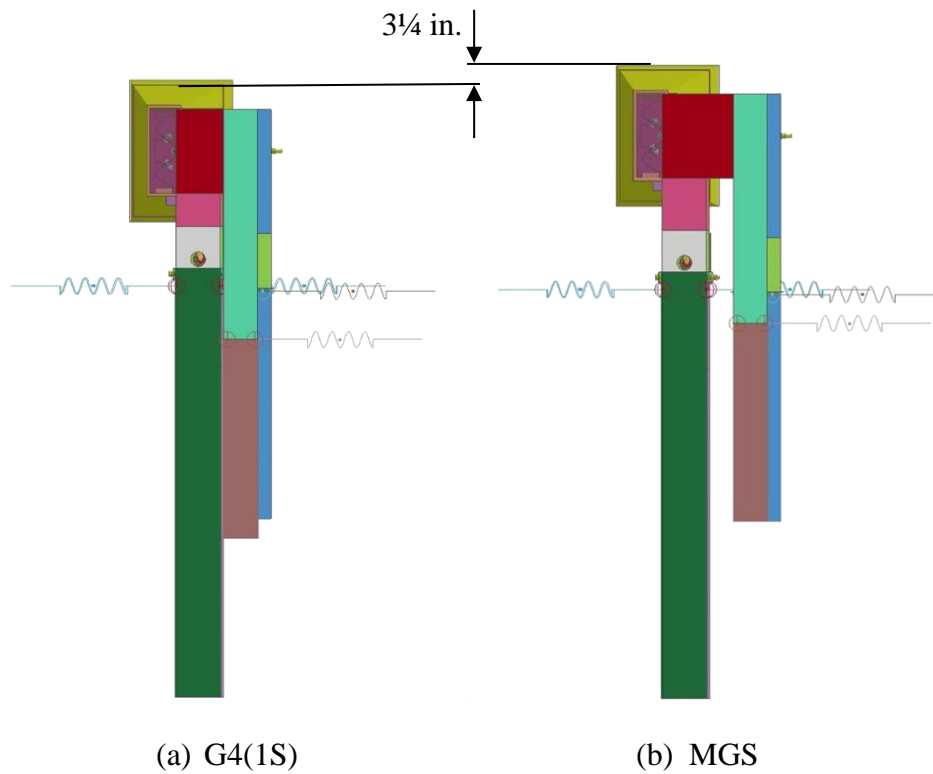


Figure 5. Cross Sections Through End Terminal and Guardrail Model (a) Modified G4(1S) and (b) MGS



Figure 6. 50-ft (15.2-m) Long End Terminal System

5.1.1 End Terminal System

The 50-ft (15.2-m) long end terminal system included component models of the impact head, W-beam guardrail, anchorage, and CRT post assemblies. The details of each component are described in the following sections.

5.1.1.1 Impact Head

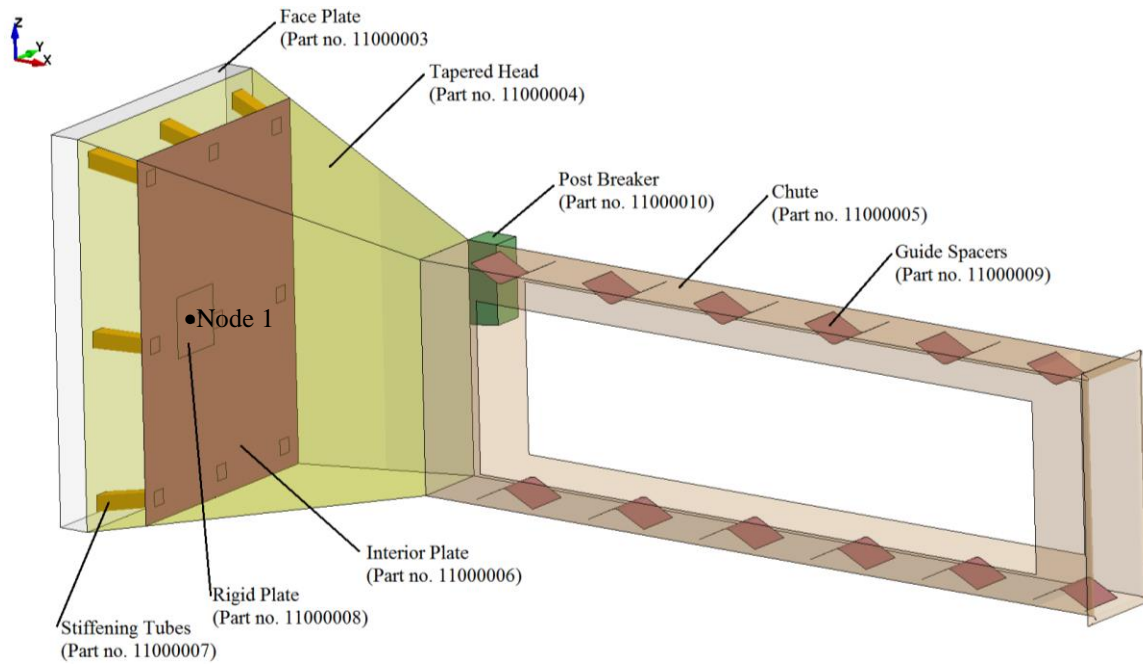
The parts and details of the impact head are shown in Figure 7 and Table 7. The impact head consisted of a $\frac{3}{16}$ -in. (4.8-mm) thick shell-element face plate, tapered head, and chute. The downstream end of the chute had a 180-degree, $\frac{1}{2}$ -in. (12.7-mm) diameter rounded corner to prevent contact problems from occurring when the chute impacted posts and blockouts. The chute's interior had several rounded $\frac{1}{8}$ -in. (3.175-mm) thick shell-element guide spacers merged to the chute to keep the W-beam rail centered vertically in the chute. A 2-in. (50.8-mm) long x 2-in. (50.8-mm) wide x 4.9-in. (124.2-mm) tall solid-element post breaker was attached to the chute upstream of post no. 1. All component interfaces were connected using merged nodes. All parts were modeled with a deformable steel material, with the exception of the chute, which was modeled with a rigid steel material. Using average dimensions of the end terminal systems combined with the internal structure added to the head, the weight of the generic impact head was 243 lb (110 kg).

Table 7. Impact Head Model Parts

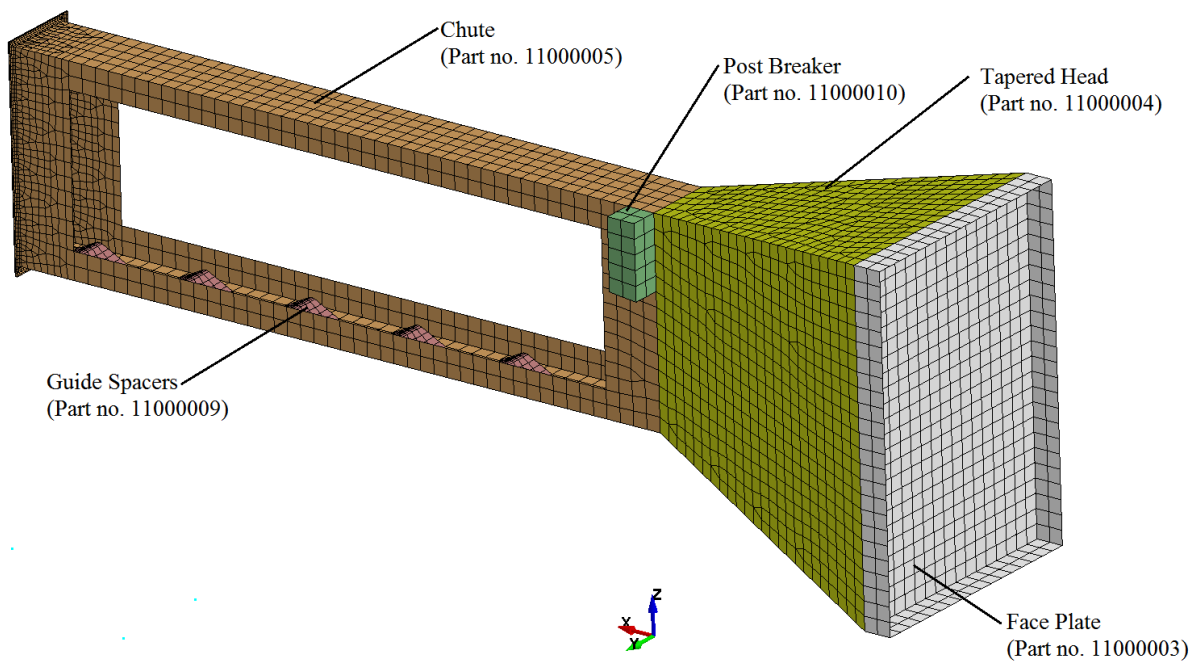
Part Description	Part Number	Material Type	Element Type	Element Thickness in. (mm)
Face Plate	11000003	24 - Piecewise Linear Plasticity	Shell – 8	3/16 (4.7625)
Tapered Head	11000004	24 - Piecewise Linear Plasticity	Shell – 8	3/16 (4.7625)
Chute	11000005	20 - Rigid	Shell – 8	3/16 (4.7625)
Interior Plate	11000006	24 - Piecewise Linear Plasticity	Shell – 8	1/2 (12.7)
Stiffening Tubes	11000007	24 - Piecewise Linear Plasticity	Shell – 8	3/16 (4.7625)
Rigid Plate	11000008	20 - Rigid	Shell – 8	0.008 (0.2)
Guide Spacers	11000009	24 - Piecewise Linear Plasticity	Shell – 8	1/8 (3.175)
Post Breaker	11000010	24 - Piecewise Linear Plasticity	Solid – 1	NA

NA = not applicable

The energy absorbing mechanism was not modeled for the generic end terminal system due to the variability between systems. Since the internal structure of the impact head did not include the energy-absorbing mechanism, nine approximately 1-in. (25-mm) square, $\frac{3}{16}$ -in. (4.8-mm) thick shell-element steel tubes connected the face plate and to a $\frac{1}{2}$ -in. (12.7-mm) thick shell-element internal plate that spanned the height and width of the tapered impact head to add rigidity to the head. The internal plate was located at $5\frac{3}{4}$ in. (146 mm) longitudinally from the impact face plate, which was approximately where the W-beam rail exits from the side on existing impact heads. A rigid plate was merged to the internal plate, which is where the end terminal force was applied.



Frontside Isometric (parts shown transparent)



Backside Isometric

Figure 7. Impact Head Model

An average force representative of the forces produced by the energy absorbing mechanisms was utilized. As shown in Table 6, the overall range of the representative end terminal systems was 10.5 to 22.5 kips (46.7 to 100 kN). There was no determination whether higher or lower values in the force range would be more critical, so a representative force in the middle of the range was desired.

The average force was applied to the impact head at Node no. 1, as shown in Figure 7, using the keyword *LOAD_MOTION_NODE. Node no. 1 was located laterally at the centerline of the rail and attached to the rigid plate. The keyword *LOAD_MOTION_NODE specified that if the local x-translational velocity of Node no. 1 was between 0.2 and 268.4 mph (0.01 and 120 mm/ms), then a constant -11.2 kip (-50 kN) force was applied in the x-direction and a constant -1.1 kip (-5 kN) force was applied in the y-direction at Node no. 1 in the local coordinate system. The value of 11.2 kips (50 kN) was selected, because it was toward the lower end of the average force range exerted by actual end terminals in full-scale crash testing. However, the 11.2 kips (50 kN) value in the simulation only accounted for the energy-absorbing mechanism, whereas the average forces determined from full-scale crash testing accounted for the energy-absorbing mechanism in the impact head, post fracture, vehicle deformation, and other energies. Therefore, the actual average force in simulation was expected to be higher than 11.2 kips (50 kN) due to post fracture, vehicle deformation, and other energies. The -1.1 kip (-5 kN) lateral force was selected as 10 percent of the longitudinal force as the actual force level was unknown. If the model did not behavior similar to actual terminals, these force levels could be varied.

5.1.1.2 W-beam Guardrail

The W-beam rail was modeled with Type 16 (fully integrated) shell elements, and material model *MAT_PIECEWISE_LINEAR_PLASTICITY representative of AASHTO M180 steel with no failure defined. The average element size was 0.37 in. x 0.97 in. (9.3 mm x 24.7 mm) with a finer mesh of approximately 1/4 in. (6.4 mm) around bolt holes in the rail.

The first rail splice was located at the midspan between post nos. 3 and 4. The splices were located at the midspans between posts in both the MGS and modified G4(1S) models. The splice location may affect where the guardrail buckles during full-scale crash testing. However, due to the modeling methodology to simulate the energy-absorbing mechanism, the simulated guardrail was not loaded in compression like an actual installation, so the guardrail buckling location when loaded in compression in the simulations was not very accurate. The guardrail buckling location for the 15-degree angle impacts may be closer to reality since the rail buckle is primarily caused by lateral force exerted by the vehicle rather than the compression load imparted to the rail from the impact head.

*DEFINE_CONSTRUCTION_STAGES, *DEFINE_STAGED_CONSTRUCTION_PART, and *CONTROL_STAGED_CONSTRUCTION were used to sequentially delete the W-beam segments as a function of time for visualization. The timing of part deletion was determined for each individual simulation. When the W-beam part was deleted, the mass was also deleted, which would normally extend to the side of the end terminal head after exiting the energy-absorbing mechanism. In most simulations, the deletion of parts did not significantly alter the system or vehicle performance, so it only contributed to the visualization.

5.1.1.3 Anchorage

The end terminal anchorage was adapted from the MGS downstream anchorage design [16] and consisted of two BCT posts in soil tubes, a groundline strut spanning post nos. 1 and 2, a cable anchor bracket attached to the backside of the W-beam rail, a cable anchor spanning from the cable anchor bracket through the groundline hole in post no. 1, and an anchor bearing plate, as shown in Figure 8. Multiple parts make up each of these systems, including bolt connections between parts.

The wood material model used for the BCT posts was developed previously using material model *MAT_ISOTROPIC_ELASTIC_FAILURE [16]. The region near the groundline of BCT post nos. 1 and 2 had a plastic failure strain defined, while the other BCT post regions had no failure defined. The BCT posts were constructed of type 3 (fully integrated quadratic 8-node element with nodal rotations) solid elements in the fracturable area.

Most end terminals do not include a standard post-to-rail bolt at post no. 1. Rather, no bolt is present to allow the post to release easily, and a bracket is attached to the side of post no. 1, which supports the impact head. This configuration was replicated in the simulation with an approximately 2-in. x 2-in. x 2-in. (50.8-mm x 50.8-mm x 50.4-mm) solid element support tied to the front face of post no. 1.

A cable anchor bracket attached the backside of the W-beam guardrail with the anchorage cable. The cable anchor bracket disengages when hit in an end-on impact in energy-absorbing end terminal systems. However, the cable anchor brackets utilized in actual end terminals were not utilized, because many of the brackets are proprietary. Therefore, the downstream anchorage cable anchor bracket was modelled. However, the anchor bracket is not intended to disengage when impacted. Thus, disengagement was simulated by deleting the part at the appropriate time using the construction stages that were utilized to delete the W-beam guardrail. The trajectory of the impact head was monitored in the simulations to determine if the impacts could cause the cable release bracket to fail to disengage.

5.1.1.4 CRT Post Assembly

The CRT post assembly was initially developed by Weiland, et al. [37]. The post assembly consists of several parts, as shown in Figure 9:

- 1) CRT post with a failure region near groundline and non-failure regions elsewhere
- 2) Soil tube with soil springs
- 3) Blockout
- 4) Post-to-guardrail bolt assembly, as shown in Figure 10
- 5) Guardrail bolt slot with refined mesh

The wood material model used for the CRT posts was developed previously using an elasto-plastic material (*MAT_PIECEWISE_LINEAR_PLASTICITY) with a failure criterion based on a maximum plastic strain [37]. The material model was representative of Southern Yellow Pine, which is the material used in the manufacturing of CRT posts. The parameters used in the wood material model are shown in Table 8. The region near the groundline of the CRT

posts had a plastic failure strain defined, while the other CRT post regions did not. The CRT posts were constructed using solid elements with a fully integrated, selectively reduced element formulation. The soil tubes and soil springs were defined to represent typical soil stiffness used during full-scale crash testing. Bogie vehicle impacts into CRT posts in the strong and weak axes were compared to simulations with the same set-up. Based on the correlation with the physical bogie tests, degrees of deflection, and modes of failure, the wood material model used for the CRT posts was considered validated.

The blockouts were fully integrated, selectively reduced element formulation with an elastic material. It is difficult to predict breakout fracture and disengagement from the posts, and often the blockouts do not disengage from the posts. Therefore, the blockouts were not defined with a material with failure.

Table 8. CRT Post Properties

Density kg/mm ³	Young's Modulus GPa	Poisson's Ratio	Yield Strength GPa	Tangent Modulus GPa	Plastic Failure Strain
6.274 E-07	11.0	0.30	6.0 E-03	250.0 E-03	120.0 E-03

The preload in the post to guardrail bolts was determined through field testing to an average of 6.7 kips (30 kN) [37]. The *INITIAL_STRESS_SECTION card was utilized to apply a 23.2 ksi (160 MPa) initial stress at a cross-section near the center of each bolt to obtain a preload of 6.7 kips (30 kN). The CRT post assembly was calibrated to accurately model bolt pullout and general post behavior. Further details of the post model can be found in Weiland, et al. [37].

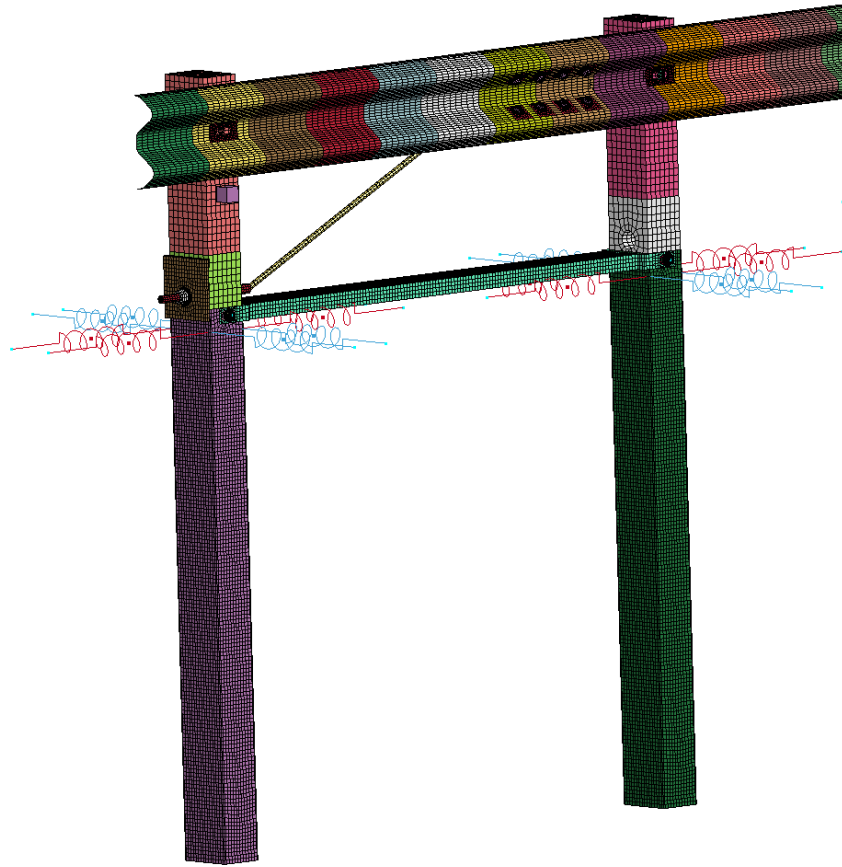
Typically in impacts on the end of guardrail end terminals, the W-beam rail tears at the slots as the post bolts release. The mesh around the guardrail slot was refined to enhance bolt release. However, no failure is defined in the W-beam guardrail material model, so tearing cannot occur. Without failure in the material, significant rail deformations occurred when the post bolt heads did not release easily and snagged on the W-beam elements, as shown in Figure 11a before release and Figure 11b after release at post no. 3. This led to instabilities in the simulations, especially in impacts with the 2270P model where large W-beam deformations occurred. The mesh around the guardrail slots was refined and other contact definitions were explored, but significant rail deformations and simulation instabilities still occurred.

To account for the lack of guardrail material failure, parameters on the *CONTROL_SHELL card were activated to delete excessively distorted elements:

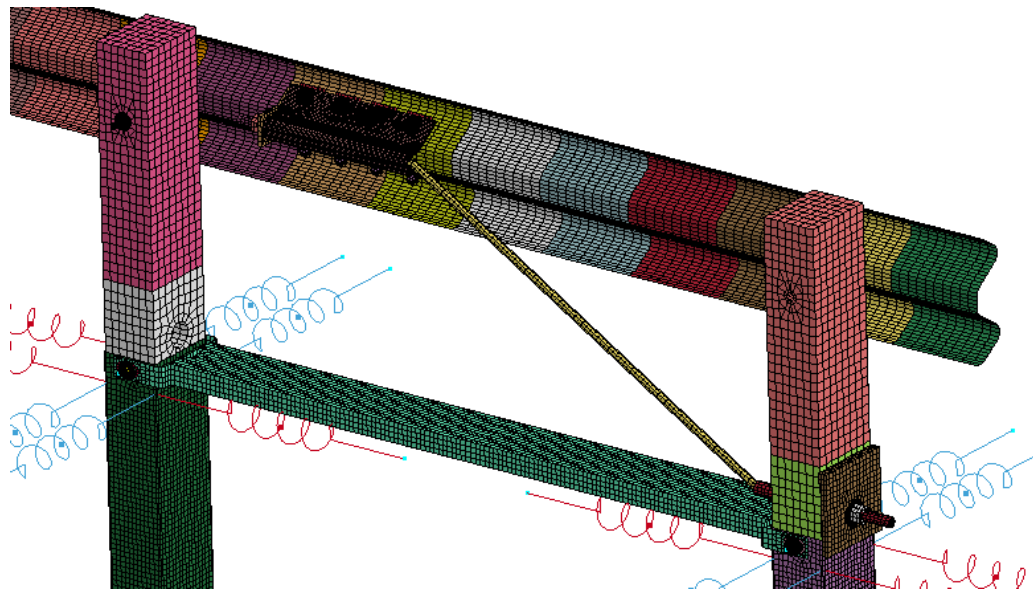
stretch = 1 (stretch ratio of element diagonals for element deletion)

nfail1 = 1 (delete element if highly distorted under-integrated shell elements)

delfr = 1 (delete shell elements whose neighboring shell elements have failed)



Frontside Isometric



Backside Isometric

Figure 8. End Terminal Anchorage Model

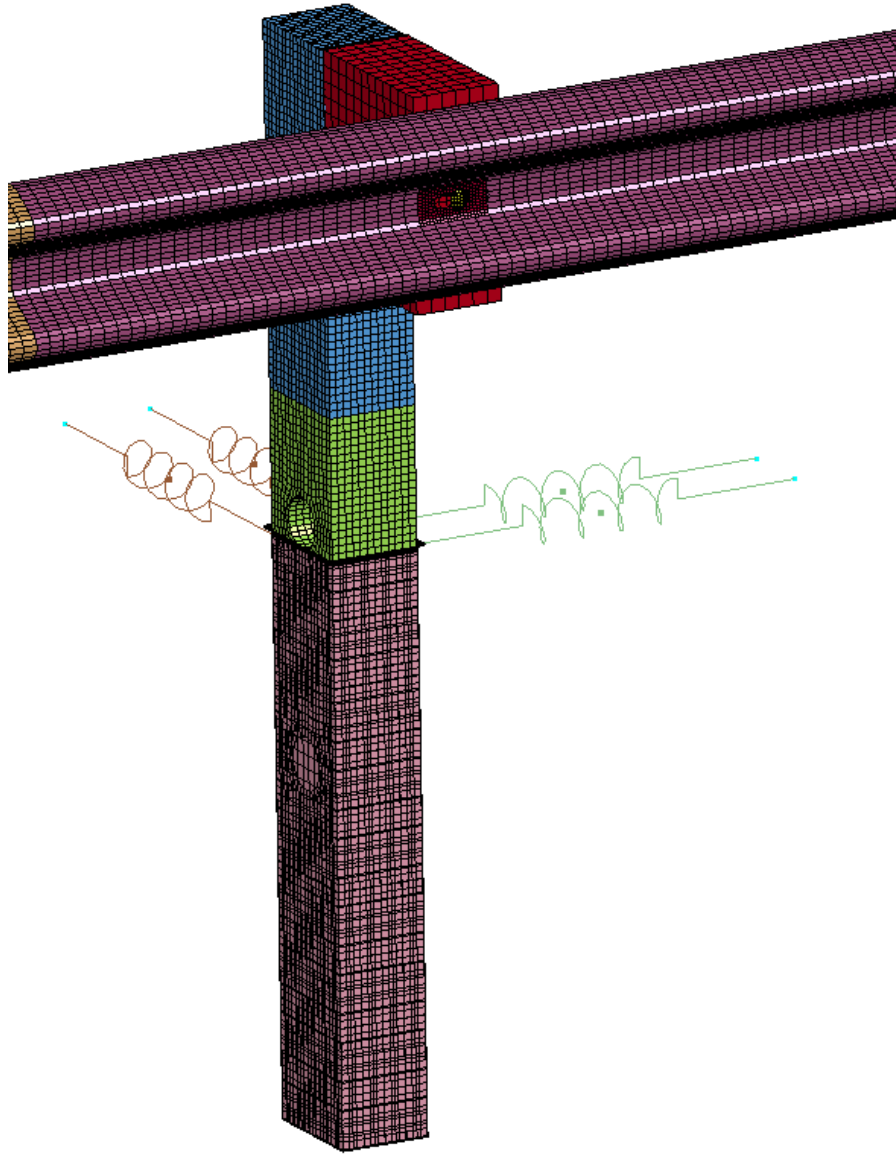


Figure 9. CRT Post Assembly Model

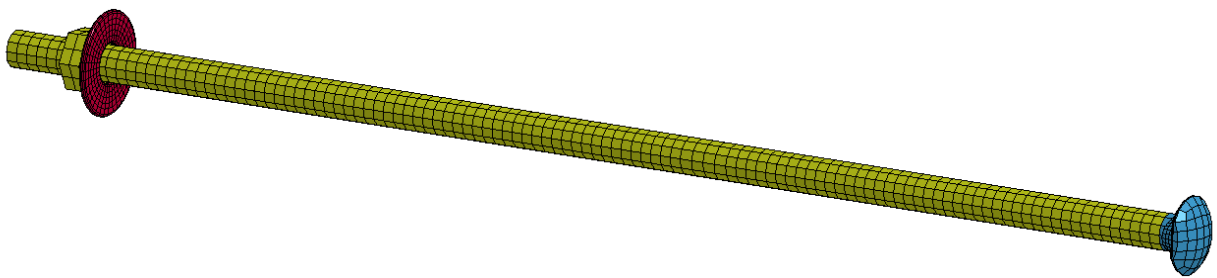
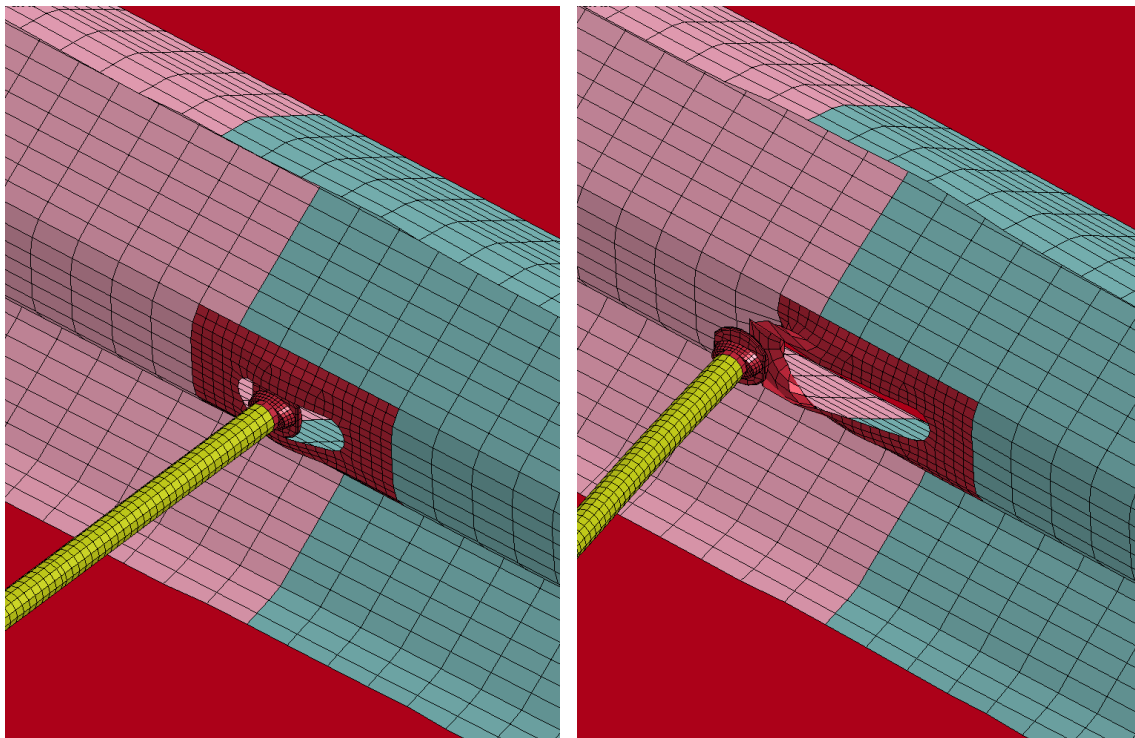


Figure 10. Post-to-Guardrail Bolt Model

When element deletion is active, LS-PrePost allows two different modes to view the element deletion patterns: on the deformed part shape and on the undeformed part shape. On the deformed part shape, it can be difficult to see which elements are deleted. However, on the undeformed part shape, it is much easier to discern which elements were deleted. The guardrail deformation at post no. 3 with element deletion active is shown in Figure 12a. When significant deformation occurred, some elements were deleted, which prevented significant snagging and simulation instability. The undeformed guardrail state with deleted elements and the deformed guardrail state with deleted elements at post no. 3 are shown in Figure 12b. However, the number and location of deleted elements at each post differed as the deformation varied. An example of the undeformed guardrail state with deleted elements at post no. 7 is shown in Figure 12c. The distorted element deletion modeling technique was not predictive of where actual tearing occurred in the guardrail but was used to overcome the lack of guardrail material failure.



(a) Before bolt release (post no. 3)

(b) After bolt release (post no. 3)

Figure 11. Bolt Head Snagging and Deformation Around Guardrail Slot

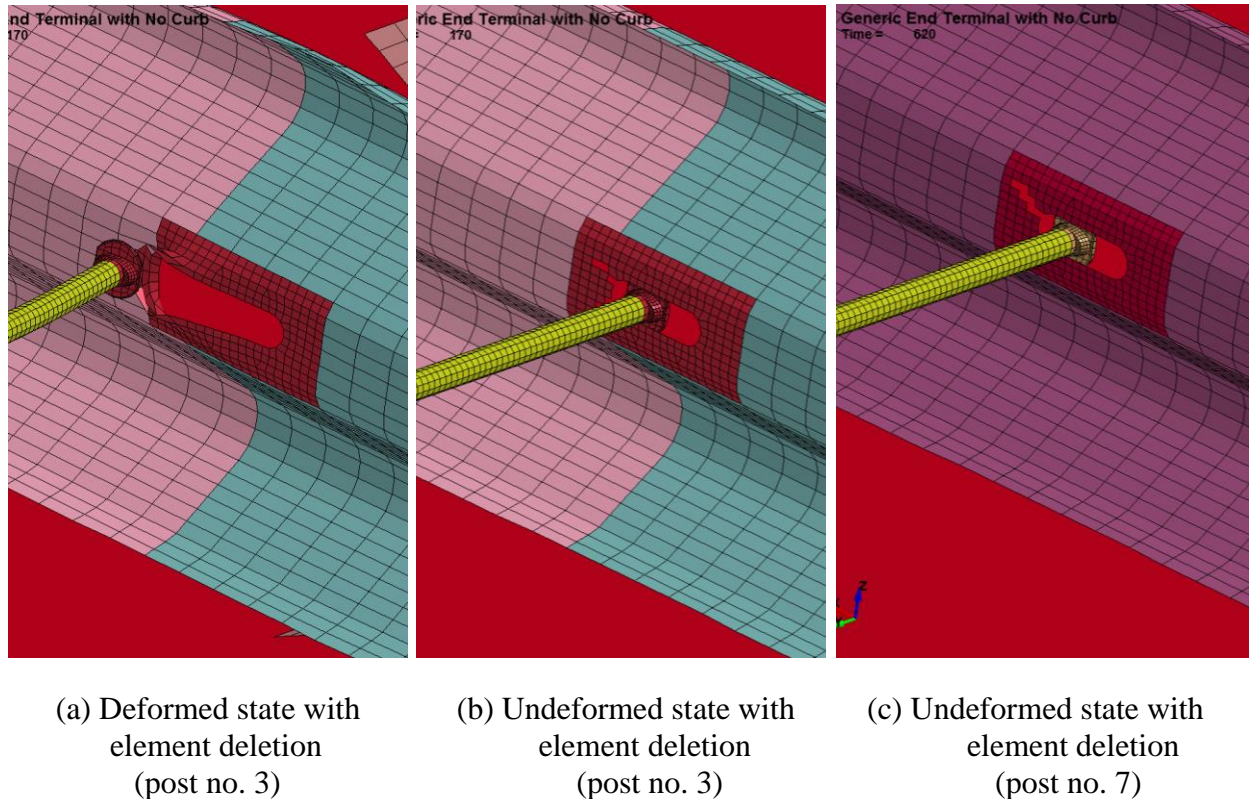


Figure 12. Bolt Head Deformation with Distorted Element Deletion

5.1.2 Strong Post Guardrail Model

A 175-ft (53.3-m) MGS model was previously validated against NCHRP Report 350 test no. 3-10 and MASH 2009 test no. 3-11 impacts on the length-of-need [38]. This model was modified with the end terminal system previously described. During impact events on the end of the end terminal, the vehicles should not travel much beyond the 50-ft (15.2-m) long end terminal system. Therefore, the rest of the guardrail system was not modified from the standard MGS model, apart from changing from 12 in. to 8 in. (305 mm to 203 mm) deep blockouts and a 31-in. to 27¾-in. (787-mm to 705-mm) rail height for the modified G4(1S) configuration.

5.2 Vehicle Models

Four vehicle models were used to evaluate the end terminal. The NCHRP Report 350 820C vehicle was the Geo Metro small car, and the 2000P vehicle was the Chevrolet c2500 pickup truck. The MASH 2009 1100C vehicle was the Toyota Yaris small car, and the 2270P vehicle was the Chevrolet Silverado pickup truck.

5.2.1 Geo Metro (820C)

A Geo Metro vehicle model, shown in Figure 13, was originally created by National Crash Analysis Center (NCAC) and then improved upon and obtained from Politecnico di Milano, Italy. This model was later modified by MwRSF personnel for use in roadside safety

applications. A Roadside Safety Verification and Validation Program (RSVVP) analysis was conducted with the 1,984-lb (900-kg) Geo Metro model impacting the MGS model according to NCHRP Report 350 test no. 3-10 [38].

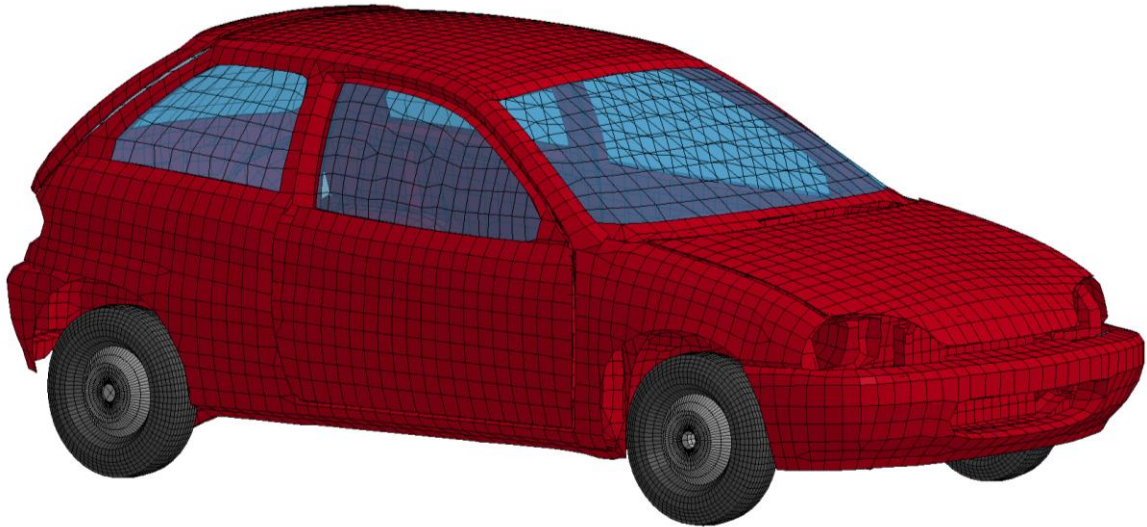


Figure 13. Geo Metro Model

5.2.2 Chevrolet c2500 (2000P)

A Chevrolet c2500 vehicle model, shown in Figure 14, was originally developed by NCAC and later modified by MwRSF personnel for use in roadside safety applications. The c2500 vehicle models weighs 4,572 lb (2,074 kg).

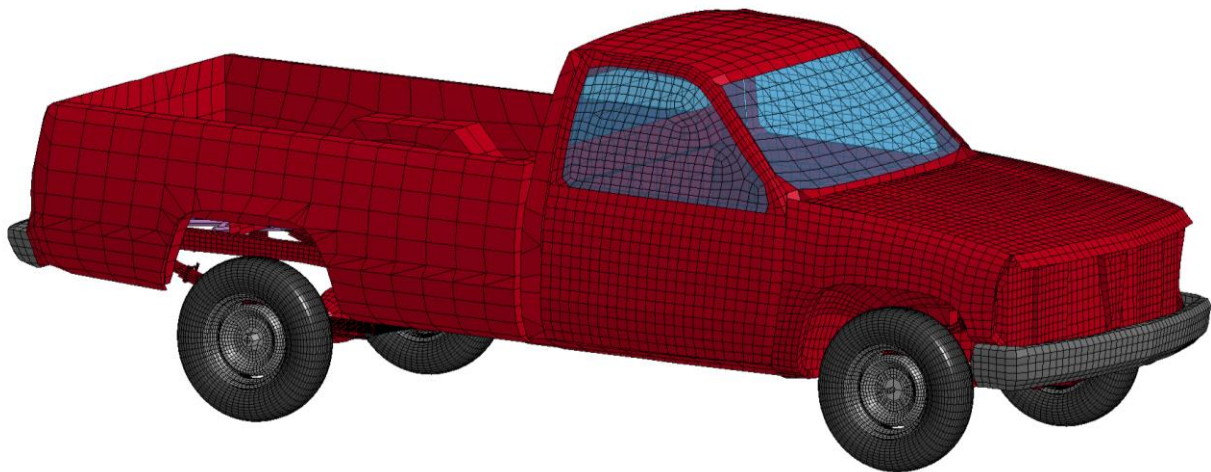


Figure 14. Chevrolet c2500 Model

5.2.3 Toyota Yaris (1100C)

A Toyota Yaris model, shown in Figure 15, was originally created by NCAC and later modified by MwRSF personnel for use in roadside safety applications. The 2,776-lb (1,259-kg) Toyota Yaris model was validated by NCAC with several frontal impact events [39], and the MGS model has been validated with other vehicle models. The Toyota Yaris vehicle model had a test inertial mass of 2,425 lb (1,100 kg) and an additional mass of 351 lb (159 kg), which included the mass of two front-seated occupants, for a total mass of 2,776 lb (1,259 kg). A RSVVP analysis was conducted with the Toyota Yaris model impacting the MGS model according to MASH 2009 test no. 3-10 [40].



Figure 15. Toyota Yaris Model

5.2.4 Chevrolet Silverado (2270P)

A Chevrolet Silverado vehicle model, shown in Figure 16, was originally developed by NCAC and later modified by MwRSF personnel for use in roadside safety applications. This particular vehicle is a reduced version 3 Silverado model, which weighs 5,000 lb (2,270 kg) [41]. Tire deflation and disengagement were not enabled in the simulations. A RSVVP analysis was conducted with the Chevrolet Silverado model impacting the MGS model according to MASH 2009 test no. 3-11 [40].

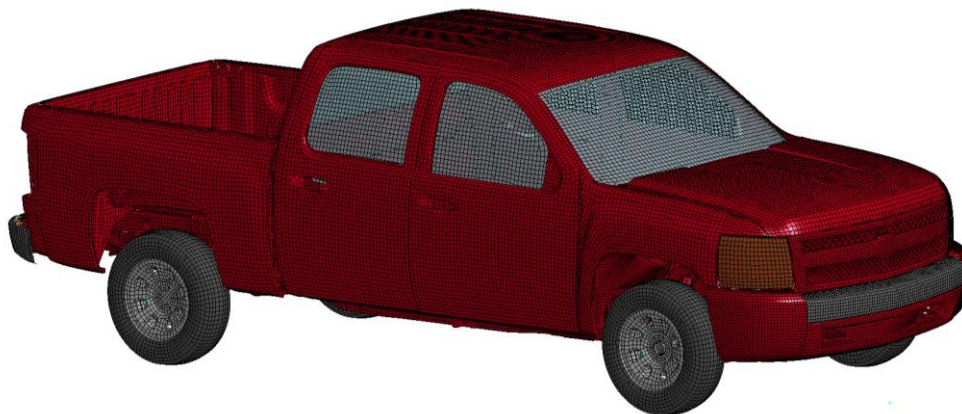


Figure 16. Chevrolet Silverado Reduced V3 Model

6 SIMULATIONS ON LEVEL TERRAIN

Eight different test numbers from NCHRP Report 350 and MASH 2009 were simulated on the generic end terminal installed on MGS and modified G4(1S), as follows:

- 1) NCHRP Report 350 test no. 3-30 - 820C small car (Geo) impacting end at 0 deg at quarter point offset
- 2) NCHRP Report 350 test no. 3-31 - 2000P pickup truck (C2500) impacting end at 0 deg
- 3) NCHRP Report 350 test no. 3-32 - 820C small car (Geo) impacting end at 15 deg
- 4) NCHRP Report 350 test no. 3-33 - 2000P pickup truck (C2500) impacting end at 15 deg
- 5) MASH 2009 test no. 3-30 - 1100C small car (Yaris) impacting end at 0 deg at quarter point offset
- 6) MASH 2009 test no. 3-31 - 2270P pickup truck (Silverado) impacting end at 0 deg
- 7) MASH 2009 test no. 3-32 - 1100C small car (Yaris) impacting end at 5/15 deg
- 8) MASH 2009 test no. 3-33 - 2270P pickup truck (Silverado) impacting end at 5/15 deg

Full-scale crash testing did not exist for all of these impact conditions, so all simulations could not be compared to existing systems in all cases. However, the simulations were conducted to provide additional results for comparison.

Specific simulation results that were evaluated included occupant risk measures, vehicle stability, guardrail feed length, average end terminal forces, rail buckle location, and vehicle and system damage. The occupant risk measures included longitudinal and lateral occupant impact velocities (OIV) and occupant ridedown accelerations (ORA) that were calculated using acceleration data with a minimum 10,000 Hz frequency from the local c.g. node of the vehicle and then processed as defined in MASH 2009.

The average end terminal force was calculated based on the procedure established by Coon to provide an equivalent comparison to the full-scale crash tests [20-21]. Using conservation of momentum and assuming the initial impact is perfectly plastic, the combined velocity, V_c , of the terminal head and vehicle can be calculated just after the initial impact from Equation 6.1. The kinetic energy, KE_c , can be calculated at that initial combined state from Equation 6.2. The kinetic energy, KE_d , when the vehicle departs from the rail or when the impact head stops extruding guardrail can be calculated from Equation 6.3. Applying conservation of energy, kinetic energy at the initial combined state, KE_c , can also be calculated with Equation 6.4. The average force can be found by rearranging these equations, as shown in Equation 6.5.

$$V_c = \frac{V_i M_v + V_h M_h}{M_v + M_h} = \frac{V_i M_v}{M_v + M_h} \quad (6.1)$$

where

V_i = initial velocity of vehicle

M_v = mass of vehicle

V_h = velocity of end terminal head initially = 0

M_h = mass of impact head = 110 kg (243 lb)

$$KE_c = 0.5(M_v + M_h)V_c^2 \quad (6.2)$$

$$KE_d = 0.5(M_v + M_h)V_d^2 \quad (6.3)$$

where

V_d is the velocity of the vehicle as it departs from the rail or when the impact head stops extruding guardrail

$$KE_c = KE_d + E_{rail} \quad (6.4)$$

where

E_{rail} = energy dissipated by rail = $F_{ave}d$

F_{ave} = average force required to displace the head along the rail

d = distance the head is displaced or feed length

$$F_{ave} = \frac{KE_c - KE_d}{d} \quad (6.5)$$

The procedure to determine average end terminal force is only valid when the velocity of the vehicle and the impact head are the same throughout the impact event. This only occurs in the simulations of NCHRP Report 350 and MASH 2009 test no. 3-31.

6.1.1 NCHRP Report 350 Test No. 3-30

NCHRP Report 350 test no. 3-30 involves an 820C small car impacting at 62 mph (99.8 km/h) and at 0 degrees with the centerline of the system aligned with the quarter point offset of the vehicle's bumper. Many end terminal systems have been tested at the shallow quarter point offset, as shown in Figure 17. Since the performance of the deep quarter point offset, shown in Figure 18, is largely unknown, impacts with both quarter point offsets were simulated.

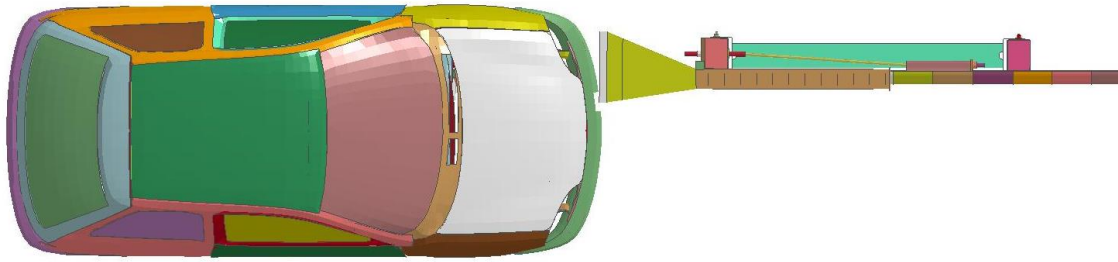


Figure 17. NCHRP Report 350 Test No. 3-30, Shallow Quarter-Point Offset Impact

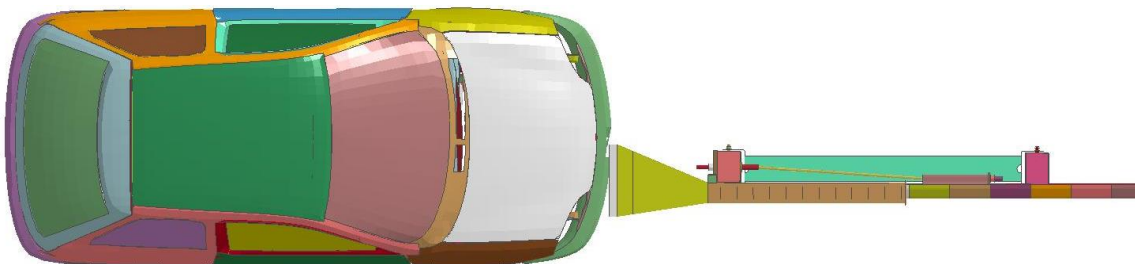


Figure 18. NCHRP Report 350 Test No. 3-30, Deep Quarter-Point Offset Impact

6.1.1.1 Shallow Quarter-Point Offset

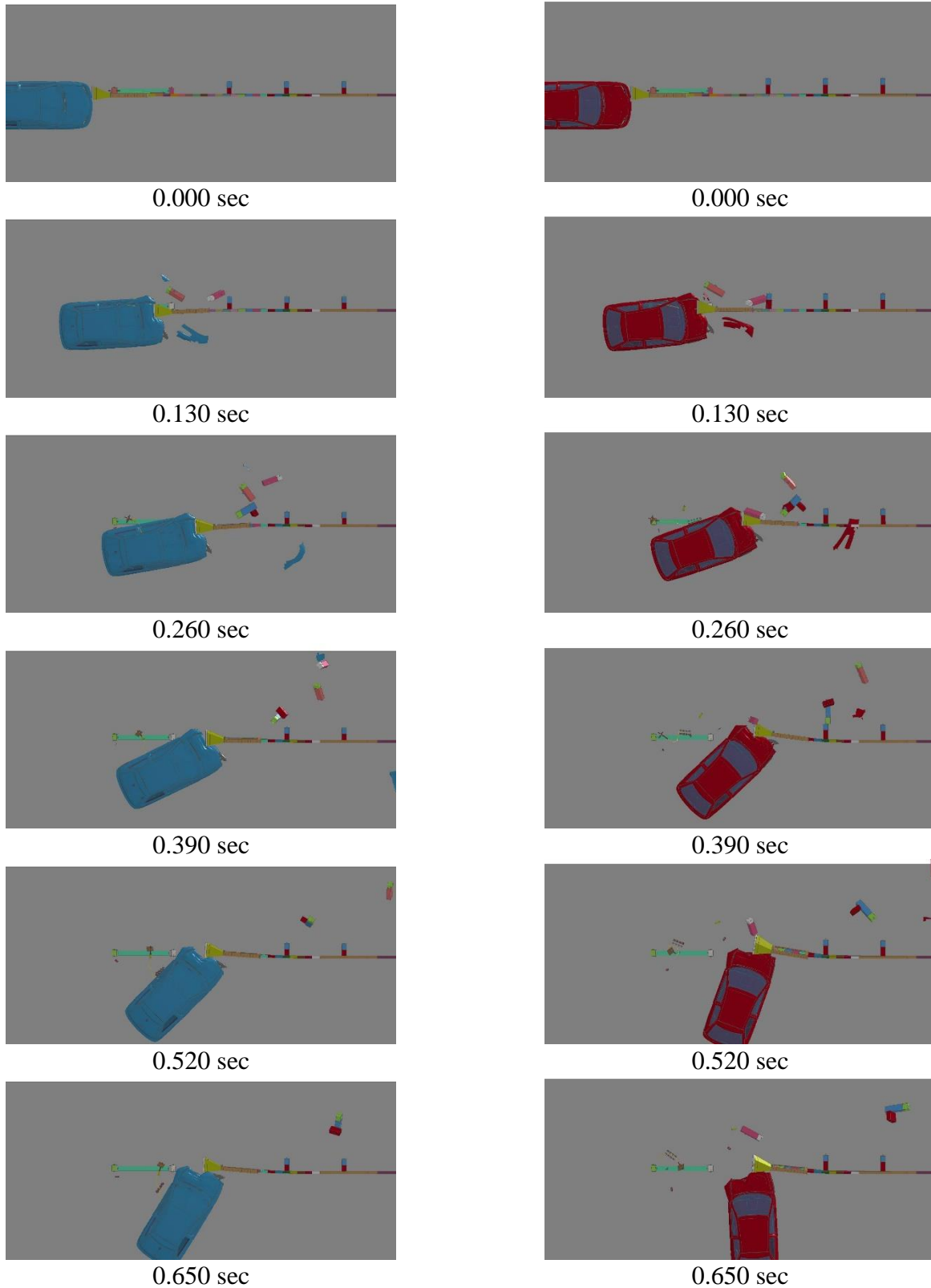
In simulation nos. NCHRP-30-shallow-G41S and NCHRP-30-shallow-MGS, the 820C small car impacted the end terminals installed on modified G4(1S) and MGS, respectively, at the shallow-quarter point offset. Sequential photographs are shown in Figure 19 (overhead view) and Figure 20 (downstream view). The longitudinal and lateral ORAs and OIVs are shown in Table 9. The distance the impact head translated, or the feed length, and the buckle location are also shown in Table 9.

The 820C model impacted the impact head installed on modified G4(1S). The impact head translated downstream along 12.5 ft (3.8 m) of guardrail, impacting the BCT posts and one of the CRT posts. The first three posts fractured near the groundline. The car yawed toward the traffic side of the system, and the impact head stopped translating downstream 360 ms after impact. The guardrail did not buckle, but the simulation model rail buckling should be used cautiously as the rail does not have typical compressive loads as a result of not modeling the energy-absorbing mechanism in the impact head. The longitudinal OIV was -36.1 ft/s (-11.0 m/s), which is close to the 39.4 ft/s (12 m/s) limit specified in NCHRP Report 350. No significant occupant compartment deformation occurred.

The 820C model impacted the impact head installed on MGS. The impact head translated downstream along 13.3 ft (4.1 m) of guardrail, impacting the BCT posts and one of the CRT posts. The first three posts fractured near groundline. The car yawed toward the traffic side of the system, and the impact head stopped translating downstream 360 ms after impact. The guardrail began to buckle at post no. 4, but the model rail buckling should be used cautiously as the rail does not have typical compressive loads as a result of not modeling the energy-absorbing mechanism in the impact head. The longitudinal ORA was -22.5 g's, which is over the NCHRP Report 350 limit of 20 g's. The high acceleration occurred when a post-to-rail bolt snagged as it tried to release. As discussed previously, rail release when impacted end-on was not calibrated due to not modeling steel material failure, including tearing. No significant occupant compartment deformation occurred.

Table 9. NCHRP Report 350 Test No. 3-30, Shallow Quarter-Point Offset

Simulation No.	NCHRP-30-shallow-G41S	NCHRP-30-shallow-MGS
Test Number	NCHRP 350 3-30 (Shallow)	NCHRP 350 3-30 (Shallow)
System	G41S	MGS
Longitudinal OIV, ft/s (m/s)	-36.1 (-11.0)	-31.2 (-9.5)
Lateral OIV, ft/s (m/s)	-3.9 (-1.2)	2.0 (-0.3)
Longitudinal ORA, g's	-17.1	-22.5
Lateral ORA, g's	5.7	7.6
Maximum Roll Angle, deg	4.0	-1.2
Maximum Pitch Angle, deg	2.2	1.8
Maximum Yaw Angle, deg	58.3	93
Guardrail Feed Length, ft (m)	12.5 (3.8)	13.3 (4.1)
Buckle Location	None	Post no. 4



Simulation No. NCHRP-30-Shallow-G41S

Simulation No. NCHRP-30-Shallow-MGS

Figure 19. NCHRP Report 350 Test No. 3-30, Shallow Quarter-Point Offset, Overhead View

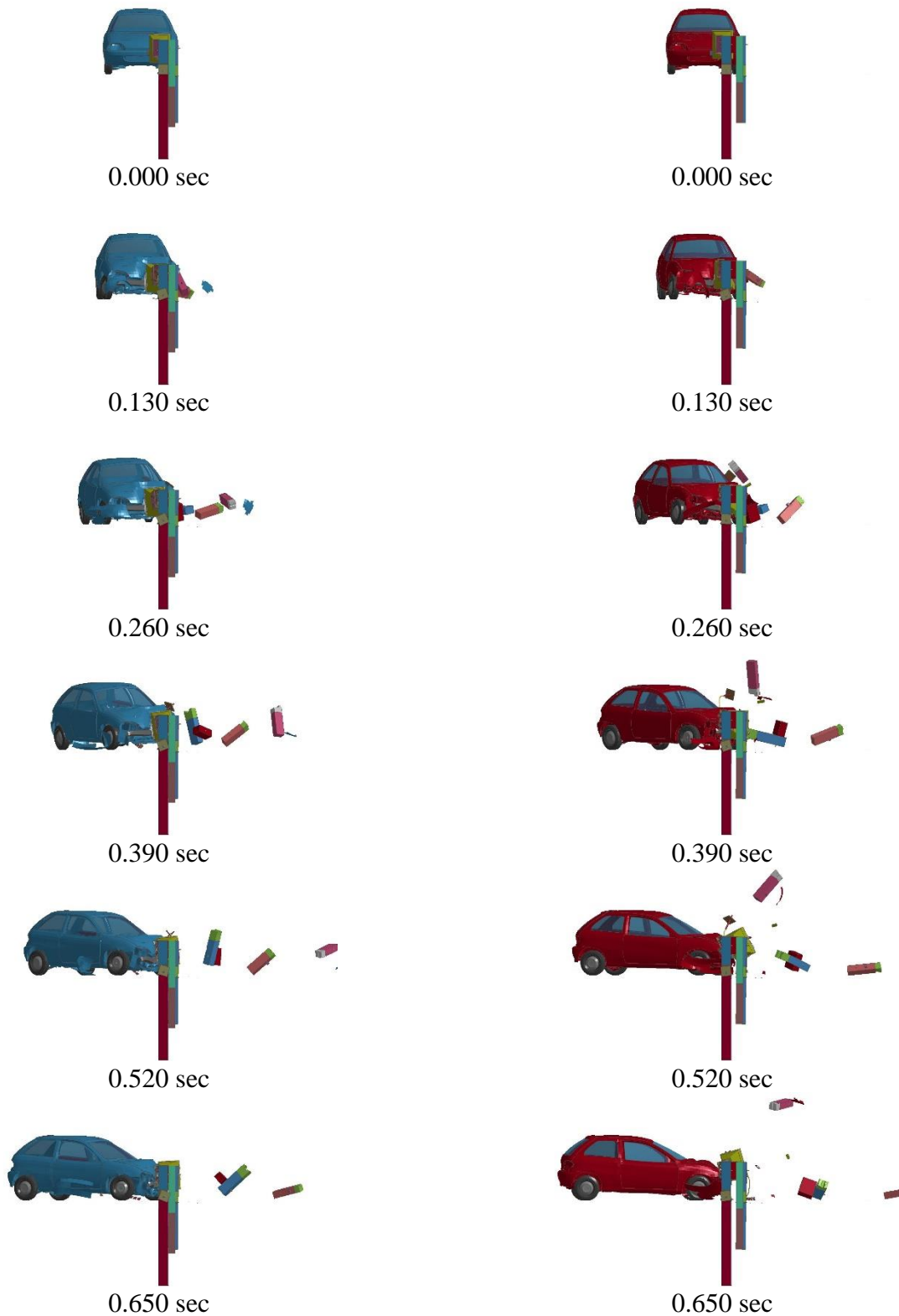


Figure 20. NCHRP Report 350 Test No. 3-30, Shallow Quarter-Point Offset, Downstream View

6.1.1.2 Deep Quarter-Point Offset

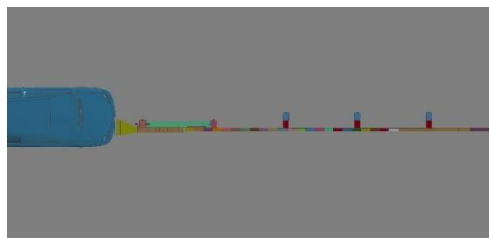
In simulation nos. NCHRP-30-deep-G41S and NCHRP-30-deep-MGS, the 820C small car impacted the end terminals installed on modified G4(1S) and MGS, respectively, at the deep quarter-point offset. Sequential photographs are shown in Figure 21 (overhead view) and Figure 22 (downstream view). The longitudinal and lateral ORAs and OIVs are shown in Table 10. The distance the impact head translated, or the feed length, and the buckle location are also shown in Table 10.

The 820C model impacted the impact head installed on modified G4(1S). The impact head translated downstream along 14.2 ft (4.3 m) of guardrail, impacting the BCT posts and one of the CRT posts. The first three posts fractured near the groundline. The car yawed toward the non-traffic side of the system, and the impact head stopped translating downstream 340 ms after impact. The guardrail buckled at post no. 5, but rail buckling should be used cautiously as the rail does not have typical compressive loads as a result of not modeling the energy-absorbing mechanism in the impact head. No significant occupant compartment deformation occurred.

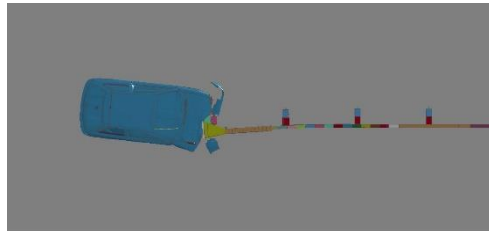
The 820C model impacted the impact head installed on MGS. The impact head translated downstream along 13.3 ft (4.1 m) of guardrail, impacting the BCT posts and one of the CRT posts. The first four posts fractured near the groundline. The car yawed toward the non-traffic side of the system, and the impact head stopped translating downstream 300 ms after impact. The guardrail buckled at post no. 5, but rail buckling should be used cautiously as the rail does not have typical compressive loads as a result of not modeling the energy-absorbing mechanism in the impact head. No significant occupant compartment deformation occurred.

Table 10. NCHRP Report 350 Test No. 3-30, Deep Quarter-Point Offset

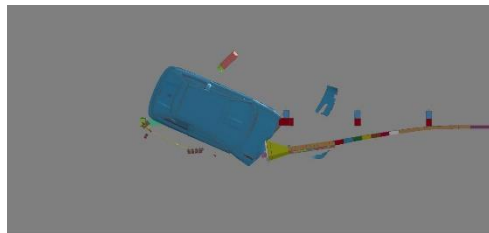
Simulation No.	NCHRP-30-deep-G41S	NCHRP-30-deep-MGS
Test Number	NCHRP 350 3-30 (Deep)	NCHRP 350 3-30 (Deep)
System	G41S	MGS
Longitudinal OIV, ft/s (m/s)	-29.9 (-9.1)	-29.9 (-9.1)
Lateral OIV, ft/s (m/s)	-2.3 (-0.7)	-3.0 (-0.9)
Longitudinal ORA, g's	-10.2	-9.8
Lateral ORA, g's	-7.3	-8.6
Maximum Roll Angle, deg	1.7	2.4
Maximum Pitch Angle, deg	2.8	2.3
Maximum Yaw Angle, deg	-133.8	-122.9
Guardrail Feed Length, ft (m)	14.2 (4.3)	13.3 (4.1)
Buckle Location	Post no. 5	Post no. 5



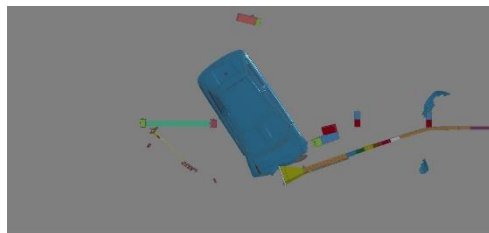
0.000 sec



0.130 sec



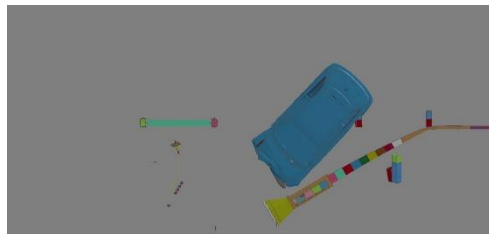
0.260 sec



0.390 sec

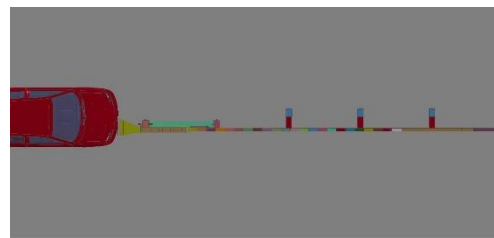


0.520 sec

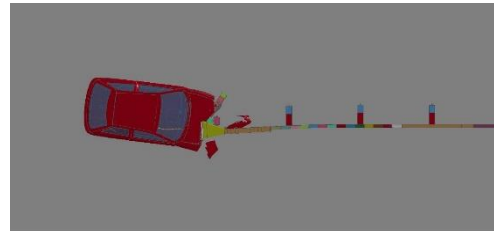


0.650 sec

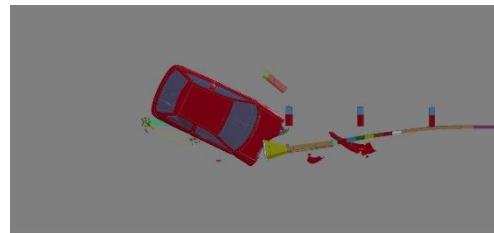
Simulation No. NCHRP-30-Deep-G41S



0.000 sec



0.130 sec



0.260 sec



0.390 sec



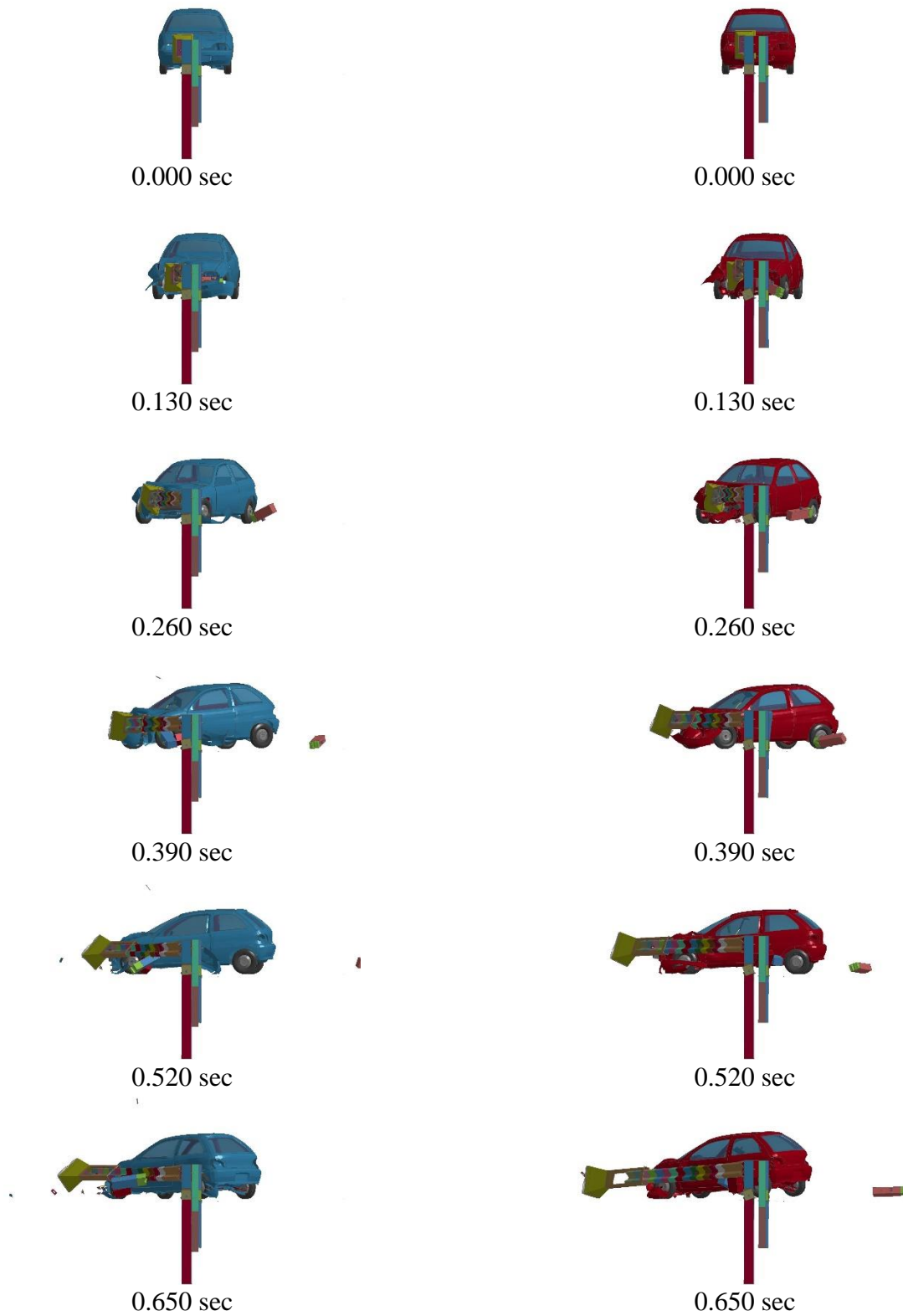
0.520 sec



0.650 sec

Simulation No. NCHRP-30-Deep-MGS

Figure 21. NCHRP Report 350 Test No. 3-30, Deep Quarter-Point Offset, Overhead View



Simulation No. NCHRP-30-Deep-G41S

Simulation No. NCHRP-30-Deep-MGS

Figure 22. NCHRP Report 350 Test No. 3-30, Deep Quarter-Point Offset, Downstream View

6.1.2 NCHRP Report 350 Test No. 3-31

NCHRP Report 350 test no. 3-31 involves a 2000P pickup truck impacting at 62 mph (99.8 km/h) and at 0 degrees with the centerline of the system aligned with the centerline of the vehicle, as shown in Figure 23. In simulation nos. NCHRP-31-G41S and NCHRP-31-MGS, the 2000P pickup truck impacted the end terminals installed on modified G4(1S) and MGS, respectively. Sequential photographs are shown in Figure 24 (overhead view) and Figure 25 (downstream view). The longitudinal and lateral ORAs and OIVs are shown in Table 11. The distance the impact head translated, or the feed length, and the buckle location are also shown in Table 11. Using conservation of momentum utilized during the development of the crash reconstruction procedure for end terminals established by Coon, the average end terminal force was calculated based on the mass of the vehicle and guardrail feed length, also shown in Table 11.

The 2000P model impacted the impact head installed on modified G4(1S). The impact head translated downstream along 34.1 ft (10.4 m) of guardrail, impacting the BCT posts and five of the CRT posts. The first seven posts fractured near the groundline. The truck yawed slightly toward the traffic side of the system, and the impact head stopped translating downstream 660 ms after impact. The post-to-rail bolt at post no. 7 snagged as it tried to release from the W-beam guardrail, which resulted in a significant longitudinal load imparted to the W-beam guardrail, a buckle at post no. 7, and the vehicle stopping. Due to this longitudinal load and buckle, the downstream BCT anchorage posts fractured and every post-to-rail bolt released from the W-beam guardrail. This phenomenon was not realistic. No significant occupant compartment deformation occurred.

The 2000P model impacted the impact head installed on MGS. The impact head translated downstream along 36.4 ft (11 m) of guardrail, impacting the BCT posts and five of the CRT posts. The first six posts fractured near the groundline. The truck yawed slightly toward the traffic side of the system, and the impact head stopped translating downstream 900 ms after impact. The guardrail did not buckle. No significant occupant compartment deformation occurred.

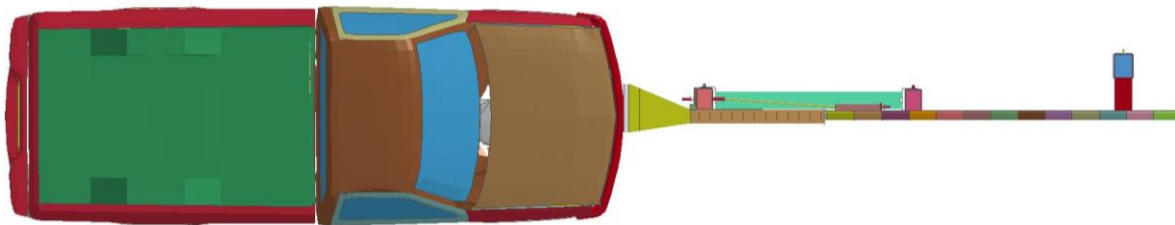


Figure 23. NCHRP Report 350, Test No. 3-31 Impact

Table 11. NCHRP Report 350 Test No. 3-31

Simulation No.	NCHRP-31-G41S	NCHRP-31 -MGS
Test Number	NCHRP 350 3-31	NCHRP 350 3-31
System	G41S	MGS
Longitudinal OIV, ft/s (m/s)	-21.0 (-6.4)	-20.0 (-6.1)
Lateral OIV, ft/s (m/s)	-1.0 (-0.3)	-1.3 (-0.4)
Longitudinal ORA, g's	-16.0	-13.9
Lateral ORA, g's	5.0	-7.3
Maximum Roll Angle, deg	-1.1	-1.3
Maximum Pitch Angle, deg	1.6	1.8
Maximum Yaw Angle, deg	16.6	13.4
Guardrail Feed Length, ft (m)	34.1 (10.4)	36.4 (11.1)
Buckle Location	None	None
Average Terminal Force, kips (kN)	16.1 (71.8)	15.3 (68.2)

6.1.3 NCHRP Report 350 Test No. 3-32

NCHRP Report 350 test no. 3-32 involves an 820C small car impacting at 62 mph (99.8 km/h) and at 15 degrees with the centerline of the system aligned with the centerline of the vehicle, as shown in Figure 26. In simulation nos. NCHRP-32-G41S and NCHRP-32-MGS, the 820C small car impacted the end terminals installed on modified G4(1S) and MGS, respectively. Sequential photographs are shown in Figure 27 (overhead view) and Figure 28 (downstream view). The longitudinal and lateral ORAs and OIVs are shown in Table 12. The distance the impact head translated, or the feed length, and the buckle location are also shown in Table 12.

The 820C model impacted the impact head installed on modified G4(1S). The impact head translated downstream along 8.7 ft (2.7 m) of guardrail, impacting the BCT posts and one of the CRT posts. The first two posts fractured near the groundline. The rail gated, which allowed the vehicle to traverse behind the system, and the impact head stopped translating downstream 185 ms after impact. The impact head remained engaged with the front of the vehicle for longer than what has occurred in full-scale crash testing, which may partially be attributed to the impact head and vehicle nodes becoming entangled. When the impact head model disengaged from the front bumper and hood, the impact head twisted and translated upward. The impact head typically releases to the side of the vehicle in full-scale crash testing, and not upward as observed in the model. The guardrail buckled at post no. 3, but rail buckling should be used cautiously as the rail does not have typical compressive loads as a result of not modeling the energy-absorbing mechanism in the impact head. No significant occupant compartment deformation occurred.

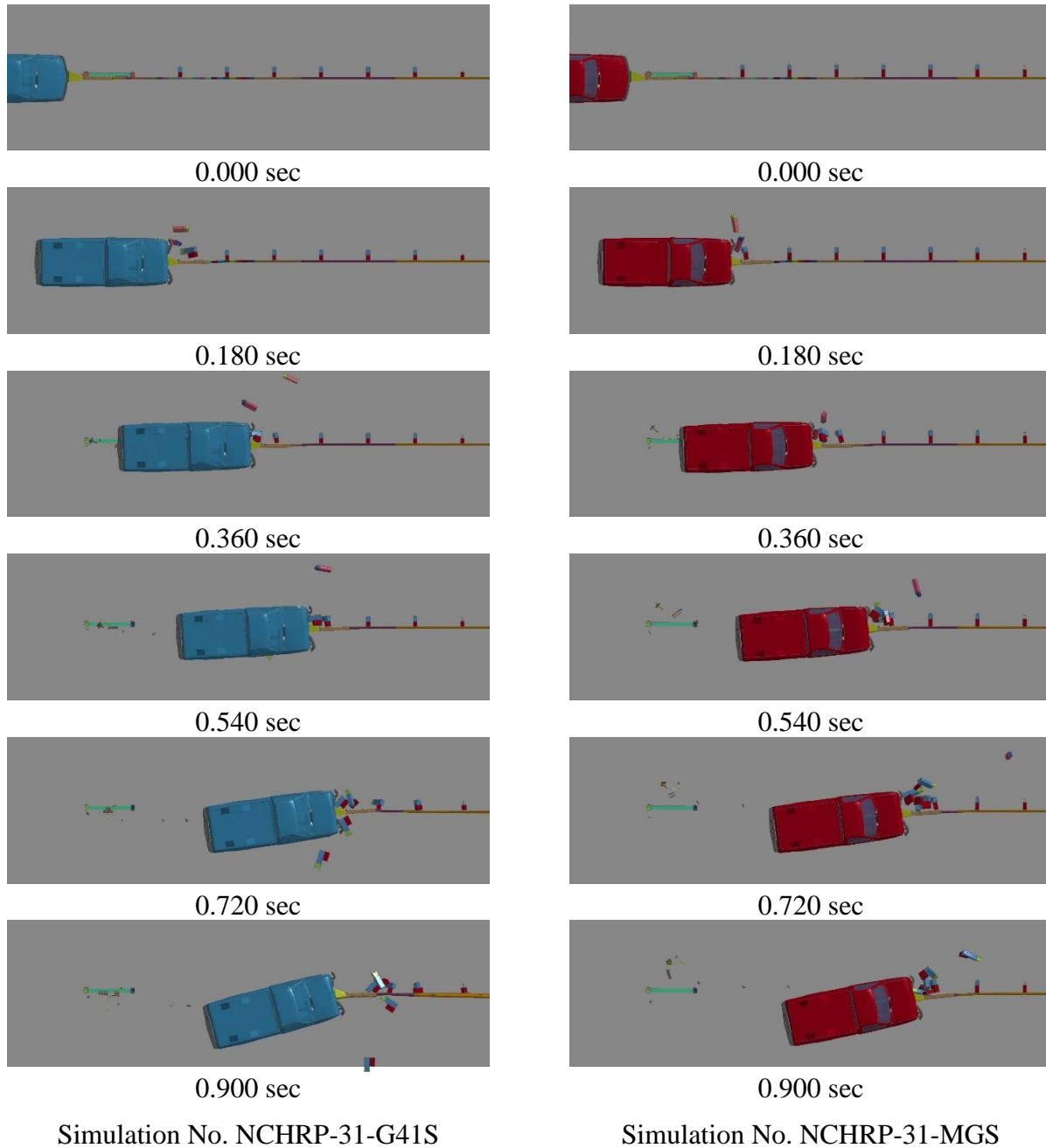


Figure 24. NCHRP Report 350 Test No. 3-31, Overhead View

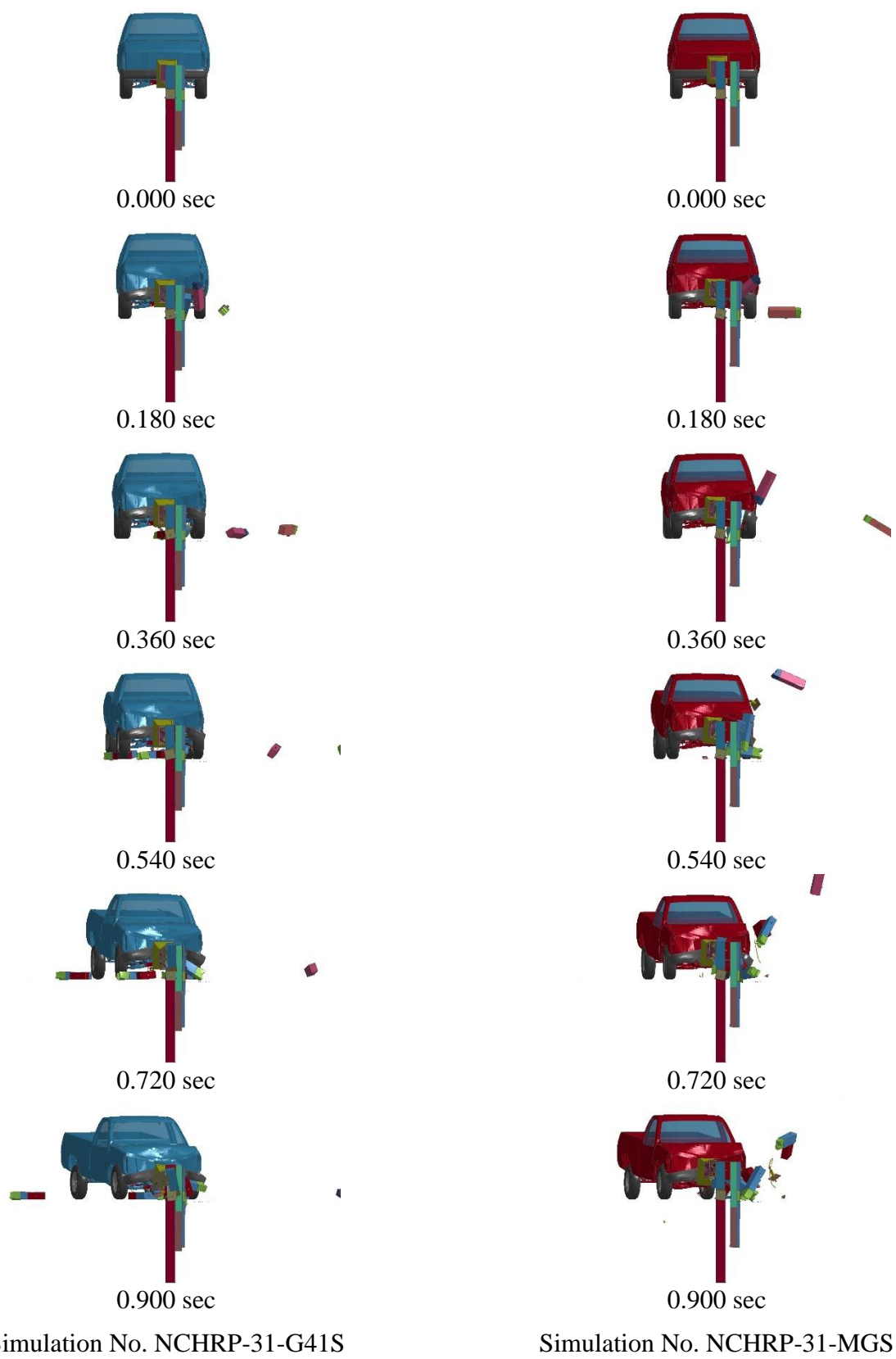


Figure 25. NCHRP Report 350 Test No. 3-31, Downstream View

The 820C model impacted the impact head installed on MGS. The impact head translated downstream along 8.7 ft (2.7 m) of guardrail, impacting the BCT posts and one of the CRT posts. The first two posts fractured near the groundline. The rail gated, which allowed the vehicle to traverse behind the system, and the impact head stopped translating downstream 195 ms after impact. The impact head remained engaged with the front of the vehicle for longer than what has occurred in full-scale crash testing, which may partially be attributed to the impact head and vehicle nodes becoming entangled. When the impact head model disengaged from the front bumper and hood, the impact head twisted and translated upward. The impact head typically releases to the side of the vehicle in full-scale crash testing, and not upward as observed in the model. The guardrail buckled at post no. 3, but rail buckling should be used cautiously as the rail does not have typical compressive loads as a result of not modeling the energy-absorbing mechanism in the impact head. No significant occupant compartment deformation occurred.

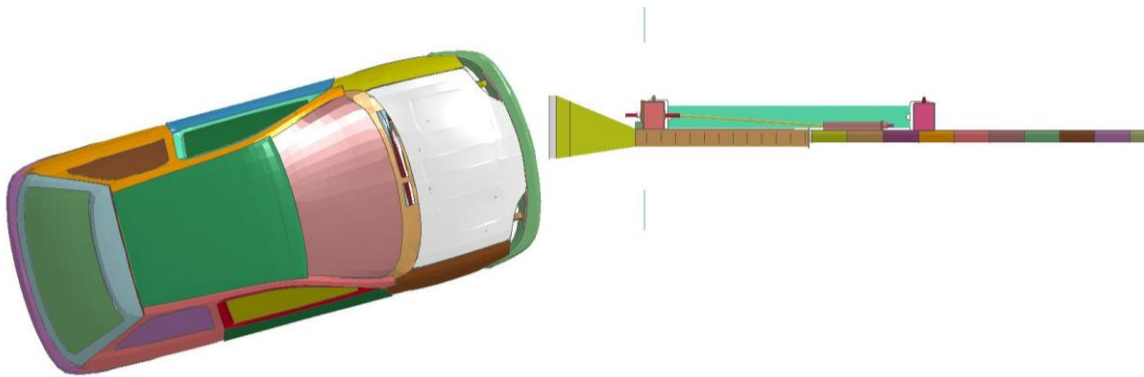
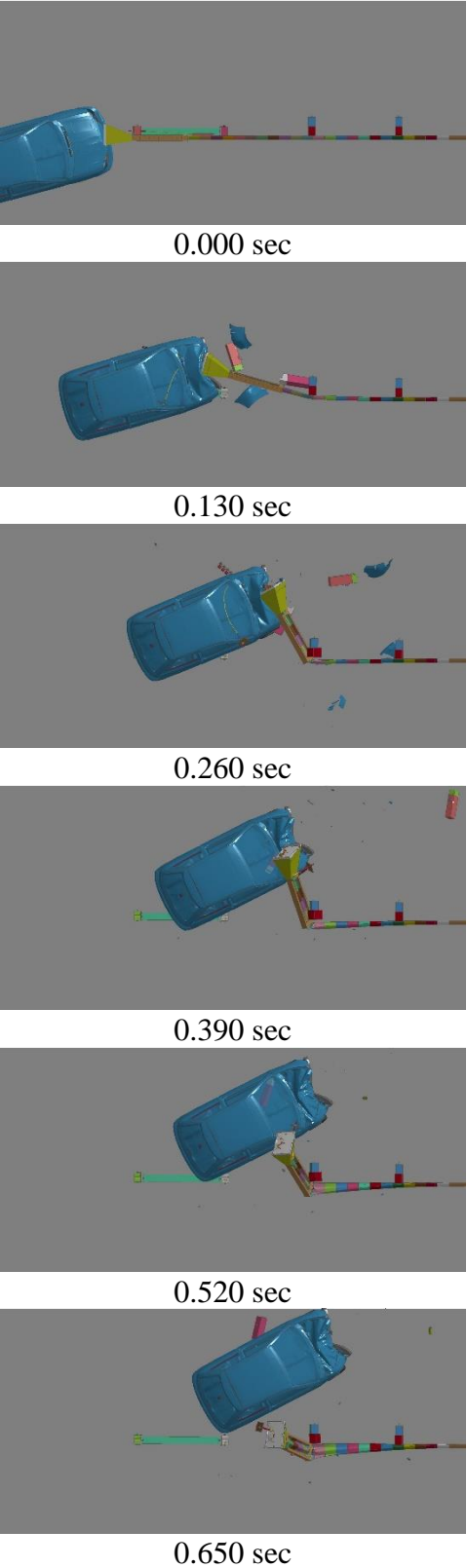


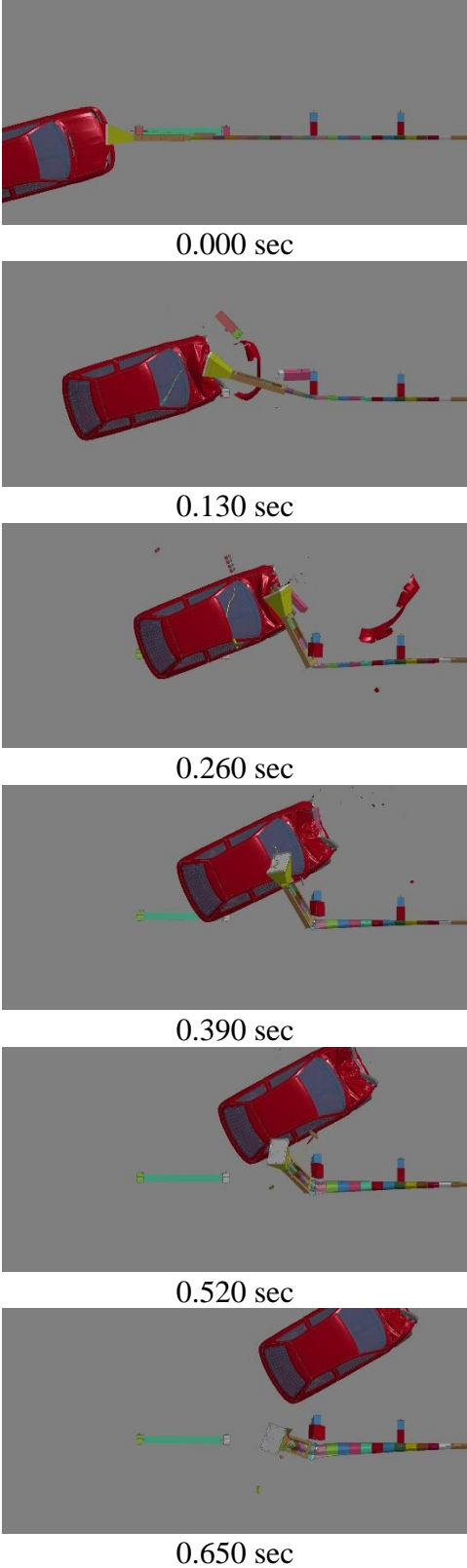
Figure 26. NCHRP Report 350 Test No. 3-32 Impact

Table 12. NCHRP Report 350 Test No. 3-32

Simulation No.	NCHRP-32-G41S	NCHRP-32 -MGS
Test Number	NCHRP 350 3-32	NCHRP 350 3-32
System	G41S	MGS
Longitudinal OIV, ft/s (m/s)	-32.5 (-9.9)	-32.2 (-9.8)
Lateral OIV, ft/s (m/s)	2.0 (0.6)	2.3 (0.7)
Longitudinal ORA, g's	-13.0	-8.9
Lateral ORA, g's	9.2	5.1
Maximum Roll Angle, deg	2.5	1.3
Maximum Pitch Angle, deg	2.4	2.0
Maximum Yaw Angle, deg	12.3	14.7
Guardrail Feed Length, ft (m)	8.7 (2.6)	8.7 (2.6)
Buckle Location	Post no. 3	Post no. 3



Simulation No. NCHRP-32-G41S



Simulation No. NCHRP-32-MGS

Figure 27. NCHRP Report 350 Test No. 3-32, Overhead View

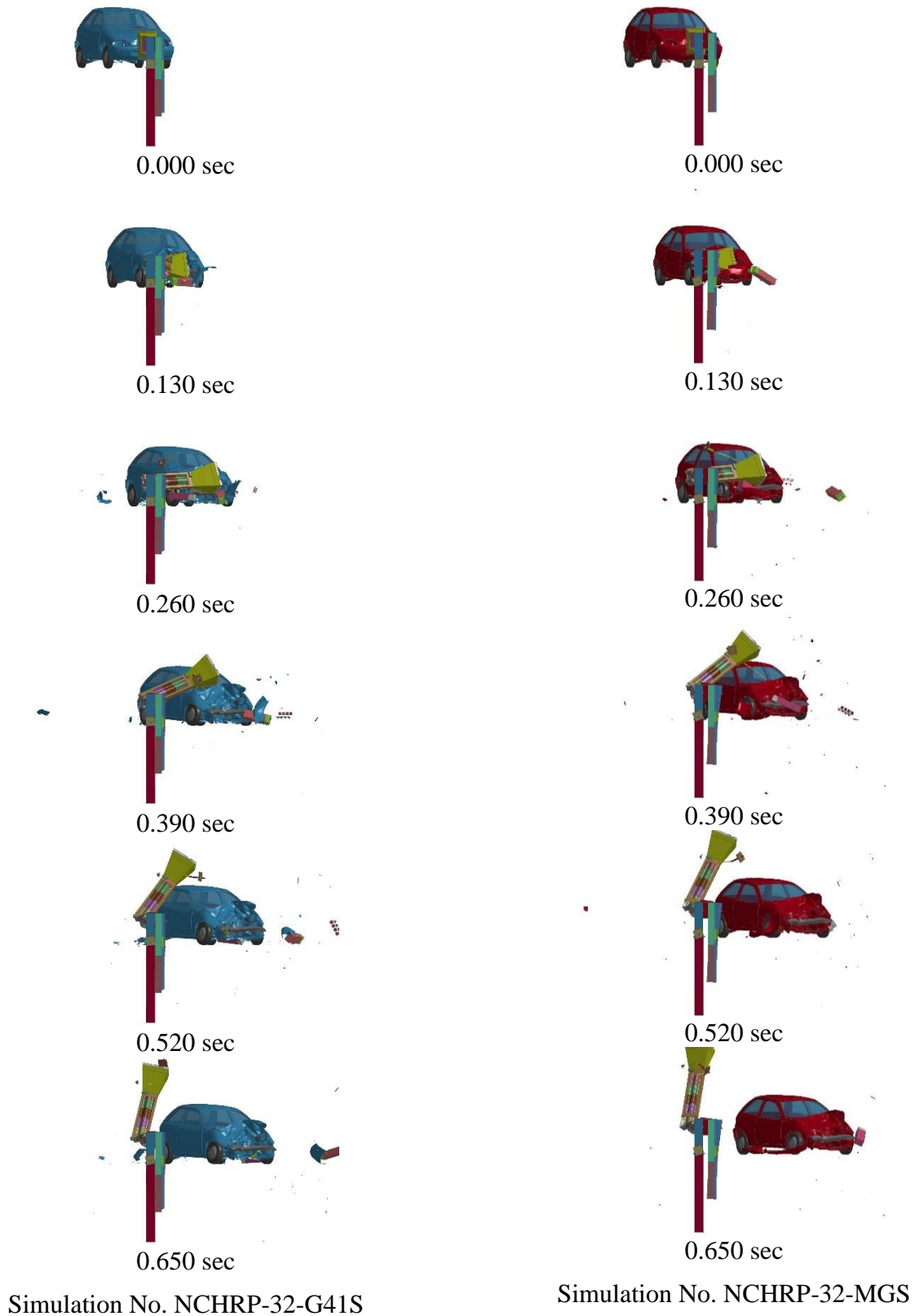


Figure 28. NCHRP Report 350 Test No. 3-32, Downstream View

6.1.4 NCHRP Report 350 Test No. 3-33

NCHRP Report 350 test no. 3-33 involves a 2000P pickup truck impacting at 62 mph (99.8 km/h) and at 15 degrees with the centerline of the system aligned with the centerline of the vehicle, as shown in Figure 29. In simulation nos. NCHRP-33-G41S and NCHRP-33-MGS, the 2000P pickup truck impacted the end terminals installed on modified G4(1S) and MGS, respectively. Sequential photographs are shown in Figure 30 (overhead view) and Figure 31 (downstream view). The longitudinal and lateral ORAs and OIVs are shown in Table 13. The distance the impact head translated, or the feed length, and the buckle location are also shown in Table 13.

The 2000P model impacted the impact head installed on modified G4(1S). The impact head translated downstream along 9.7 ft (3.0 m) of guardrail, impacting the BCT posts and one of the CRT posts. The first three posts fractured near the groundline. The rail gated, which allowed the vehicle to traverse behind the system, and the impact head stopped translating downstream 160 ms after impact. The guardrail buckled at post no. 3, but rail buckling should be used cautiously as the rail does not have typical compressive loads as a result of not modeling the energy-absorbing mechanism in the impact head. The impact head attached to the front of the truck due to nodes entangling. However, this phenomenon is not expected to occur during an actual impact event. No significant occupant compartment deformation occurred.

The 2000P model impacted the impact head installed on MGS. The impact head translated downstream along 9.0 ft (2.7 m) of guardrail, impacting the BCT posts and one of the CRT posts. The first three posts fractured near the groundline. The rail gated, which allowed the vehicle to traverse behind the system, and the impact head stopped translating downstream 160 ms after impact. The guardrail buckled 13 in. (330 mm) downstream from post no. 3, but rail buckling should be used cautiously as the rail does not have typical compressive loads as a result of not modeling the energy-absorbing mechanism in the impact head. No significant occupant compartment deformation occurred.

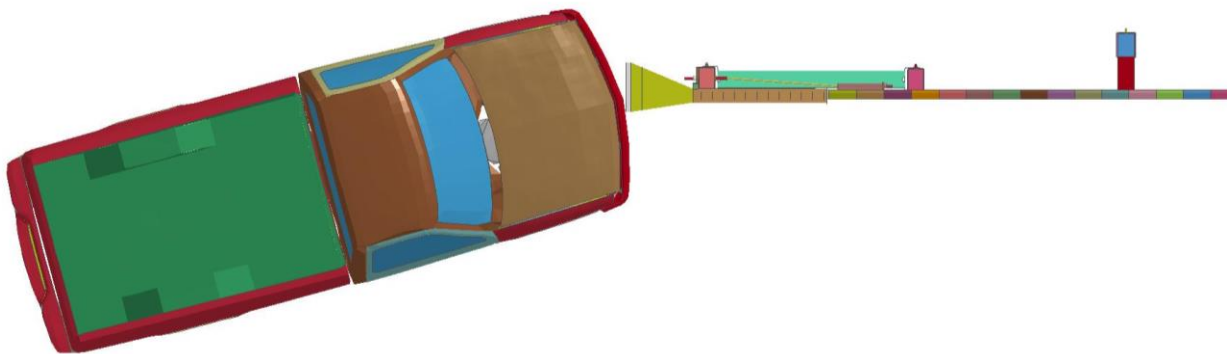
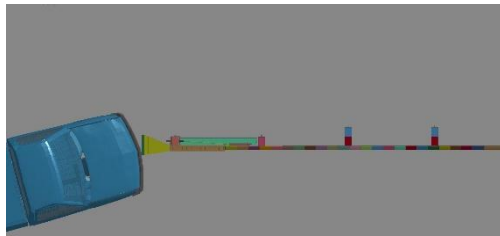


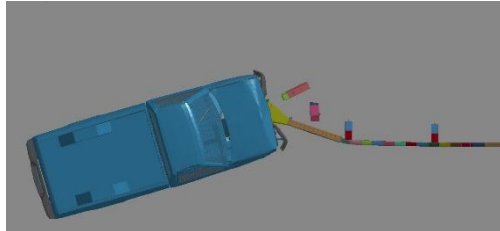
Figure 29. NCHRP Report 350 Test No. 3-33 Impact

Table 13. NCHRP Report 350 Test No. 3-33

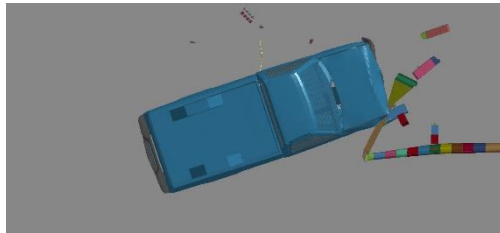
Simulation No.	NCHRP-33-G41S	NCHRP-33 -MGS
Test Number	NCHRP 350 3-33	NCHRP 350 3-33
System	G41S	MGS
Longitudinal OIV, ft/s (m/s)	-21.7 (-6.6)	-21.3 (-6.5)
Lateral OIV, ft/s (m/s)	1.0 (0.3)	2.6 (0.8)
Longitudinal ORA, g's	-8.5	-7.9
Lateral ORA, g's	11.0	9.2
Maximum Roll Angle, deg	2.7	-3.9
Maximum Pitch Angle, deg	-2.4	-2.7
Maximum Yaw Angle, deg	38.6	9.4
Guardrail Feed Length, ft (m)	9.7 (3.0)	9.0 (2.7)
Buckle Location	Post no. 3	13 in. DS from Post no. 3



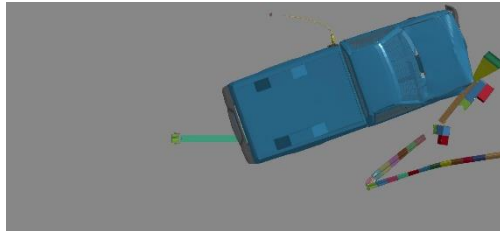
0.000 sec



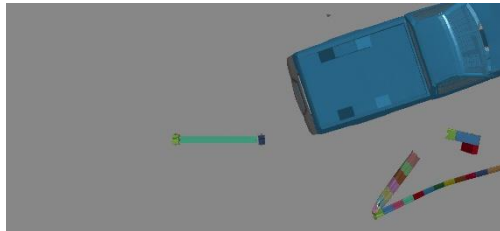
0.130 sec



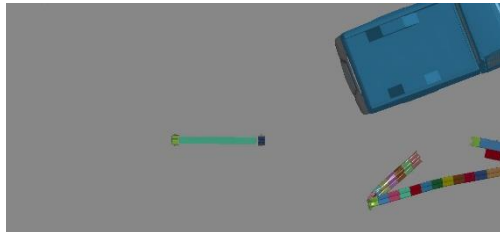
0.260 sec



0.390 sec

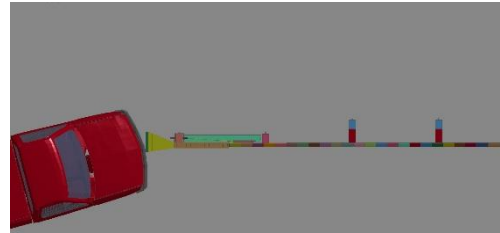


0.520 sec

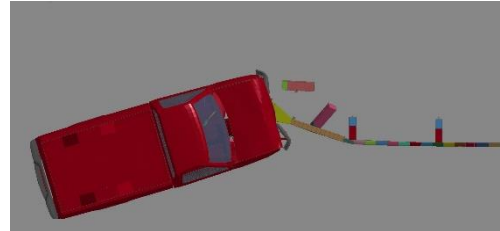


0.650 sec

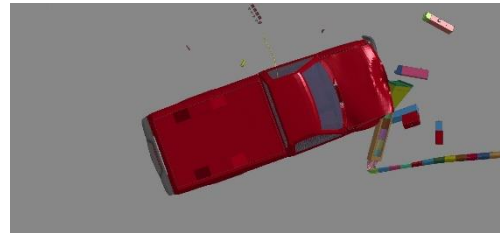
Simulation No. NCHRP-33-G41S



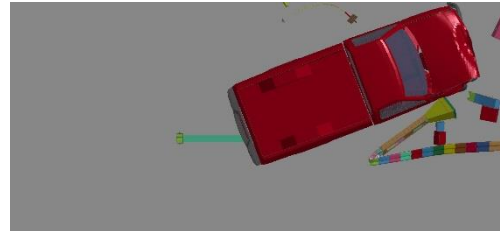
0.000 sec



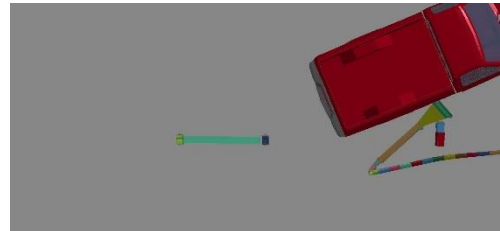
0.130 sec



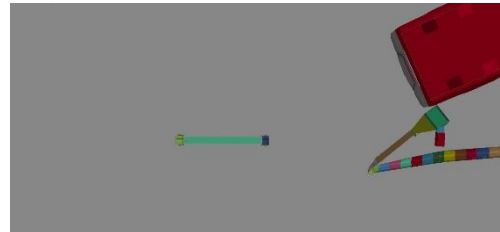
0.260 sec



0.390 sec



0.520 sec



0.650 sec

Simulation No. NCHRP-33-MGS

Figure 30. NCHRP Report 350 Test No. 3-33, Overhead View

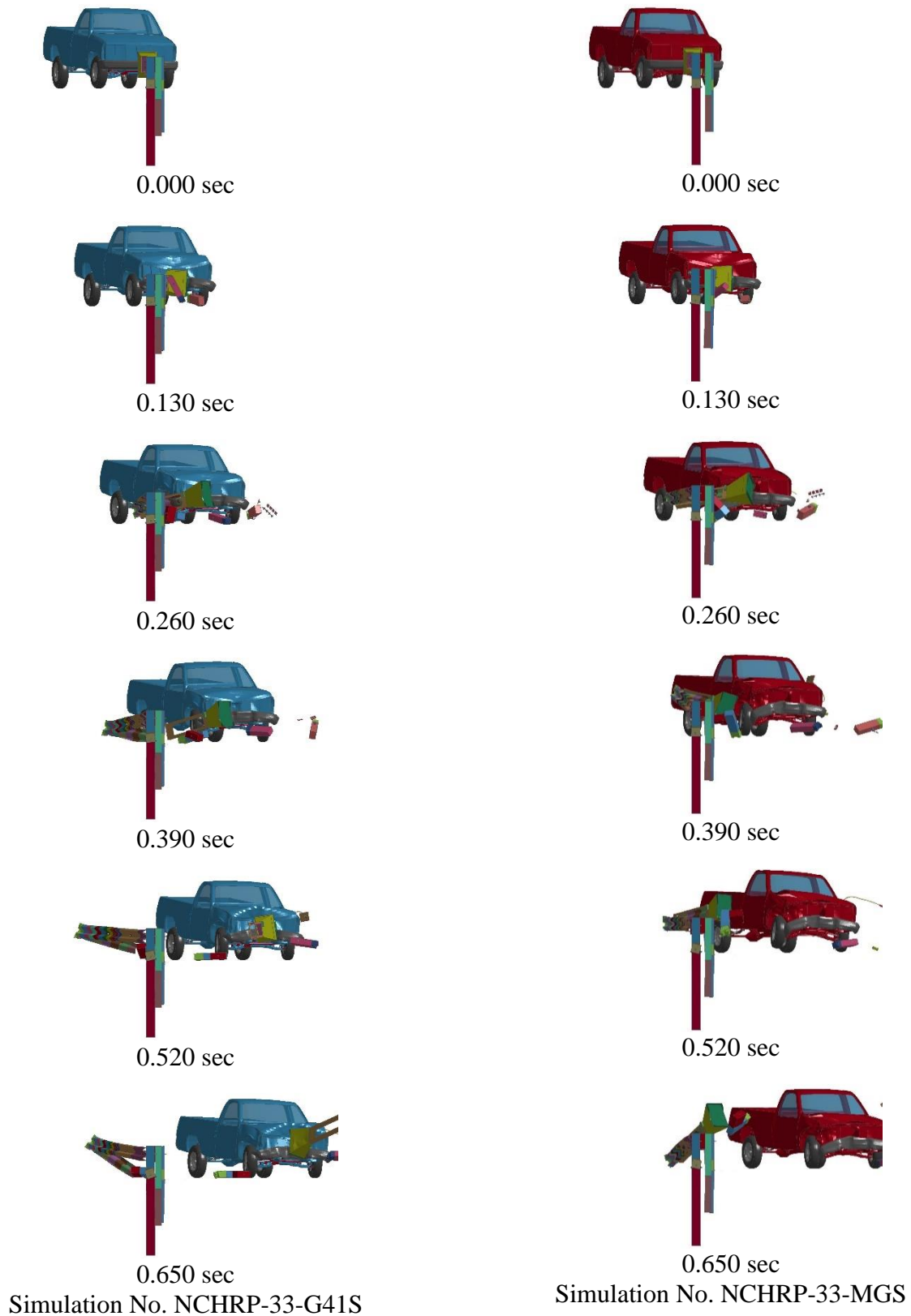


Figure 31. NCHRP Report 350 Test No. 3-33, Downstream View

6.1.5 MASH 2009 Test No. 3-30

MASH 2009 test no. 3-30 involves an 1100C small car impacting at 62 mph (99.8 km/h) and at 0 degrees with the centerline of the system aligned with the quarter point offset of the vehicle's bumper. Typically, the system is tested at the shallow quarter point offset, as shown in Figure 32. Since the performance of the deep quarter-point offset, shown in Figure 33, is largely unknown, impacts with both quarter point offsets were simulated.

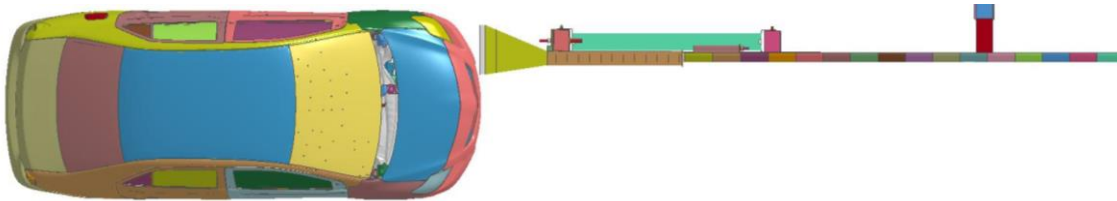


Figure 32. MASH 2009 Test No. 3-30, Shallow Quarter-Point Offset Impact

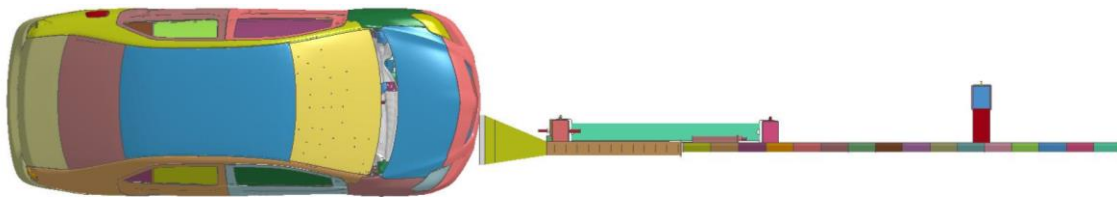


Figure 33. MASH 2009 Test No. 3-30, Deep Quarter-Point Offset Impact

6.1.5.1 Shallow Quarter-Point Offset

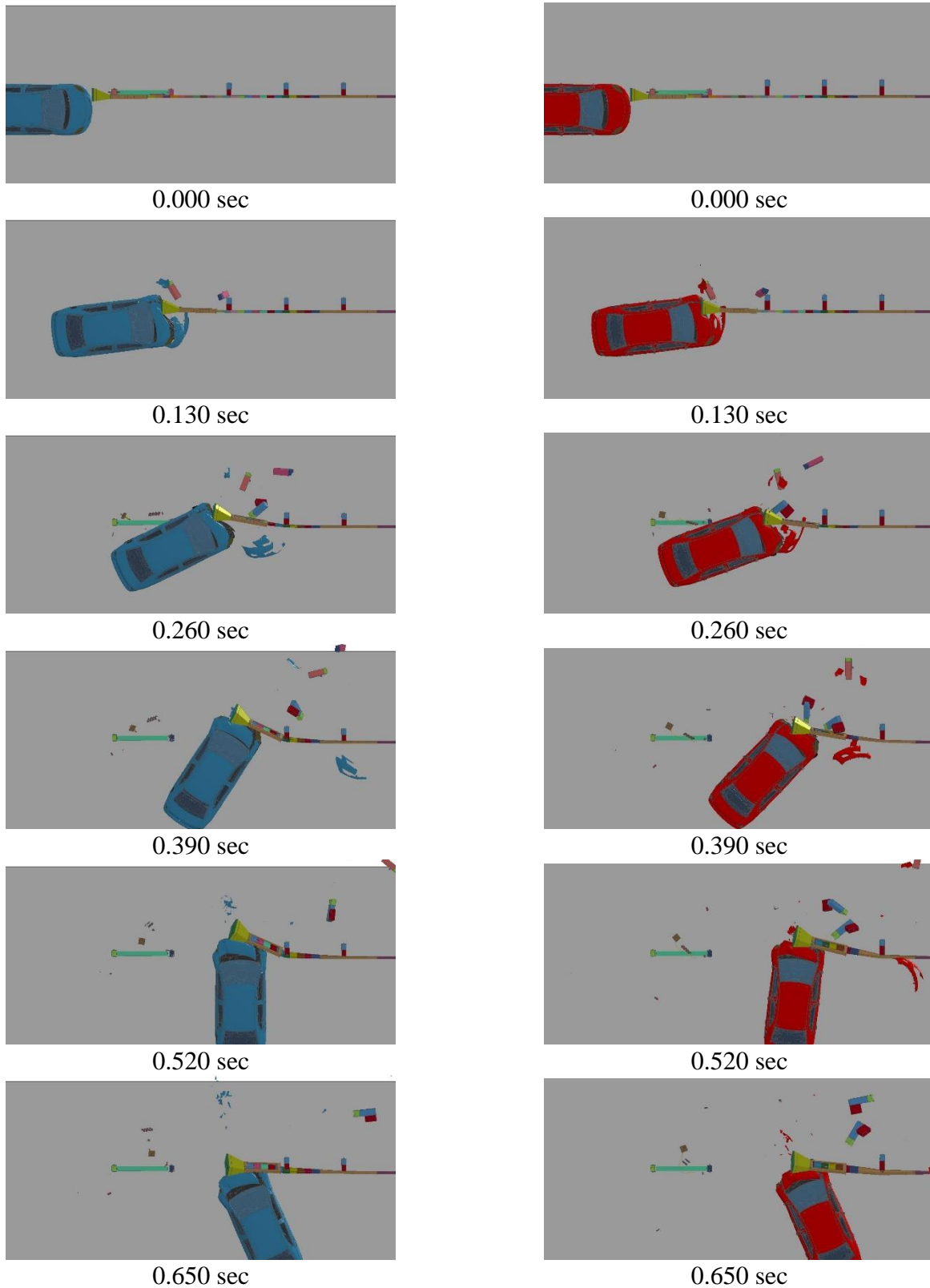
In simulation nos. MASH-30-shallow-G41S and MASH-30-shallow-MGS, the 1100C small car impacted the end terminals installed on modified G4(1S) and MGS, respectively, at the shallow quarter-point offset. Sequential photographs are shown in Figure 34 (overhead view) and Figure 35 (downstream view). The longitudinal and lateral ORAs and OIVs, distance the impact head translated, or the feed length, and the buckle location are shown in Table 14.

The 1100C model impacted the impact head installed on modified G4(1S). The impact head translated downstream along 14.8 ft (4.5 m) of guardrail, impacting the BCT posts and two of the CRT posts. The first three posts fractured near the groundline. The car yawed toward the traffic side of the system, and the impact head stopped translating downstream 359 ms after impact. The guardrail began to buckle at post no. 4, but rail buckling should be used cautiously as the rail does not have typical compressive loads as a result of not modeling the energy-absorbing mechanism in the impact head. The impact head attached to the front of the car model due to nodes entangling. However, this phenomenon is not expected to occur during an actual impact event. No significant occupant compartment deformation occurred.

The 1100C model impacted the impact head installed on MGS. The impact head translated downstream along 17.6 ft (5.4 m) of guardrail, impacting the BCT posts and two of the CRT posts. The first four posts fractured near the groundline. The car yawed toward the traffic side of the system, and the impact head stopped translating downstream 428 ms after impact. The guardrail began to buckle at post no. 5, but rail buckling should be used cautiously as the rail does not have typical compressive loads as a result of not modeling the energy-absorbing mechanism in the impact head. The impact head attached to the front of the car model due to nodes entangling. However, this phenomenon is not expected to occur during an actual impact event. No significant occupant compartment deformation occurred.

Table 14. MASH 2009 Test No. 3-30, Shallow Quarter-Point Offset

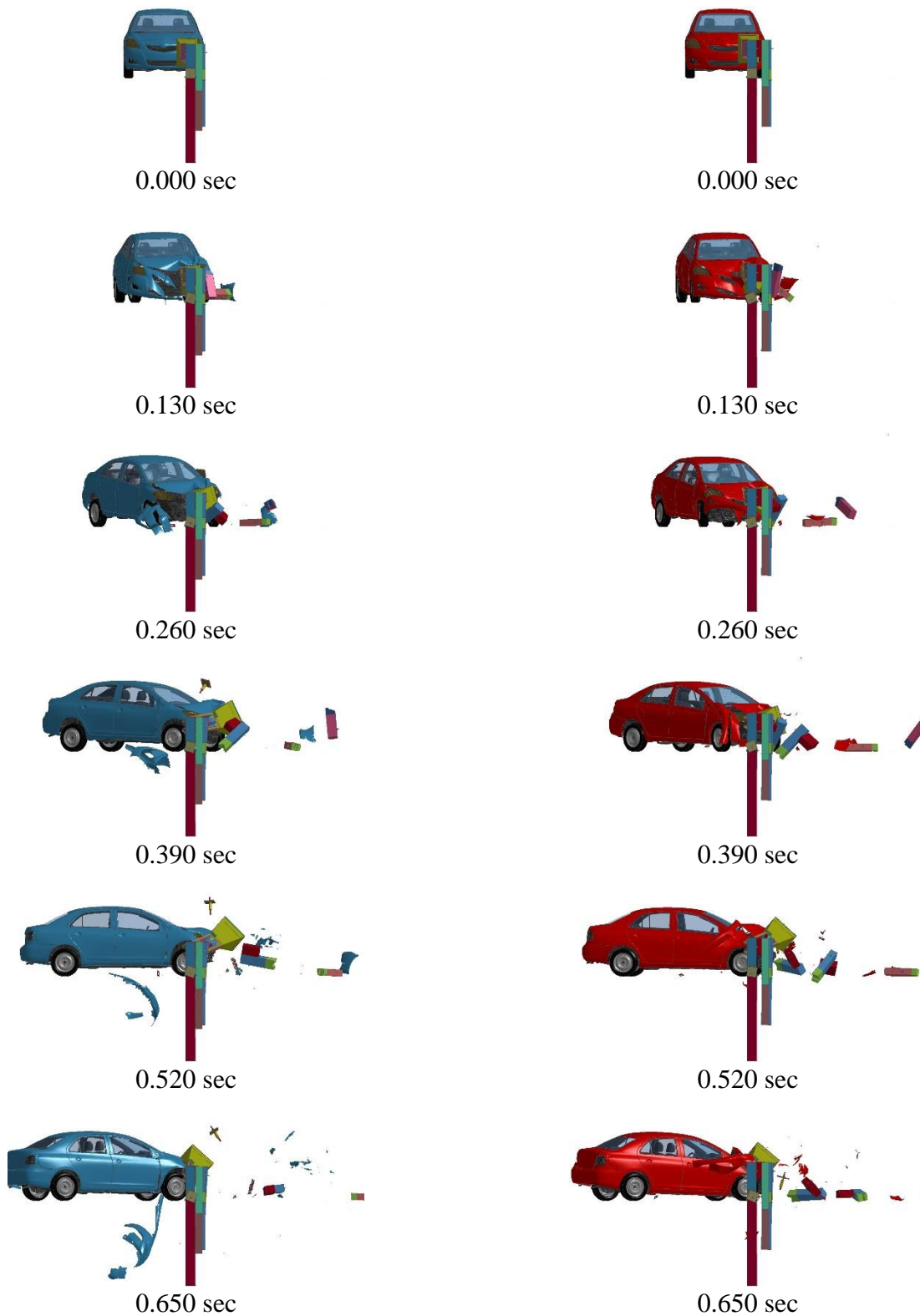
Simulation No.	MASH-30-shallow-G41S	MASH-30-shallow-MGS
Test Number	MASH 2009 3-30 (Shallow)	MASH 2009 3-30 (Shallow)
System	G41S	MGS
Longitudinal OIV, ft/s (m/s)	-28.2 (-8.6)	-25.6 (-7.8)
Lateral OIV, ft/s (m/s)	0.7 (0.2)	0.0 (0.0)
Longitudinal ORA, g's	-19.7	-12.9
Lateral ORA, g's	14.4	9.5
Maximum Roll Angle, deg	2.8	2.4
Maximum Pitch Angle, deg	3.9	3.4
Maximum Yaw Angle, deg	113.9	113.6
Guardrail Feed Length, ft (m)	14.8 (4.5)	17.6 (5.4)
Buckle Location	Post no. 4	Post no. 5



Simulation No. MASH-30-Shallow-G41S

Simulation No. MASH-30-Shallow-MGS

Figure 34. MASH 2009 Test No. 3-30, Shallow Quarter-Point Offset, Overhead View



Simulation No. MASH-30-Shallow-G41S

Simulation No. MASH-30-Shallow-MGS

Figure 35. MASH 2009 Test No. 3-30, Shallow Quarter-Point Offset, Downstream View

6.1.5.2 Deep Quarter-Point Offset

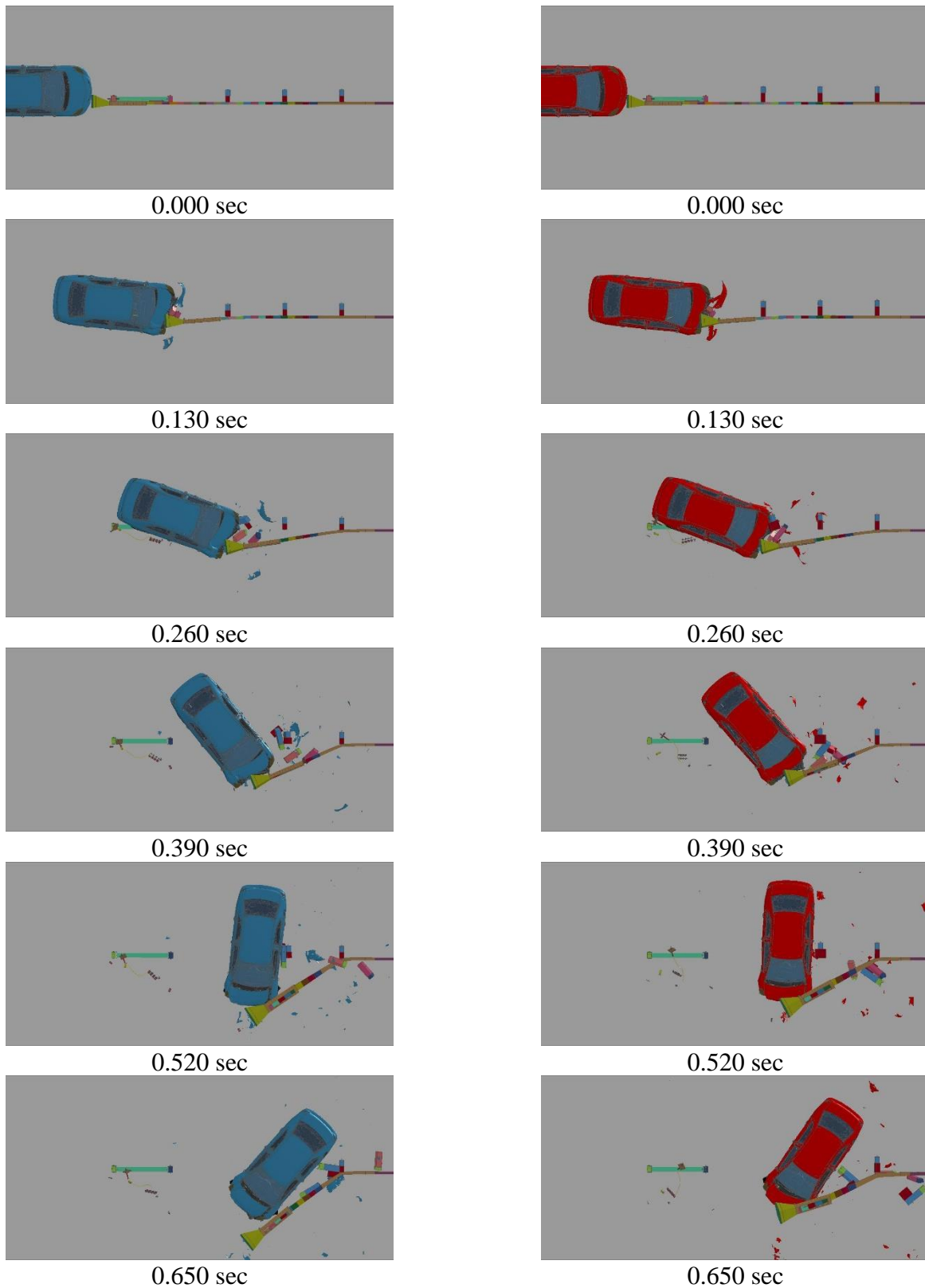
In simulation nos. MASH-30-deep-G41S and MASH-30-deep-MGS, the 1100C small car impacted the end terminals installed on modified G4(1S) and MGS, respectively, at the deep quarter-point offset. Sequential photographs are shown in Figure 36 (overhead view) and Figure 37 (downstream view). The longitudinal and lateral ORAs and OIVs are shown in Table 15. The distance the impact head translated, or the feed length, and the buckle location are also shown in Table 15.

The 1100C model impacted the impact head installed on modified G4(1S). The impact head translated downstream along 16.8 ft (5.1 m) of guardrail, impacting the BCT posts and one of the CRT posts. The first four posts fractured near the groundline. The car yawed toward the non-traffic side of the system, and the impact head stopped translating downstream 370 ms after impact. The guardrail buckled at post no. 5, but rail buckling should be used cautiously as the rail does not have typical compressive loads as a result of not modeling the energy-absorbing mechanism in the impact head. No significant occupant compartment deformation occurred.

The 1100C model impacted the impact head installed on MGS. The impact head translated downstream along 16.8 ft (5.1 m) of guardrail, impacting the BCT posts and one of the CRT posts. The first four posts fractured near the groundline. The car yawed toward the non-traffic side of the system, and the impact head stopped translating downstream 380 ms after impact. The guardrail buckled at post no. 5, but rail buckling should be used cautiously as the rail does not have typical compressive loads as a result of not modeling the energy-absorbing mechanism in the impact head. No significant occupant compartment deformation occurred.

Table 15. MASH 2009 Test No. 3-30, Deep Quarter-Point Offset

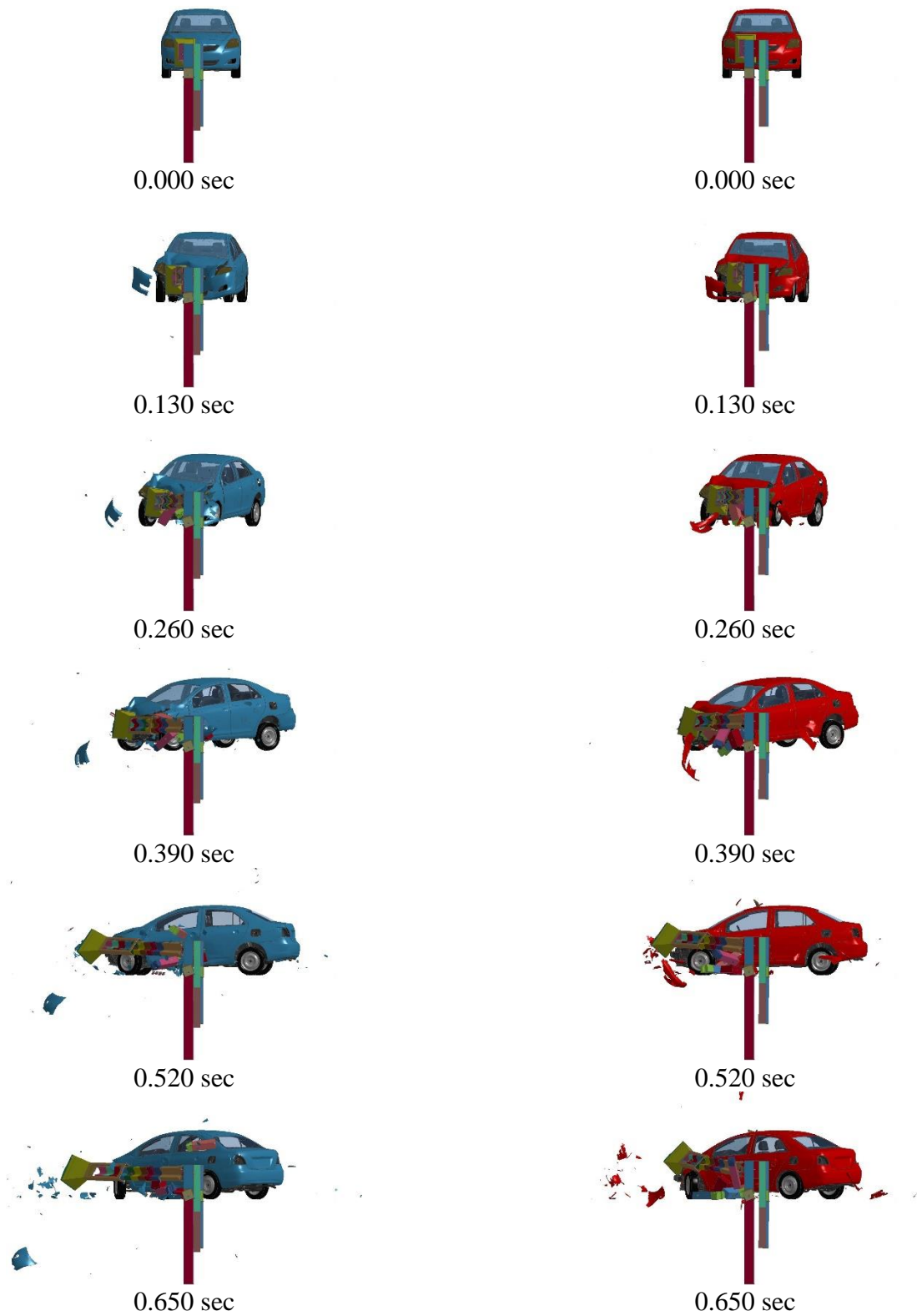
Simulation No.	MASH-30-deep-G41S	MASH-30-deep-MGS
Test Number	MASH 2009 3-30 (Deep)	MASH 2009 3-30 (Deep)
System	G41S	MGS
Longitudinal OIV, ft/s (m/s)	-27.9 (-8.5)	-27.6 (-8.4)
Lateral OIV, ft/s (m/s)	-1.0 (-0.3)	-0.3 (-0.1)
Longitudinal ORA, g's	-8.3	-11.3
Lateral ORA, g's	-9.3	-7.8
Maximum Roll Angle, deg	-3.9	-3.5
Maximum Pitch Angle, deg	3.6	4.3
Maximum Yaw Angle, deg	-132.2	-124.5
Guardrail Feed Length, ft (m)	16.8 (5.1)	16.8 (5.1)
Buckle Location	Post no. 5	Post no. 5



Simulation No. MASH-30-Deep-G41S

Simulation No. MASH-30-Deep-MGS

Figure 36. MASH 2009 Test No. 3-30, Deep Quarter-Point Offset, Overhead View



Simulation No. MASH-30-Deep-G41S

Simulation No. MASH-30-Deep-MGS

Figure 37. MASH 2009 Test No. 3-30, Deep Quarter-Point Offset, Downstream View

6.1.6 MASH 2009 Test No. 3-31

MASH 2009 test no. 3-31 involves a 2270P pickup truck impacting at 62 mph (99.8 km/h) and at 0 degrees with the centerline of the system aligned with the centerline of the vehicle, as shown in Figure 38. In simulation nos. MASH-31-G41S and MASH-31-MGS, the 2270P pickup truck impacted the end terminals installed on modified G4(1S) and MGS, respectively. Sequential photographs are shown in Figure 39 (overhead view) and Figure 40 (downstream view). The longitudinal and lateral ORAs and OIVs are shown in Table 16. The distance the impact head translated, or the feed length, and the buckle location are also shown in Table 16. Using conservation of momentum utilized during the development of the crash reconstruction procedure for end terminals established by Coon, the average end terminal force was calculated based on the mass of the vehicle and guardrail feed length, also shown in Table 16.

The 2270P model impacted the impact head installed on modified G4(1S). The impact head translated downstream along 44.6 ft (13.6 m) of guardrail, impacting the BCT posts and six of the CRT posts. The first seven posts fractured near the groundline. The truck remained aligned with the guardrail throughout the impact event, and the impact head stopped translating downstream 1070 ms after impact. The guardrail did not buckle. No significant occupant compartment deformation occurred.

The 2270P model impacted the impact head installed on MGS. The impact head translated downstream along 44.4 ft (13.5 m) of guardrail, impacting the BCT posts and six of the CRT posts. The first seven posts fractured near the groundline. The truck remained aligned with the guardrail throughout the impact event, and the impact head stopped translating downstream 1090 ms after impact. The guardrail did not buckle. No significant occupant compartment deformation occurred.

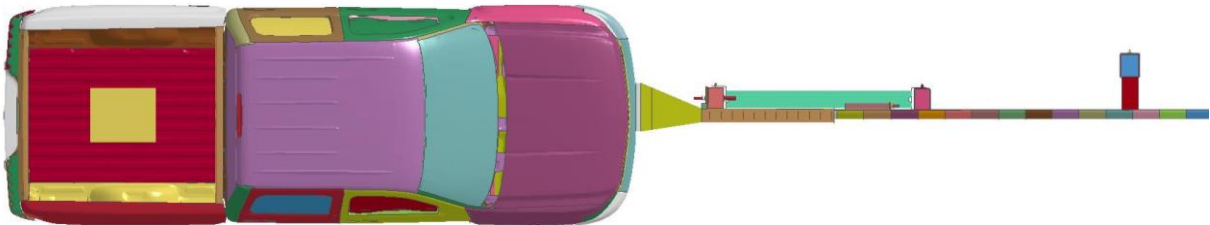
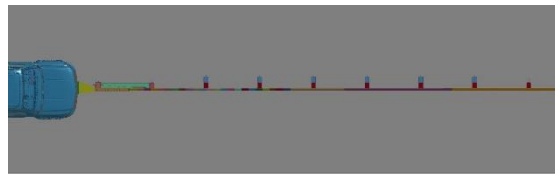


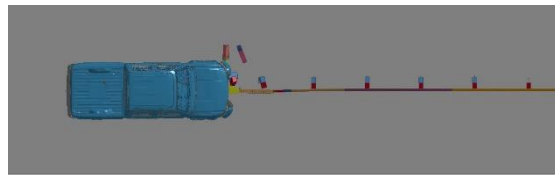
Figure 38. MASH 2009 Test No. 3-31 Impact

Table 16. MASH 2009 Test No. 3-31

Simulation No.	MASH-31-G41S	MASH-31-MGS
Test Number	MASH 2009 3-31	MASH 2009 3-31
System	G41S	MGS
Longitudinal OIV, ft/s (m/s)	-18.7 (-5.7)	-18.4 (-5.6)
Lateral OIV, ft/s (m/s)	-0.3 (-0.1)	-0.3 (-0.1)
Longitudinal ORA, g's	-14.1	-11.4
Lateral ORA, g's	3.8	3.7
Maximum Roll Angle, deg	2.2	4.0
Maximum Pitch Angle, deg	1.5	2.0
Maximum Yaw Angle, deg	1.0	1.7
Guardrail Feed Length, ft (m)	44.6 (13.6)	44.4 (13.5)
Buckle Location	None	None
Average Terminal Force, kips (kN)	13.8 (61.4)	13.9 (61.7)



0.000 sec



0.230 sec



0.460 sec



0.690 sec

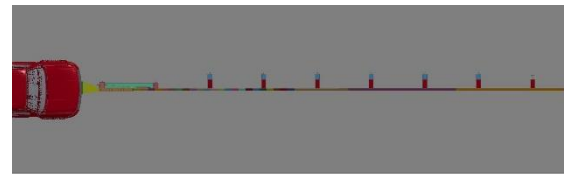


0.920 sec

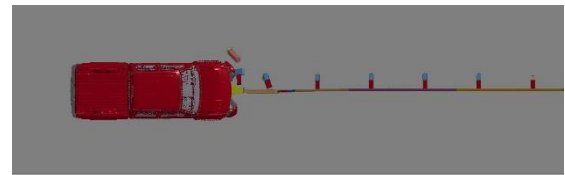


1.150 sec

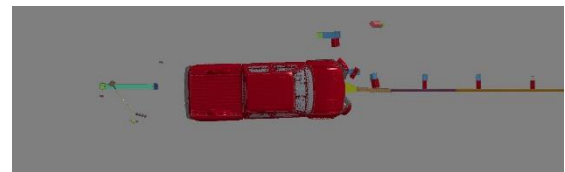
Simulation No. MASH-31-G41S



0.000 sec



0.230 sec



0.460 sec



0.690 sec



0.920 sec



1.150 sec

Simulation No. MASH-31-MGS

Figure 39. MASH 2009 Test No. 3-31, Overhead View



Simulation No. MASH-31-G41S



Simulation No. MASH-31-MGS

Figure 40. MASH 2009 Test No. 3-31, Downstream View

6.1.7 MASH 2009 Test No. 3-32

MASH 2009 test no. 3-32 involves an 1100C small car impacting at 62 mph (99.8 km/h) and at an angle between 5 and 15 degrees with the centerline of the system aligned with the centerline of the vehicle. Although MASH 2009 recommends that gating redirective terminals are tested closer to the 5-degree value, both the 5-degree and 15-degree impact angles were simulated, as shown in Figures 41 and 42, respectively.

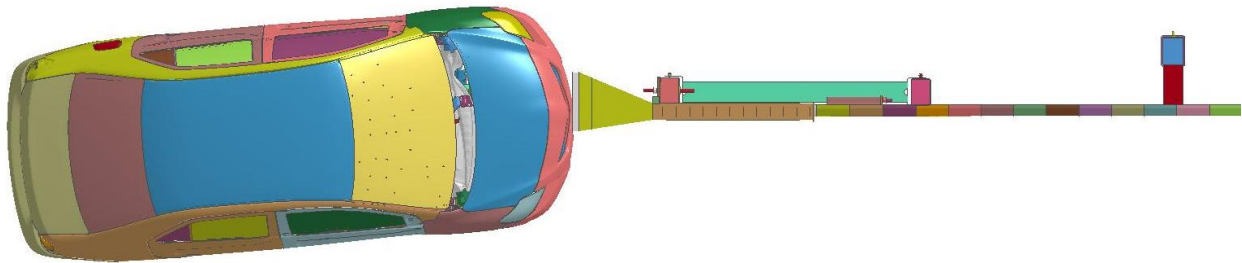


Figure 41. MASH 2009 Test No. 3-32 at 5-Degree Impact

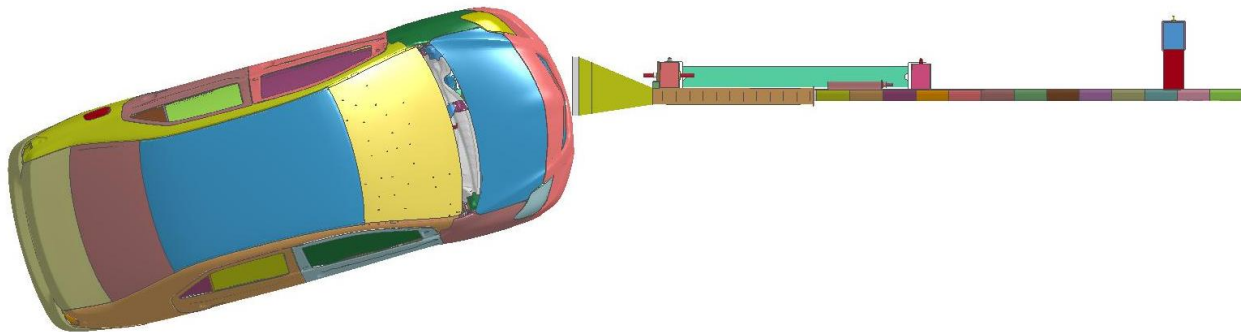


Figure 42. MASH 2009 Test No. 3-32 at 15-Degree Impact

6.1.7.1 5-Degree Impact Angle

In simulation nos. MASH-32-5deg-G41S and MASH-32-5deg-MGS, the 1100C small car impacted the end terminals installed on modified G4(1S) and MGS, respectively, at an angle of 5 degrees. Sequential photographs are shown in Figure 44 (overhead view) and Figure 45 (downstream view). The longitudinal and lateral ORAs and OIVs are shown in Table 17. The distance the impact head translated, or the feed length, and the buckle location are also shown in Table 17.

The 1100C model impacted the impact head installed on modified G4(1S). The impact head translated downstream along 20.5 ft (6.2 m) of guardrail, impacting the BCT posts and two of the CRT posts. The first four posts fractured near the groundline. The car yawed slightly toward the non-traffic side of the system, and the impact head stopped translating downstream 530 ms after impact. The guardrail did not buckle, but rail buckling should be used cautiously as the rail does not have typical compressive loads as a result of not modeling the energy-absorbing

mechanism in the impact head. The longitudinal ORA during the impact with the modified G4(1S) model was -22.4 g's and occurred at 278 ms after impact, at the same time the chute impacted post no. 4. The post-to-rail bolt experienced significant snagging as the rail tried to release from the post, which created a high longitudinal acceleration, as shown in Figure 43. This high longitudinal acceleration corresponded to a 4.5 mph (2 m/s) decrease in the longitudinal velocity over a 10 ms time frame. Typically, the rail releases from the post much more easily, so the longitudinal ORA value may be artificially high due to problems associated with modeling rail release. The rail release snagging was not seen in the impact with the MGS. No significant occupant compartment deformation occurred.

The 1100C model impacted the impact head installed on MGS. The impact head translated downstream along 20.7 ft (6.3 m) of guardrail, impacting the BCT posts and two of the CRT posts. The first four posts fractured near the groundline. The car yawed slightly toward the non-traffic side of the system, and the impact head stopped translating downstream 541 ms after impact. The guardrail did not buckle, but rail buckling should be used cautiously as the rail does not have typical compressive loads as a result of not modeling the energy-absorbing mechanism in the impact head. No significant occupant compartment deformation occurred.

Table 17. MASH 2009 Test No. 3-32 at 5 Degrees

Simulation No.	MASH-32-5deg-G41S	MASH-32-5deg-MGS
Test Number	MASH 2009 3-32 (5 deg)	MASH 2009 3-32 (5 deg)
System	G41S	MGS
Longitudinal OIV, ft/s (m/s)	-25.9 (-7.9)	-25.9 (-7.9)
Lateral OIV, ft/s (m/s)	-0.7 (-0.2)	-0.3 (-0.1)
Longitudinal ORA, g's	-22.4	-14.2
Lateral ORA, g's	3.8	-3.4
Maximum Roll Angle, deg	-1.6	1.4
Maximum Pitch Angle, deg	3.7	3.8
Maximum Yaw Angle, deg	-20.1	-26.4
Guardrail Feed Length, ft (m)	20.5 (6.2)	20.7 (6.3)
Buckle Location	None	None

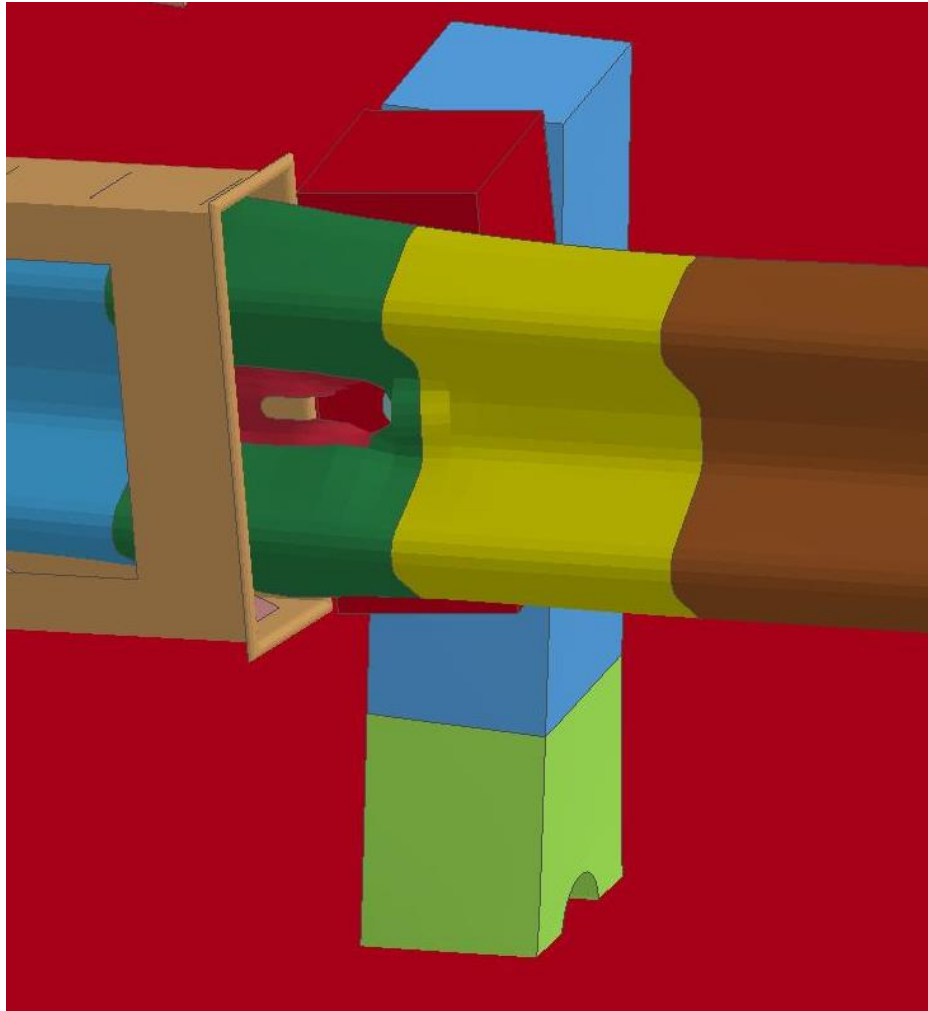
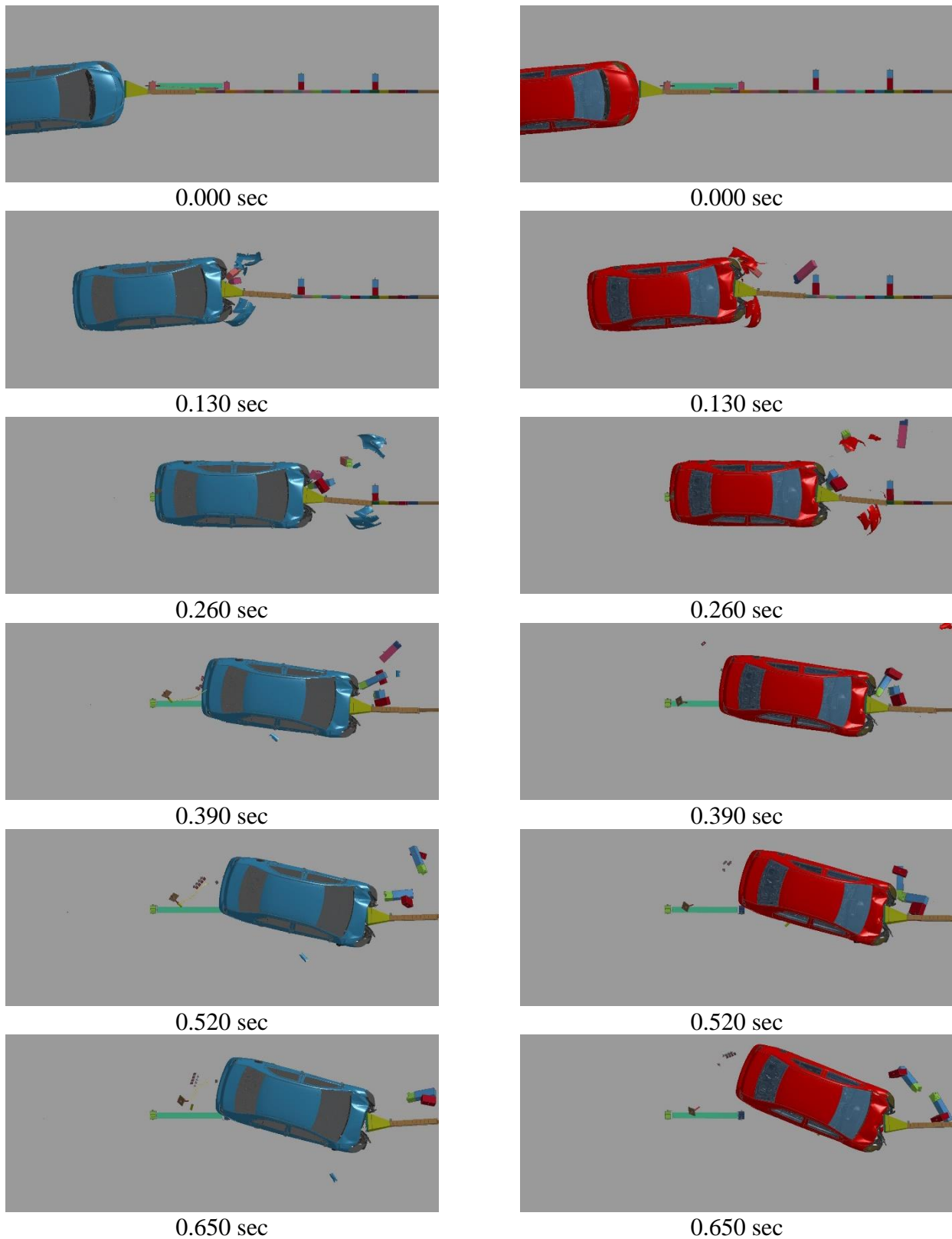


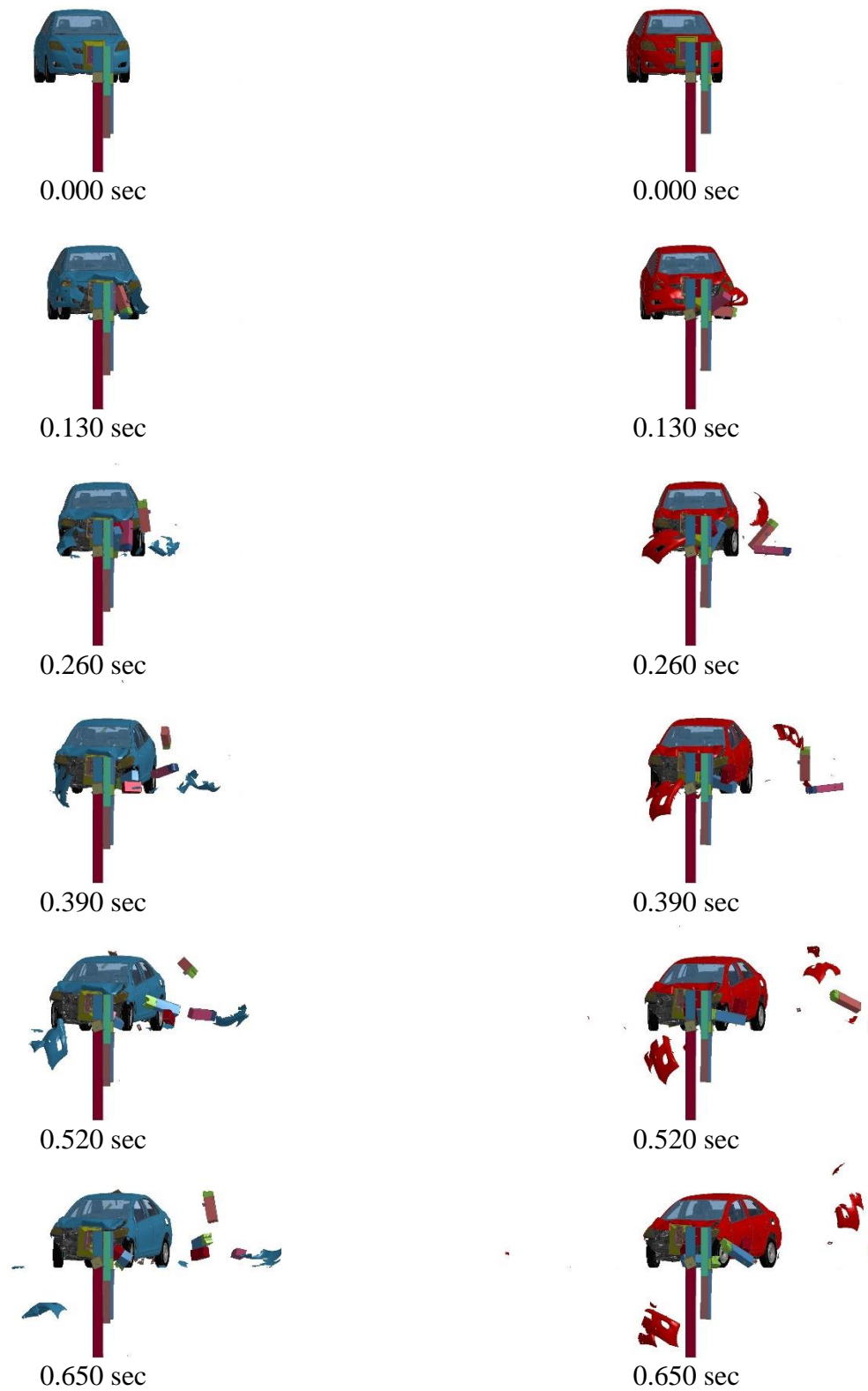
Figure 43. Post-to-Rail Bolt Snag



Simulation No. MASH-32-5deg-G41S

Simulation No. MASH-32-5deg-MGS

Figure 44. MASH 2009 Test No. 3-32 at 5 Degrees, Overhead View



Simulation No. MASH-32-5deg-G41S

Simulation No. MASH-32-5deg-MGS

Figure 45. MASH 2009 Test No. 3-32 at 5 Degrees, Downstream View

6.1.7.2 15-Degree Impact Angle

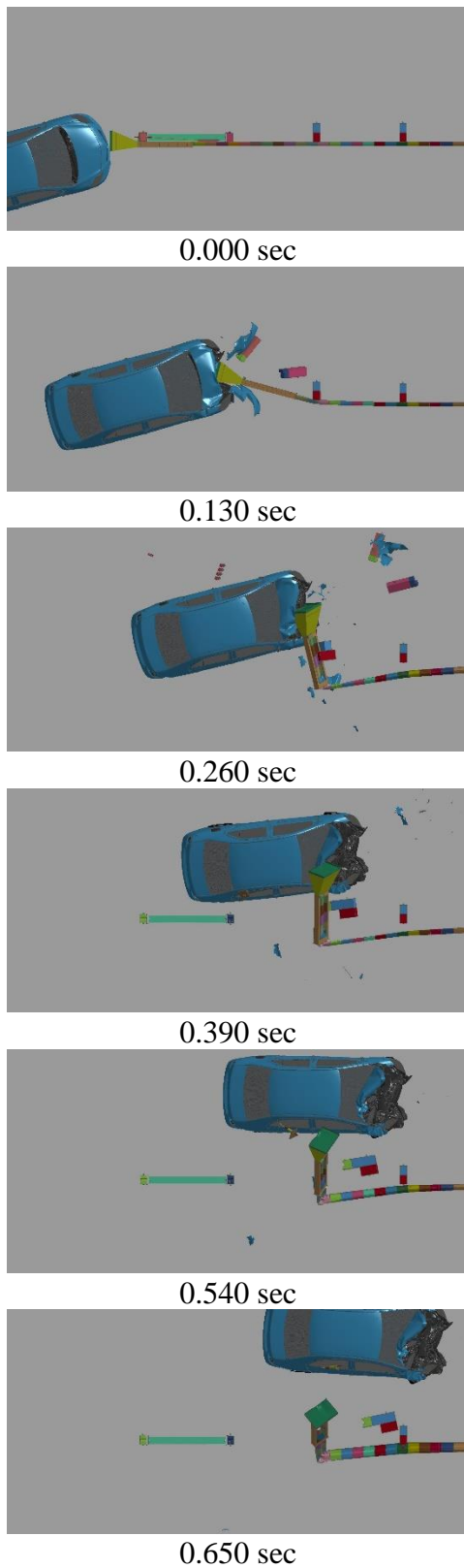
In simulation nos. MASH-32-15deg-G41S and MASH-32-15deg-MGS, the 1100C small car impacted the end terminals installed on modified G4(1S) and MGS, respectively, at an angle of 15 degrees. Sequential photographs are shown in Figure 46 (overhead view) and Figure 47 (downstream view). The longitudinal and lateral ORAs and OIVs are shown in Table 18. The distance the impact head translated, or the feed length, and the buckle location are also shown in Table 18.

The 1100C model impacted the impact head installed on modified G4(1S). The impact head translated downstream along 9.0 ft (2.7 m) of guardrail, impacting the BCT posts and one of the CRT posts. The first three posts fractured near the groundline. The rail gated, which allowed the vehicle to traverse behind the system, and the impact head stopped translating downstream 170 ms after impact. The guardrail buckled at post no. 3, but rail buckling should be used cautiously as the rail does not have typical compressive loads as a result of not modeling the energy-absorbing mechanism in the impact head. The impact head nodes snagged on the front and hood of the car due to nodes entangling, which caused the car to yaw. However, this phenomenon is not expected to occur during an actual impact event. No significant occupant compartment deformation occurred.

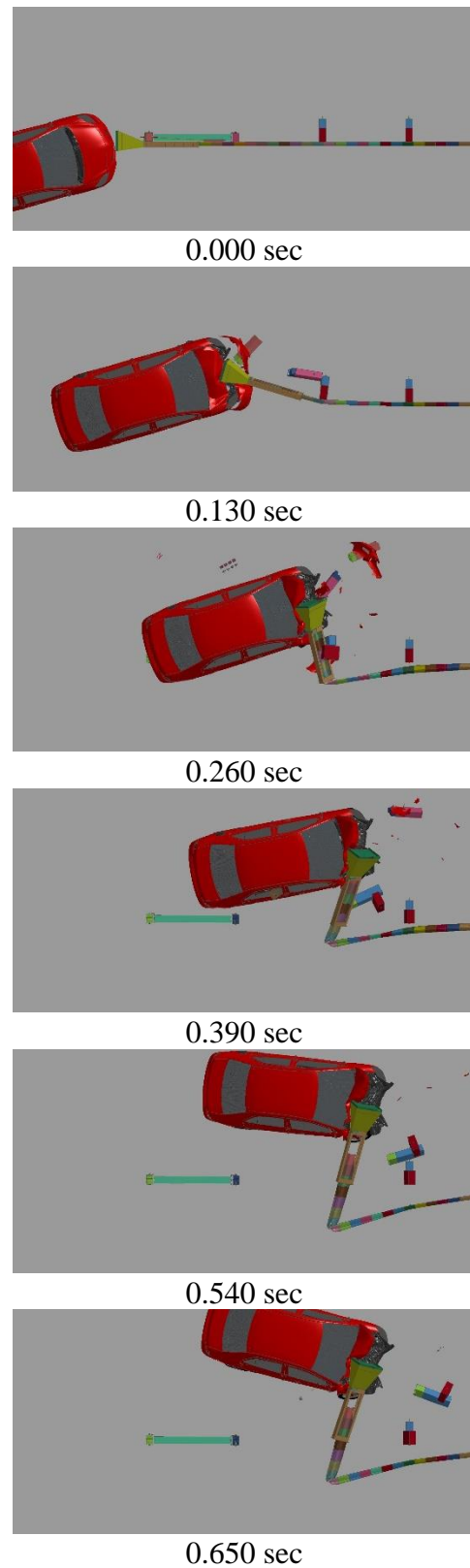
The 1100C model impacted the impact head installed on MGS. The impact head translated downstream along 9.1 ft (2.8 m) of guardrail, impacting the BCT posts and one of the CRT posts. The first three posts fractured near the groundline. The rail gated, which allowed the vehicle to traverse behind the system, and the impact head stopped translating downstream 180 ms after impact. The guardrail buckled at post no. 3, but rail buckling should be used cautiously as the rail does not have typical compressive loads as a result of not modeling the energy-absorbing mechanism in the impact head. The impact head nodes attached to the front and hood of the car due to nodes entangling, which caused the car to yaw. However, this phenomenon is not expected to occur during an actual impact event. No significant occupant compartment deformation occurred.

Table 18. MASH 2009 Test No. 3-32 at 15 Degrees

Simulation No.	MASH-32-15deg-G41S	MASH-32-15deg-MGS
Test Number	MASH 2009 3-32 (15 deg)	MASH 2009 3-32 (15 deg)
System	G41S	MGS
Longitudinal OIV, ft/s (m/s)	-26.9 (-8.2)	-26.6 (-8.1)
Lateral OIV, ft/s (m/s)	1.6 (0.5)	2.0 (0.6)
Longitudinal ORA, g's	-14.2	-10.0
Lateral ORA, g's	9.5	5.1
Maximum Roll Angle, deg	6.5	-4.9
Maximum Pitch Angle, deg	4.8	-6.2
Maximum Yaw Angle, deg	-18.5	-29.3
Guardrail Feed Length, ft (m)	9.0 (2.7)	9.1 (2.8)
Buckle Location	Post no. 3	Post no. 3

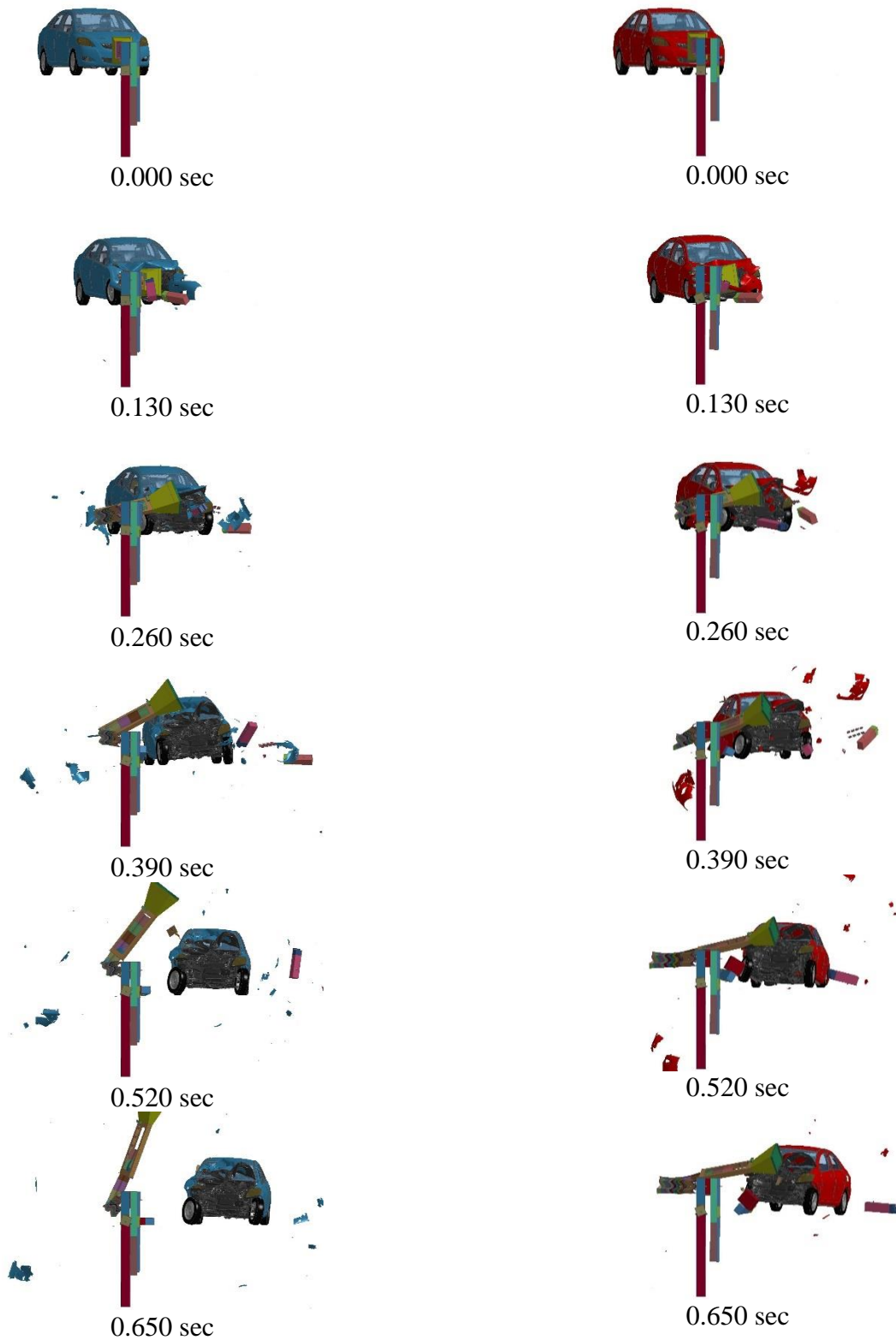


Simulation No. MASH-32-15deg-G41S



Simulation No. MASH-32-15deg-MGS

Figure 46. MASH 2009 Test No. 3-32 at 15 Degrees, Overhead View



Simulation No. MASH-32-15deg-G41S

Simulation No. MASH-32-15deg-MGS

Figure 47. MASH 2009 Test No. 3-32 at 15 Degrees, Downstream View

6.1.8 MASH 2009 Test No. 3-33

MASH 2009 test no. 3-33 involves a 2270P pickup truck impacting at 62 mph (99.8 km/h) and at an angle between 5 and 15 degrees with the centerline of the system aligned with the centerline of the vehicle. Although MASH 2009 recommends that gating redirective terminals are tested closer to the 5-degree value, both the 5-degree and 15-degree impact angles were simulated, as shown in Figures 48 and 49, respectively.

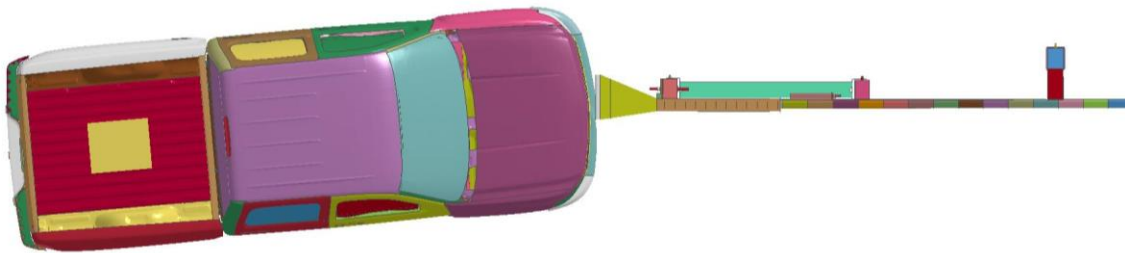


Figure 48. MASH 2009 Test No. 3-33 at 5 Degrees Impact

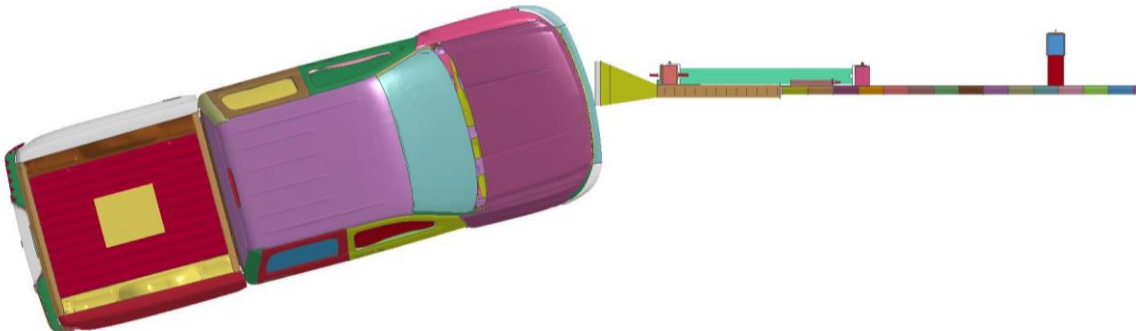


Figure 49. MASH 2009 Test No. 3-33 at 15 Degrees Impact

6.1.8.1 5-Degree Impact Angle

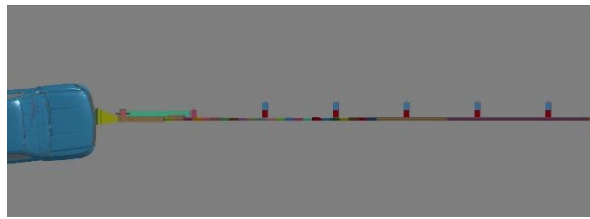
In simulation nos. MASH-33-5deg-G41S and MASH-33-5deg-MGS, the 2270P pickup truck impacted the end terminals installed on modified G4(1S) and MGS, respectively, at an angle of 5 degrees. Sequential photographs are shown in Figure 50 (overhead view) and Figure 51 (downstream view). The longitudinal and lateral ORAs and OIVs, distance the impact head translated, or the feed length, and the buckle location are shown in Table 19.

The 2270P model impacted the impact head installed on modified G4(1S). The impact head translated downstream along 27.8 ft (8.5 m) of guardrail, impacting the BCT posts and three of the CRT posts. The first six posts fractured near the groundline. The truck yawed toward the non-traffic side of the system, and the impact head stopped translating downstream 411 ms after impact. The guardrail buckled at post no. 6, but rail buckling should be used cautiously as the rail does not have typical compressive loads as a result of not modeling the energy-absorbing mechanism in the impact head. No significant occupant compartment deformation occurred.

The 2270P model impacted the impact head installed on MGS. The impact head translated downstream along 25.8 ft (7.9 m) of guardrail, impacting the BCT posts and three of the CRT posts. The first six posts fractured near the groundline. The truck yawed toward the non-traffic side of the system, and the impact head stopped translating downstream 411 ms after impact. The guardrail buckled 21 in. (533.4 mm) upstream of post no. 6, but rail buckling should be used cautiously as the rail does not have typical compressive loads as a result of not modeling the energy-absorbing mechanism in the impact head. No significant occupant compartment deformation occurred.

Table 19. MASH 2009 Test No. 3-33 at 5 Degrees

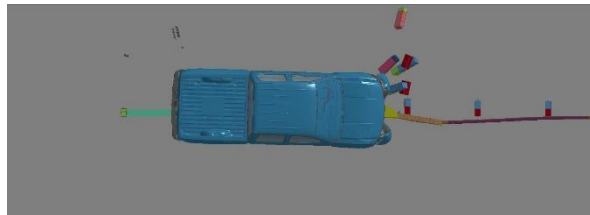
Simulation No.	MASH-33-5deg-G41S	MASH-33-5deg-MGS
Test Number	MASH 2009 3-33 (5 deg)	MASH 2009 3-33 (5 deg)
System	G41S	MGS
Longitudinal OIV, ft/s (m/s)	-20.0 (-6.1)	-19.4 (-5.9)
Lateral OIV, ft/s (m/s)	-2.6 (-0.8)	-2.6 (-0.8)
Longitudinal ORA, g's	-7.8	-9.4
Lateral ORA, g's	-2.8	-3.1
Maximum Roll Angle, deg	-2.0	3.2
Maximum Pitch Angle, deg	2.1	2.4
Maximum Yaw Angle, deg	-48.5	-58.5
Guardrail Feed Length, ft (m)	27.8 (8.5)	25.8 (7.9)
Buckle Location	Post no. 6	21 in. US of Post no. 6



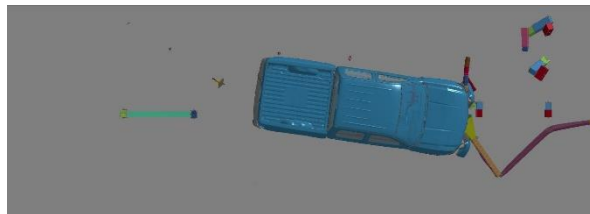
0.000 sec



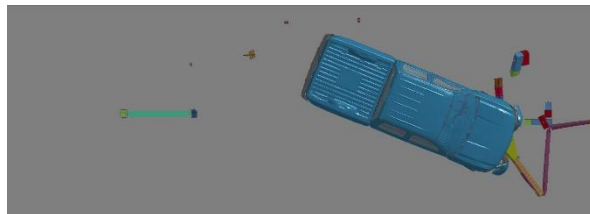
0.180 sec



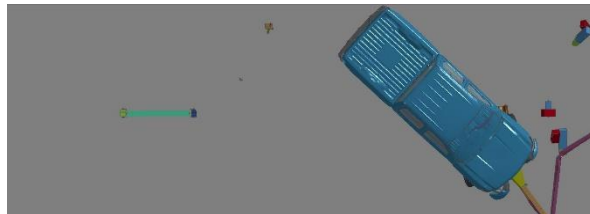
0.360 sec



0.540 sec

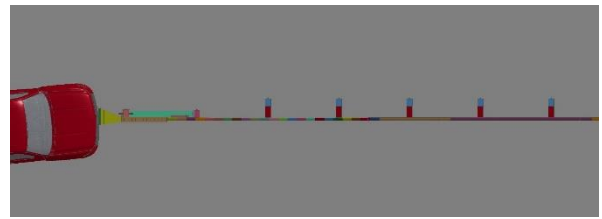


0.720 sec

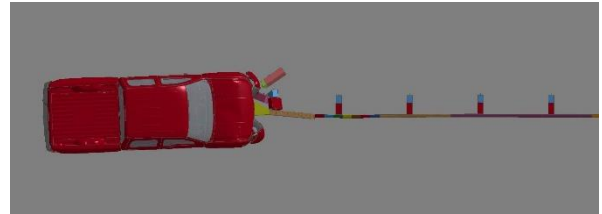


0.900 sec

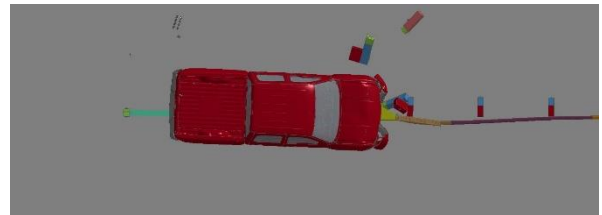
Simulation No. MASH-33-5deg-G41S



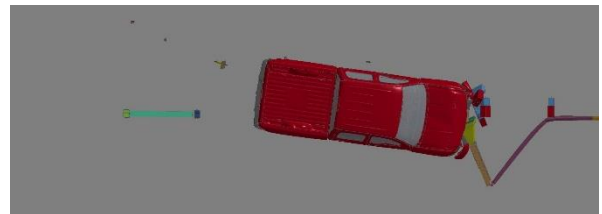
0.000 sec



0.180 sec



0.360 sec



0.540 sec



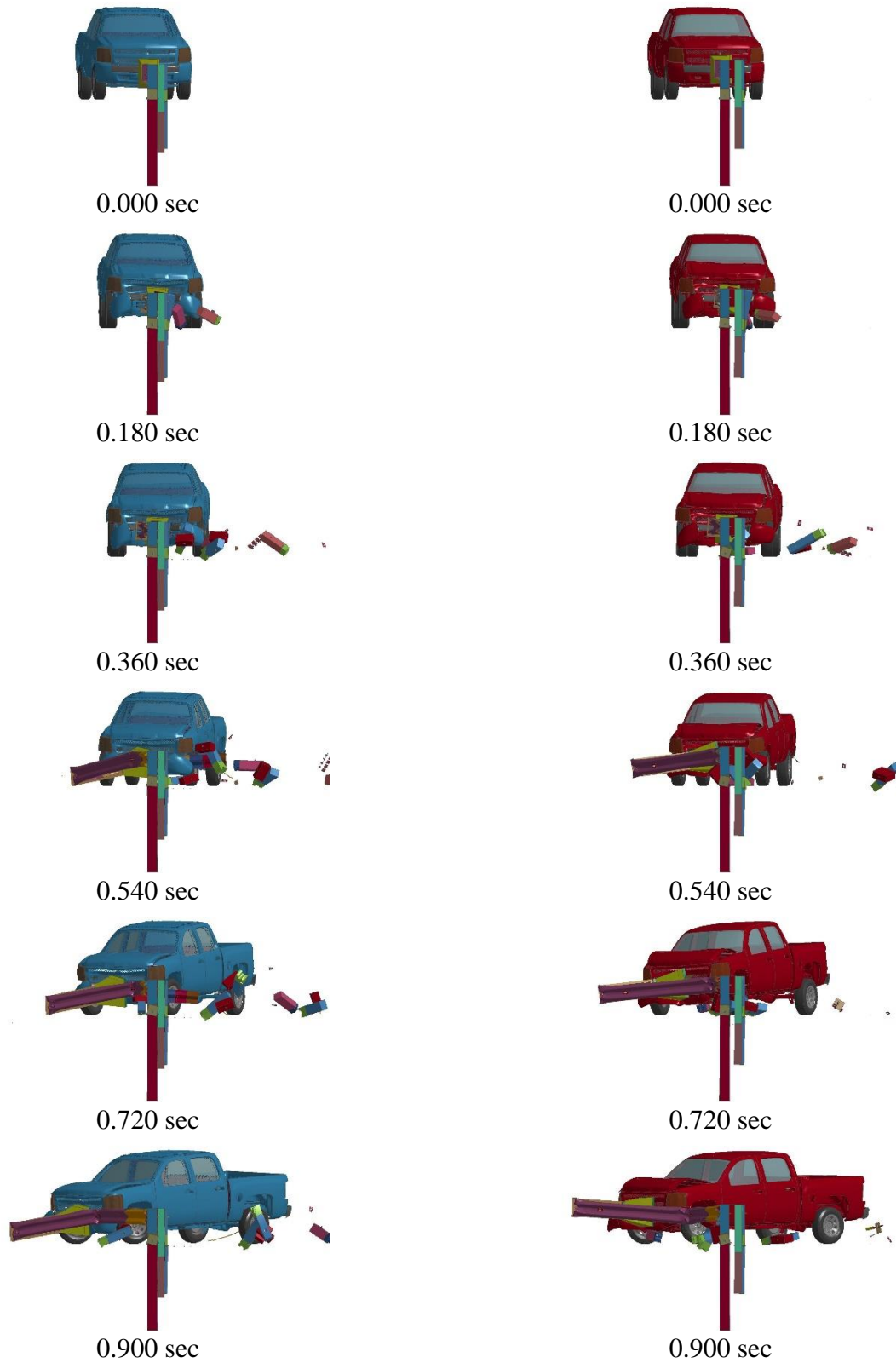
0.720 sec



0.900 sec

Simulation No. MASH-33-5deg-MGS

Figure 50. MASH 2009 Test No. 3-33 at 5 degrees, Overhead View



Simulation No. MASH-33-5deg-G41S

Simulation No. MASH-33-5deg-MGS

Figure 51. MASH 2009 Test No. 3-33 at 5 degrees, Downstream View

6.1.8.2 15-Degree Impact Angle

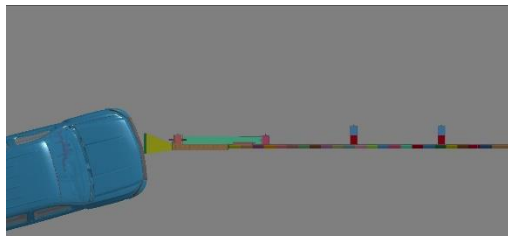
In simulation nos. MASH-33-15deg-G41S and MASH-33-15deg-MGS, the 2270P pickup truck impacted the end terminals installed on modified G4(1S) and MGS, respectively, at an angle of 15 degrees. Sequential photographs are shown in Figure 52 (overhead view) and Figure 53 (downstream view). The longitudinal and lateral ORAs and OIVs are shown in Table 20. A positive longitudinal ORA value occurred in the impact with the modified G4(1S). This value may have been caused by the impact head snagging on the side of the vehicle after it had gated behind the system, which happened at the same time as the positive ORA and is believed to be unrealistic. The distance the impact head translated, or the feed length, and the buckle location are also shown in Table 20.

The 2270P model impacted the impact head installed on modified G4(1S). The impact head translated downstream along 4.8 ft (1.5 m) of guardrail, impacting the BCT posts. The first three posts fractured near the groundline. The rail gated, which allowed the vehicle to traverse behind the system, and the impact head stopped translating downstream 80 ms after impact. The guardrail buckled 26 in. (660.4 mm) downstream of post no. 2, but rail buckling should be used cautiously as the rail does not have typical compressive loads as a result of not modeling the energy-absorbing mechanism in the impact head. No significant occupant compartment deformation occurred.

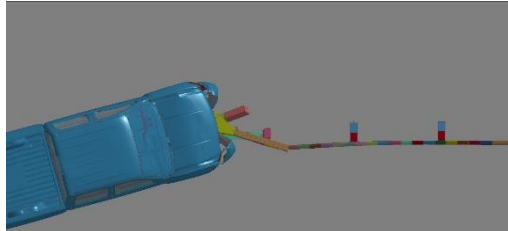
The 2270P model impacted the impact head installed on MGS. The impact head translated downstream along 4.7 ft (1.5 m) of guardrail, impacting the BCT posts. The first three posts fractured near the groundline. The rail gated, which allowed the vehicle to traverse behind the system, and the impact head stopped translating downstream 89 ms after impact. The guardrail buckled 25 in. (635 mm) downstream of post no. 2, but rail buckling should be used cautiously as the rail does not have typical compressive loads as a result of not modeling the energy-absorbing mechanism in the impact head. No significant occupant compartment deformation occurred.

Table 20. MASH 2009 Test No. 3-33 at 15 Degrees

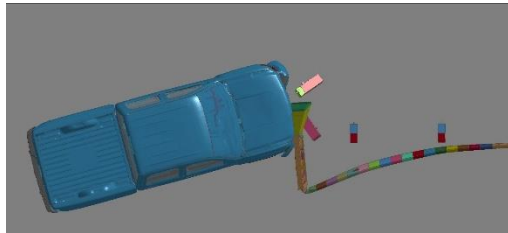
Simulation No.	MASH-33-15deg-G41S	MASH-33-15deg-MGS
Test Number	MASH 2009 3-33 (15 deg)	MASH 2009 3-33 (15 deg)
System	G41S	MGS
Longitudinal OIV, ft/s (m/s)	-21.3 (-6.5)	-20.7 (-6.3)
Lateral OIV, ft/s (m/s)	1.0 (0.3)	1.6 (0.5)
Longitudinal ORA, g's	4.8	-6.9
Lateral ORA, g's	3.9	3.8
Maximum Roll Angle, deg	-1.3	1.6
Maximum Pitch Angle, deg	1.1	1.7
Maximum Yaw Angle, deg	-1.4	-0.8
Guardrail Feed Length, ft (m)	4.8 (1.5)	4.7 (1.4)
Buckle Location	26 in. DS of Post no. 2	25 in. DS of Post no. 2



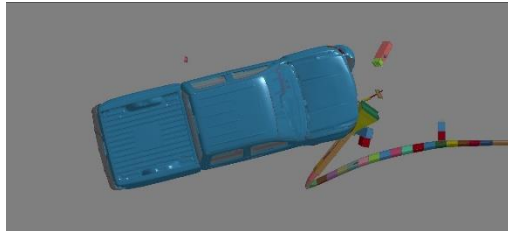
0.000 sec



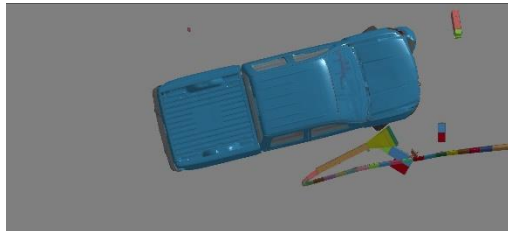
0.070 sec



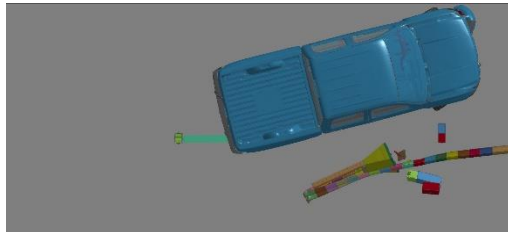
0.140 sec



0.210 sec

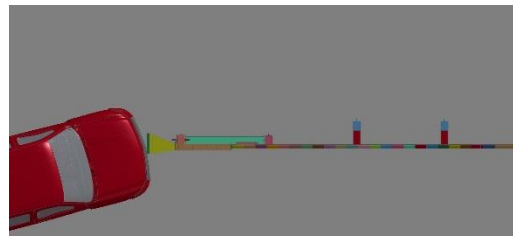


0.280 sec

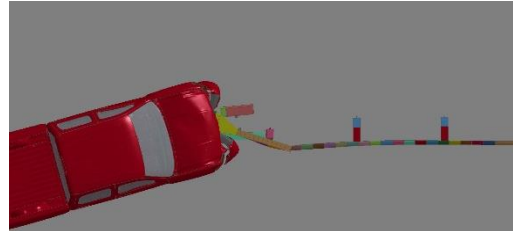


0.350 sec

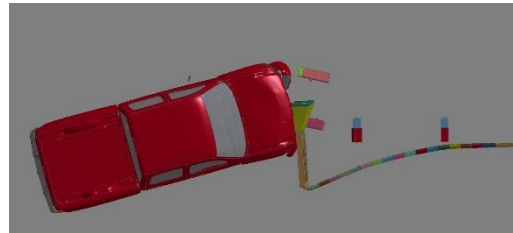
Simulation No. MASH-33-15deg-G41S



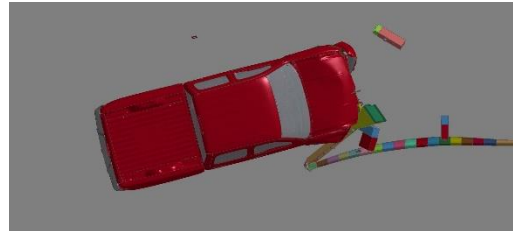
0.000 sec



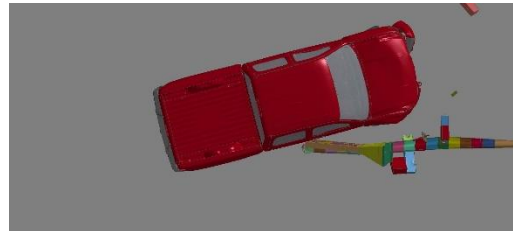
0.070 sec



0.140 sec



0.210 sec



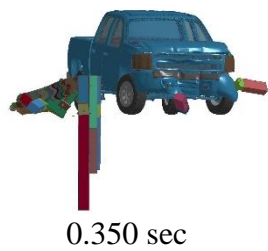
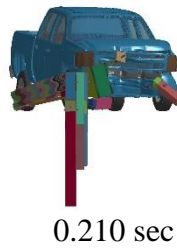
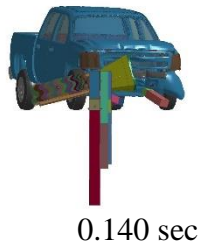
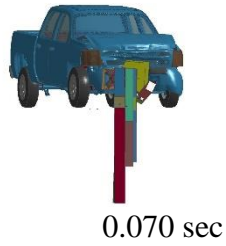
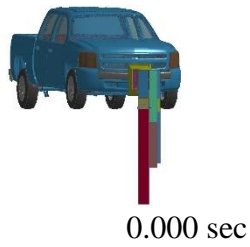
0.280 sec



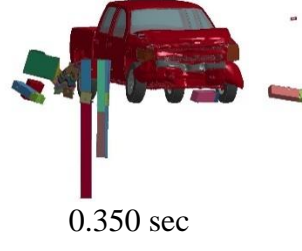
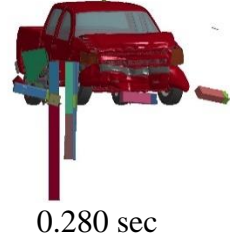
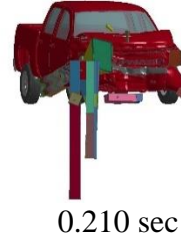
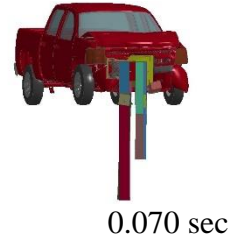
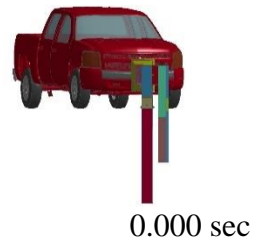
0.350 sec

Simulation No. MASH-33-15deg-MGS

Figure 52. MASH 2009 Test No. 3-33 at 15 degrees, Overhead View



Simulation No. MASH-33-15deg-G41S



Simulation No. MASH-33-15deg-MGS

Figure 53. MASH 2009 Test No. 3-33 at 15 degrees, Downstream View

7 COMPARISON OF THE END TERMINAL MODEL

At the time of this report, compression end terminals, only some NCHRP Report 350 crash test results were available. The exact terminal configuration varied in the crash tests, especially post material and type. The general system and vehicle behavior, guardrail feed lengths, and occupant risk measures were compared between available successful full-scale crash tests and the simulations conducted in Chapter 6. The simulations did not account for variance in impact conditions that occurred in the crash tests. The sign convention on OIV and ORA values also varied between crash tests and simulations. Thus, only the magnitude of these values was compared. The longitudinal and lateral OIVs and ORAs determined in the simulations likely do not provide a representative comparison to the crash tests. The discrepancies occurred due to the fact that the actual energy-absorbing mechanism for each end terminal was not modeled, and several simplifications occurred in the vehicle and rail model that may not accurately represent these values. However, they were included for comparison here and will be more useful when comparing simulations with and without curbs.

7.1 NCHRP Report 350 Test No. 3-30

7.1.1 27¾-in. (706-mm) Tall W-Beam End Terminal Impacts

Several full-scale crash tests have been conducted according to NCHRP Report 350 test no. 3-30 on approximately 27¾-in. (706-mm) tall end terminal systems installed on W-beam guardrail systems such as G4(1S) and G4(2W). Results from these tests and the corresponding simulations are shown in Table 21. Sequential photographs from the simulations and select tests are shown in Figures 54 through 56. The longitudinal OIVs and ORAs were typically higher in the simulations than the crash tests, which may be attributed to some variations between the model and actual systems. For instance, the mass of the model impact head is greater than some of the as-tested end terminals. Several of the crash tests also utilized proprietary steel post breakaway posts, which may breakaway more easily and consistently than wood post model. Additionally, the impact head contact with the front of the vehicle created some entangled nodes and contact interference, which likely elevated forces. The feed lengths of the simulations were representative of the crash tests.

7.1.2 31-in. (787-mm) Tall W-Beam End Terminal Impacts

Several full-scale crash tests have been conducted according to NCHRP Report 350 test no. 3-30 on approximately 31-in. (787-mm) tall end terminal systems installed on W-beam guardrail systems like MGS. Results from these tests and the corresponding simulation are shown in Table 22. Sequential photographs from the simulations and select tests are shown in Figures 57 and 58. . The longitudinal OIVs and ORAs were typically higher in the simulations than the crash tests, which may be attributed to some variations between the model and actual systems. For instance, the mass of the model impact head is greater than some of the as-tested end terminals. Several of the crash tests also utilized proprietary steel post breakaway posts, which may breakaway more easily and consistently than wood post model. Additionally, the impact head contact with the front of the vehicle created some entangled nodes and contact interference, which likely elevated forces. The high longitudinal ORA in simulation no. NCHRP 3-30 shallow-qtr-pt occurred when a post-to-rail bolt snagged as it tried to release. As discussed

previously, rail release when impacted end-on was not calibrated due to not modeling steel material failure, including tearing. The feed lengths of the simulations were representative of the crash tests.

Table 21. NCHRP Report 350 Test No. 3-30, 27¾ in. (706 mm) Tall, Results Comparison

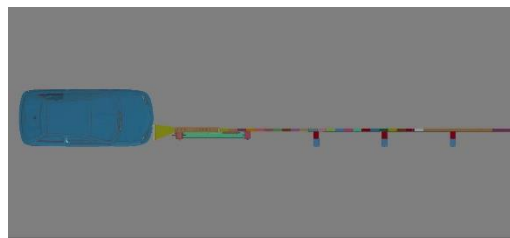
End Terminal System	Test No.	Ref. No.	Feed Length ft (m)	Long. OIV ft/s (m/s)	Lat. OIV ft/s (m/s)	Long. ORA g's	Lat. ORA g's
Simulation G4(1S)	NCHRP 3-30 shallow-qtr-pt	-	12.5 (3.8)	36.1 (11.0)	3.9 (1.2)	17.1	5.7
Simulation G4(1S)	NCHRP 3-30 deep-qtr-pt	-	14.2 (4.3)	29.9 (9.1)	2.3 (0.7)	10.2	7.3
ET-Plus	ET27-30	27	16 (4.9)*	24.6 (7.5)	1.31 (.4)	14	6.8
ET-Plus	220547-4	24	16 (4.9)	26.9 (8.2)	2.63 (.8)	11	4.8
ET-2000	6001-1	25	NA	30.6 (9.3)	NA	17.3	NA
FLEAT	FLEAT-1	31	11.8 (3.6)	22.0 (6.7)	7.56 (2.3)	8.4	8.9
FLEAT	FLT2P-3	34	20.3 (6.2)	25.3 (7.7)	0.33 (0.1)	13.3	5.2
SKT	SBD-4	35	14.1 (4.3)	21.1 (6.4)	11.8 (3.6)	5.6	3.9
SKT	SP-1	32	13 (4.0)*	27.6 (8.4)	11.5 (3.5)	12.1	10.8
BEST	BEST-8	23	6 (1.8)	33.2 (10.1)	9.2 (2.8)	16.7	4.9

NA = not available

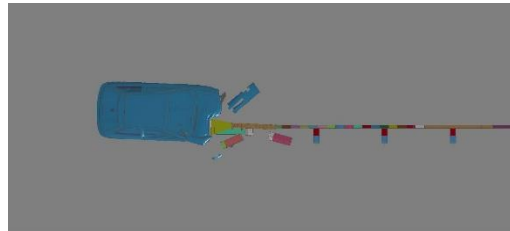
*Values were estimated from sequential and post-test photographs

Table 22. NCHRP Report 350 Test No. 3-30, 31 in. (787 mm) Tall, Results Comparison

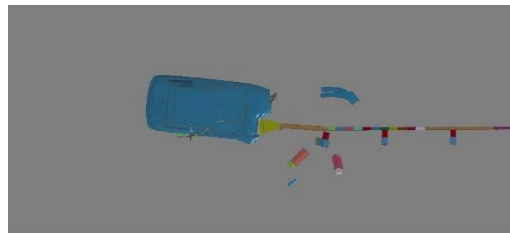
End Terminal System	Test No.	Ref. No.	Feed Length ft (m)	Long. OIV ft/s (m/s)	Lat. OIV ft/s (m/s)	Long. ORA g's	Lat. ORA g's
Simulation MGS	NCHRP 3-30 shallow-qtr-pt	-	13.3 (4.1)	31.2 (9.5)	2.0 (0.6)	22.5	7.6
Simulation MGS	NCHRP 3-30 deep-qtr-pt	-	13.3 (4.1)	29.9 (9.1)	3.0 (0.9)	9.8	8.6
ET-Plus	ET31-30	28	13 (4.0)	26.9 (8.2)	1.31 (0.4)	11.8	8.7
ET-Plus	220601-2	29	17.8 (5.4)	27.3 (8.3)	0.99 (0.3)	14	4.3
FLEAT	FLEAT-8	32	16 (4.9)	25.6 (7.8)	0.99 (0.3)	12.2	6.6



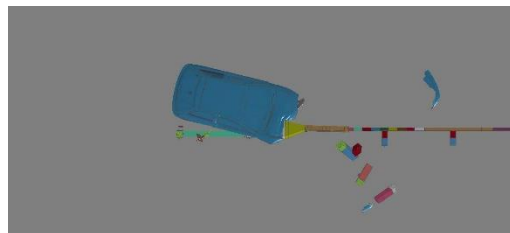
0.000 sec



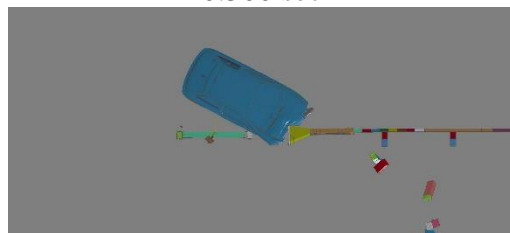
0.100 sec



0.200 sec



0.300 sec

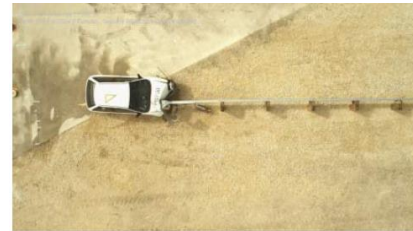


0.400 sec

Simulation No. NCHRP-30-shallow-G41S



0.000 sec



0.100 sec



0.200 sec



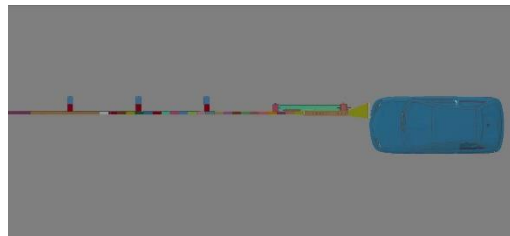
0.300 sec



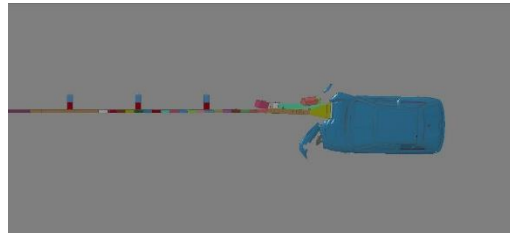
0.400 sec

ET-Plus - Test No. ET27-30

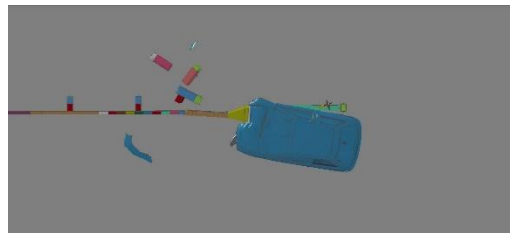
Figure 54. NCHRP Report 350 Test No. 3-30, 27¾ in. (706 mm) Tall



0.000 sec

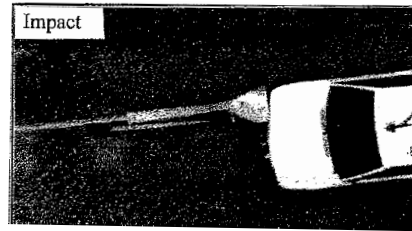


0.070 sec

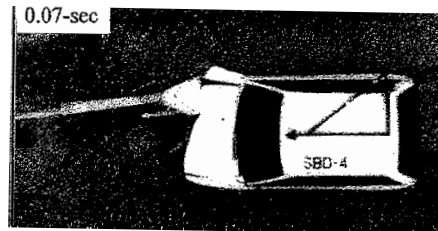


0.250 sec

Simulation No. NCHRP-30-shallow-G41S



0.000 sec



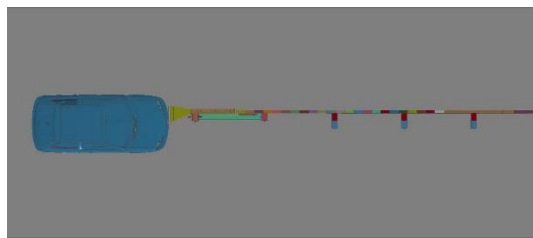
0.070 sec



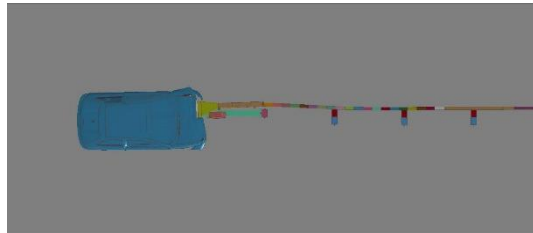
0.250 sec

SKT - Test No. SBD-4

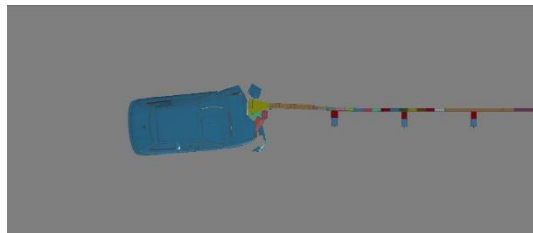
Figure 55. NCHRP Report 350 Test No. 3-30, 27¾ in. (706 mm) Tall



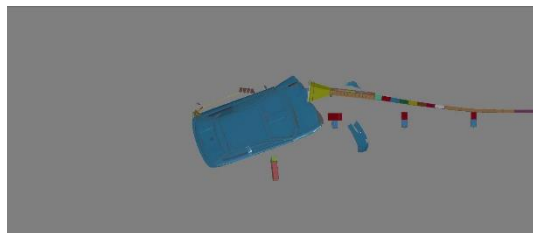
0.000 sec



0.050 sec



0.120 sec

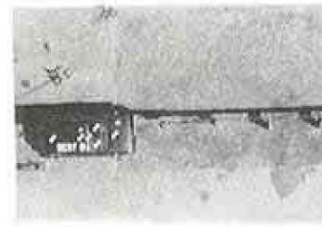


0.240 sec



0.460 sec

Simulation No. NCHRP-30-deep-G41S



0.000 sec



0.050 sec



0.120 sec



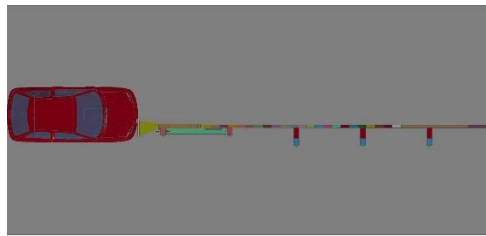
0.240 sec



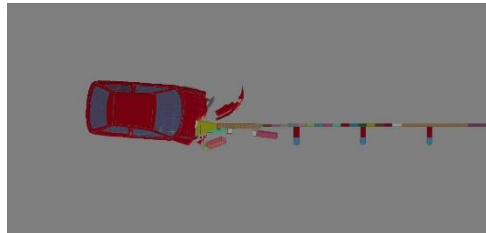
0.460 sec

BEST - Test No. BEST-8

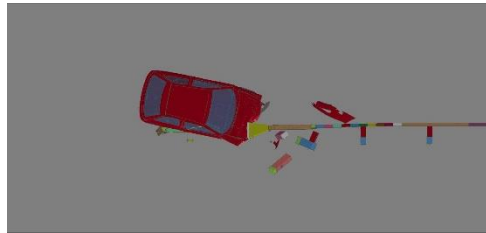
Figure 56. NCHRP Report 350 Test No. 3-30, 27¾ in. (706 mm) Tall



0.000 sec



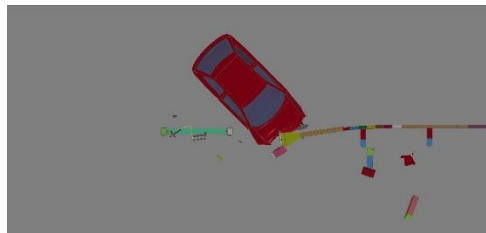
0.100 sec



0.200 sec



0.300 sec



0.400 sec

Simulation No. NCHRP-30-shallow-MGS



0.000 sec



0.100 sec



0.200 sec



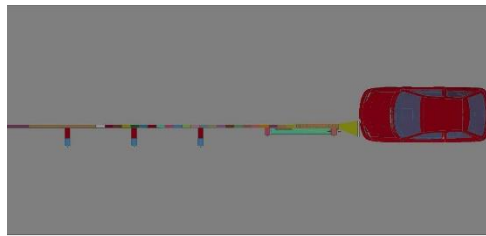
0.300 sec



0.400 sec

ET-Plus - Test No. ET31-30

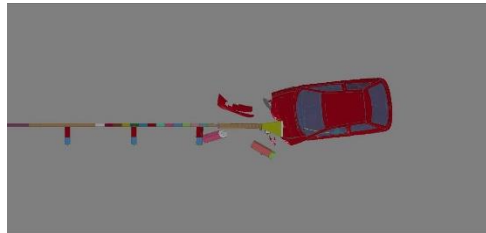
Figure 57. NCHRP Report 350 Test No. 3-30, 31 in. (787 mm) Tall



0.000 sec



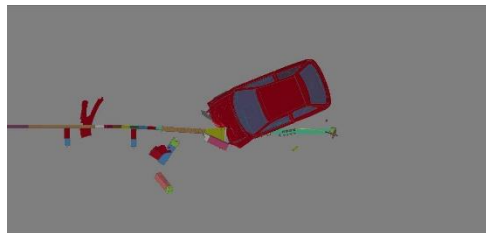
0.000 sec



0.130 sec



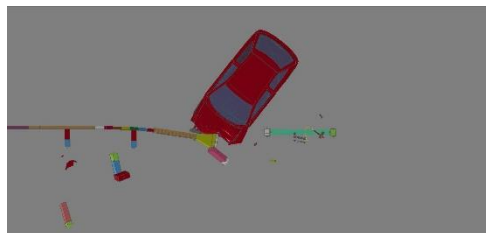
0.132 sec



0.280 sec



0.280 sec



0.430 sec



0.426 sec

Simulation No. NCHRP-30-shallow-MGS

FLEAT - Test No. FLEAT-8

Figure 58. NCHRP Report 350 Test No. 3-30, 31 in. (787 mm) Tall

7.2 NCHRP Report 350 Test No. 3-31

7.2.1 27¾-in. (706-mm) Tall W-Beam End Terminal Impacts

Several full-scale crash tests have been conducted according to NCHRP Report 350 test no. 3-31 on approximately 27¾-in. (706-mm) tall end terminal systems installed on W-beam guardrail systems like G4(1S) and G4(2W). Results from these tests and the corresponding simulation are shown in Table 23. Sequential photographs from the simulation and select tests are shown in Figures 59 through 61. The longitudinal ORA was typically higher in the simulation than the crash tests. The feed length in the simulation was representative of the crash tests. The average end terminal force was calculated to be 16.1 kips (71.8 kN) in the simulation, which was near the center of the targeted range.

Table 23. NCHRP Report 350 Test No. 3-31, 27¾ in. (706 mm) Tall, Results Comparison

End Terminal System	Test No.	Ref. No.	Feed Length ft (m)	Long. OIV ft/s (m/s)	Lat. OIV ft/s (m/s)	Long. ORA g's	Lat. ORA g's
Simulation G4(1S)	NCHRP 3-31	-	34.1 (10.4)	21.0 (6.4)	1.0 (0.3)	16.0	5.0
ET-Plus	ET27-31	27	37.4 (11.4)	23.3 (7.1)	0.99 (0.3)	9.2	5.0
ET-2000 Plus	400001-LET1	30	38.1 (11.6)	20.4 (6.2)	0.33 (0.1)	6.9	2.8
ET-2000	400001-XTI3	42	24.6 (7.5)	20.0 (6.1)	4.3 (1.3)	5.5	3.1
ET-2000	220510-5	25	24.9 (7.6)	26.6 (8.1)	3.3 (1.0)	13.0	6.5
ET-2000	520201-1	26	24.9 (7.6)	25.0 (7.6)	1.6 (0.5)	11.9	2.7
FLEAT	FLEAT-2	31	5 (1.5)	20.4 (6.2)	5.6 (1.7)	10.4	4.2
FLEAT	FLEAT-3	31	28 (8.5)	20.4 (6.2)	0.66 (0.2)	7.0	6.7
SKT	SBD-3	35	52.5 (16)	19.4 (5.9)	4.9 (1.5)	7.6	5.4
BEST	BEST-9	23	29.2 (8.9)	22.7 (6.9)	3.3 (1.0)	13.3	2.8

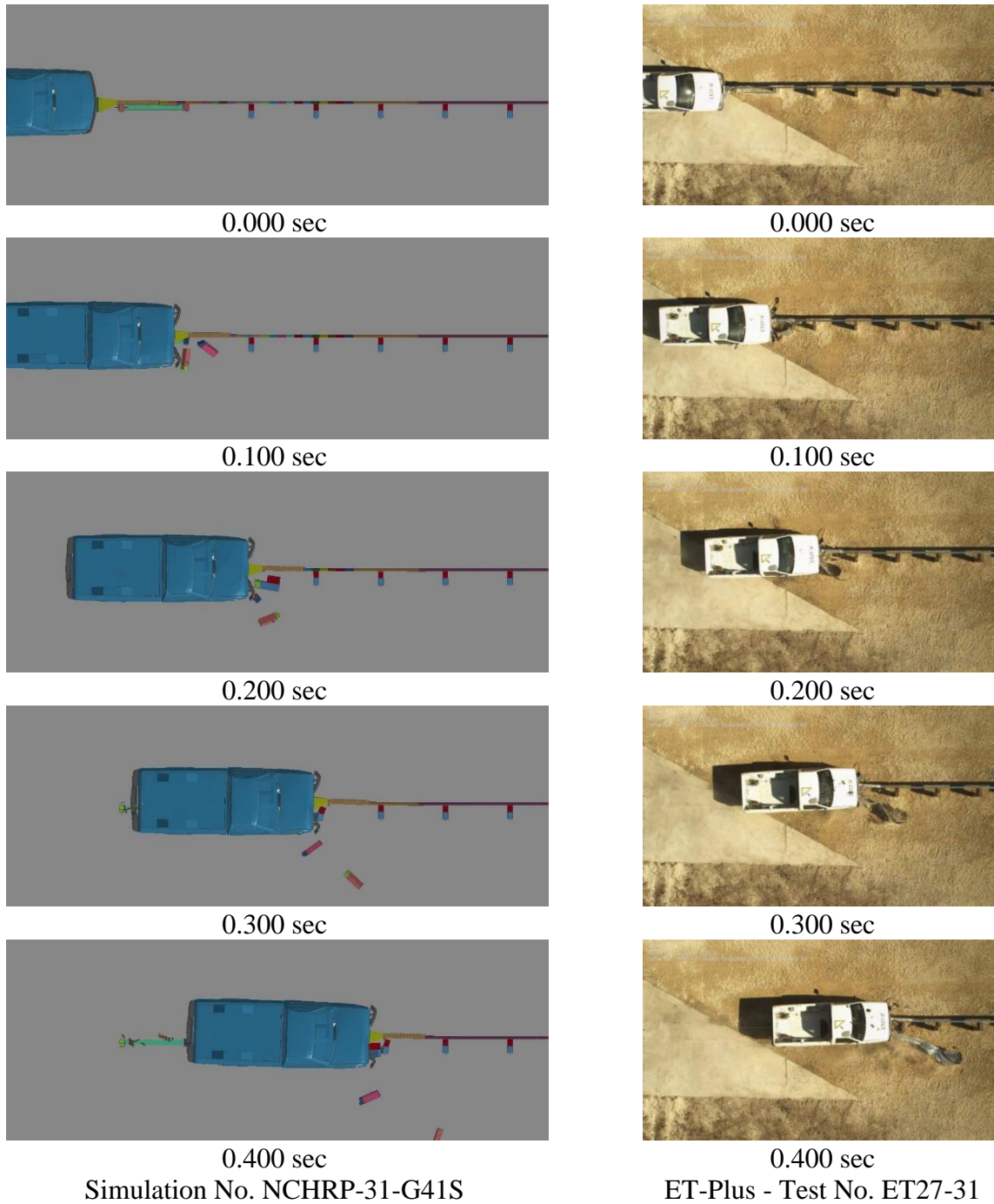


Figure 59. NCHRP Report 350 Test No. 3-31, 27¾ in. (706 mm) Tall

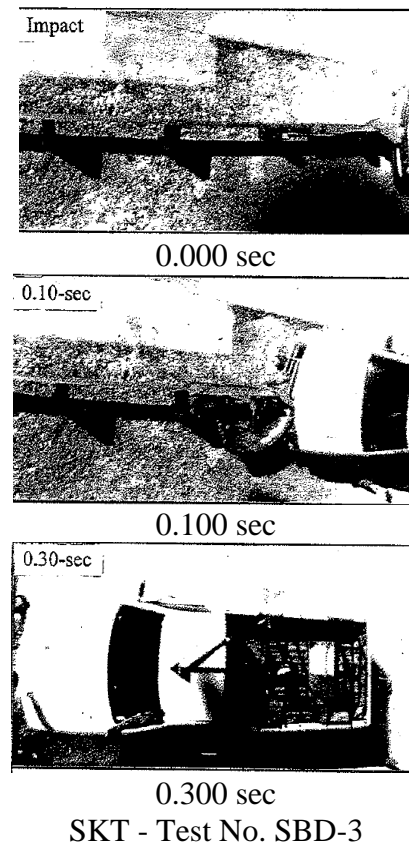
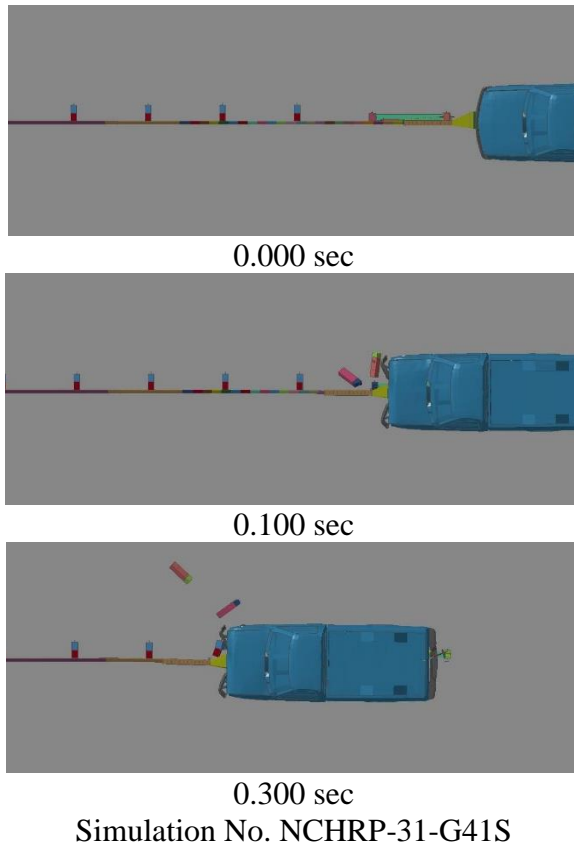


Figure 60. NCHRP Report 350 Test No. 3-31, 27¾ in. (706 mm) Tall

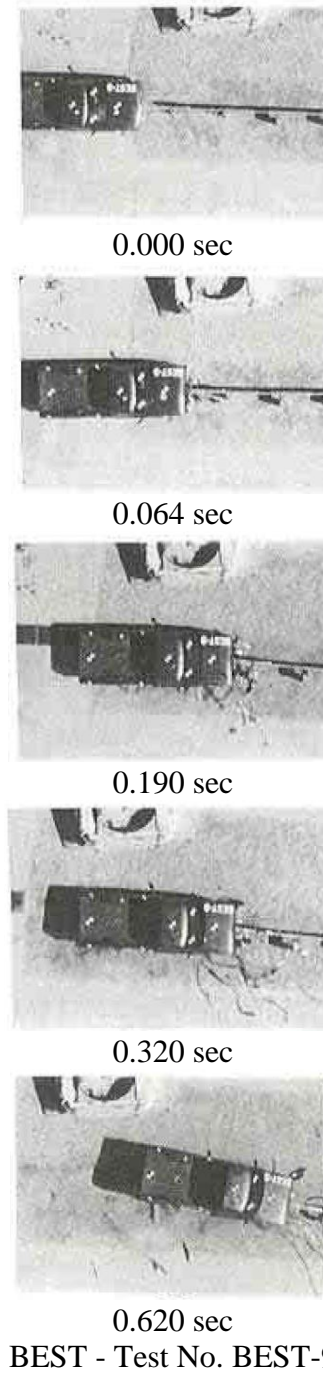
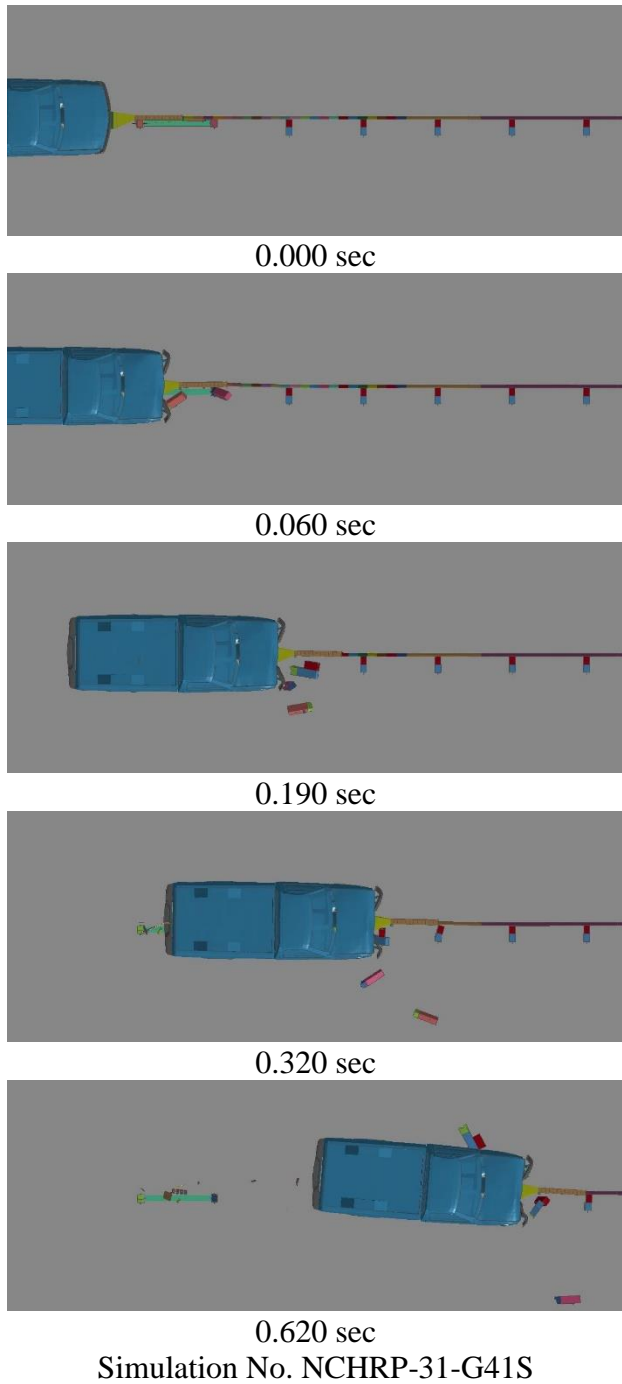


Figure 61. NCHRP Report 350 Test No. 3-31, 27³/₄ in. (706 mm) Tall

7.2.2 31-in. (787-mm) Tall W-Beam End Terminal Impacts

Two full-scale crash tests have been conducted according to NCHRP Report 350 test no. 3-31 on approximately 31-in. (787-mm) tall end terminal systems installed on W-beam guardrail systems like MGS. Results from these tests and the corresponding simulation are shown in Table 24. Sequential photographs from the simulation and select tests are shown in Figures 62 and 63. The longitudinal OIVs and ORAs were typically higher in the simulations than the crash tests. The feed length in the simulation was lower than the two crash tests. It was expected that the feed lengths may increase slightly with an increase in rail height as the c.g. height of the truck is more closely aligned with the c.g. height of end terminal. It was difficult to calibrate the representative end terminal simulation with only two crash tests for comparison. However, the feed length was representative of the 27¾-in. (706-mm) tall guardrail with more comparison data points, and the average end terminal force was calculated to be 15.3 kips (68.2 kN) in the 31-in. (787-mm) tall guardrail simulation, which was near the center of the targeted range.

Table 24. NCHRP Report 350 Test No. 3-31, 31 in. (787 mm) Tall, Results Comparison

End Terminal System	Test No.	Ref. No.	Feed Length ft (m)	Long. OIV ft/s (m/s)	Lat. OIV ft/s (m/s)	Long. ORA g's	Lat. ORA g's
Simulation MGS	NCHRP 3-31	-	36.4 (11.1)	20.0 (6.1)	1.3 (0.4)	13.9	7.3
ET-Plus	ET31-31	28	50.9 (15.5)	19.4 (5.9)	0.66 (0.2)	8.0	7.0
SKT	SMG-1	32	57.5 (17.5)	18.4 (5.6)	0.99 (0.3)	8.7	5.7

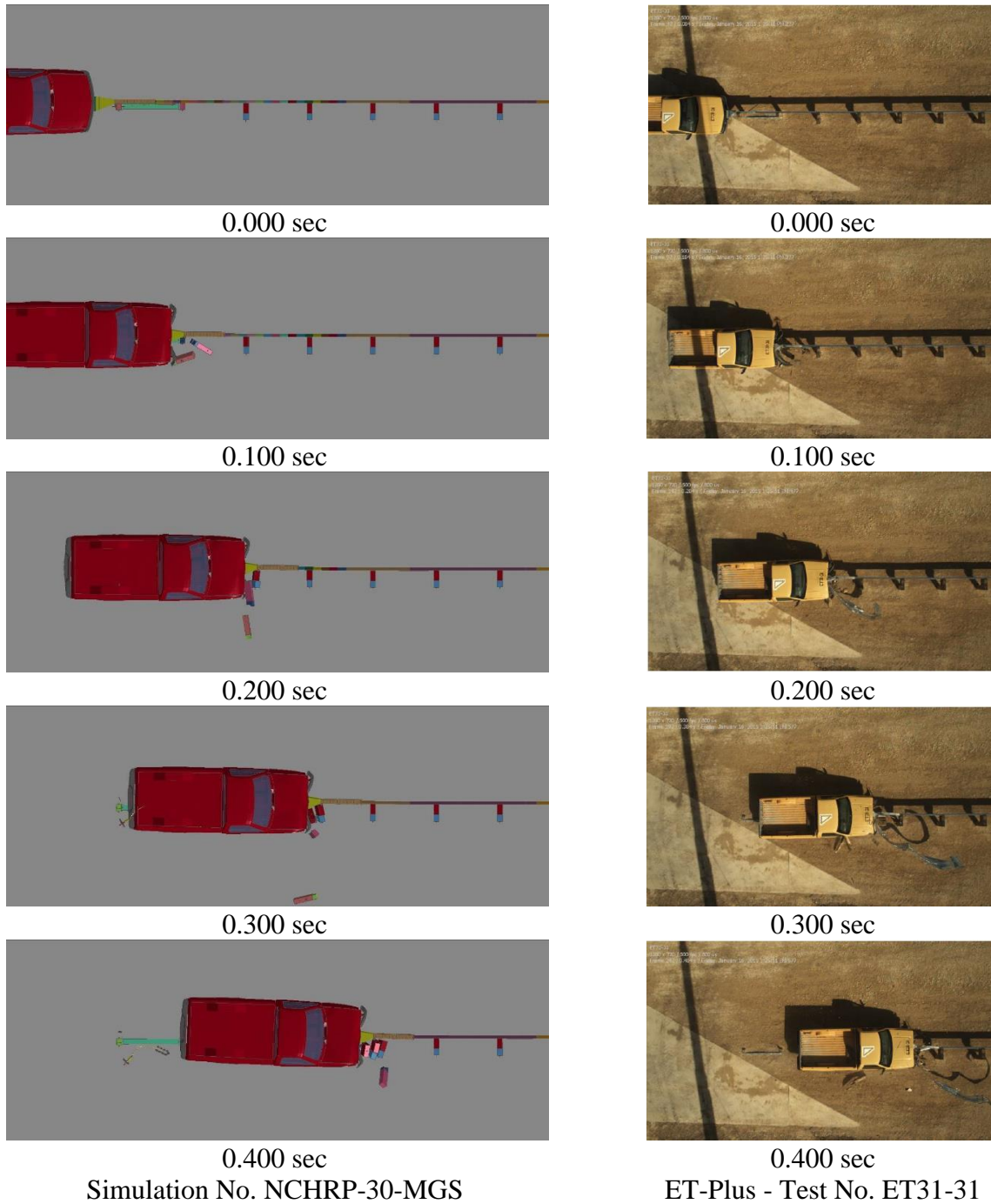


Figure 62. NCHRP Report 350 Test No. 3-31, 31 in. (787 mm) Tall

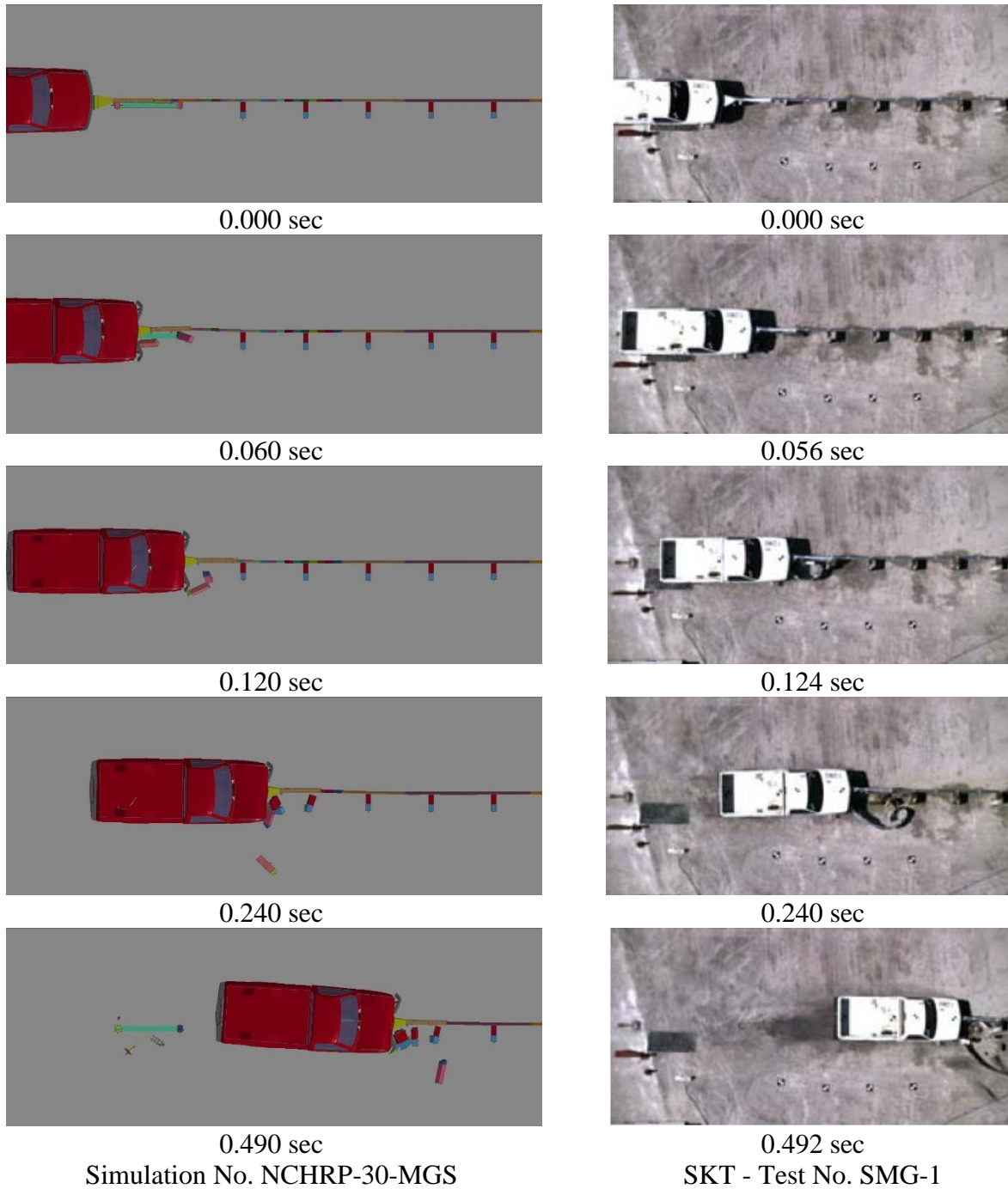


Figure 63. NCHRP Report 350 Test No. 3-31, 31 in. (787 mm) Tall

7.3 NCHRP Report 350 Test No. 3-32

7.3.1 27¾-in. (706-mm) Tall W-Beam End Terminal Impacts

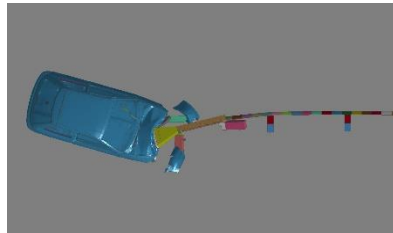
Several full-scale crash tests have been conducted according to NCHRP Report 350 test no. 3-32 on approximately 27¾-in. (706-mm) tall end terminal systems installed on W-beam guardrail systems like G4(1S) and G4(2W). Results from these tests and the corresponding simulation are shown in Table 25. Sequential photographs from the simulation and select tests are shown in Figures 64 through 66. The impact head remained engaged with the front of the vehicle in the simulation for longer than what has occurred in full-scale crash testing, which may partially be attributed to the impact head and vehicle nodes becoming entangled. When the impact head model disengaged from the front bumper and hood, the impact head twisted and translated upward. The impact head typically releases to the side of the vehicle in full-scale crash testing, and not upward as observed in the model. The ORAs were typically higher, and the lateral OIVs were lower in the simulation than the crash tests. The guardrail with the 15-degree impact angle in the crash tests almost always buckled between post nos. 1 and 3 and varied within this range, and this buckling corresponded to the feed lengths. However, the feed length in the simulation was representative of the crash tests even with the variance.

Table 25. NCHRP Report 350 Test No. 3-32, 27¾ in. (706 mm) Tall, Results Comparison

End Terminal System	Test No.	Ref. No.	Feed Length ft (m)	Long. OIV ft/s (m/s)	Lat. OIV ft/s (m/s)	Long. ORA g's	Lat. ORA g's
Simulation G4(1S)	NCHRP 3-32	-	8.7 (2.7)	32.5 (9.9)	2.0 (0.6)	13.0	9.2
ET-Plus	ET27-32	27	3 (0.9)	27.9 (8.5)	4.9 (1.5)	4.1	3.3
ET-2000	220510-3	25	7.9 (2.4)	29.6 (9.0)	7.9 (2.4)	7.4	5.9
ET-2000	400001-XTI2	42	8.6 (2.6)	26.9 (8.2)	5.3 (1.6)	5.6	4.3
SKT	SBD-5	35	13.5 (4.1)	24.3 (7.4)	4.9 (1.5)	9.6	3.1
BEST	BEST-4	23	4.2 (1.3)	32.9 (10)	3.9 (1.2)	12	4.7



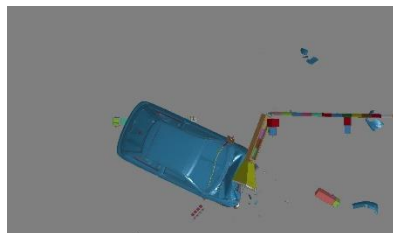
0.000 sec



0.100 sec



0.200 sec

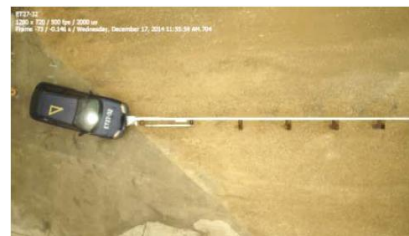


0.300 sec



0.400 sec

Simulation No. NCHRP-32-G41S



0.000 sec



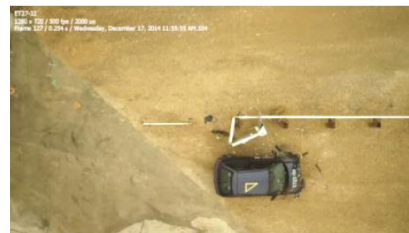
0.100 sec



0.200 sec



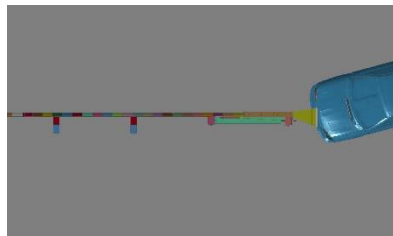
0.300 sec



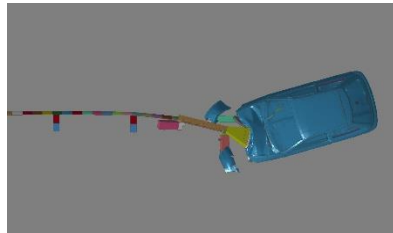
0.400 sec

ET-Plus - Test No. ET27-32

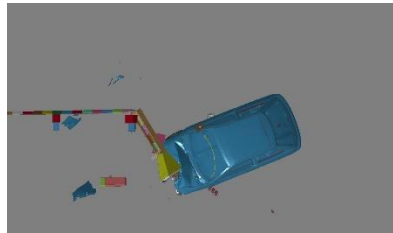
Figure 64. NCHRP Report 350 Test No. 3-32, 27¾ in. (706 mm) Tall



0.000 sec



0.100 sec

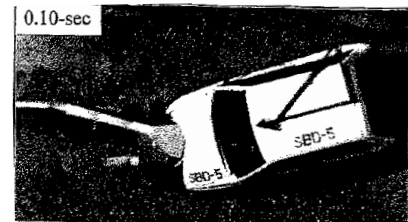


0.250 sec

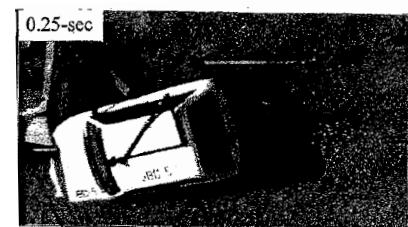
Simulation No. NCHRP-32-G41S



0.000 sec



0.100 sec



0.250 sec

SKT - Test No. SBD-5

Figure 65. NCHRP Report 350 Test No. 3-32, 27¾ in. (706 mm) Tall



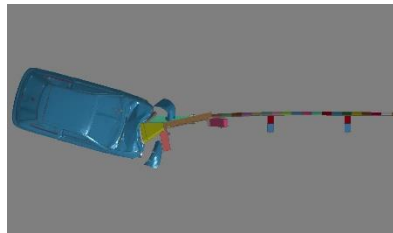
0.000 sec



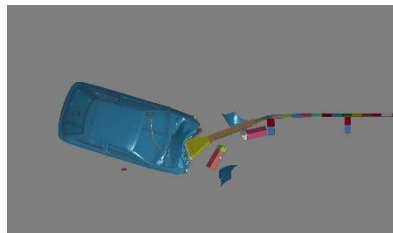
0.020 sec



0.040 sec

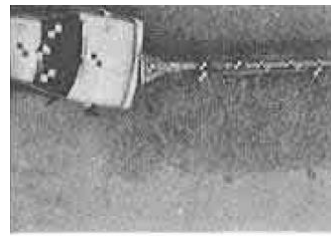


0.080 sec



0.150 sec

Simulation No. NCHRP-32-G41S



0.000 sec



0.022 sec



0.044 sec



0.080 sec



0.145 sec

BEST - Test No. BEST-4

Figure 66. NCHRP Report 350 Test No. 3-32, 27¾ in. (706 mm) Tall

7.3.2 31-in. (787-mm) Tall W-Beam End Terminal Impacts

One full-scale crash test has been conducted according to NCHRP Report 350 test no. 3-32 on approximately 31-in. (787-mm) tall end terminal systems installed on W-beam guardrail systems like MGS. Results from the test and the corresponding simulation are shown in Table 26. Sequential photographs from the simulation and the test are shown in Figure 67. The impact head remained engaged with the front of the vehicle in the simulation for longer than what has occurred in full-scale crash testing, which may partially be attributed to the impact head and vehicle nodes becoming entangled. When the impact head model disengaged from the front bumper and hood, the impact head twisted and translated upward. The impact head typically releases to the side of the vehicle in full-scale crash testing, and not upward as observed in the model. The longitudinal OIV was higher and the lateral OIV was lower in the simulation as compared to the crash test. The feed length was representative of the crash test. However, it was difficult to calibrate the representative end terminal using only one crash test with this configuration and impact conditions.

Table 26. NCHRP Report 350 Test No. 3-32, 31 in. (787 mm) Tall, Results Comparison

End Terminal System	Test No.	Ref. No.	Feed Length ft (m)	Long. OIV ft/s (m/s)	Lat. OIV ft/s (m/s)	Long. ORA g's	Lat. ORA g's
Simulation MGS	NCHRP 3-32	-	8.7 (2.7)	32.2 (9.8)	2.3 (0.7)	8.9	5.1
ET-Plus	ET31-32	28	9.5 (2.9)	26.0 (7.9)	4.3 (1.3)	6.4	6.3



0.000 sec



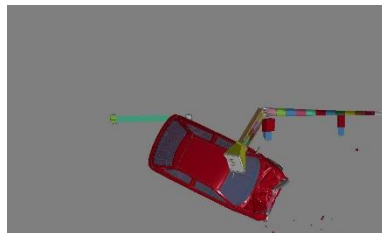
0.100 sec



0.200 sec



0.300 sec



0.400 sec

Simulation No. NCHRP-32-MGS



0.000 sec



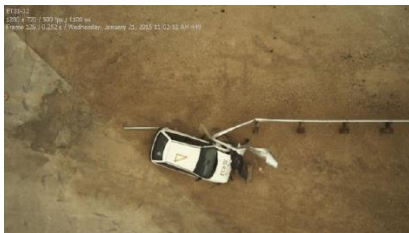
0.100 sec



0.200 sec



0.300 sec



0.400 sec

ET-Plus - Test No. ET31-32

Figure 67. NCHRP Report 350, Test No. 3-32, 31 in. (787 mm) Tall

7.4 NCHRP Report 350 Test No. 3-33

7.4.1 27¾-in. (706-mm) Tall W-Beam End Terminal Impacts

Several full-scale crash tests have been conducted according to NCHRP Report 350 test no. 3-33 on approximately 27¾-in. (706-mm) tall end terminal systems installed on W-beam guardrail systems like G4(1S) and G4(2W). Results from these tests and the corresponding simulation are shown in Table 27. Sequential photographs from the simulation and select tests are shown in Figures 68 and 69. The longitudinal OIV was higher and the lateral OIV was smaller in the simulation than the crash tests. The guardrail with the 15-degree impact angle in the crash tests almost always buckled between post nos. 1 and 3 and varied within this range, and this buckling corresponded to the feed lengths. However, the feed length in the simulation was representative of the crash tests even with the variance.

Table 27. NCHRP Report 350 Test No. 3-33, 27¾ in. (706 mm) Tall, Results Comparison

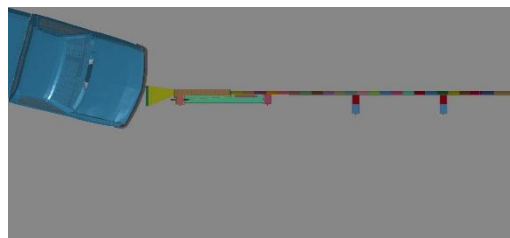
End Terminal System	Test No.	Ref. No.	Feed Length ft (m)	Long. OIV ft/s (m/s)	Lat. OIV ft/s (m/s)	Long. ORA g's	Lat. ORA g's
Simulation G4(1S)	NCHRP 3-33	-	9.7 (3.0)	21.7 (6.6)	1.0 (0.3)	8.5	11.0
ET-Plus	ET27-33	27	3 (0.9)	14.8 (4.5)	5.0 (1.5)	7.6	4.6
ET-2000	220510-4	25	13.5 (4.1)	18.1 (5.5)	5.3 (1.6)	4.0	3.1
SKT	SBD-6	35	13.5 (4.1)	16.8 (5.1)	5.9 (1.8)	13.9	13.3
BEST	BEST-10	23	7 (2.1)	20.4 (6.2)	7.6 (2.3)	17.5	10.0

7.4.2 31-in. (787-mm) Tall W-Beam End Terminal Impacts

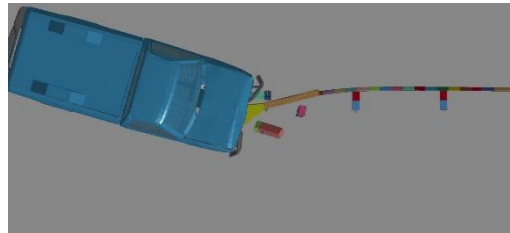
One full-scale crash test has been conducted according to NCHRP Report 350 test no. 3-33 on approximately 31-in. (787-mm) tall end terminal systems installed on W-beam guardrail systems like MGS. Results from the test and the corresponding simulation are shown in Table 28. Sequential photographs from the simulation and the test are shown in Figure 70. The longitudinal OIV was higher and the lateral OIV was lower in the simulation than the crash test. The feed length was representative of the crash test. However, it was difficult to calibrate the representative end terminal with only one crash test using this configuration.

Table 28. NCHRP Report 350 Test No. 3-33, 31 in. (787 mm) Tall, Results Comparison

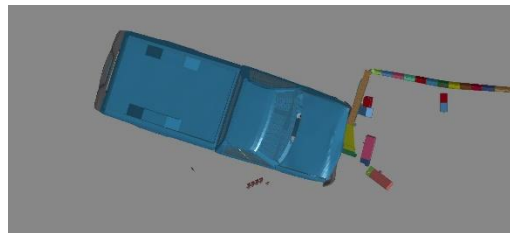
End Terminal System	Test No.	Ref. No.	Feed Length ft (m)	Long. OIV ft/s (m/s)	Lat. OIV ft/s (m/s)	Long. ORA g's	Lat. ORA g's
Simulation MGS	NCHRP 3-33	-	9 (2.7)	21.3 (6.5)	2.6 (0.8)	7.9	9.2
ET-Plus	ET31-33	28	9.5 (2.9)	15.4 (4.7)	6.6 (2.0)	9.0	6.7



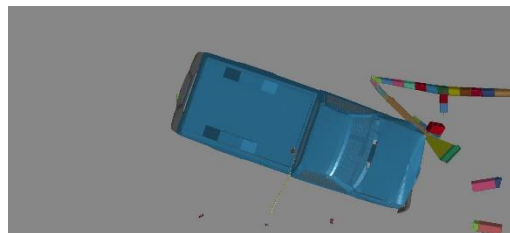
0.000 sec



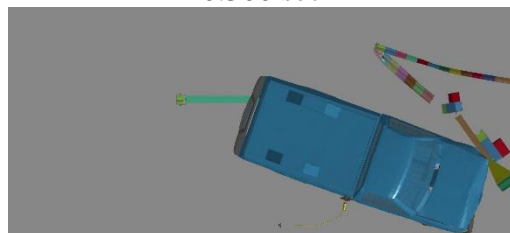
0.100 sec



0.200 sec



0.300 sec



0.400 sec

Simulation No. NCHRP-33-G41S



0.000 sec



0.100 sec



0.200 sec



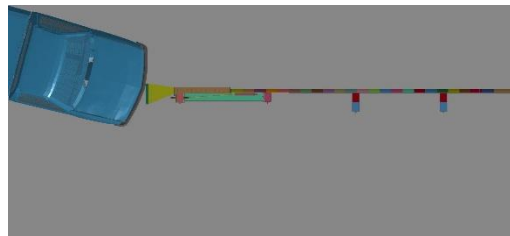
0.300 sec



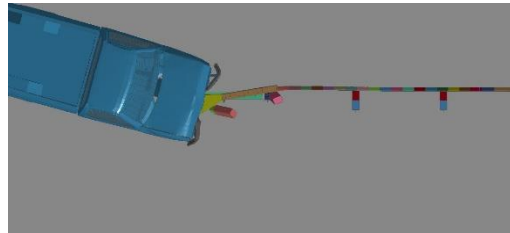
0.400 sec

ET-Plus - Test No. ET27-33

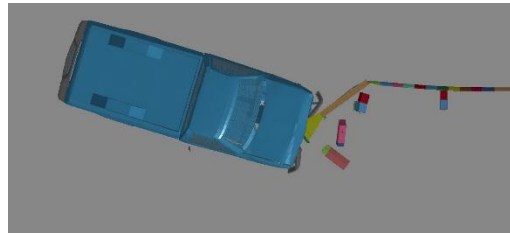
Figure 68. NCHRP Report 350 Test No. 3-33, 27¾ in. (706 mm) Tall



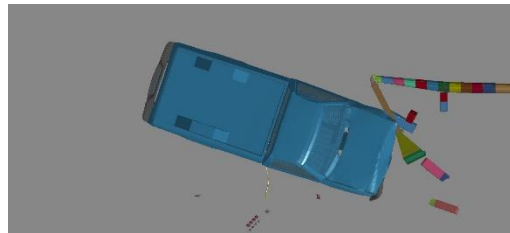
0.000 sec



0.060 sec



0.160 sec



0.260 sec

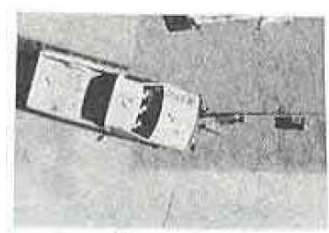


0.430 sec

Simulation No. NCHRP-33-G41S



0.000 sec



0.064 sec



0.156 sec



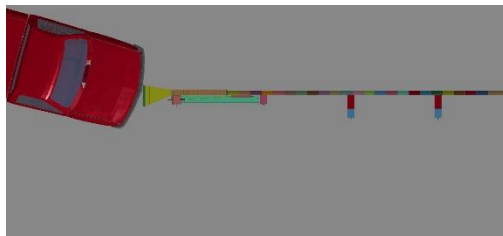
0.266 sec



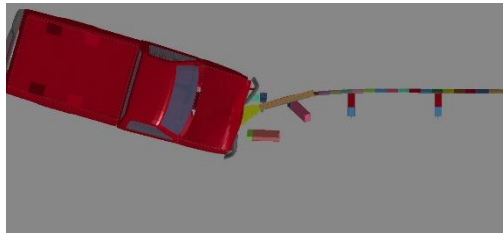
0.434 sec

BEST - Test No. BEST-10

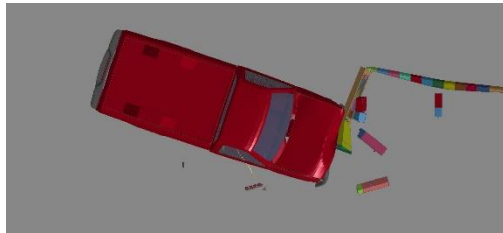
Figure 69. NCHRP Report 350 Test No. 3-33, 27¾ in. (706 mm) Tall



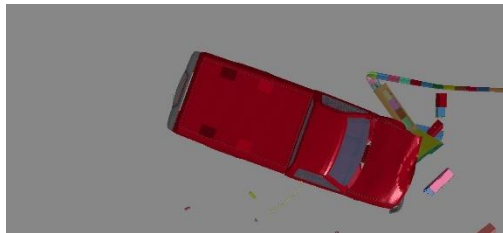
0.000 sec



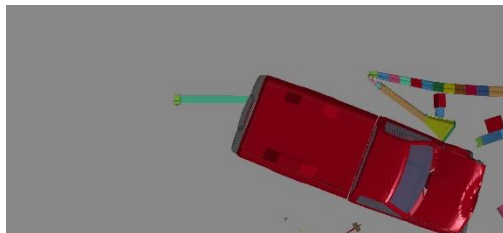
0.100 sec



0.200 sec



0.300 sec



0.400 sec

Simulation No. NCHRP-33-MGS



0.000 sec



0.100 sec



0.200 sec



0.300 sec



0.400 sec

ET-Plus - Test No. ET31-33

Figure 70. NCHRP Report 350 Test No. 3-33, 31 in. (787 mm) Tall

7.5 Discussion

In the NCHRP Report 350 test no. 3-31 crash tests, the average rail feed lengths with 31-in. (787-mm) tall guardrail were significantly greater than observed with the 27 $\frac{3}{4}$ -in. (706-mm) tall guardrail. The average terminal force for NCHRP Report 350 test no. 3-31 simulations was calculated to be 16.1 kips (71.8 kN) for 27 $\frac{3}{4}$ -in. (706-mm) tall guardrail and 15.3 kips (68.2 kN) for 31-in. (787-mm) tall guardrail, which was near the middle of the desired range of 10.5 to 22.5 kips (46.7 to 100.1 kN).

The overall vehicle and system behavior and guardrail feed length were compared and calibrated to match NCHRP Report 350 test nos. 3-30, 3-31, 3-32, and 3-33 crash tests. The rail feed lengths were similar to the crash tests in almost every simulation. The rail buckle locations were also very similar for NCHRP Report 350 test nos. 3-32 and 3-33. The vehicle roll, pitch, and yaw were similar for all simulations and crash tests, except MASH 2009 test no. 3-30, which demonstrated inaccurate rail buckling that affected yaw. The lateral and longitudinal OIV and ORA in all but two simulations were below the limits established in NCHRP Report 350 or MASH 2009. NCHRP Report 350 test no. 3-30 with 31-in. (787-mm) tall guardrail and MASH 2009 test no. 3-32 at a 5-degree impact angle with 27 $\frac{3}{4}$ -in. (706-mm) tall guardrail exceeded the longitudinal ORA value of 20 g's. However, the high acceleration occurred when a post-to-rail bolt snagged as it tried to release. As discussed previously, rail release when impacted end-on was not calibrated due to not modeling steel material failure, including tearing. In addition, all of the simulations tended to overpredict occupant risk measures when compared to crash tests. Since none of the specific end terminals were modeled, the occupant risk values were not expected to compare with crash tests and were calculated to compare trends between simulations. Due to the fact that a specific end terminal was not modeled and simplifications were incorporated within the model, limited conclusions can be made regarding the performance of the terminal beyond the initial impact head contact and rail feed.

Of note, very few crash tests with a 31 in. (787-mm) tall guardrail height were available. Overall, the comparisons were reasonably close. However, due to the limited results, the model cannot likely encompass the performance of all end terminal systems that would be seen across multiple end terminal crash tests.

8 SIMULATIONS WITH CURBS

Simulations with curbs were conducted with the MGS model according to MASH 2009 impact conditions. Several curb configurations were selected based on the survey results and sponsor direction including:

- 1) curb heights of 2 in., 4 in., and 6 in. (51 mm, 102 mm, and 152 mm);
- 2) wedge and vertical curb shapes; and
- 3) curb toe lateral offset 0 in., 6 in., 6 ft (0 mm, 152 mm, 1,829 mm) away from front face of guardrail.

The curb shapes that were evaluated are shown in Figure 71. The top edge of the curbs were rounded to prevent contact problems with the vehicle tires.

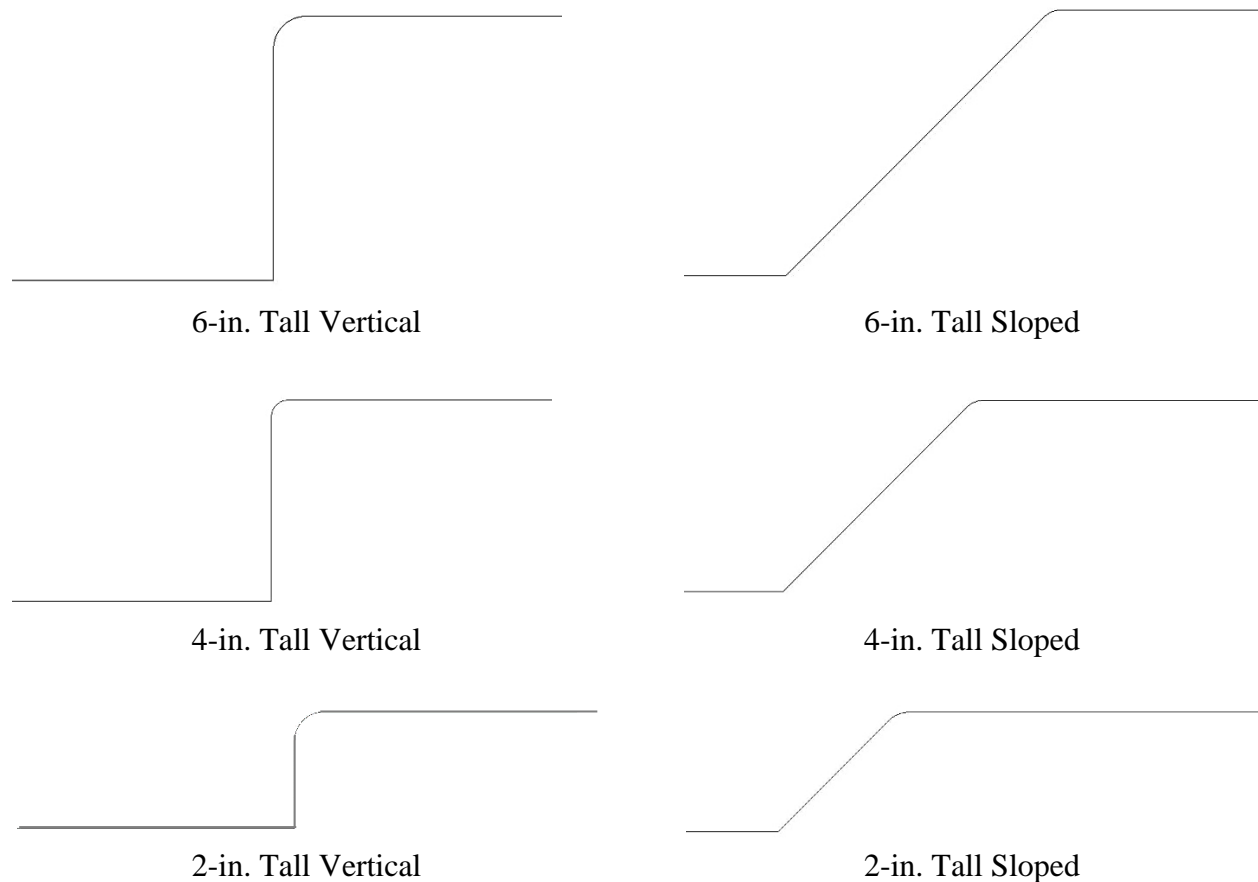


Figure 71. Curb Shapes

For each curb configuration, up to seven simulations were evaluated according to MASH 2009 TL-3 impact conditions:

- 1) 1100C small car (Yaris) impacting end at 0 deg at shallow quarter point offset (MASH 2009 test no. 3-30)

- 2) 1100C small car (Yaris) impacting end at 0 deg at deep quarter point offset (MASH 2009 test no. 3-30)
- 3) 2270P pickup truck (Silverado) impacting end at 0 deg (MASH 2009 test no. 3-31)
- 4) 1100C small car (Yaris) impacting end at 5 deg (MASH 2009 test no. 3-32)
- 5) 1100C small car (Yaris) impacting end at 15 deg (MASH 2009 test no. 3-32)
- 6) 2270P pickup truck (Silverado) impacting end at 5 deg (MASH 2009 test no. 3-33)
- 7) 2270P pickup truck (Silverado) impacting end at 15 deg (MASH 2009 test no. 3-33)

MASH 2009 test no. 3-31 was only simulated with 6-in. (152-mm) tall curbs as the curb had a minimal effect, and shorter curbs were likely to have an insignificant effect on the vehicle and terminal performance.

When curbs are installed adjacent to longitudinal barriers at small lateral offsets, the guardrail height is generally relative to the roadway surface, or the toe of the curb. When curbs are installed with large lateral offsets in front of longitudinal barriers, the guardrail height is generally installed relative to the groundline at the base of the posts, or usually the crown of the curb. However, the definition of small and large lateral offsets is subjective and can vary between State DOTs.

Manufacturers typically provide an end terminal system with the breakaway features located at the groundline (i.e., 31 in. (787 mm) below the top of the guardrail). However, if the curb is installed near the face of the guardrail, and there is soil fill behind the curb, the guardrail height would be 31 in. (787 mm) above the roadway surface (i.e., the top of the guardrail would be 25 in. (635 mm) above the groundline and 31 in. (787 mm) above the roadway if a 6-in. (152-mm) tall curb is utilized). This height discrepancy would interfere with the breakaway features of the end terminal system unless the end terminal rail transitioned to a greater height or the breakaway features were adjusted. Additional post embedment also creates a stiffer guardrail system when impacted along the length of the system. If no soil fill is placed in the area behind the curb, then the roadway surface and the groundline around the posts would be at the same level. The sponsor suggested that the curb would typically be installed with soil fill, the end terminals would be installed with the standard breakaway features located at the groundline, and guardrail height for an installation with a 6-in. (152-mm) tall curb would be 37 in. (940 mm) above the roadway, as shown in Figure 72. Thus, this configuration was modeled in the curb simulations.

When the toe of the curb is aligned with the face of the guardrail or offset 6 in. (152 mm), it can be very difficult or impossible to install the anchor posts, which typically have no offset blocks, without interfering with the curb. Many State DOTs noted that they flare tangent terminals at a 1:25 or 1:50 flare to allow room to install the anchor posts. However, in the model, the tangent terminals remained tangent to the roadway and interference occurred between the curb and anchor posts. This inference was not problematic in the model as no contact was defined between the posts and curb.

The curb and ground were meshed with fully-constrained rigid shell elements. A mesh was utilized on the curb radii, and a larger mesh was utilized elsewhere. A typical curb mesh is shown in Figure 73.

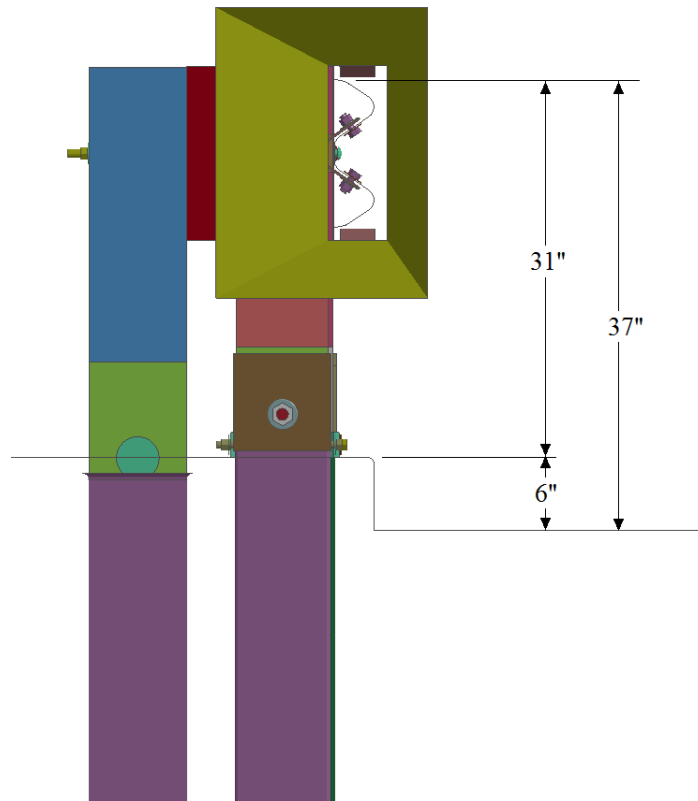


Figure 72. Typical End Terminal Installation Adjacent to 6-in. (152-mm) Tall Curb

8.1 Results

Specific simulation parameters were evaluated, including vehicle interaction with the impact head, occupant risk measures, vehicle stability, and guardrail feed length. The occupant risk measures included longitudinal and lateral OIVs and ORAs that were calculated using acceleration data with a minimum 10,000 Hz frequency from the local c.g. node of the vehicle and then processed as defined in MASH 2009. Roll, pitch, and yaw Euler angles were extracted from the local c.g. node of the vehicle and processed as defined in MASH 2009. Vehicle and impact head interaction was measured as the height of initial bumper contact on the impact head relative to the baseline simulation as well as visually monitoring the contact.

The sloped and vertical 6-in. (152-mm) tall curbs were initially simulated with each of the impact conditions. In the MASH 2009 test no. 3-31 simulations, the curb minimally affected occupant risk measures, vehicle stability, feed lengths, and overall end terminal performance. Thus, it was believed that 2-in. (51-mm) and 4-in. (102-mm) tall curbs would also minimally affect the end terminal performance, and these simulations were not conducted.

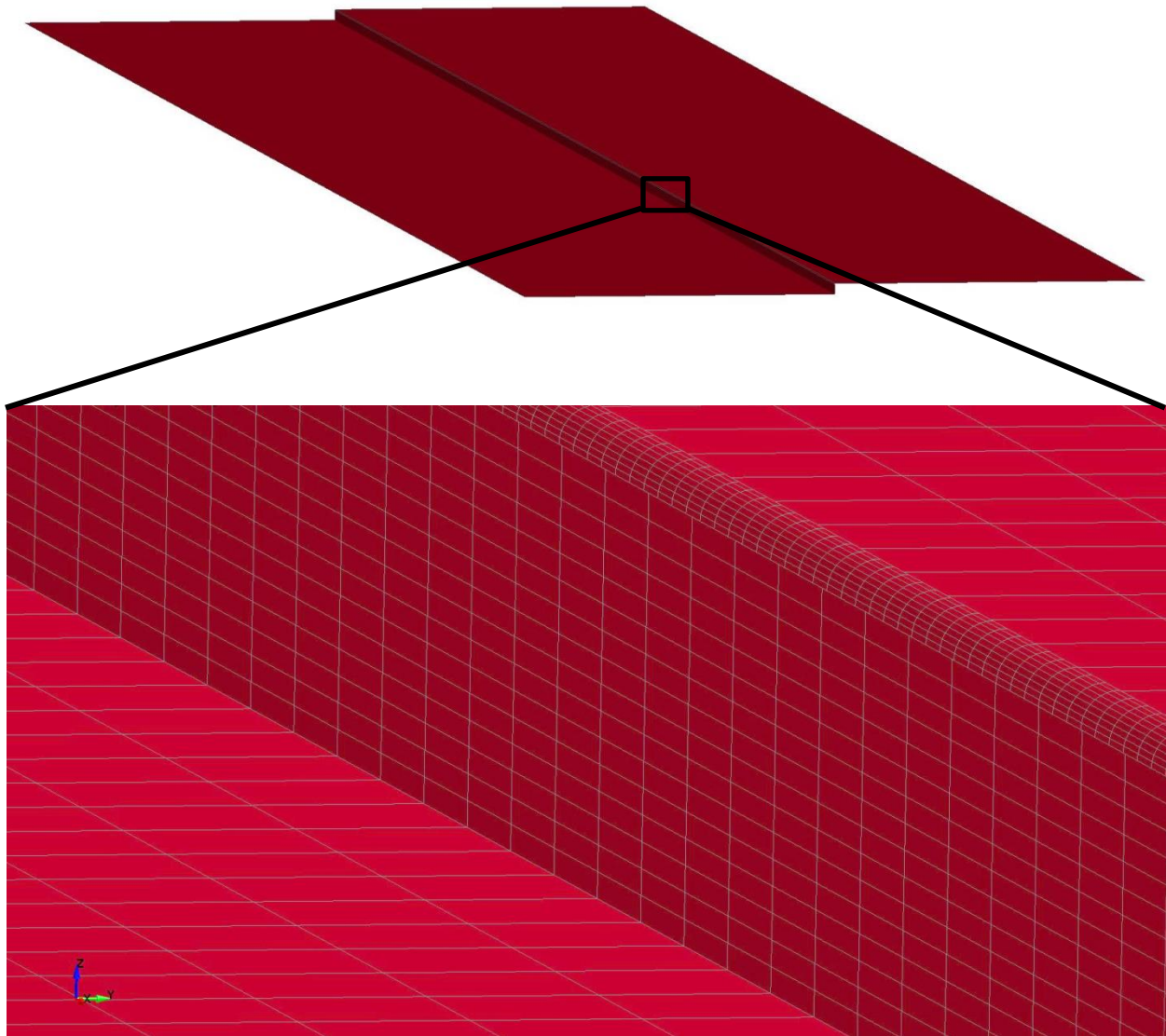


Figure 73. Typical Curb Mesh Model

8.1.1 Occupant Risk Measures

The lateral and longitudinal OIVs varied minimally and were far below MASH 2009 limits in all of the simulations. Longitudinal and lateral ORAs are shown in Figures 74 through 80 for MASH 2009 test nos. 3-30 through 3-33. The presence of curbs at a 0-in. or 6-in. (152-mm) lateral offset did not affect MASH 2009 test no. 3-31. In these cases, the left side of the pickup truck was on top of the curb, the right side of the pickup truck was on the roadway, and the bumper impact height on the impact head varied minimally from the baseline simulation of the 31-in. (787-mm) tall terminals. In the simulations of MASH 2009 test no. 3-30 with a deep quarter-point offset, occupant risk was minimally affected by the presence of curbs for the same reason as MASH 2009 test no. 3-31. However, MASH 2009 test no. 3-30 with a shallow quarter-point offset on a 6-in. (152-mm) tall vertical curb at a 6-in. (152-mm) lateral offset had a the

longitudinal ORA of 20 g's, which was more than 50 percent greater than the baseline simulation and near the MASH 2009 limit. Thus, the tall vertical curb significantly affected occupant risk measures.

In MASH 2009 test no. 3-32 with a 5-degree impact angle, high longitudinal ORAs occurred due to significant post-to-rail bolt snag as the rail tried to release away from post nos. 3 and 4. This behavior occurred in all MASH 2009 test no. 3-32 5-degree simulations as the car pushed upward on the impact head and guardrail due to the presence of sloped and vertical curbs. In the 4-in. (102-mm) tall sloped curb simulation, the rail buckled shortly after impact. Sequential photographs of the MASH 2009 test no. 3-32 5-degree impact with no curb and 2-in. (51-mm) and 4-in. (102-mm) tall sloped curb simulations are shown in Figures 88 and 89. The maximum roll and pitch angles also increased, and the feed lengths decreased with curbs. While the post-to-rail release was not calibrated as mentioned previously, the slight uplift on the impact head and guardrail that was accentuated by the curb is likely to occur. However, it is unknown if the altered head trajectory would affect rail release without full-scale crash testing.

Longitudinal ORAs typically increased with the presence of curbs in MASH 2009 test no. 3-32 at a 15-degree impact angle. However, some of these values seemed unrealistically high as the impact head mesh sometimes became entangled in the bumper and engine hood of the Yaris, which caused a spike in the acceleration trace. These components do not typically interlock with the vehicle in full-scale crash tests. The longitudinal and lateral ORAs in MASH 2009 test no. 3-33 at 5- and 15-degree impact angles varied by less than 3 g's from the baseline and were well below MASH 2009 limits.

None of the simulations showed an inherent behavior that would cause the system to fail MASH 2009 criteria, unless post-to-rail bolt release became hindered, especially during shallow-angle impacts. However, this behavior could not be fully evaluated with simulation.

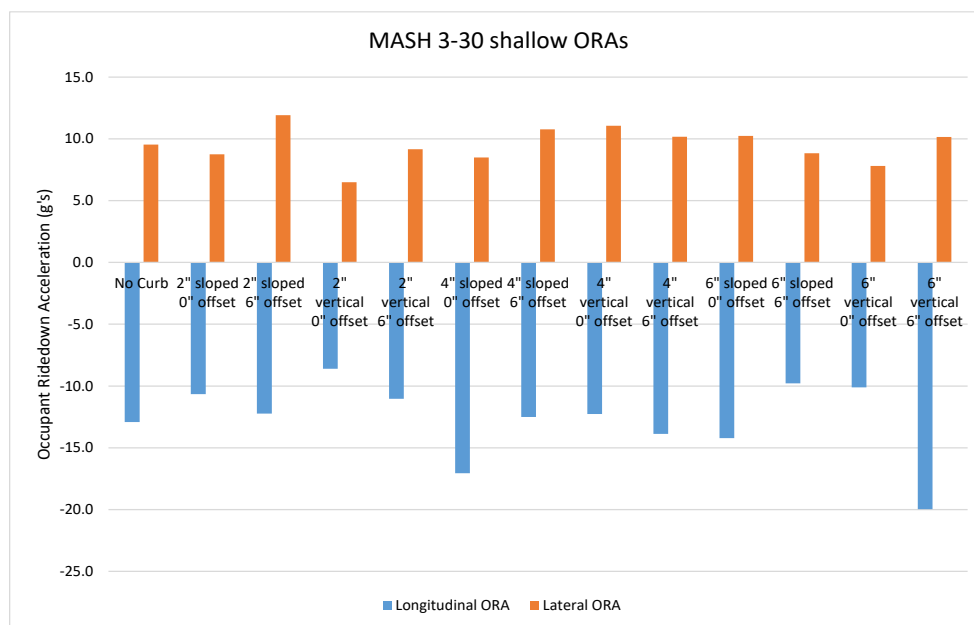


Figure 74. End Terminal with Curb Simulation ORAs, MASH 2009 Test No. 3-30 with Shallow ¼-Point Offset

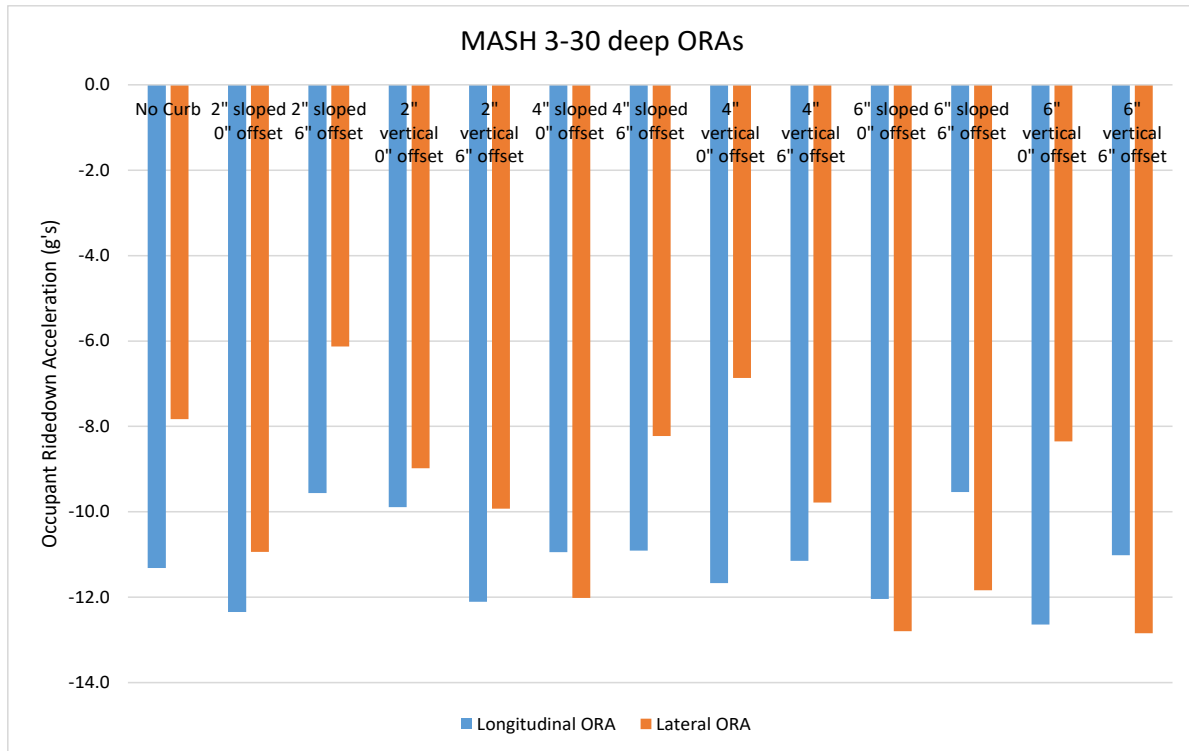


Figure 75. End Terminal with Curb Simulation ORAs, MASH 2009 Test No. 3-30 with Deep ¼-Point Offset

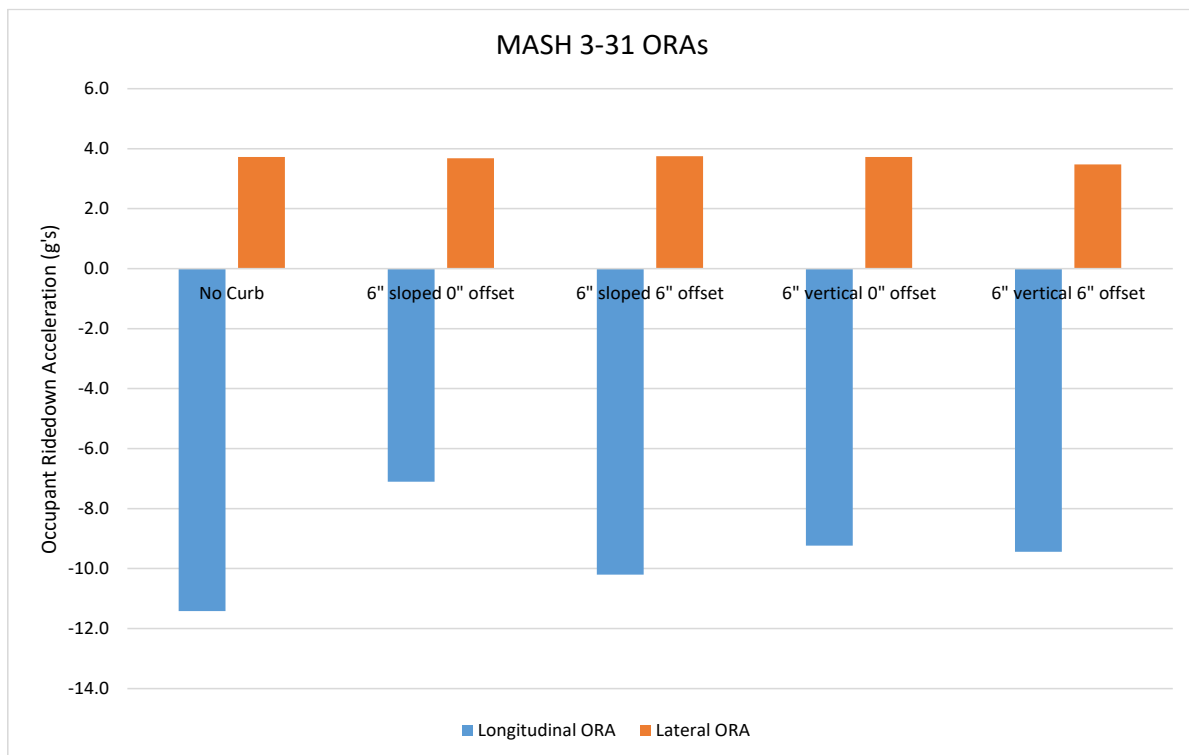


Figure 76. End Terminal with Curb Simulation ORAs, MASH 2009 Test No. 3-31

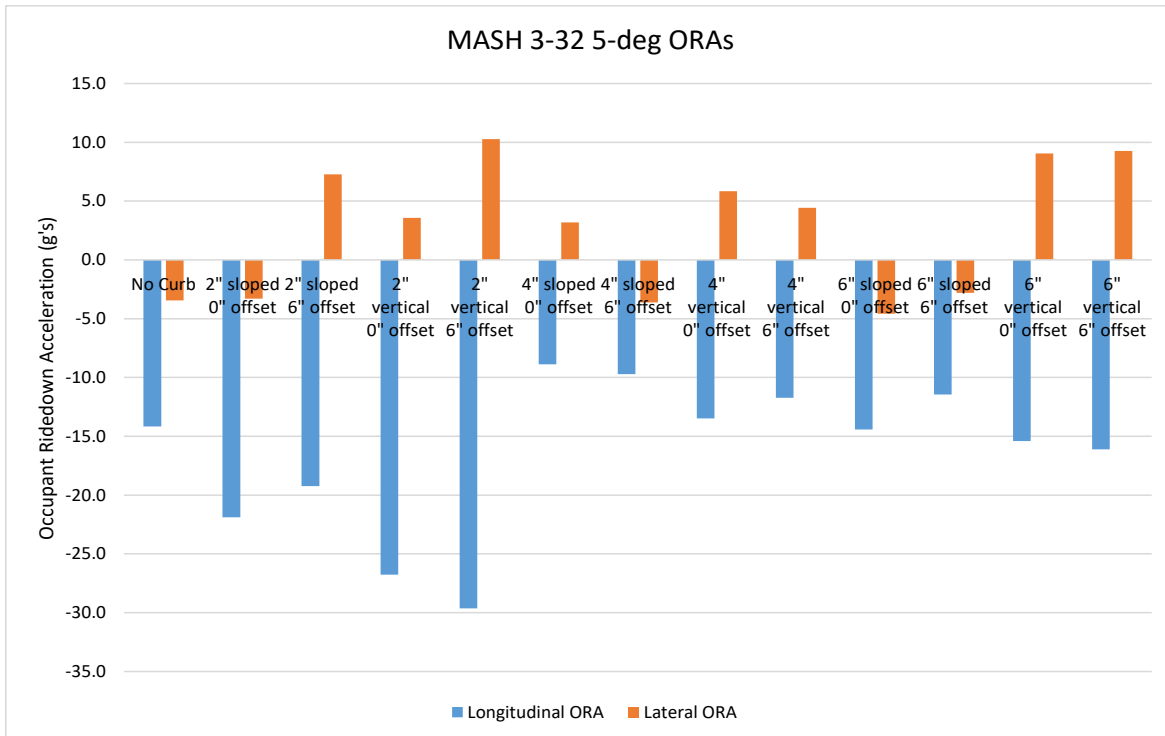


Figure 77. End Terminal with Curb Simulation ORAs, MASH 2009 Test No. 3-32 at 5-deg Impact Angle

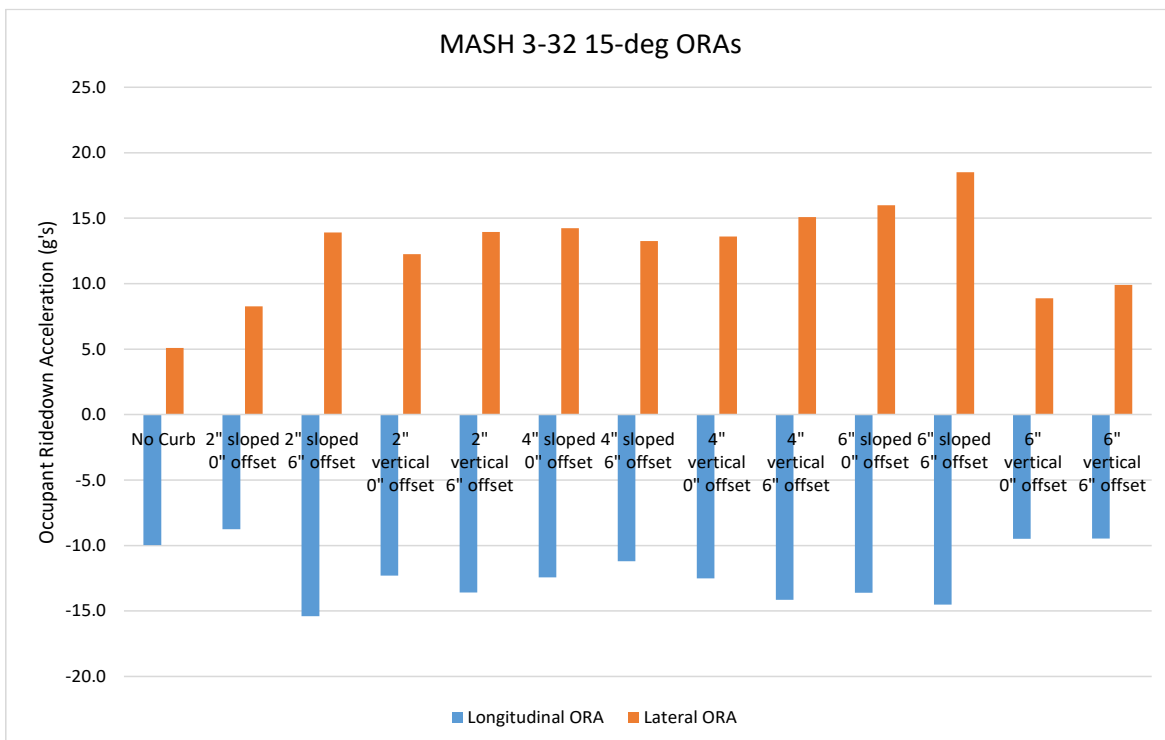


Figure 78. End Terminal with Curb Simulation ORAs, MASH 2009 Test No. 3-32 at 15-deg Impact Angle

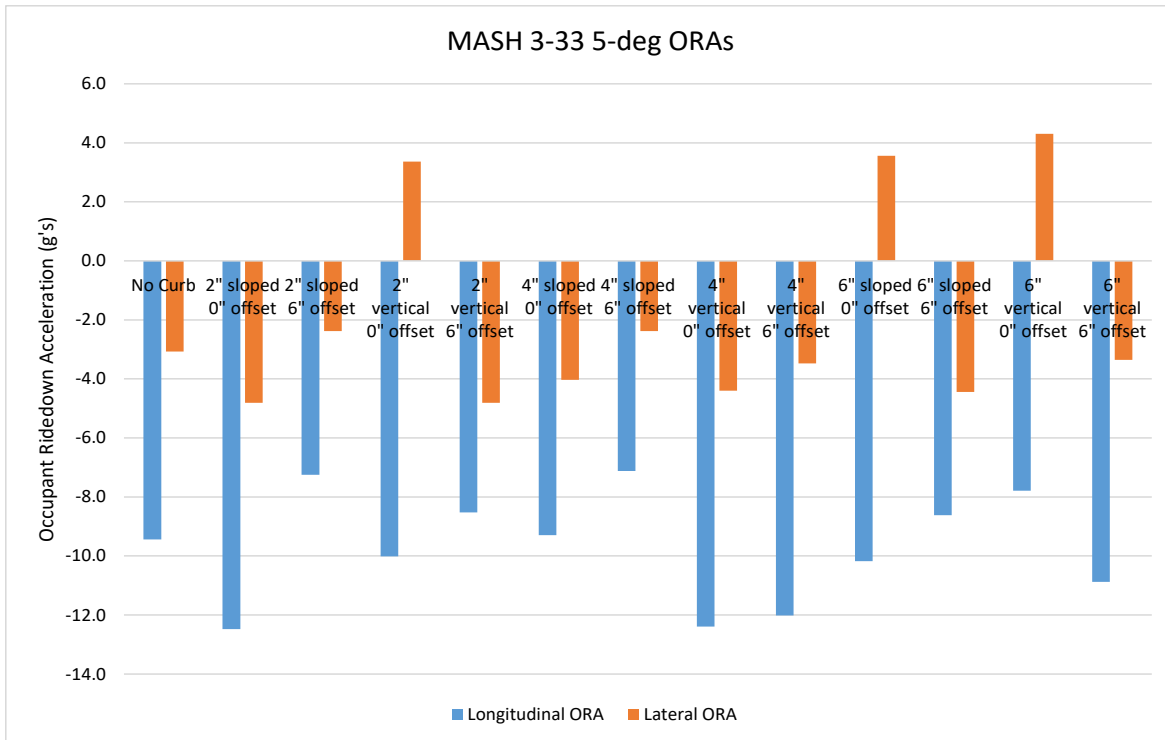


Figure 79. End Terminal with Curb Simulation ORAs, MASH 2009 Test No. 3-33 at 5-deg Impact Angle

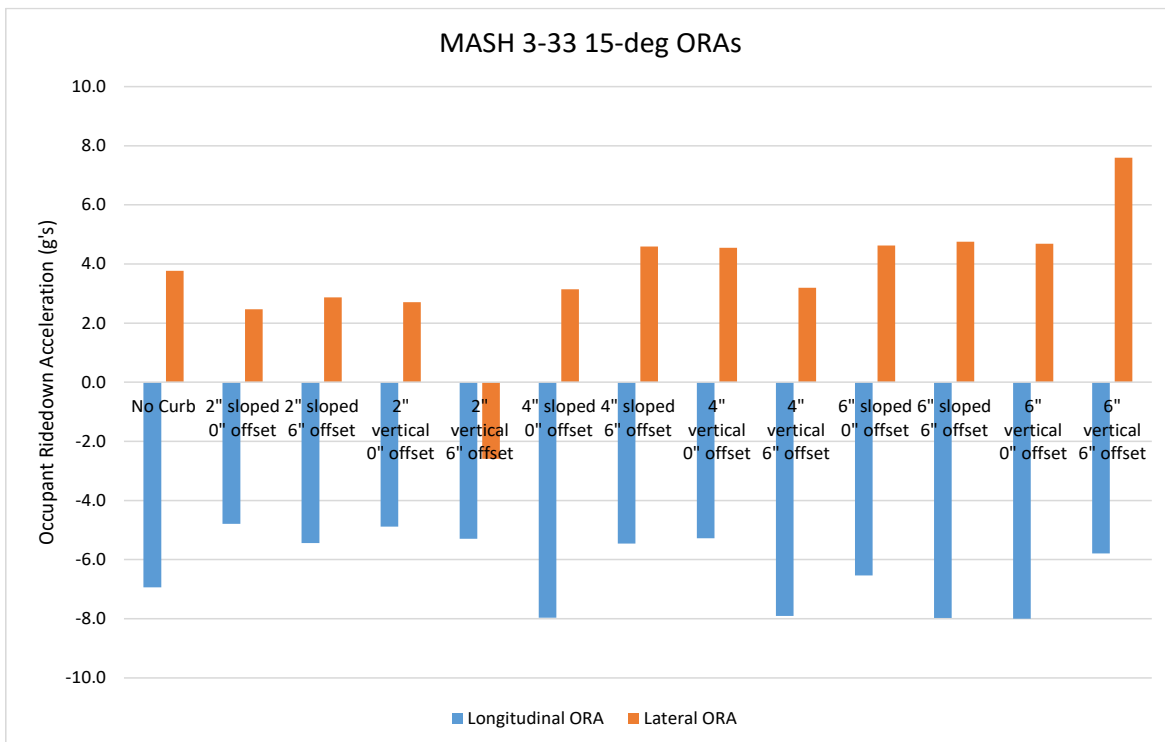


Figure 80. End Terminal with Curb Simulation ORAs, MASH 2009 Test No. 3-33 at 15-deg Impact Angle

8.2 Vehicle Stability

The roll, pitch, and yaw angles from the simulations are shown in Figures 81 through 87 for MASH 2009 test nos. 3-30 through 3-33. Since the vehicle yaws due to the quarter-point impact location in MASH 2009 test no. 3-30 with a deep quarter-point offset, the 4-in. (102-mm) and 6-in. (152-mm) tall vertical curbs noticeably affected vehicle yaw as the sidewall of the tires snagged on the curbs while the vehicle model was not tracking, as shown in Figure 90. The vertical curbs also affected the Yaris yaw motion in MASH 2009 test no. 3-32 at a 5-degree impact angle.

In MASH 2009 test no. 3-32 with a 15-degree impact angle, the vehicle pitched and yawed in the opposite direction with the curbs present. However, much of the yaw motion and increased occupant risk values were believed to be due to the impact head nodes snagging on the bumper and hood and not releasing from the vehicle, which would not be expected in full-scale crash tests. While changing the contact definition improved this behavior, it was not remedied.

In MASH 2009 test no. 3-33 with both the 5- and 15-degree impact angles, the pitch increased with increased curb heights. The roll and yaw angles varied throughout the curb heights, and no trends could be identified. The roll and pitch angles in all of the simulated MASH 2009 were low.

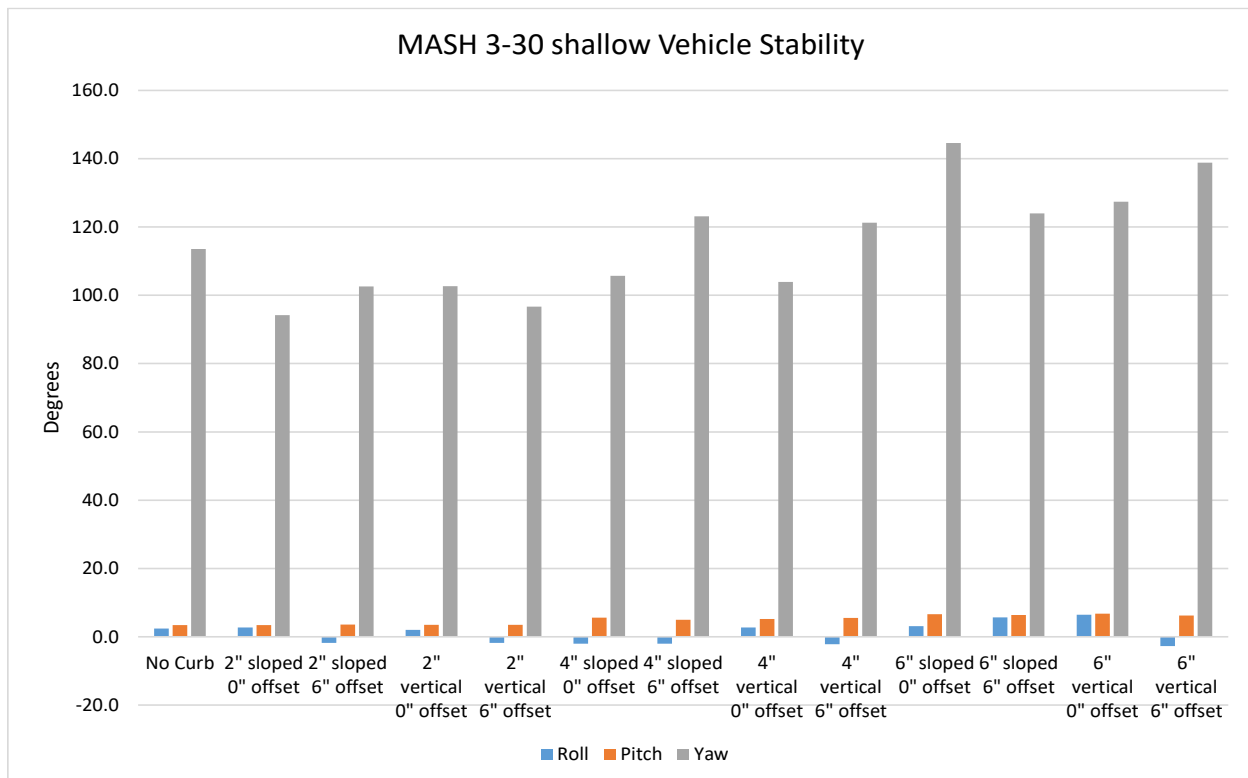


Figure 81. End Terminal with Curb Simulation Vehicle Stability, MASH 2009 Test No. 3-30 with Shallow ¼-Point Offset

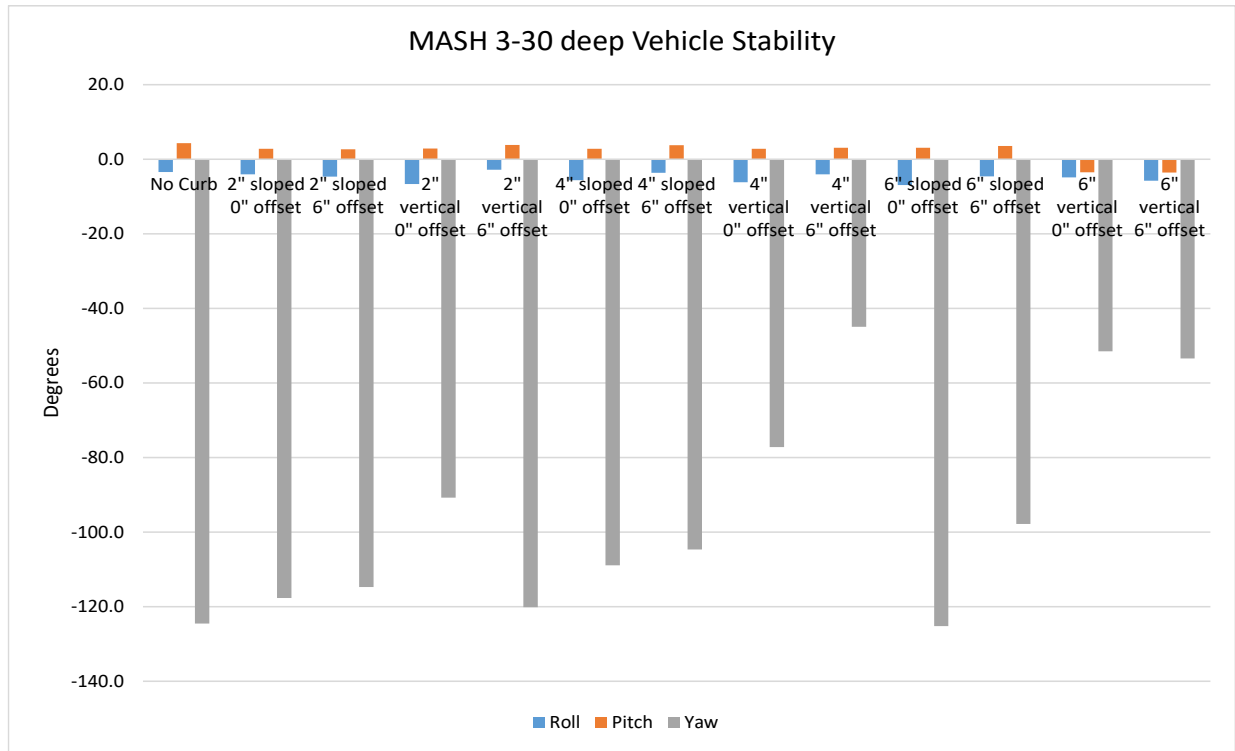


Figure 82. End Terminal with Curb Simulation Vehicle Stability, MASH 2009 Test No. 3-30 with Deep ¼-Point Offset

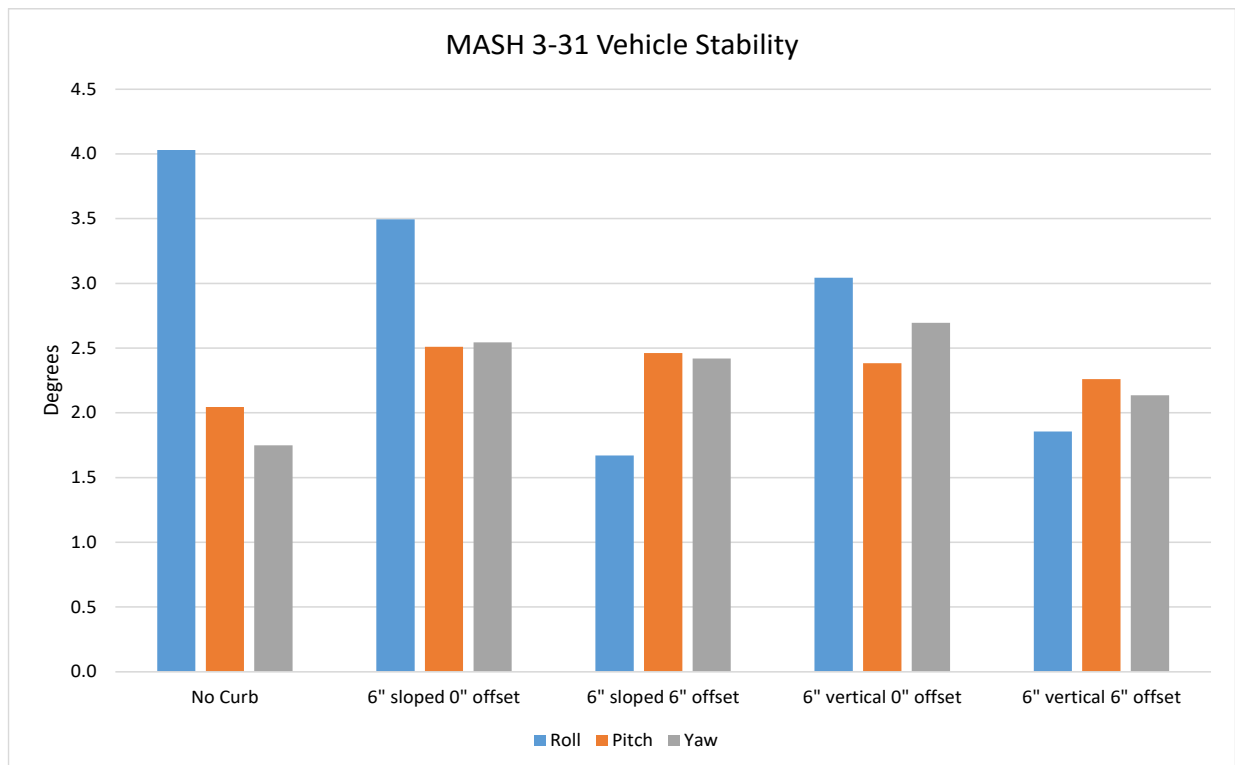


Figure 83. End Terminal with Curb Simulation Vehicle Stability, MASH 2009 Test No. 3-31

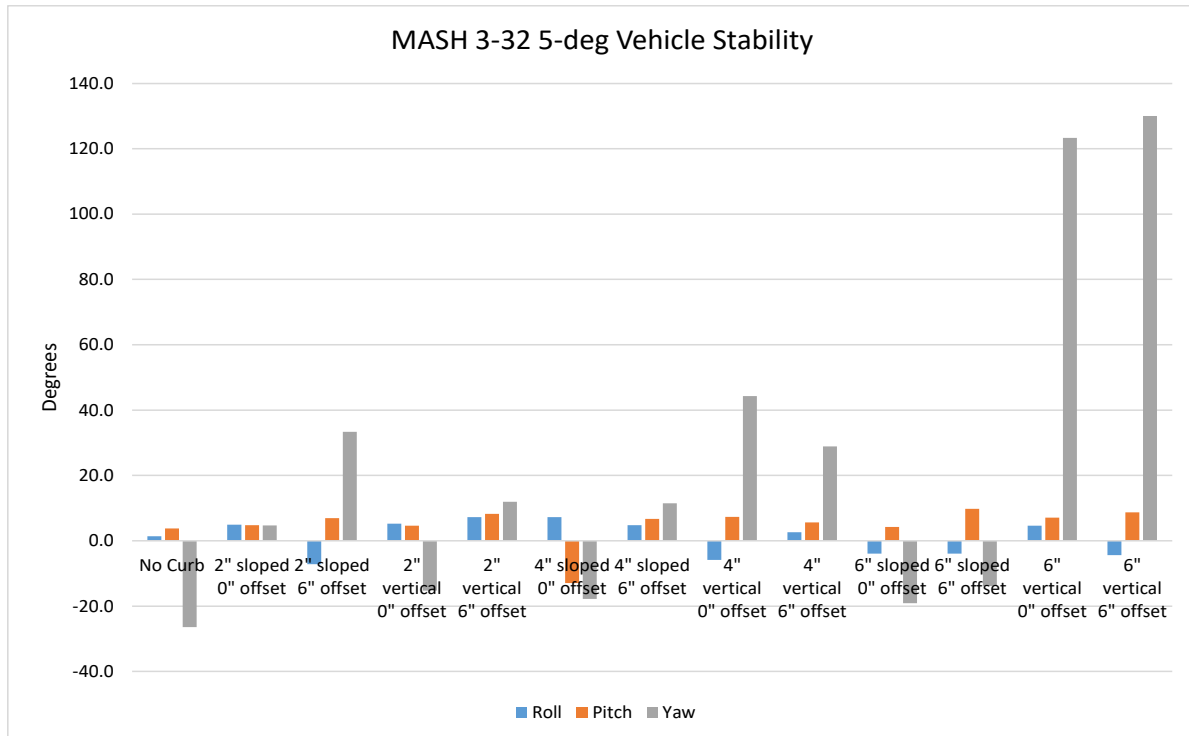


Figure 84. End Terminal with Curb Simulation Vehicle Stability, MASH 2009 Test No. 3-32 at 5-deg Impact Angle

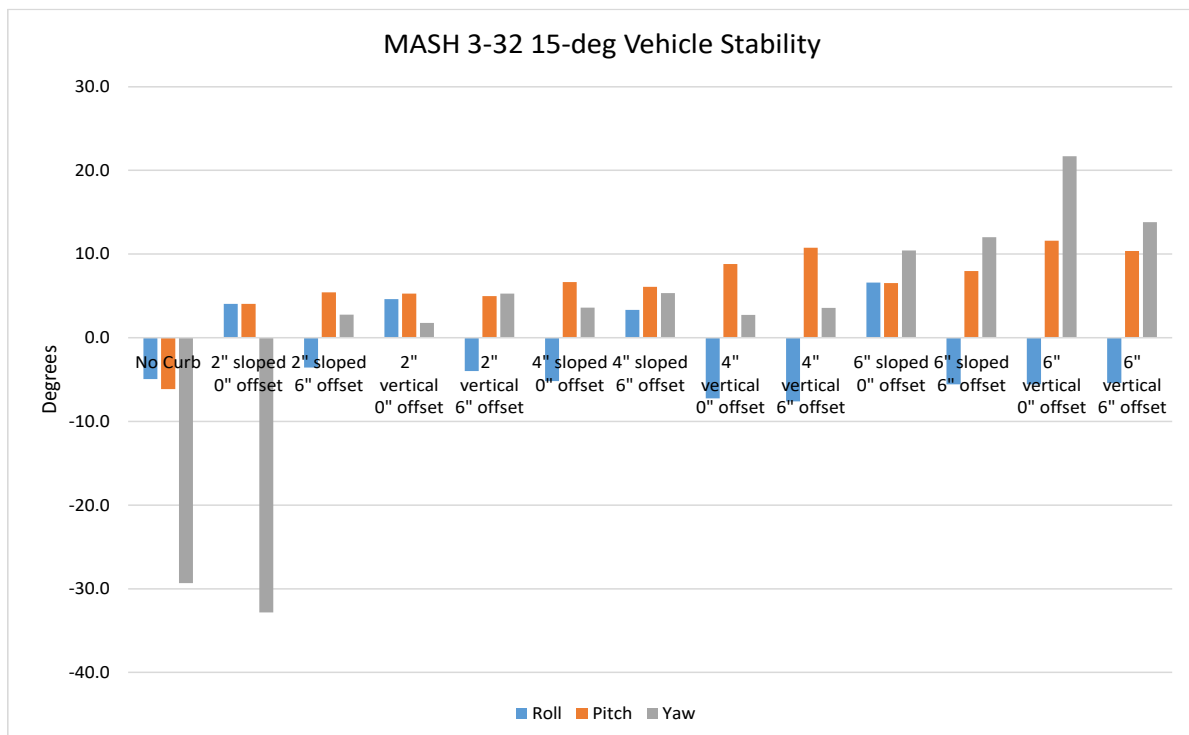


Figure 85. End Terminal with Curb Simulation Vehicle Stability, MASH 2009 Test No. 3-32 at 15-deg Impact Angle

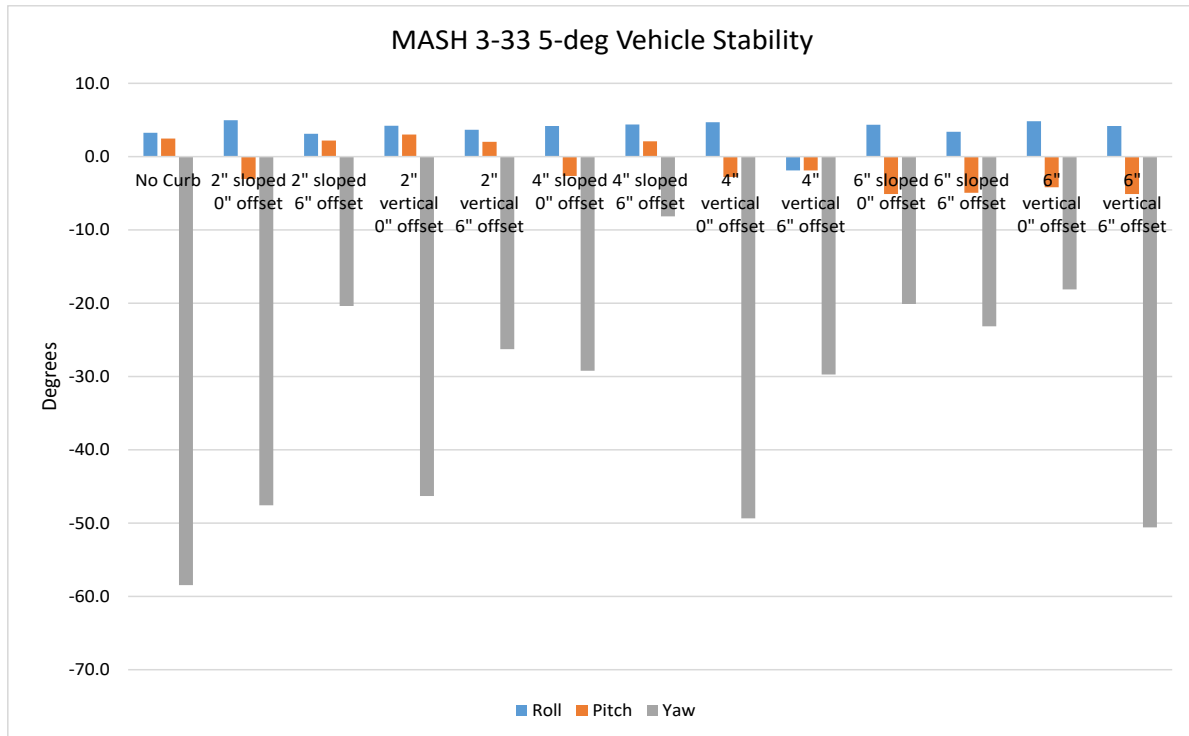


Figure 86. End Terminal with Curb Simulation Vehicle Stability, MASH 2009 Test No. 3-33 at 5-deg Impact Angle

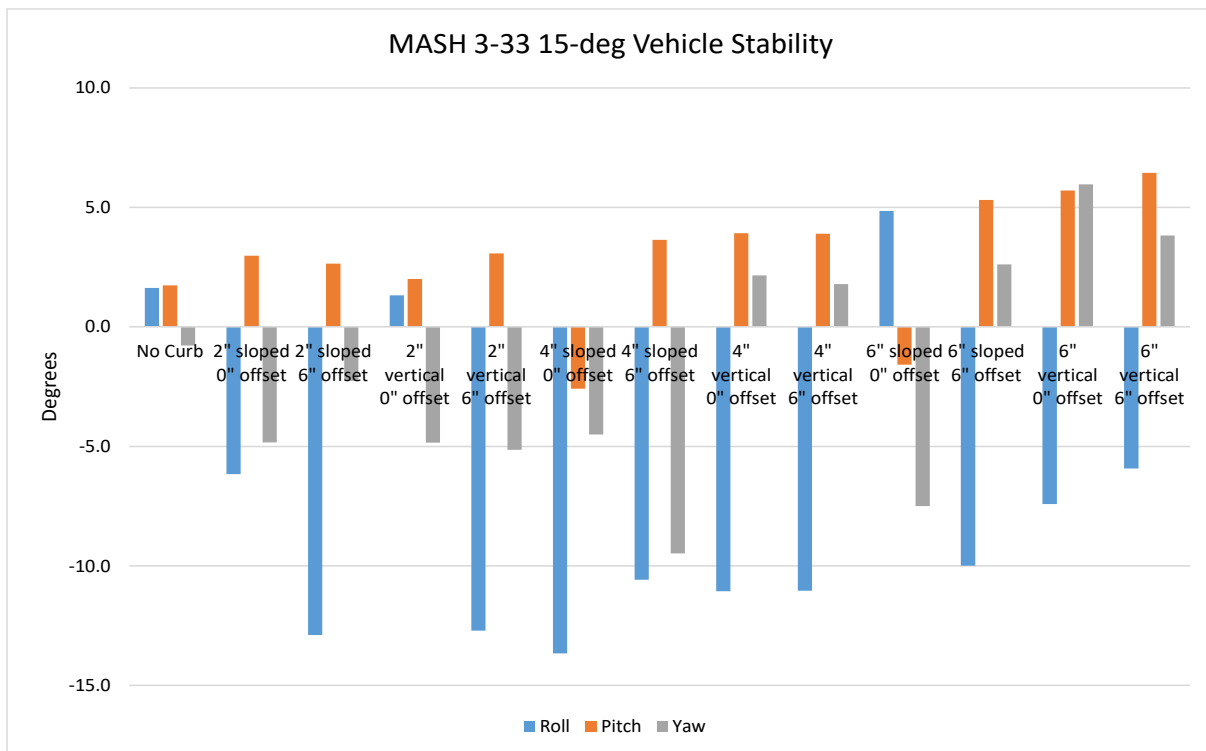


Figure 87. End Terminal with Curb Simulation Vehicle Stability, MASH 2009 Test No. 3-33 at 15-deg Impact Angle

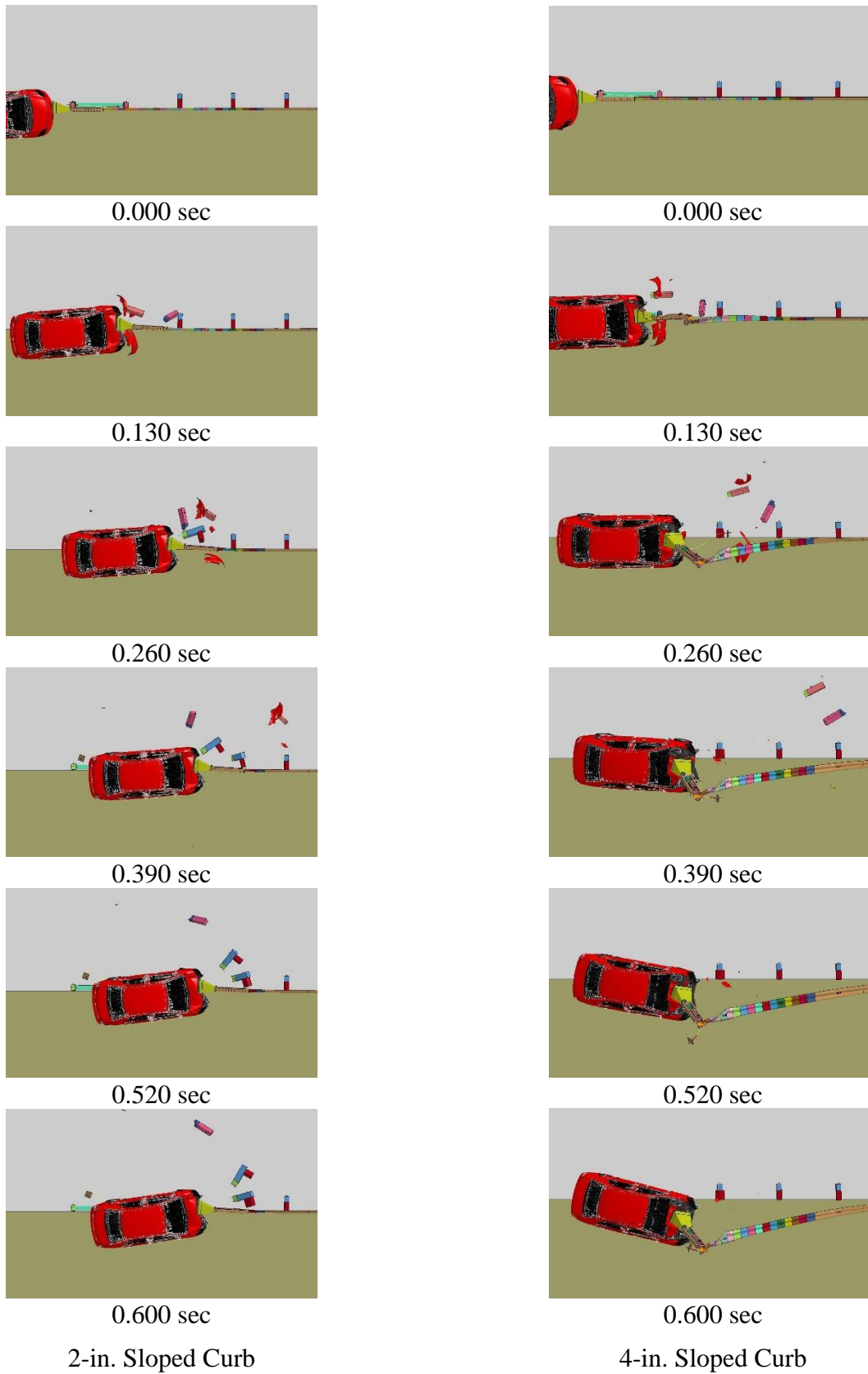


Figure 88. MASH 2009 Test No. 3-32 with Curbs, 5 Degrees, 0" Offset, Overhead View

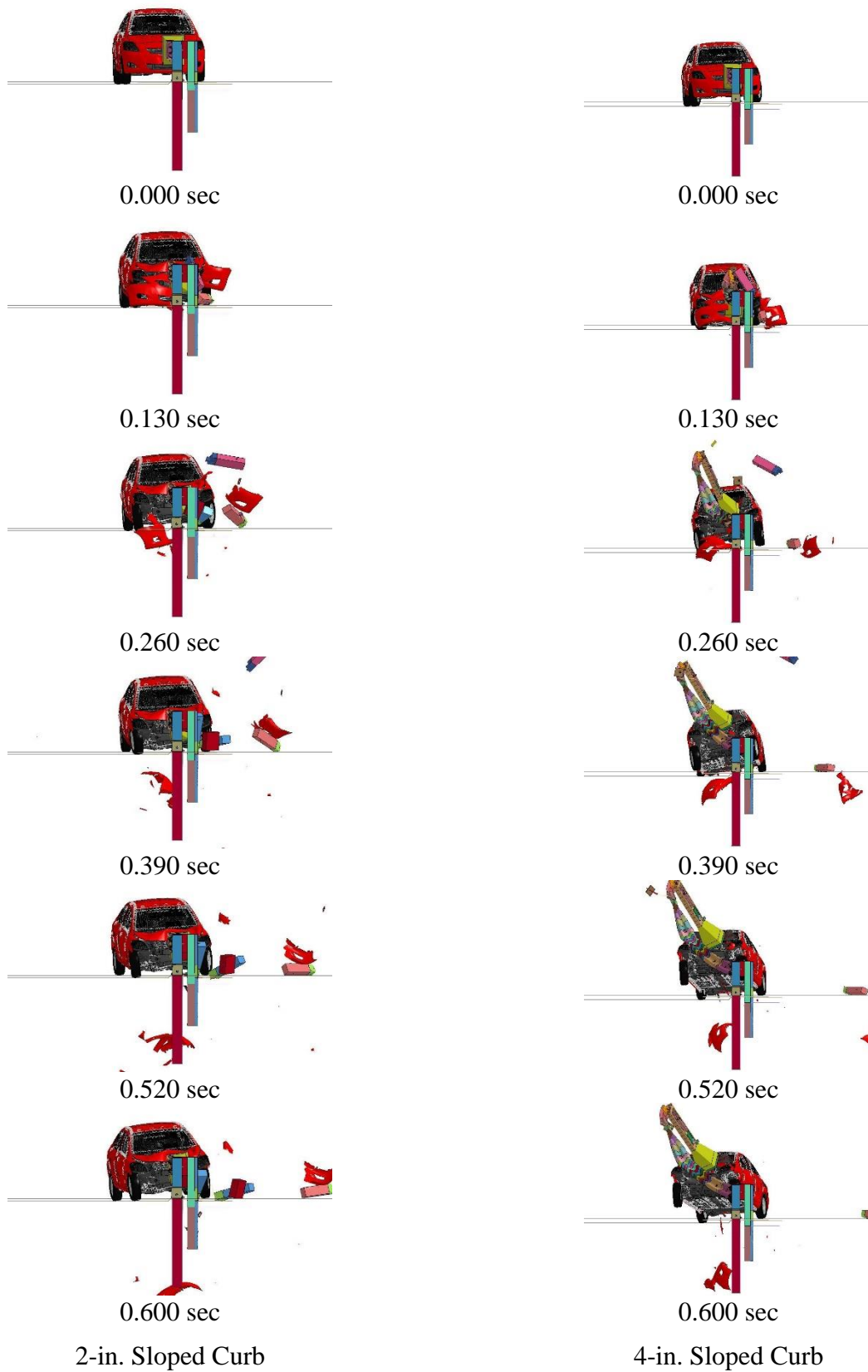
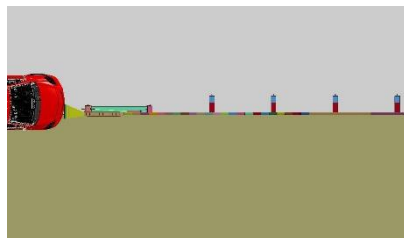
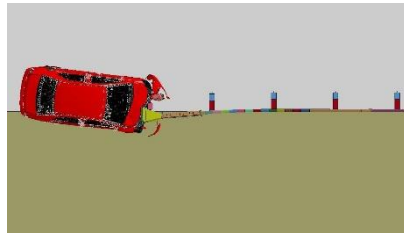


Figure 89. MASH 2009 Test No. 3-32 with Curbs, 5 Degrees, 0" Offset, Downstream View



0.000 sec



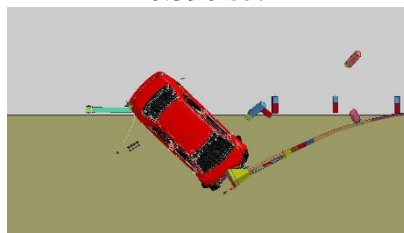
0.130 sec



0.260 sec



0.390 sec

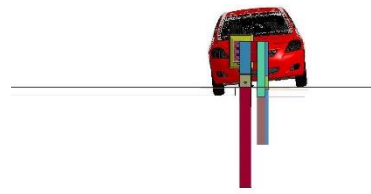


0.520 sec

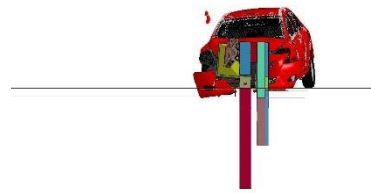


0.650 sec

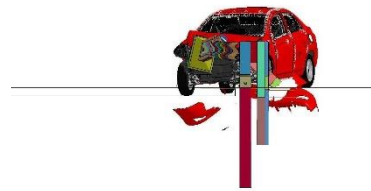
6-in. Vertical Curb, Overhead



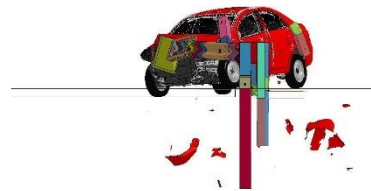
0.000 sec



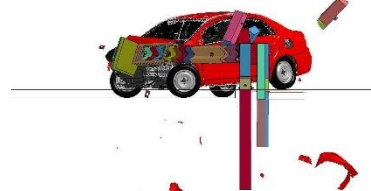
0.130 sec



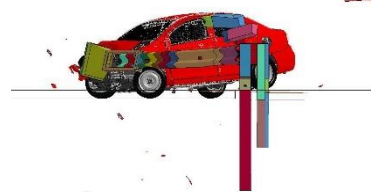
0.260 sec



0.390 sec



0.520 sec



0.650 sec

6-in. Vertical Curb, Downstream

Figure 90. MASH 2009 Test No. 3-30 with Curbs, Deep Quarter-Point, 0" Offset

8.3 Feed Lengths and Vehicle Interaction

The feed lengths from the simulations are shown in Figures 91 and 97 for MASH 2009 test nos. 3-30 through 3-33. The feed lengths did not vary significantly, except in MASH 2009 test no. 3-32 at 5-degree impact angle and MASH 2009 test no. 3-33 at a 15-degree impact angle. As mentioned previously, in all MASH 2009 test no. 3-32 5-degree simulations, the car pushed upward on the impact head and guardrail due to the presence of sloped and vertical curbs, which caused the rail to buckle prematurely in some scenarios and reduce the overall feed length. In MASH 2009 test no. 3-33 with 15-degree impacts, the rail buckled just after post no. 2 or at post no. 3, which corresponds to feed lengths of approximately 4.5 ft (1.4 m) and 9 ft (2.7 m). In historical NCHRP Report 350 and MASH 2009 test no. 3-33 crash tests, the rail typically buckled at both of these locations.

Since curbs adjacent to guardrail systems have previously caused problems for vehicle capture due to vehicle override, underride, or penetration, the height at which the vehicle impacted the impact head was monitored. The change in vertical bumper height (ΔZ) at impact relative to the baseline configuration with no curb was measured in each simulation, as shown in Table 29. The maximum increase in impact height was 4.7 in. (119.4 mm) over the baseline and occurred in simulated MASH 2009 test no. 3-32 at a 15-degree impact angle with a 6-in. (152-mm) tall sloped curb at a 6-in. (152-mm) lateral offset away from the front face of the guardrail. Most of the impact heights increased by less than 2 in. (50 mm). All of the MASH 2009 test no. 3-30 simulated impacts with a curb had a lower impact height than the baseline, but only by a maximum of 0.19 in. (4.8 mm). Overall, the change in impact height on the impact head was minimal and could not be specifically linked to a degradation in terminal performance. Since only 0-in. and 6-in. (152-mm) lateral curb offsets were evaluated, the bumper of the vehicle models often interacted with the impact head shortly after the front tires contacted the curb in angled impacts. Thus, the bumper height at impact did not vary greatly. However, at larger curb offsets, the height of the bumper upon impact may vary more significantly.

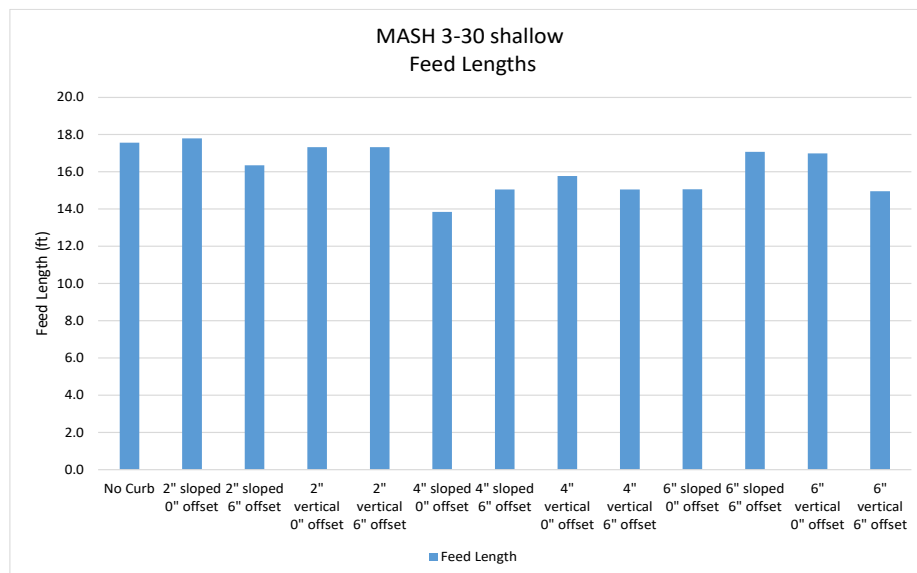


Figure 91. End Terminal with Curb Simulation Feed Length, MASH 2009 Test No. 3-30 with Shallow 1/4-Point Offset

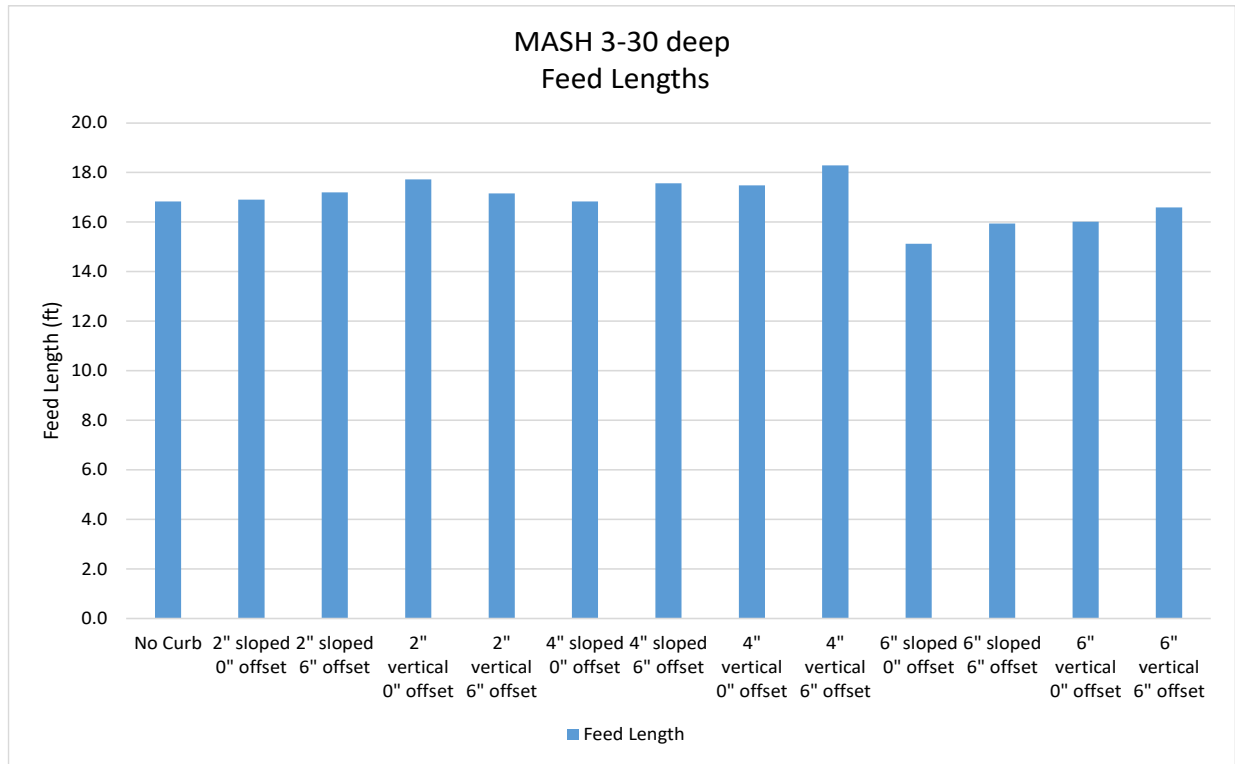


Figure 92. End Terminal with Curb Simulation Feed Length, MASH 2009 Test No. 3-30 with Deep ¼-Point Offset

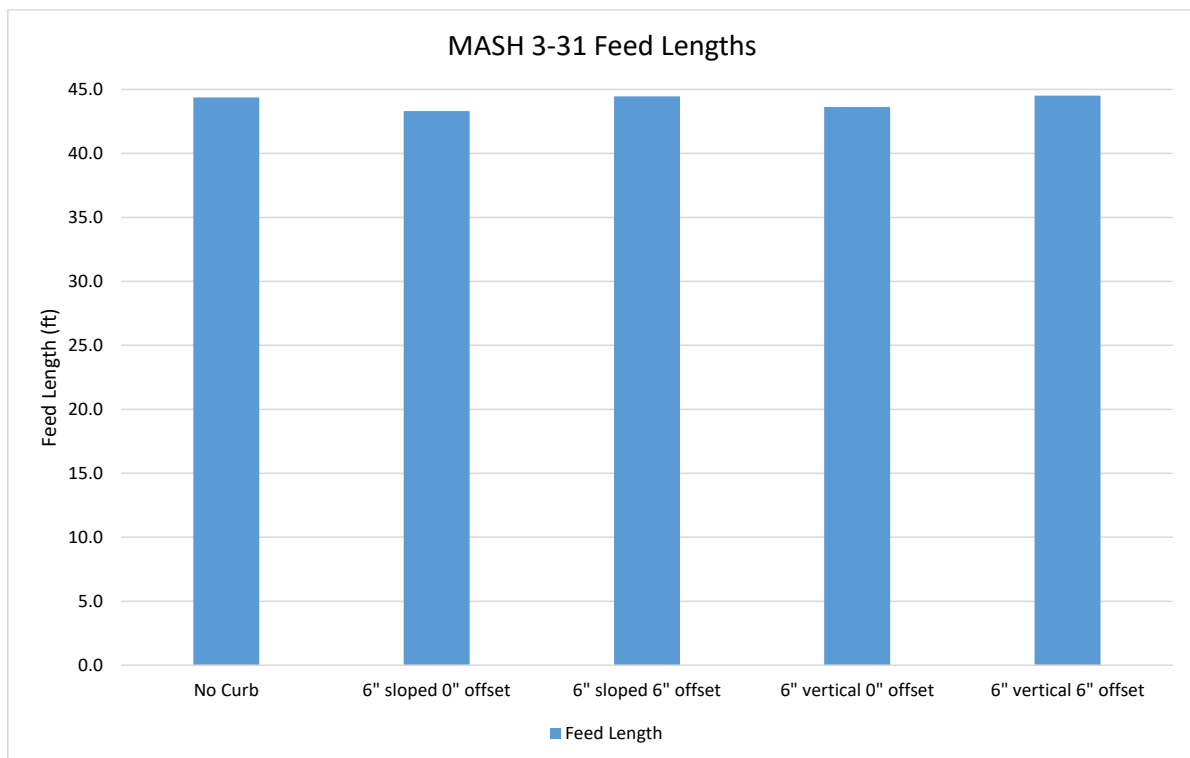


Figure 93. End Terminal with Curb Simulation Feed Length, MASH 2009 Test No. 3-31

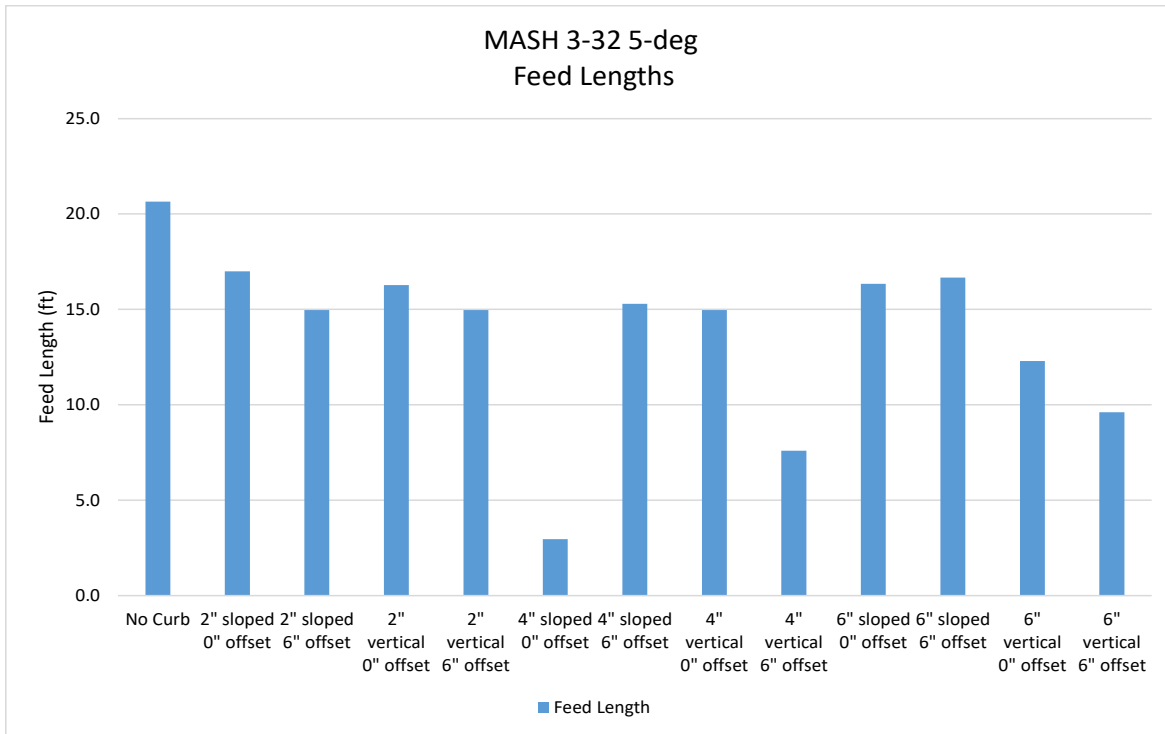


Figure 94. End Terminal with Curb Simulation Feed Length, MASH 2009 Test No. 3-32 at 5-deg Impact Angle

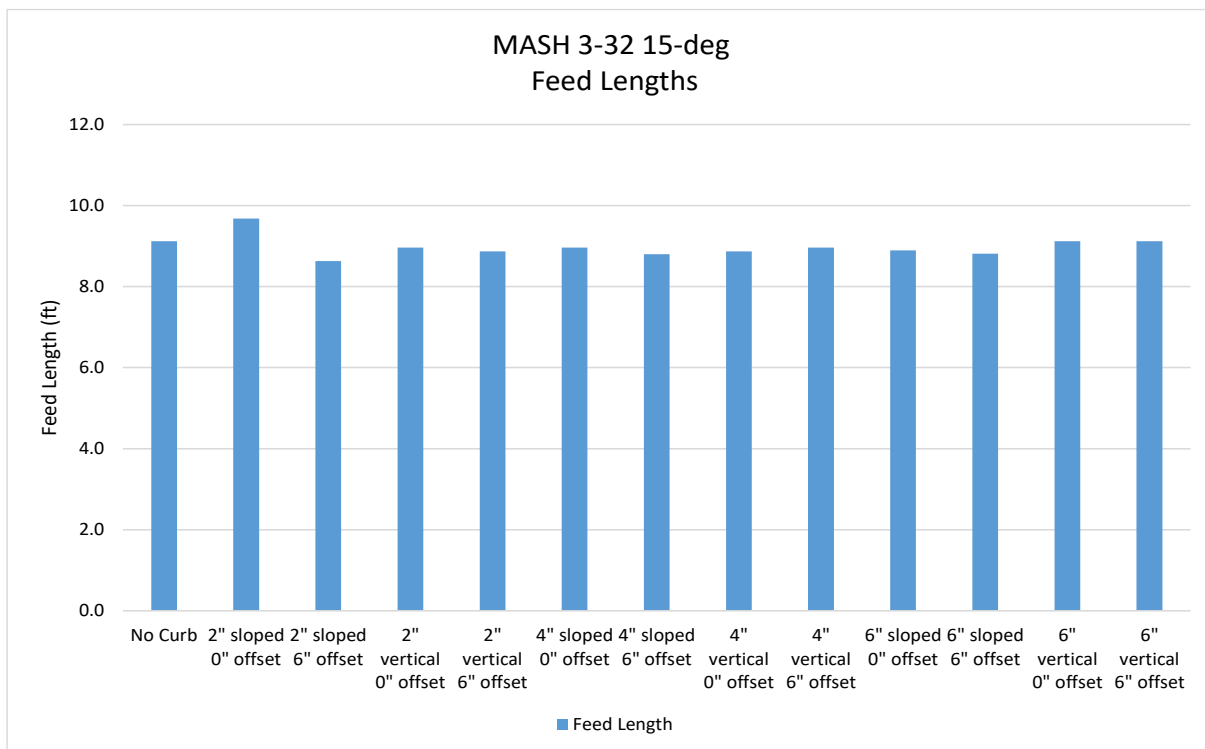


Figure 95. End Terminal with Curb Simulation Feed Length, MASH 2009 Test No. 3-32 at 15-deg Impact Angle

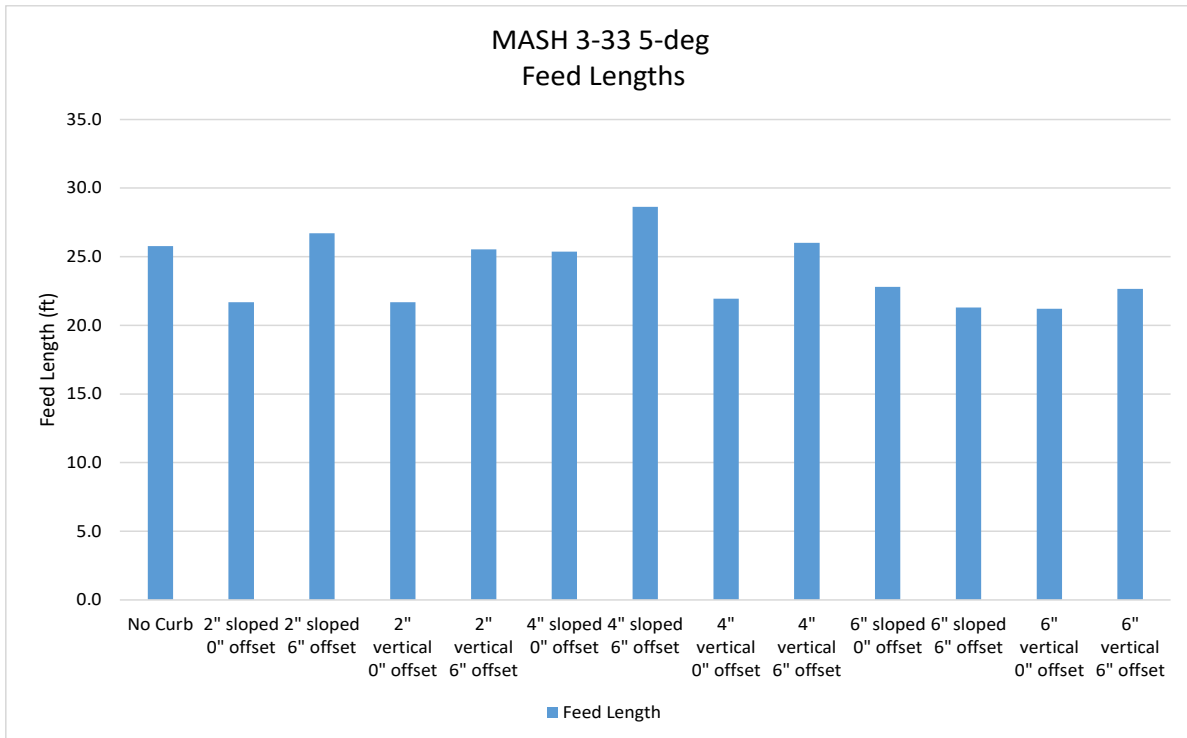


Figure 96. End Terminal with Curb Simulation Feed Length, MASH 2009 Test No. 3-33 at 5-deg Impact Angle

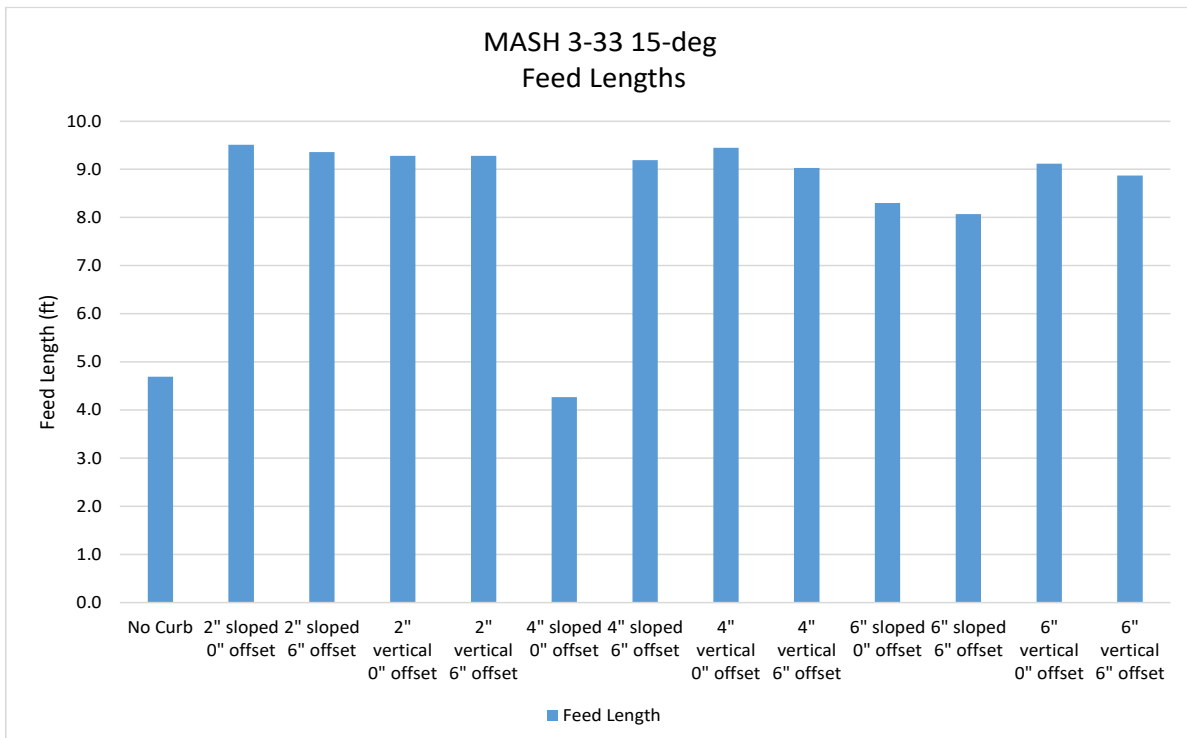


Figure 97. End Terminal with Curb Simulation Feed Length, MASH 2009 Test No. 3-33 at 15-deg Impact Angle

Table 29. Change in Vertical Bumper Height at Impact

Curb Height (in.)	Curb Shape	Curb Offset (in.)	Test No.	Angle	ΔZ Bumper at Impact (mm)	ΔZ Bumper at Impact (in.)
2	sloped	0	MASH 3-33	5 deg	4.7	0.2
2	sloped	0	MASH 3-33	15 deg	17.5	0.7
2	sloped	0	MASH 3-32	5 deg	14.5	0.6
2	sloped	0	MASH 3-32	15 deg	7.4	0.3
2	sloped	0	MASH 3-30	0-deep	-2.4	-0.1
2	sloped	0	MASH 3-30	0-shallow	-4.6	-0.2
2	vertical	0	MASH 3-33	5 deg	0.6	0.0
2	vertical	0	MASH 3-33	15 deg	16.3	0.6
2	vertical	0	MASH 3-32	5 deg	11.2	0.4
2	vertical	0	MASH 3-32	15 deg	10.5	0.4
2	vertical	0	MASH 3-30	0-deep	-2.4	-0.1
2	vertical	0	MASH 3-30	0-shallow	-4.6	-0.2
4	sloped	0	MASH 3-33	5 deg	40.2	1.6
4	sloped	0	MASH 3-33	15 deg	10.4	0.4
4	sloped	0	MASH 3-32	5 deg	44.3	1.7
4	sloped	0	MASH 3-32	15 deg	46.4	1.8
4	sloped	0	MASH 3-30	0-deep	-1.9	-0.1
4	sloped	0	MASH 3-30	0-shallow	-4.7	-0.2
4	vertical	0	MASH 3-33	5 deg	13.0	0.5
4	vertical	0	MASH 3-33	15 deg	10.9	0.4
4	vertical	0	MASH 3-32	5 deg	33.9	1.3
4	vertical	0	MASH 3-32	15 deg	56.9	2.2
4	vertical	0	MASH 3-30	0-deep	-2.0	-0.1
4	vertical	0	MASH 3-30	0-shallow	-4.8	-0.2
6	sloped	0	MASH 3-33	5 deg	70.9	2.8
6	sloped	0	MASH 3-33	15 deg	9.3	0.4
6	sloped	0	MASH 3-32	5 deg	94.0	3.7
6	sloped	0	MASH 3-32	15 deg	75.1	3.0
6	sloped	0	MASH 3-30	0-deep	-1.7	-0.1
6	sloped	0	MASH 3-30	0-shallow	-4.5	-0.2
6	vertical	0	MASH 3-33	5 deg	43.8	1.7
6	vertical	0	MASH 3-33	15 deg	18.5	0.7
6	vertical	0	MASH 3-32	5 deg	55.0	2.2
6	vertical	0	MASH 3-32	15 deg	91.8	3.6
6	vertical	0	MASH 3-30	0-deep	-1.8	-0.1
6	vertical	0	MASH 3-30	0-shallow	-4.6	-0.2
2	sloped	6	MASH 3-33	5 deg	3.0	0.1
2	sloped	6	MASH 3-33	15 deg	20.9	0.8
2	sloped	6	MASH 3-32	5 deg	9.8	0.4
2	sloped	6	MASH 3-32	15 deg	11.9	0.5
2	sloped	6	MASH 3-30	0-deep	-2.4	-0.1
2	sloped	6	MASH 3-30	0-shallow	-4.3	-0.2
2	vertical	6	MASH 3-33	5 deg	2.6	0.1
2	vertical	6	MASH 3-33	15 deg	21.6	0.9
2	vertical	6	MASH 3-32	5 deg	8.1	0.3
2	vertical	6	MASH 3-32	15 deg	12.9	0.5
2	vertical	6	MASH 3-30	0-deep	-2.4	-0.1
2	vertical	6	MASH 3-30	0-shallow	-4.1	-0.2
4	sloped	6	MASH 3-33	5 deg	35.0	1.4
4	sloped	6	MASH 3-33	15 deg	20.6	0.8
4	sloped	6	MASH 3-32	5 deg	31.6	1.2
4	sloped	6	MASH 3-32	15 deg	60.1	2.4
4	sloped	6	MASH 3-30	0-deep	-1.9	-0.1
4	sloped	6	MASH 3-30	0-shallow	-4.9	-0.2
4	vertical	6	MASH 3-33	5 deg	17.1	0.7
4	vertical	6	MASH 3-33	15 deg	28.5	1.1
4	vertical	6	MASH 3-32	5 deg	15.5	0.6
4	vertical	6	MASH 3-32	15 deg	66.3	2.6
4	vertical	6	MASH 3-30	0-deep	-2.0	-0.1
4	vertical	6	MASH 3-30	0-shallow	-5.1	-0.2
6	sloped	6	MASH 3-33	5 deg	70.9	2.8
6	sloped	6	MASH 3-33	15 deg	22.3	0.9
6	sloped	6	MASH 3-32	5 deg	62.3	2.5
6	sloped	6	MASH 3-32	15 deg	119.4	4.7
6	sloped	6	MASH 3-30	0-deep	-1.7	-0.1
6	sloped	6	MASH 3-30	0-shallow	-4.6	-0.2
6	vertical	6	MASH 3-33	5 deg	41.3	1.6
6	vertical	6	MASH 3-33	15 deg	38.1	1.5
6	vertical	6	MASH 3-32	5 deg	16.7	0.7
6	vertical	6	MASH 3-32	15 deg	101.3	4.0
6	vertical	6	MASH 3-30	0-deep	-1.8	-0.1
6	vertical	6	MASH 3-30	0-shallow	-4.6	-0.2

8.4 0-in. and 6-in. (152-mm) Lateral Offset Curbs-Discussion

Due to the small lateral curb offsets, the vehicle interaction with the impact head was minimally affected. However, larger lateral curb offsets may have a greater effect on vehicle trajectory and interaction with the impact head. The presence of curbs affected the small car impacts the most. The 4-in. (102-mm) and 6-in. (152-mm) tall vertical curbs affected vehicle yaw in the small car impacts as the tires had a more difficult time traversing the curb, especially when the tires were non-tracking. The sloped curbs minimally affected vehicle yaw. The vehicle and terminal performance was more similar to the baseline simulations with 2-in. (51-mm) tall curbs as compared to 4-in. (102-mm) and 6-in. (152-mm) tall curbs.

None of the simulations showed an inherent behavior that would cause the system to fail MASH 2009 criteria, unless post-to-rail bolt release became hindered, especially during shallow-angle impacts. However, this behavior could not be fully evaluated with simulation.

8.5 6-ft (1.8-m) Wide Curb Sidewalk Adjacent to End Terminal

Three curb configurations (2-in., 4-in. and 6-in. (51-mm, 102-mm, 152-mm) tall sloped) were simulated at a 6-ft (1.8-m) lateral offset away from the front face of the guardrail, which represented a sidewalk adjacent to the roadway. MASH 2009 test nos. 3-30 and 3-31 were not simulated with curbs as the system was expected to behave similarly to the baseline simulations, because the whole vehicle would have been on top of the curb and only would have interacted with the curb late in the event. MASH 2009 test nos. 3-32 and -33 at 5- and 15-degree impact angles were simulated. The Yaris and Silverado suspension and steering models were believed to be reacting unrealistically as the tires turned significantly almost immediately after impacting the curbs, especially at a 5-degree impact angle. Downstream sequential photographs of simulated MASH 2009 test no. 3-32 with a 5-degree impact angle are shown in Figure 98. The car model did not impact the end terminal with the 2-in. (102-mm) and 4-in. (152-mm) tall sloped curbs. With the 6-in. (152-mm) tall sloped curb, the car model impacted the end terminal, but the centerline of the vehicle was not aligned with the centerline of the impact head, which is inconsistent with the MASH 2009-specified impact conditions.

The steering and suspension performance of small cars and pickup trucks were briefly evaluated using CarSim simulated impacts into 2-in., 4-in., and 6-in. (51-mm, 102-mm, and 152-mm) tall sloped curbs at a 5-degree impact angle. A previously-calibrated midsize passenger car model and the default small passenger car and pickup truck models were utilized. In all vehicle models, the wheel steer angle varied less than one degree when impacting the curb. The small car and pickup truck models' trajectories varied by a maximum of 1 ft (0.3 m) laterally from their intended course in the simulation with the 6-in. (152-mm) tall curb. The variance in vehicle trajectory was less than 1 ft (0.3 m) laterally for the shorter curbs. Thus, it was expected that the LS-DYNA vehicle models would impact the end terminals much closer to the centerline of the vehicles if the steering and suspension models were properly calibrated.

Due to the unexpected performance of the vehicle with the shallow-angle curb impacts, the full results of the simulations were not processed. The limitations of the vehicle model suspension and steering with curb impacts should be improved for future studies.

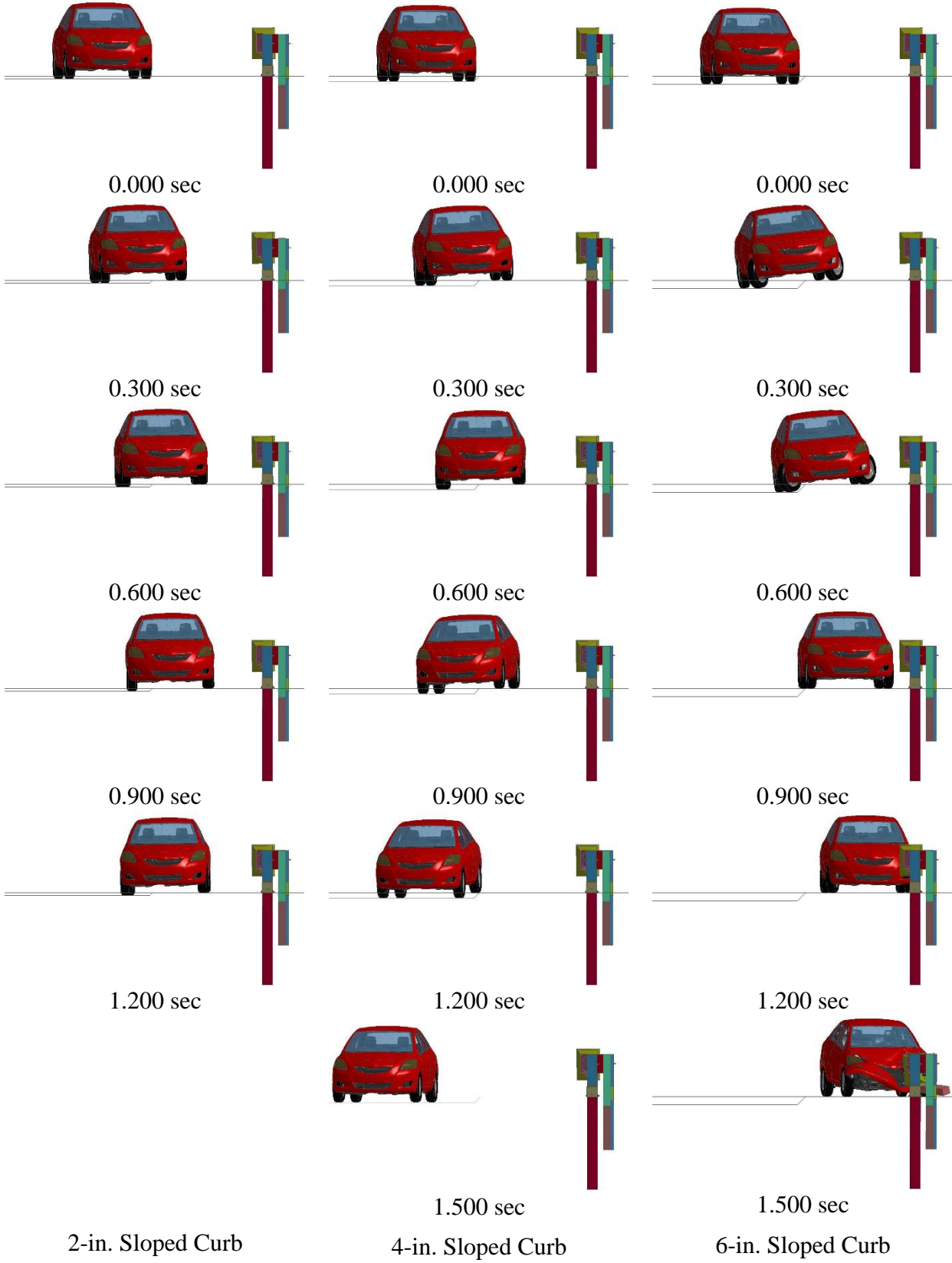


Figure 98. MASH 2009 Test No. 3-32 with Curbs, 5 Degrees, 6-ft Offset, Downstream View

9 END TERMINAL PERFORMANCE – TANGENT VS. FLARED SYSTEMS

Since many State DOTs flared their tangent energy-absorbing end terminals at a 1:25 or 1:50 flare rate, the end terminal model was modified to have a 1:25 flare rate with a 2-ft (0.6-m) lateral offset. The seven MASH 2009 TL-3 impact conditions were simulated again without a curb:

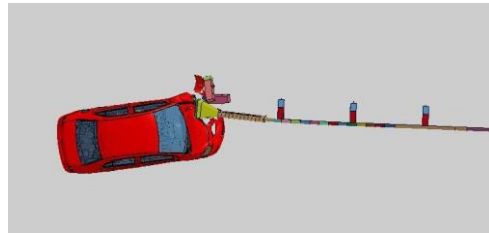
- 1) 1100C small car (Yaris) impacting end at 0 deg at shallow quarter point offset (MASH 2009 test no. 3-30)
- 2) 1100C small car (Yaris) impacting end at 0 deg at deep quarter point offset (MASH 2009 test no. 3-30)
- 3) 2270P pickup truck (Silverado) impacting end at 0 deg (MASH 2009 test no. 3-31)
- 4) 1100C small car (Yaris) impacting end at 5 deg (MASH 2009 test no. 3-32)
- 5) 1100C small car (Yaris) impacting end at 15 deg (MASH 2009 test no. 3-32)
- 6) 2270P pickup truck (Silverado) impacting end at 5 deg (MASH 2009 test no. 3-33)
- 7) 2270P pickup truck (Silverado) impacting end at 15 deg (MASH 2009 test no. 3-33)

Sequential photographs for the flared and tangent end terminal impact simulations are shown in Figures 99 through 112. The feed lengths, roll, pitch, yaw, and longitudinal and lateral ORA for each simulated impact with flared and tangent terminals are shown in Figures 113 through 118. Longitudinal and lateral OIVs varied by a maximum of 2.0 ft/s (0.6 m/s), which was considered non-significant.

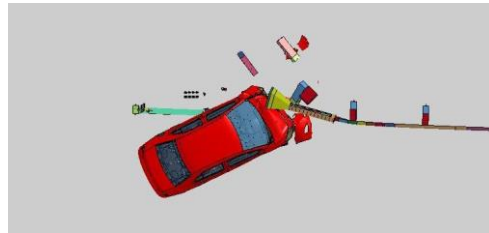
There were minimal changes in barrier performance between the tangent and flared configurations. The most notable difference was the feed length was significantly less in MASH 2009 test no. 3-33 with a 5-degree impact angle when the end terminal was flared as opposed to tangent. The flared system buckled and gated more quickly than the tangent system, which led to decreased feed lengths, as shown in Figures 109 and 110. Since the effective impact angle of the flared system was 7.3 degrees, the system began to behave more similarly to systems impacted at 15 degrees. There was no indication that this would negatively affect the system performance. As mentioned previously, the vehicle yaw in the 5- and 15-degree impacts may be inaccurate as contact between the impact head and vehicle can cause the components to become entangled, which typically does not happen in full-scale crash tests.



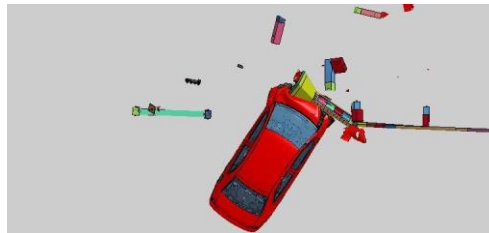
0.000 sec



0.130 sec



0.260 sec



0.390 sec

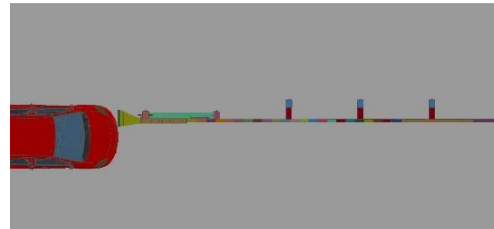


0.520 sec

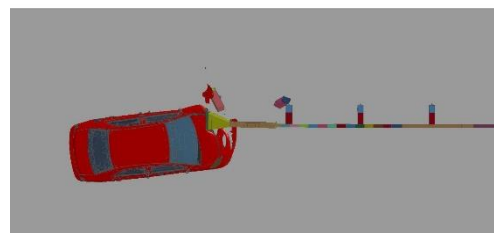


0.650 sec

Simulation No. MASH-30-Shallow-flared



0.000 sec



0.130 sec



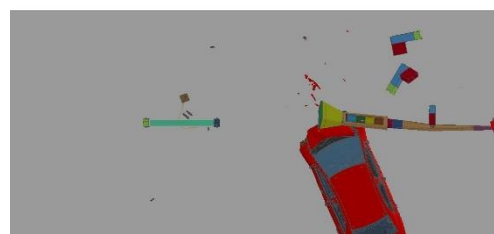
0.260 sec



0.390 sec



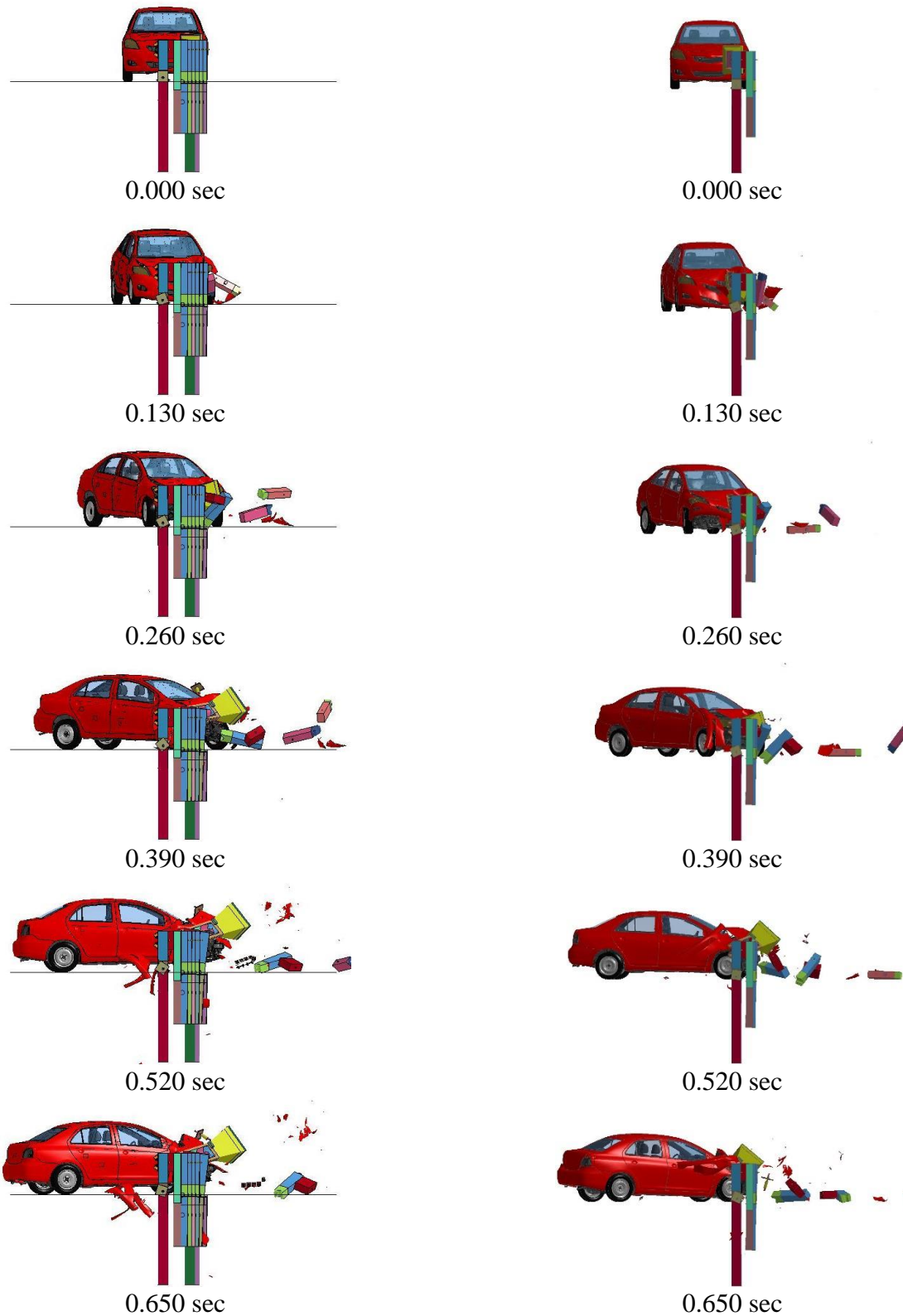
0.520 sec



0.650 sec

Simulation No. MASH-30-Shallow-MGS

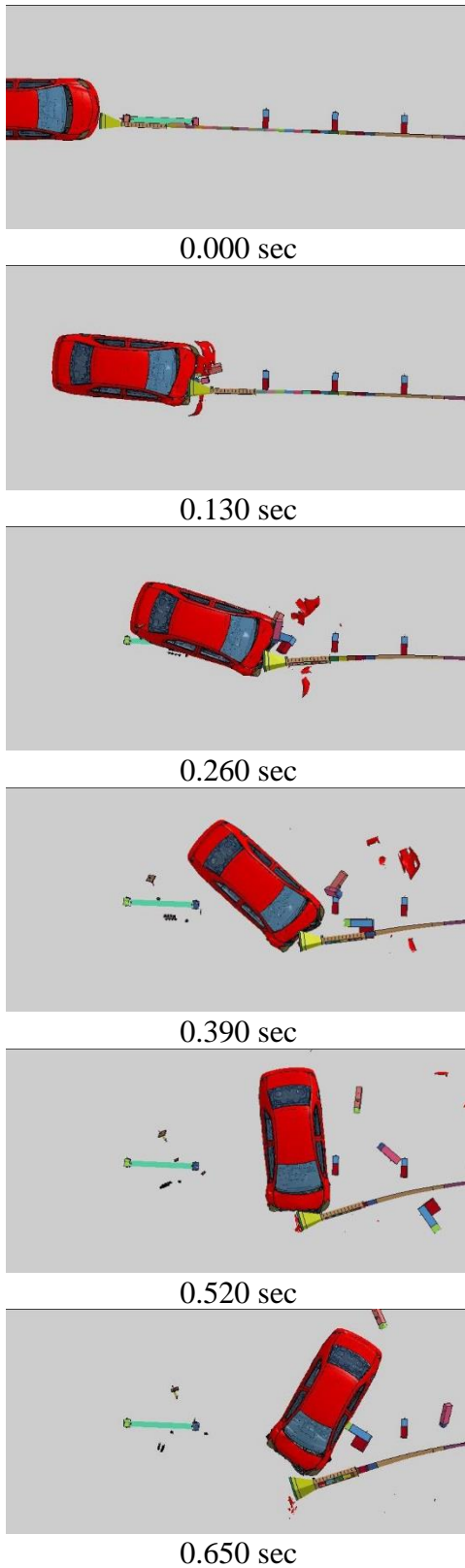
Figure 99. MASH 2009 Test No. 3-30, Shallow Quarter-Point Offset, Overhead View



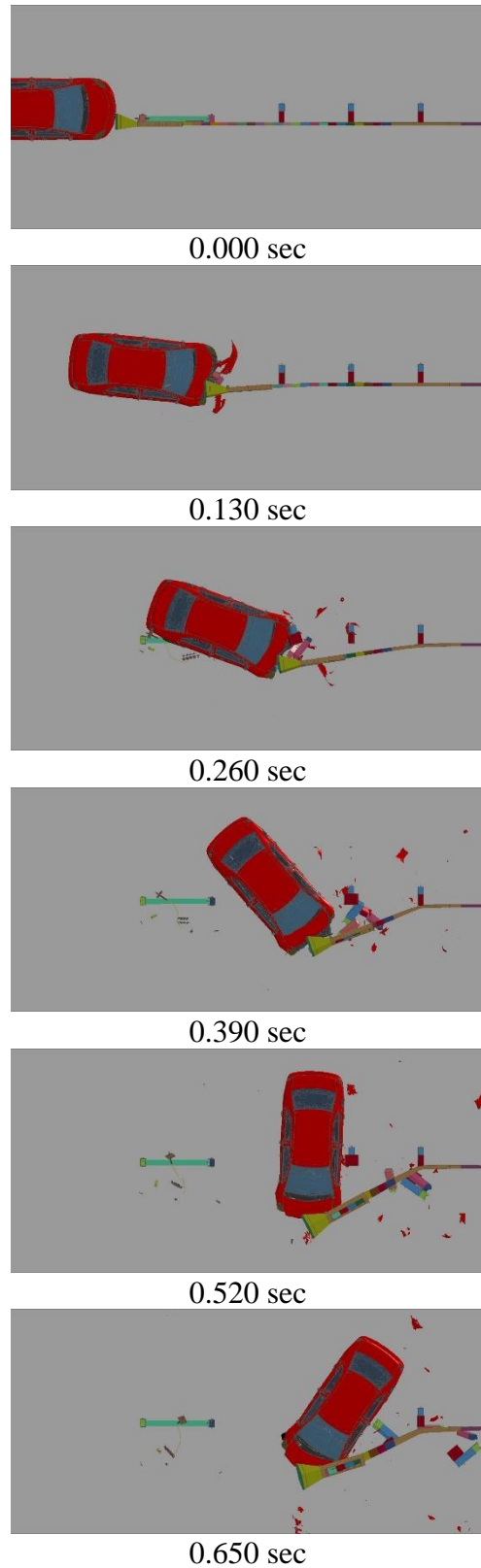
Simulation No. MASH-30-Shallow-flared

Simulation No. MASH-30-Shallow-MGS

Figure 100. MASH 2009 Test No. 3-30, Shallow Quarter-Point Offset, Downstream View

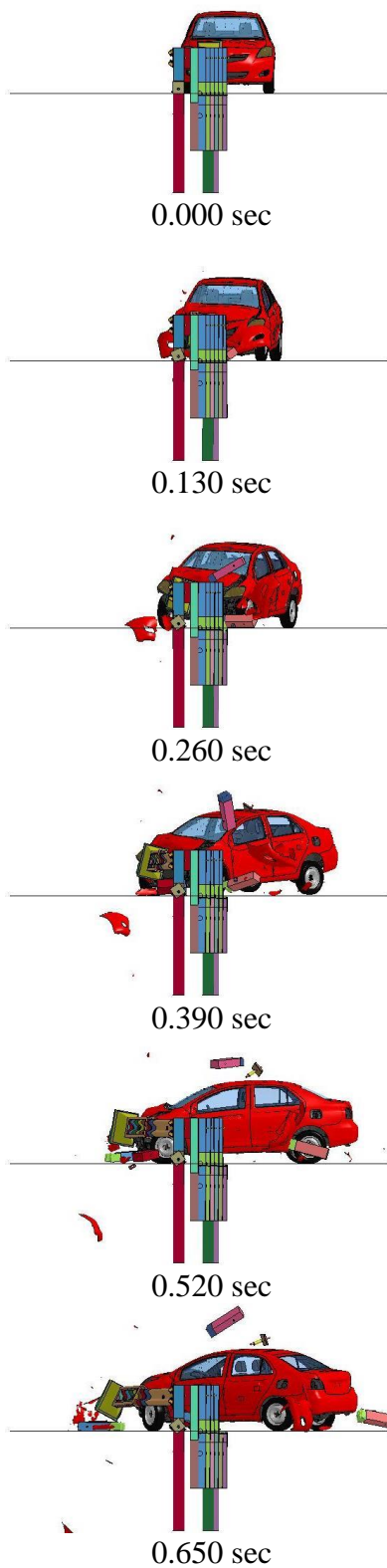


Simulation No. MASH-30-Deep-flared

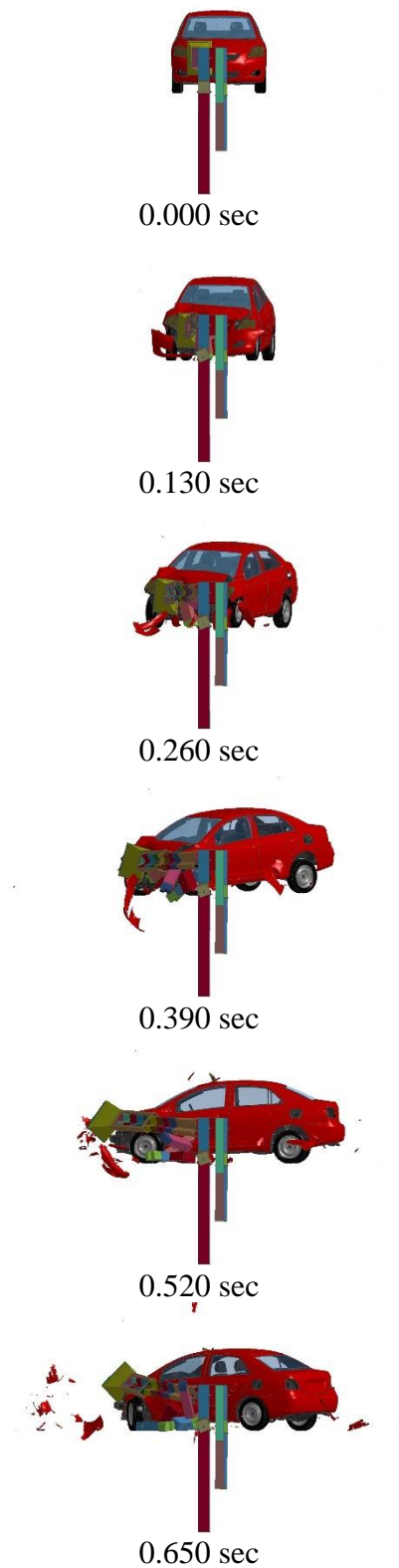


Simulation No. MASH-30-Deep-MGS

Figure 101. MASH 2009 Test No. 3-30, Deep Quarter-Point Offset, Overhead View

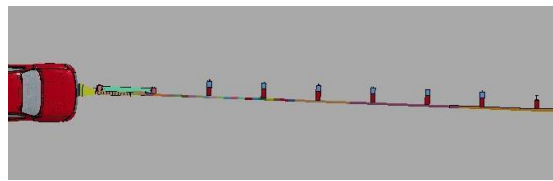


Simulation No. MASH-30-Deep-flared

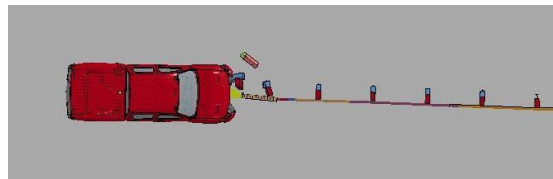


Simulation No. MASH-30-Deep-MGS

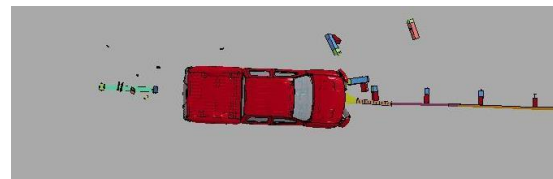
Figure 102. MASH 2009 Test No. 3-30, Deep Quarter-Point Offset, Downstream View



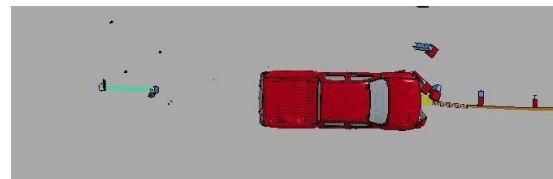
0.000 sec



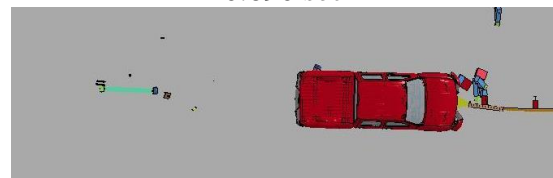
0.230 sec



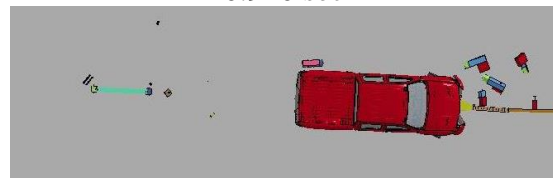
0.460 sec



0.690 sec

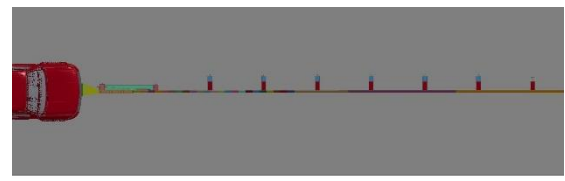


0.920 sec

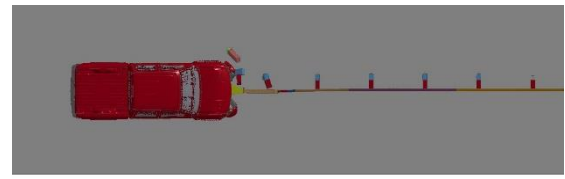


1.150 sec

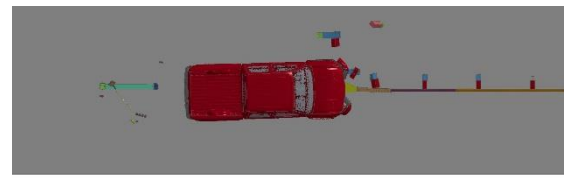
Simulation No. MASH-31-flared



0.000 sec



0.230 sec



0.460 sec



0.690 sec



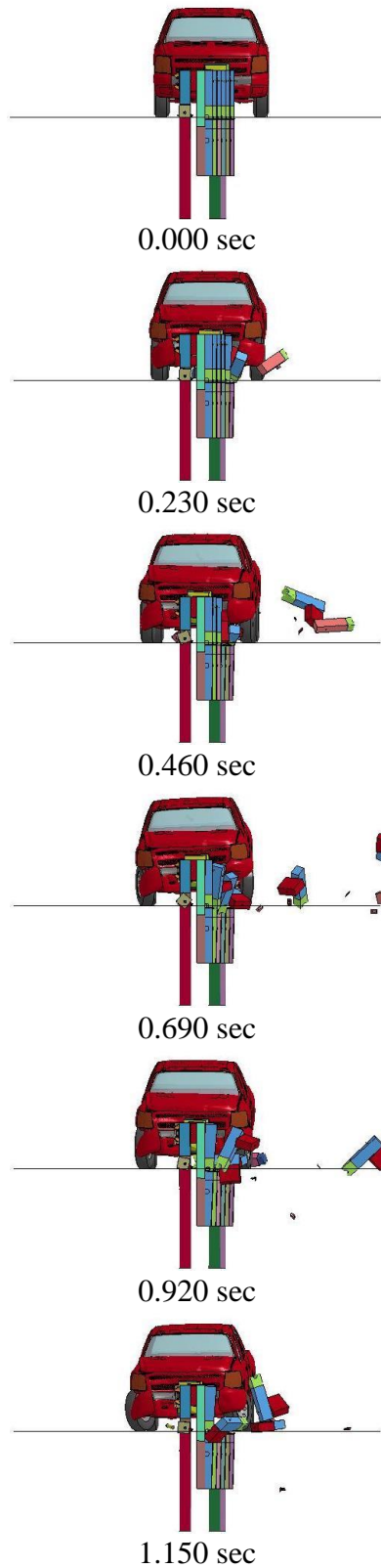
0.920 sec



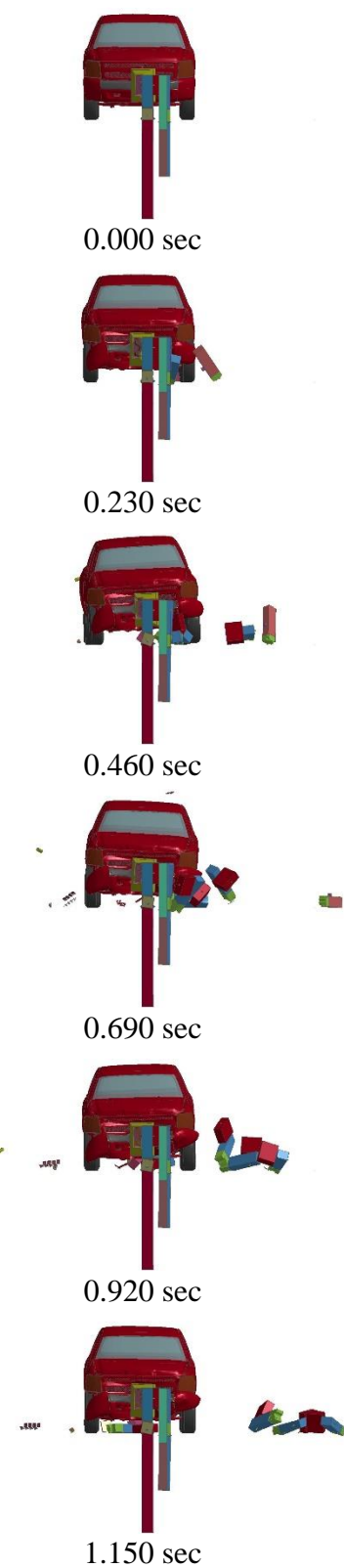
1.150 sec

Simulation No. MASH-31-MGS

Figure 103. MASH 2009 Test No. 3-31, Overhead View

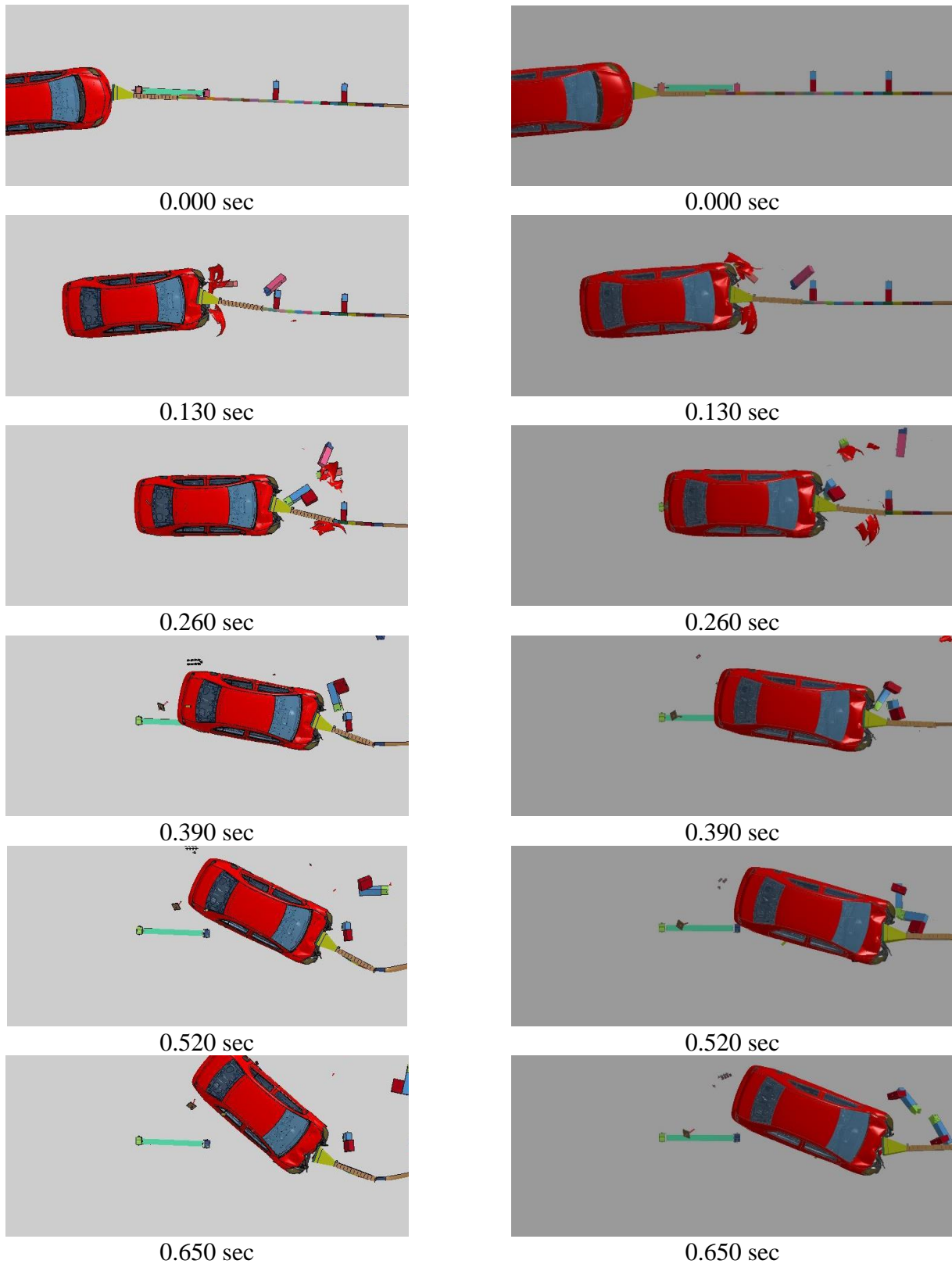


Simulation No. MASH-31-flared



Simulation No. MASH-31-MGS

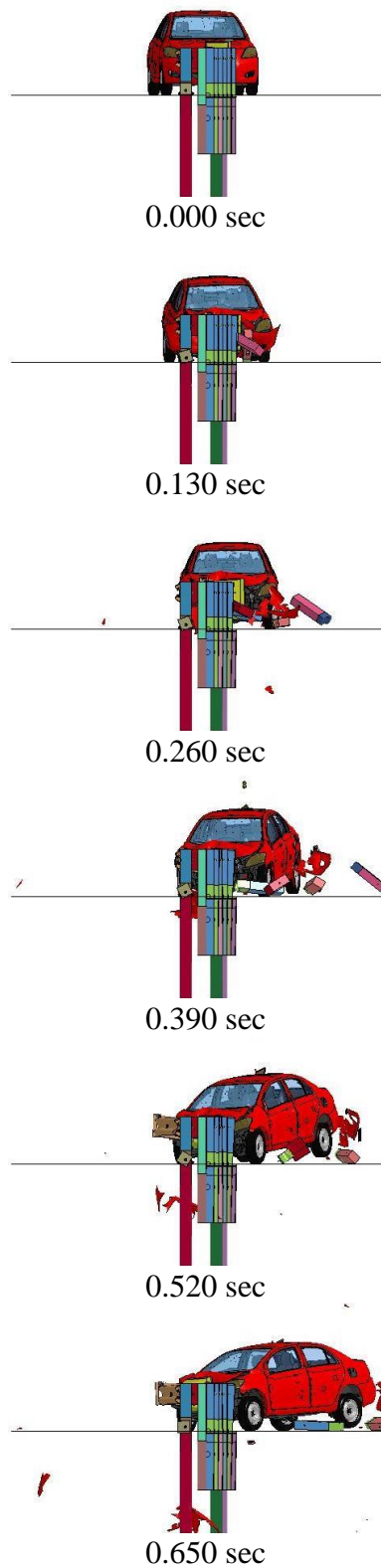
Figure 104. MASH 2009 Test No. 3-31, Downstream View



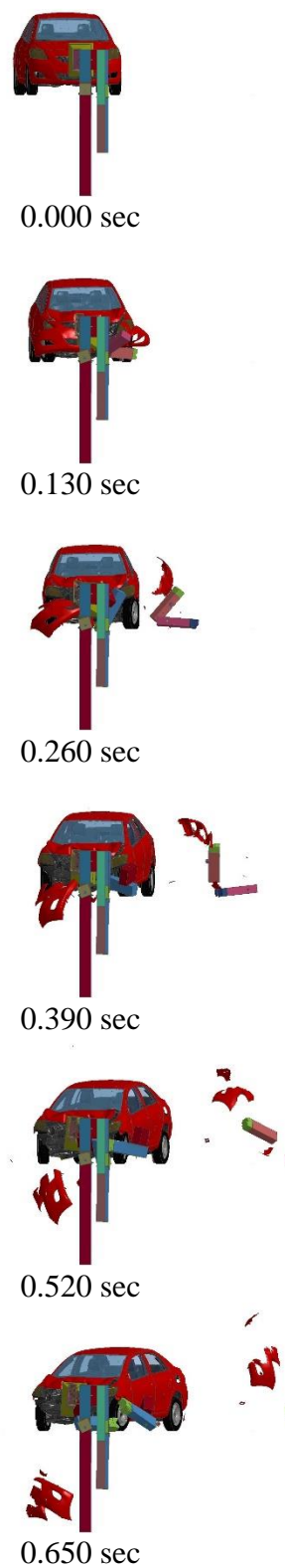
Simulation No. MASH-32-5deg-flared

Simulation No. MASH-32-5deg-MGS

Figure 105. MASH 2009 Test No. 3-32 at 5 Degrees, Overhead View



Simulation No. MASH-32-5deg-flared

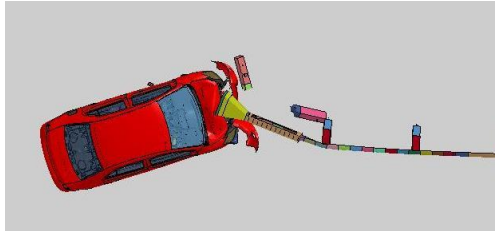


Simulation No. MASH-32-5deg-MGS

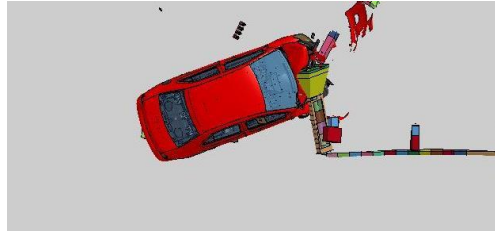
Figure 106. MASH 2009 Test No. 3-32 at 5 Degrees, Downstream View



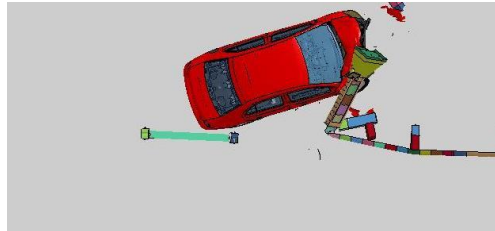
0.000 sec



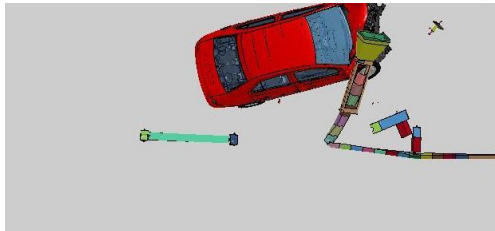
0.130 sec



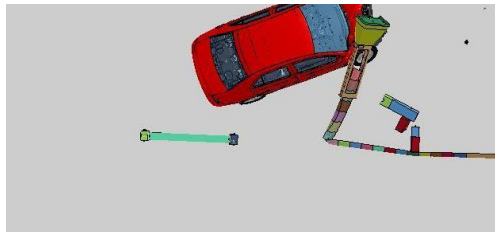
0.260 sec



0.390 sec

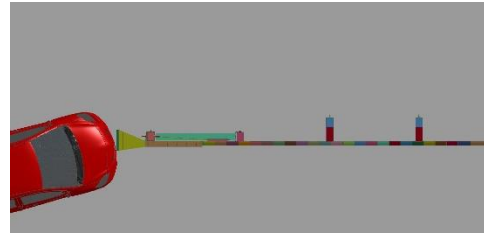


0.540 sec



0.650 sec

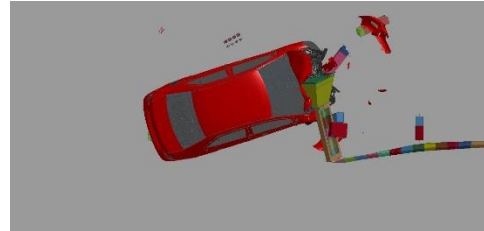
Simulation No. MASH-32-15deg-flared



0.000 sec



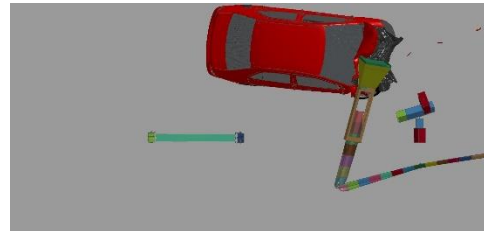
0.130 sec



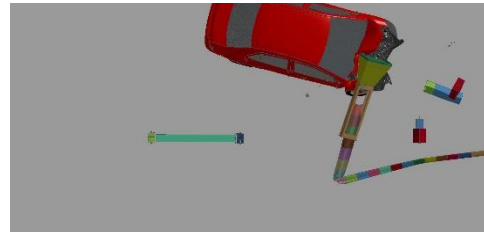
0.260 sec



0.390 sec



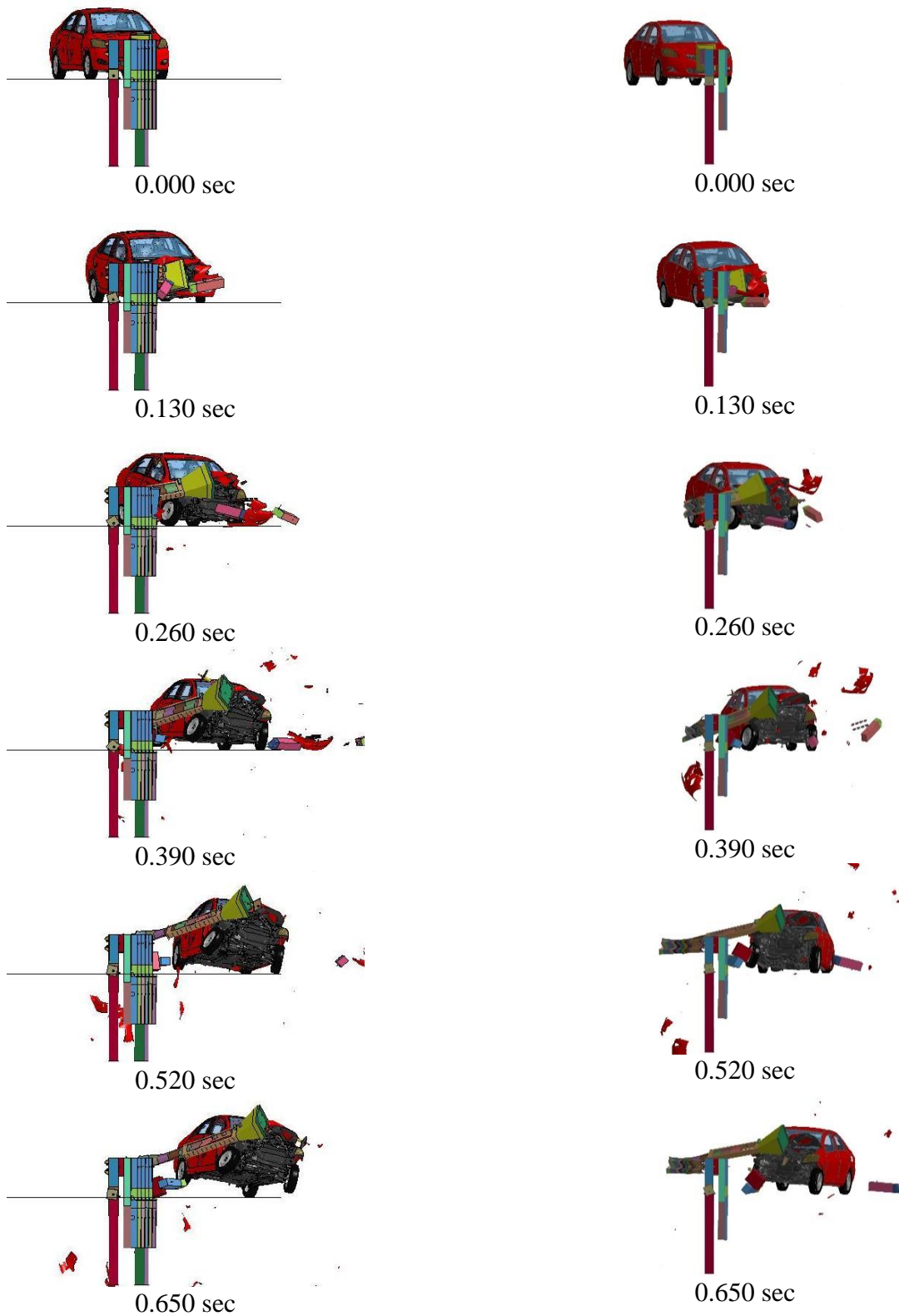
0.540 sec



0.650 sec

Simulation No. MASH-32-15deg-MGS

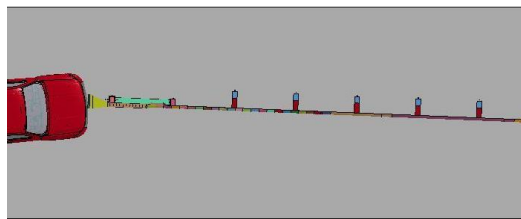
Figure 107. MASH 2009 Test No. 3-32 at 15 Degrees, Overhead View



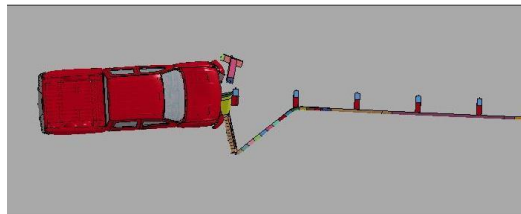
Simulation No. MASH-32-15deg-flared

Simulation No. MASH-32-15deg-MGS

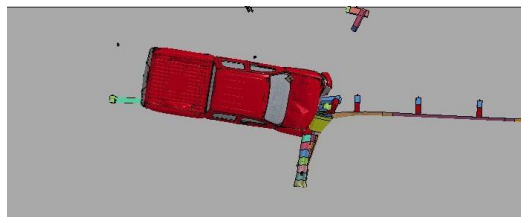
Figure 108. MASH 2009 Test No. 3-32 at 15 Degrees, Downstream View



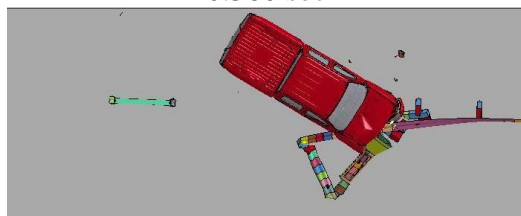
0.000 sec



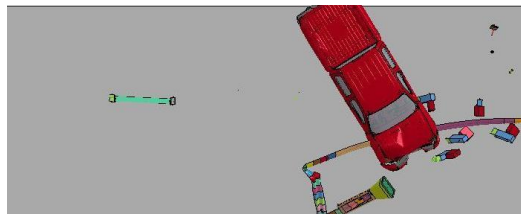
0.180 sec



0.360 sec



0.540 sec

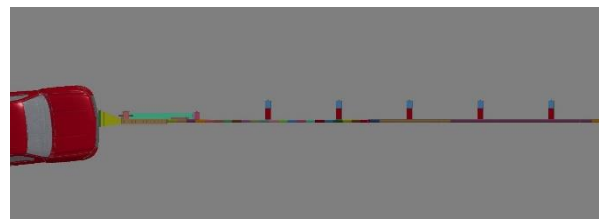


0.720 sec

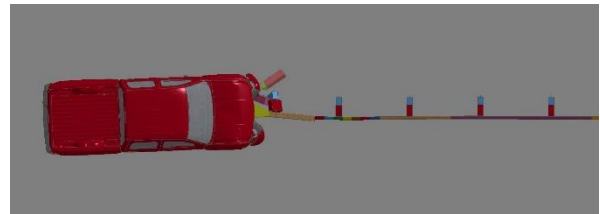


0.900 sec

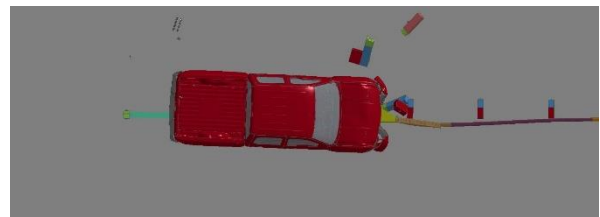
Simulation No. MASH-33-5deg-flared



0.000 sec



0.180 sec



0.360 sec



0.540 sec



0.720 sec



0.900 sec

Simulation No. MASH-33-5deg-MGS

Figure 109. MASH 2009 Test No. 3-33 at 5 degrees, Overhead View

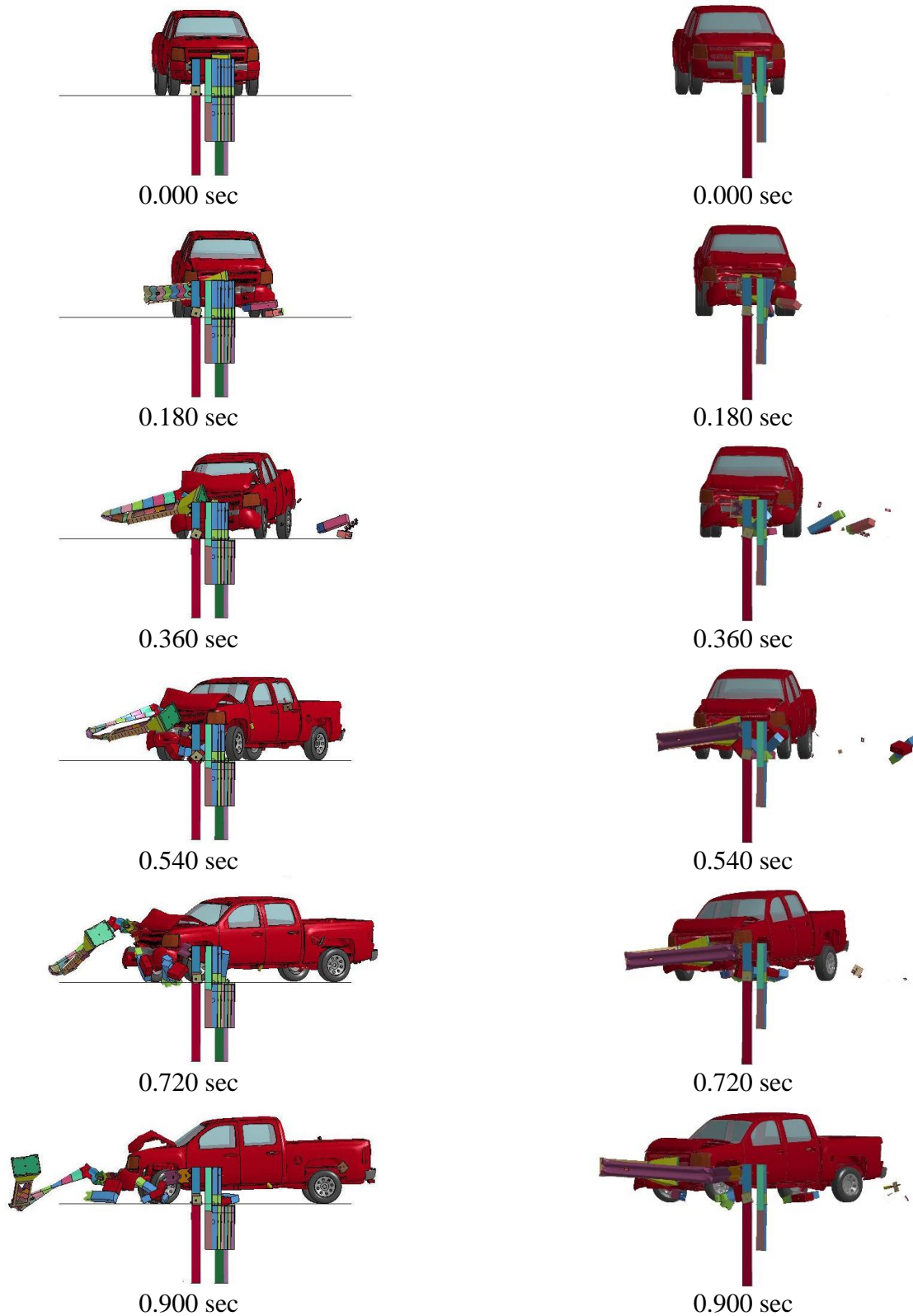
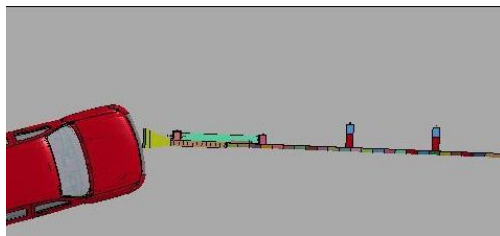
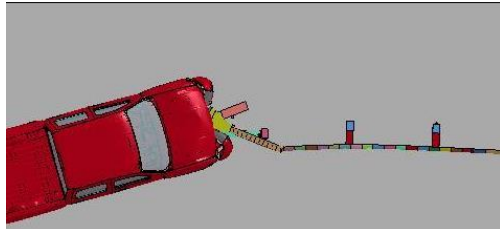


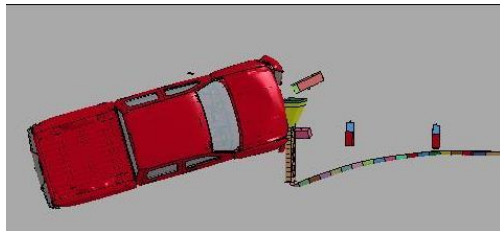
Figure 110. MASH 2009 Test No. 3-33 at 5 degrees, Downstream View



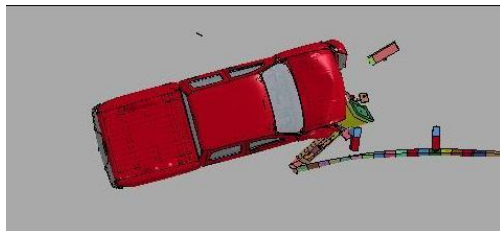
0.000 sec



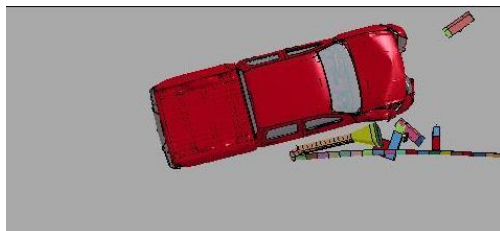
0.070 sec



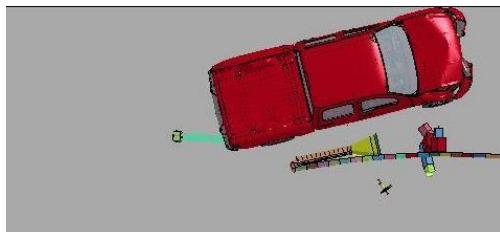
0.140 sec



0.210 sec

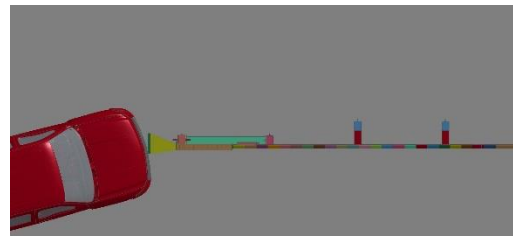


0.280 sec

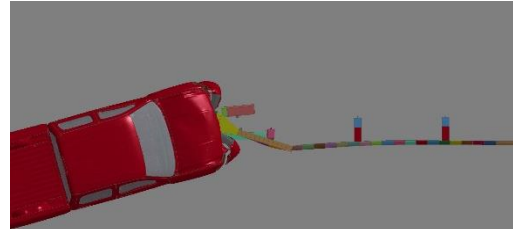


0.350 sec

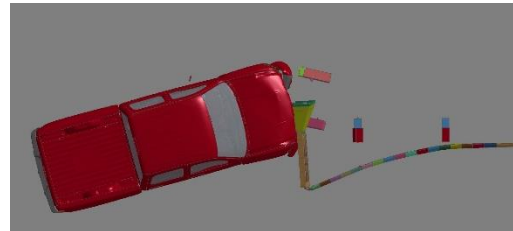
Simulation No. MASH-33-15deg-flared



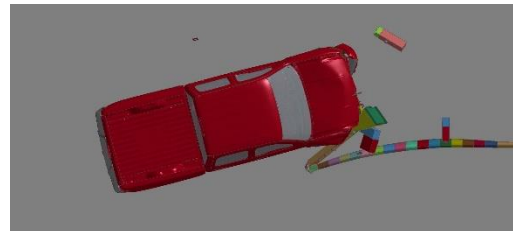
0.000 sec



0.070 sec



0.140 sec



0.210 sec



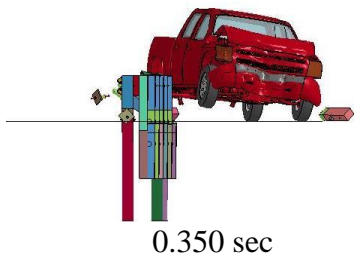
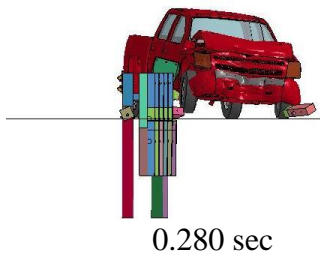
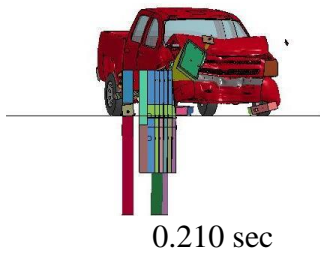
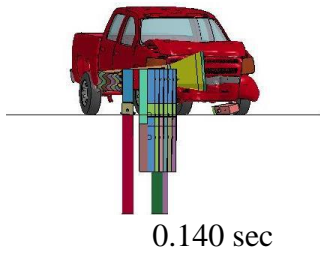
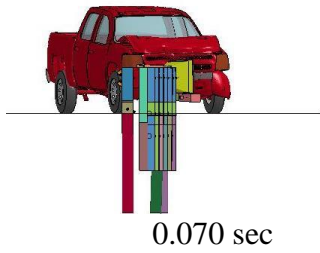
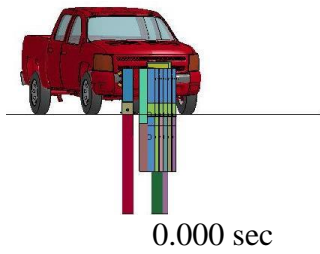
0.280 sec



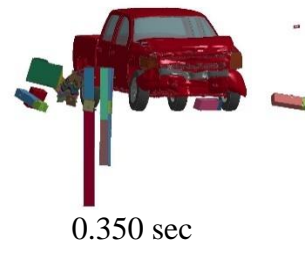
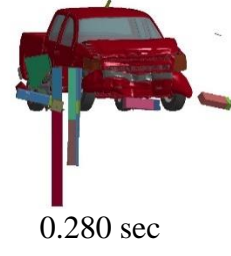
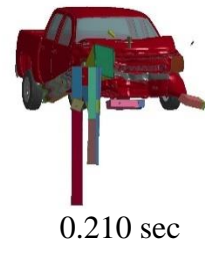
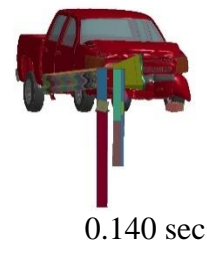
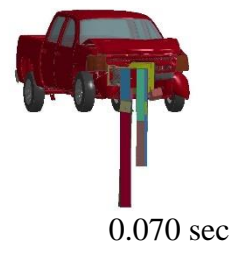
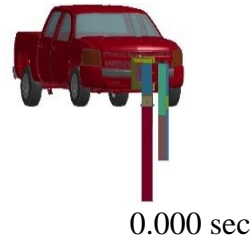
0.350 sec

Simulation No. MASH-33-15deg-MGS

Figure 111. MASH 2009 Test No. 3-33 at 15 degrees, Overhead View



Simulation No. MASH-33-15deg-flared



Simulation No. MASH-33-15deg-MGS

Figure 112. MASH 2009 Test No. 3-33 at 15 degrees, Downstream View

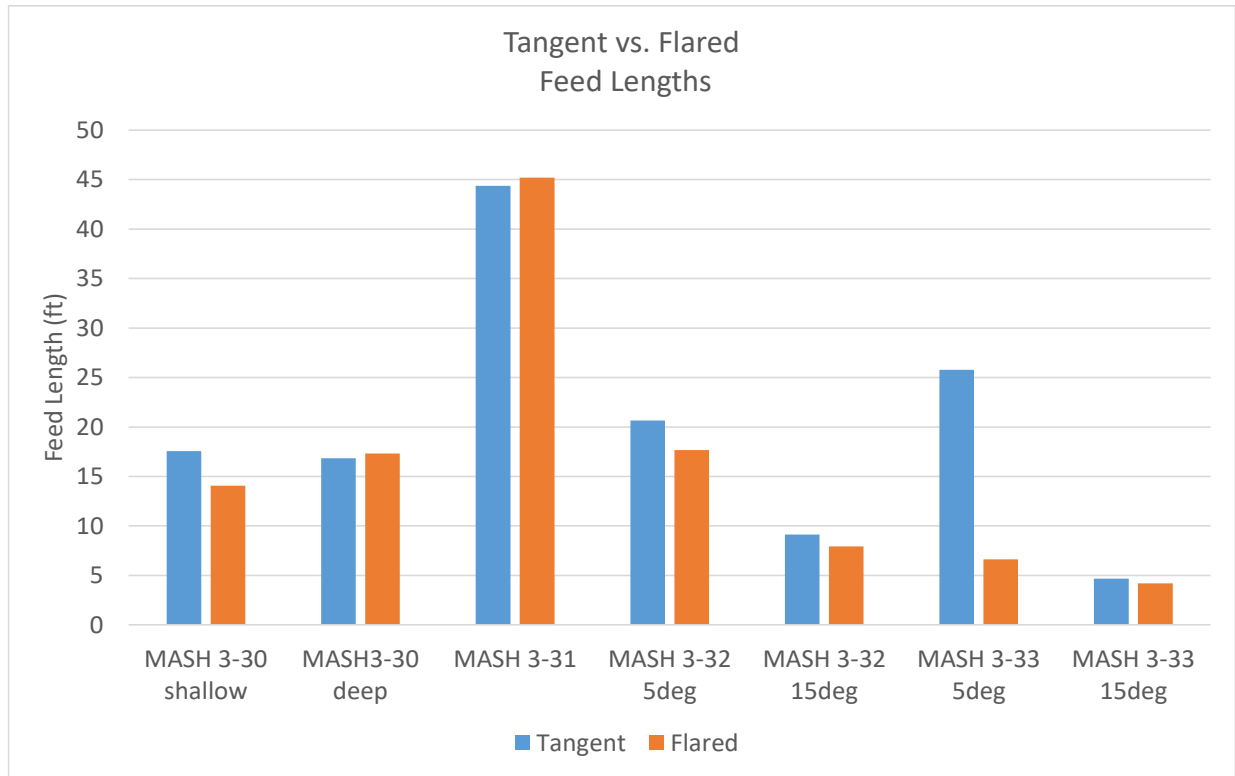


Figure 113. Tangent vs. Flared End Terminal Simulations, Feed Lengths

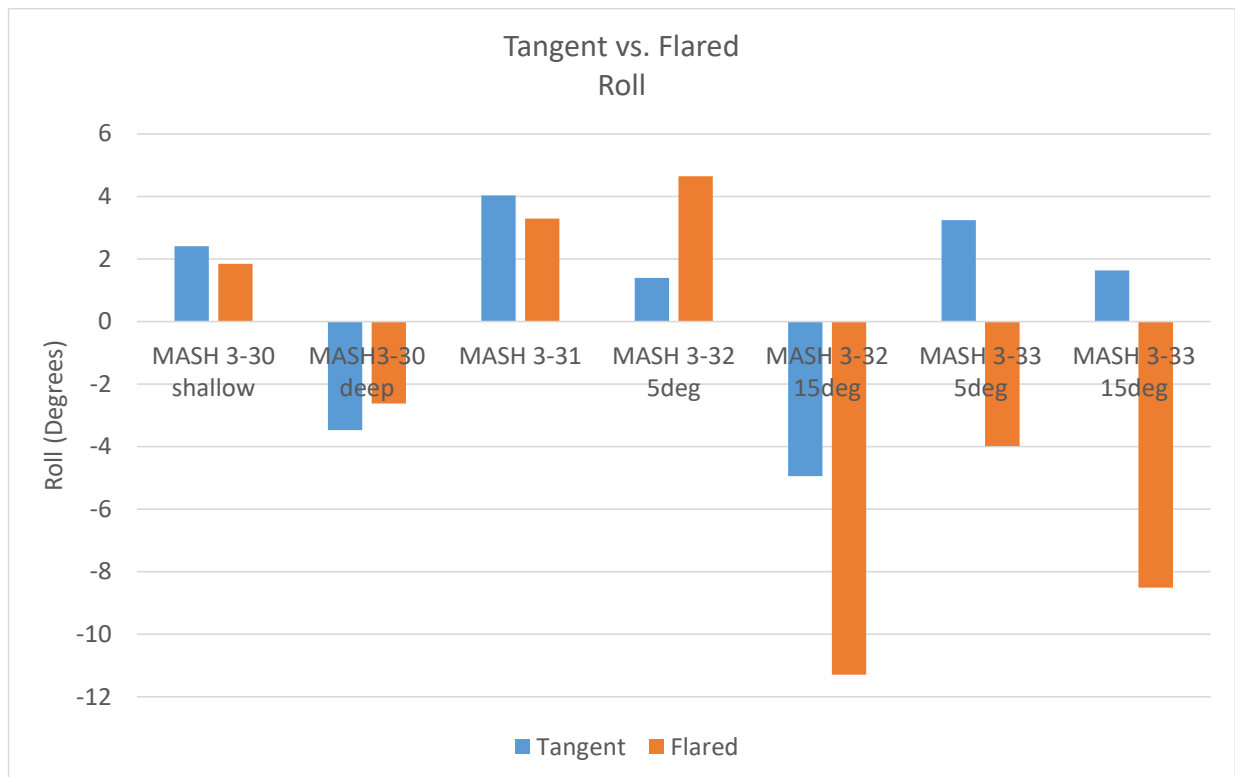


Figure 114. Tangent vs. Flared End Terminal Simulations, Vehicle Roll

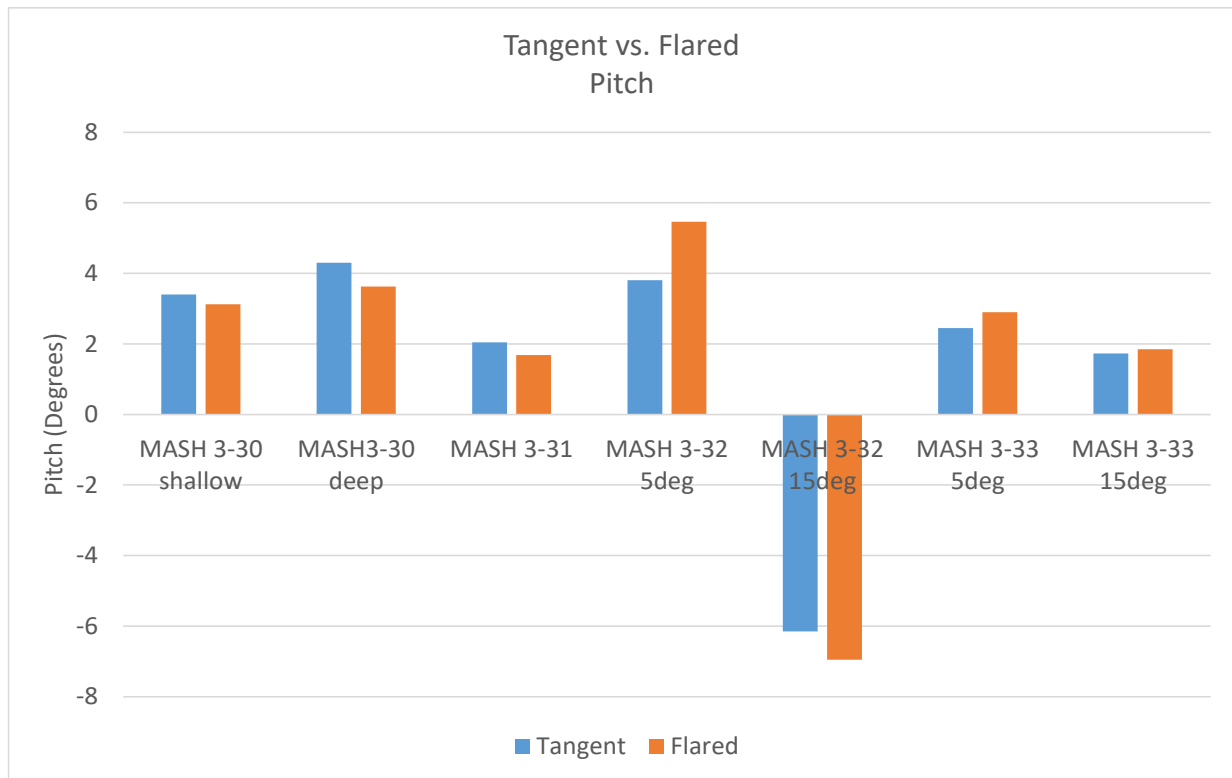


Figure 115. Tangent vs. Flared End Terminal Simulations, Vehicle Pitch

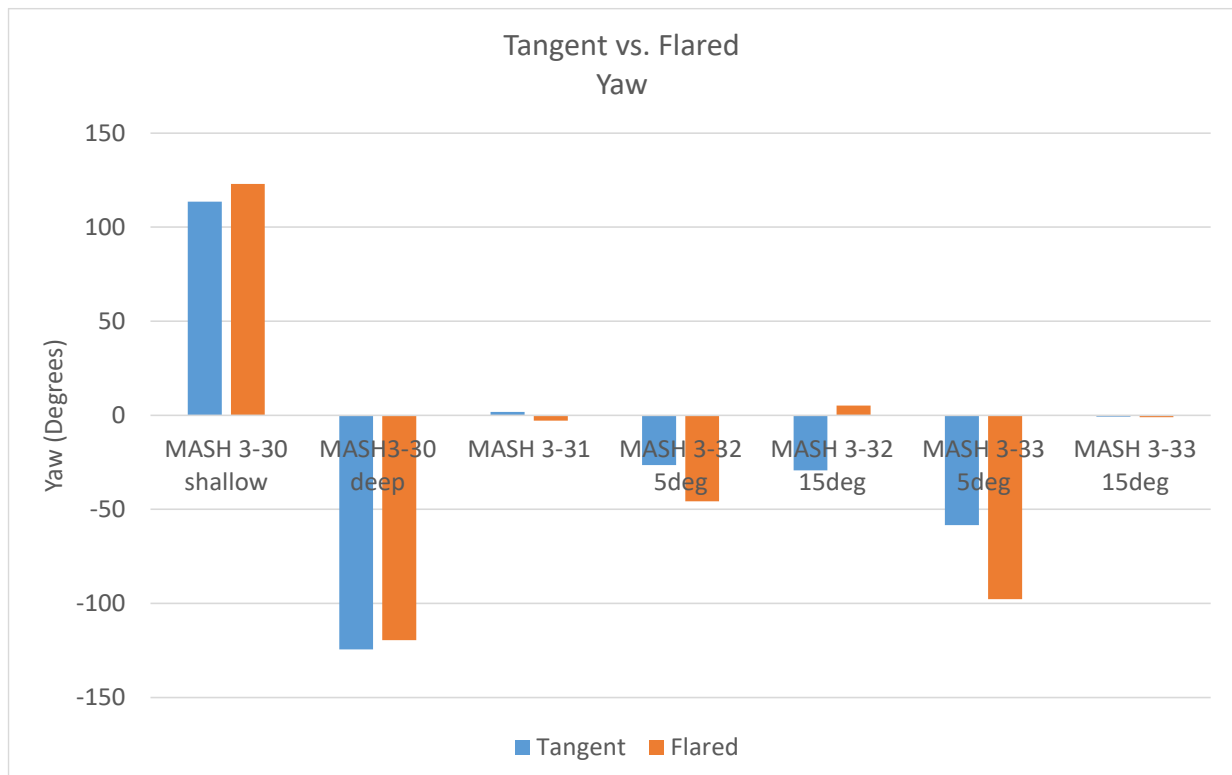


Figure 116. Tangent vs. Flared End Terminal Simulations, Vehicle Yaw

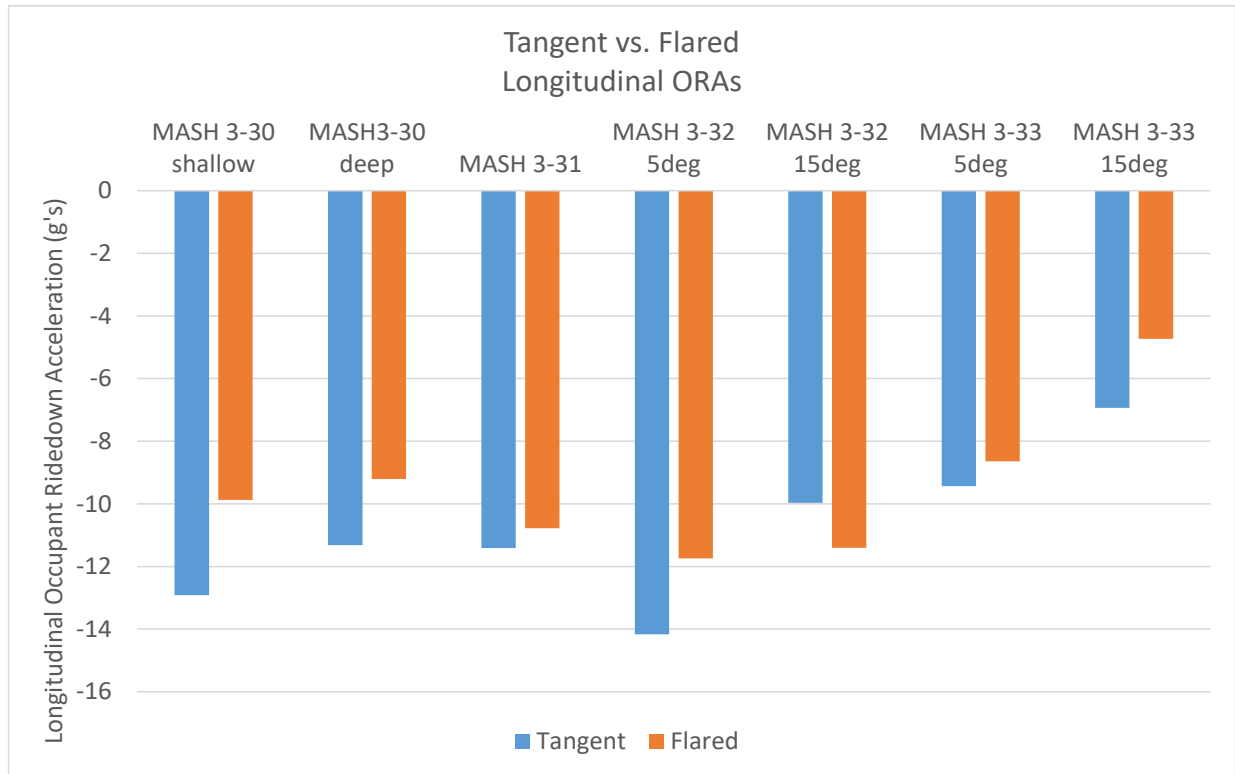


Figure 117. Tangent vs. Flared End Terminal Simulations, Longitudinal ORA

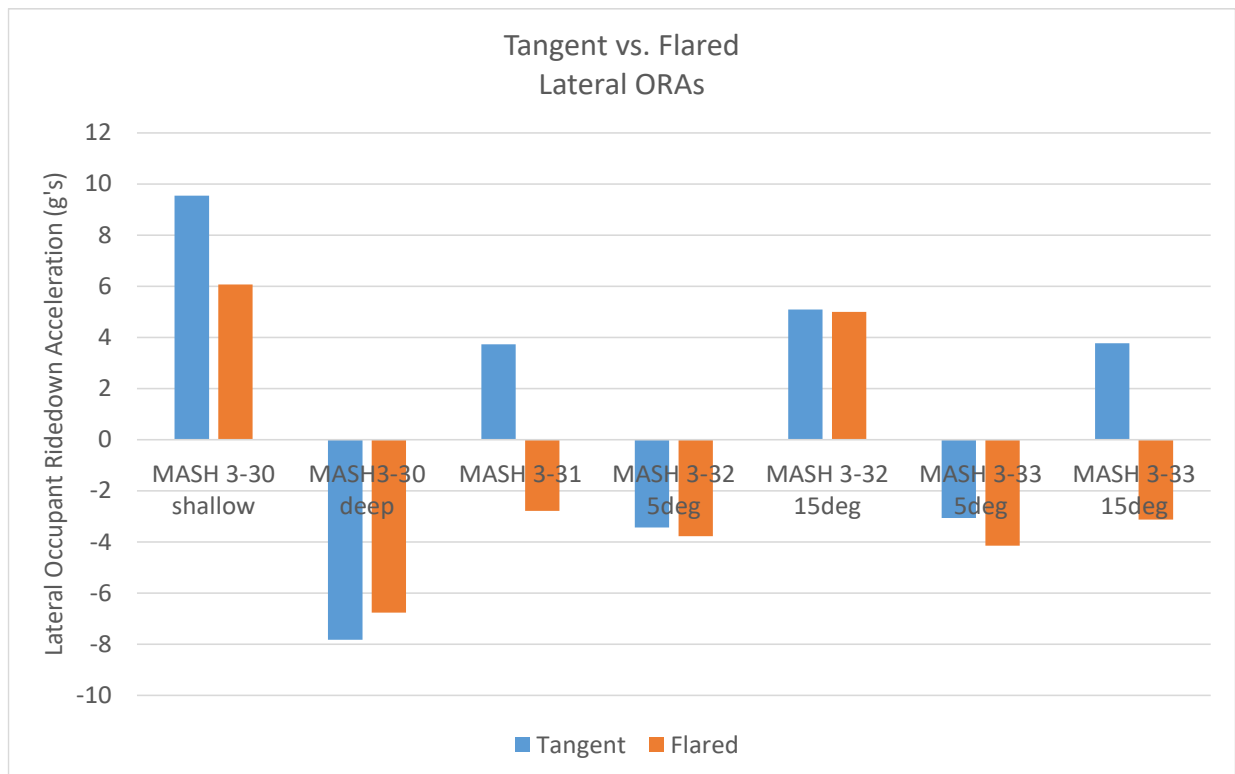


Figure 118. Tangent vs. Flared End Terminal Simulations, Lateral ORA

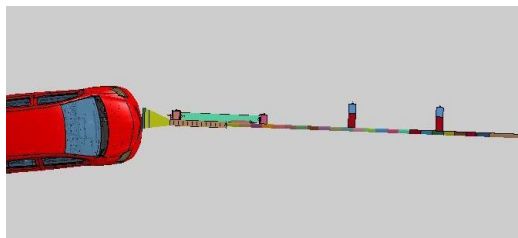
10 FLARED END TERMINAL SIMULATIONS WITH CURBS

Three sloped curb configurations (2 in., 4 in., and 6 in. (51 mm, 102 mm, and 152 mm) tall) were simulated at a 0-in. lateral offset from the face of the tangent guardrail. MASH 2009 test nos. 3-30 and 3-31 were not simulated with curbs as the system was expected to behave similarly to the flared baseline simulations, because the vehicle would have been on top of the curb and would not have interacted with the curb until late in the event. During the simulations with curbs laterally offset 0 in. and 6 in. (152 mm) from the front face of the guardrail, the change in impact height of the vehicle models in MASH 2009 test nos. 3-30 and 3-31 did not affect terminal performance. However, MASH 2009 test nos. 3-32 and 3-33 at 5- and 15-degree impact angles were simulated as the curbs may have affected vehicle and terminal performance under these impact conditions.

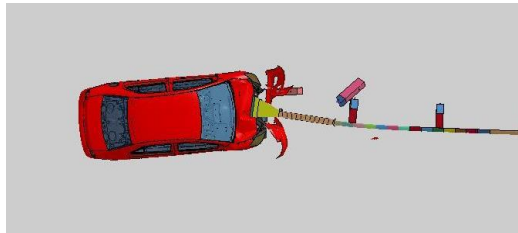
The Yaris and Silverado suspension and steering models were believed to be inaccurate as the tires turned significantly almost immediately after impacting the curbs, especially at a 5-degree impact angle. Because the curb was close to the end terminal, the heading angle of the vehicle upon impact was still close to targeted impact conditions for the 15-degree impact angles. However, some of the results at the 5-degree impact angles may not provide good comparisons as the centerline of the impact head was not at the centerline of the vehicle. The limitations with the vehicle model suspension and steering with curb impacts needs to be improved for future studies.

Sequential photographs comparing the flared end terminal impact simulations with and without curbs are shown in Figures 119 through 122. The feed lengths, roll, pitch, yaw, longitudinal and lateral ORA, and longitudinal and lateral OIV for each impact with flared and tangent terminals are shown in Figures 123 through 128.

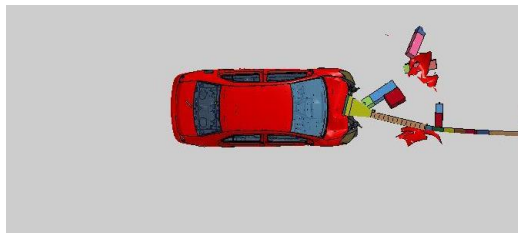
The lateral and longitudinal OIVs varied minimally in all of the simulations. The impact head nodes snagged on the Yaris hood and bumper, especially MASH 2009 test no. 3-32 5- and 15-degree impacts, which caused the vehicle to yaw and decelerate quickly. The feed lengths remained the same or decreased with the presence of curbs, except in the simulation of MASH 2009 test no. 3-33 at 15 degrees. Vehicle and terminal performance were not degraded significantly by the presence of a flared, tangent terminal with sloped curbs. Since the end terminal system was flared at a 2.3-degree angle, with a 5-degree impact angle, the effective vehicle angle of impact relative to the end terminal was 7.3 degrees. MASH 2009 test nos. 3-32 and 3-33 are to be conducted at a critical impact angle between 5 and 15 degrees. At a 5-degree impact angle, the system does not gate as easily as at a 15-degree impact angle, and the vehicle typically extrudes more guardrail through the end terminal. As the impact angle increased from 5 to 15 degrees, the system behavior changed more toward gating, which is likely why the feed length decreased for MASH 2009 test nos. 3-32 and 3-33 at a 5-degree impact angle with flared end terminals.



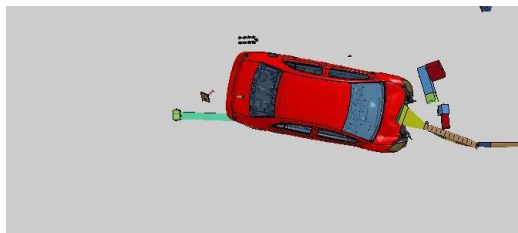
0.000 sec



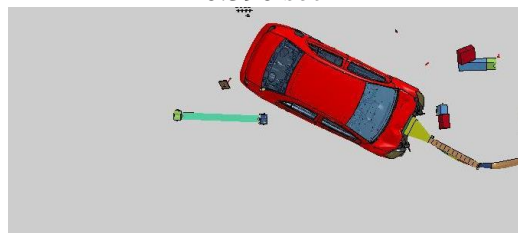
0.130 sec



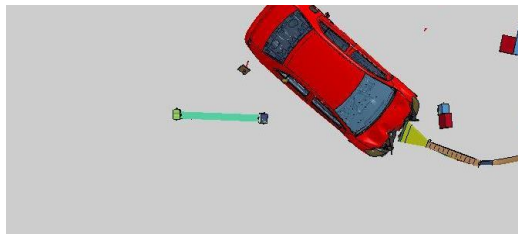
0.260 sec



0.390 sec

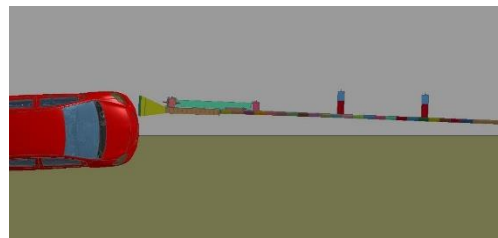


0.520 sec

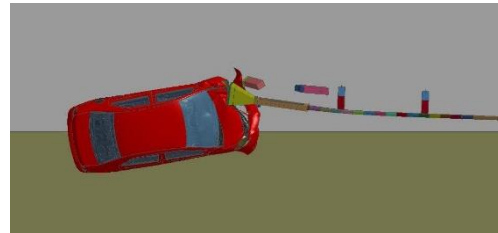


0.650 sec

Simulation No. MASH-32-5deg-flared



0.000 sec



0.130 sec



0.260 sec



0.390 sec



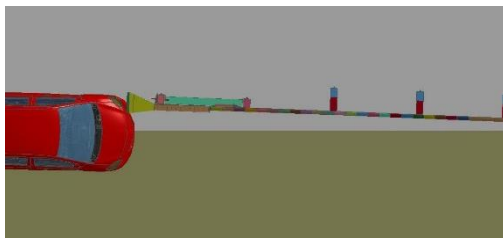
0.520 sec



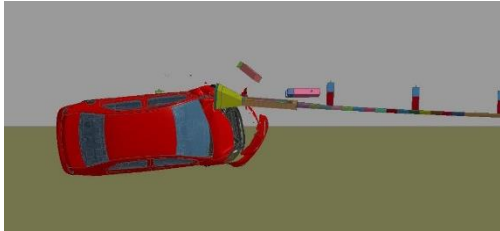
0.630 sec

Simulation No. MASH-32-5deg-flared-2"

Figure 119. MASH 2009, Test No. 3-32 at 5 Degrees, Overhead View



0.000 sec



0.130 sec



0.260 sec



0.390 sec

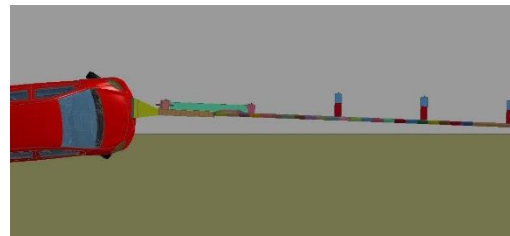


0.520 sec



0.620 sec

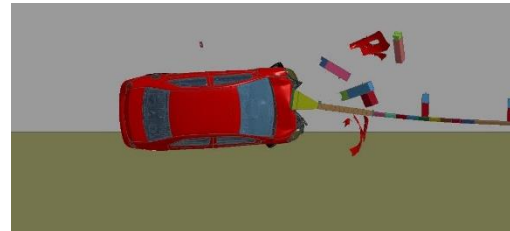
Simulation No. MASH-32-5deg-flared-4''



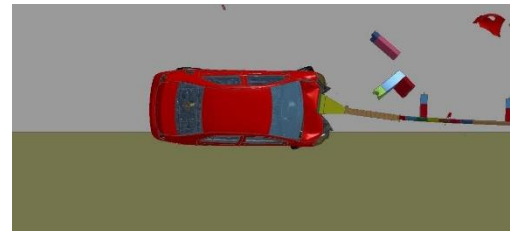
0.000 sec



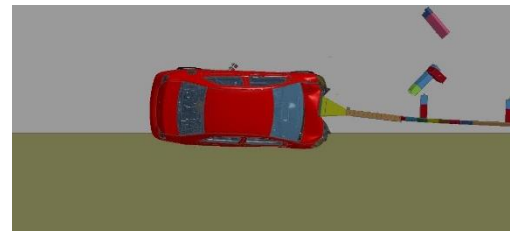
0.130 sec



0.260 sec



0.390 sec



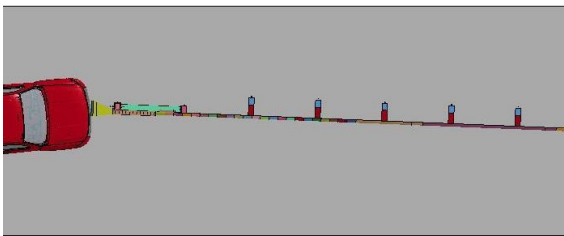
0.520 sec



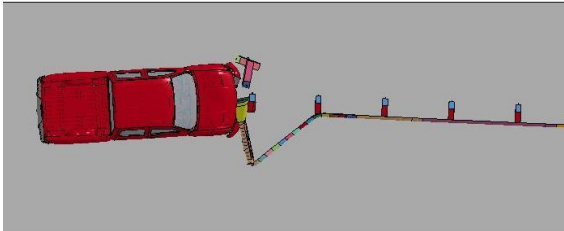
0.620 sec

Simulation No. MASH-32-5deg-flared-6''

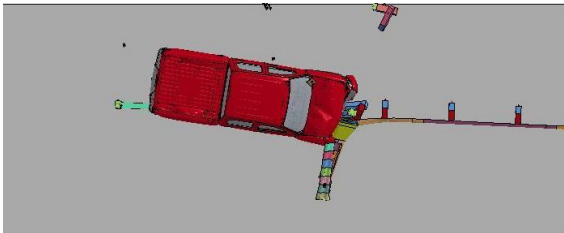
Figure 120. MASH 2009, Test No. 3-32 at 5 Degrees, Overhead View



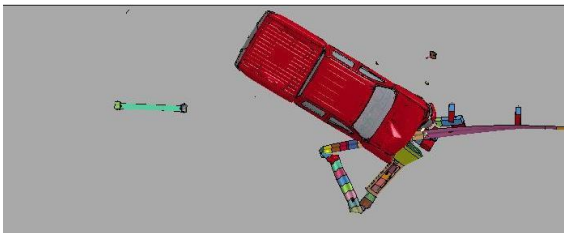
0.000 sec



0.180 sec



0.360 sec



0.540 sec

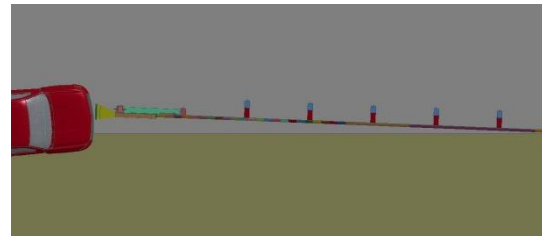


0.720 sec

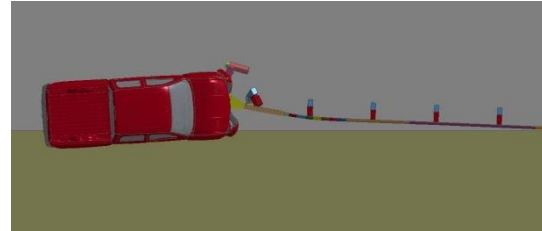


0.900 sec

Simulation No. MASH-33-5deg-flared



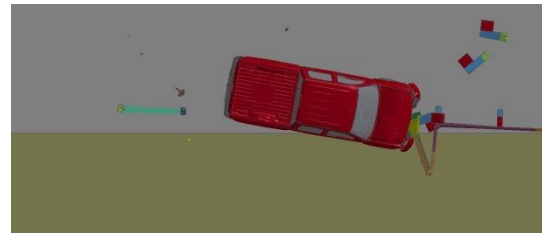
0.000 sec



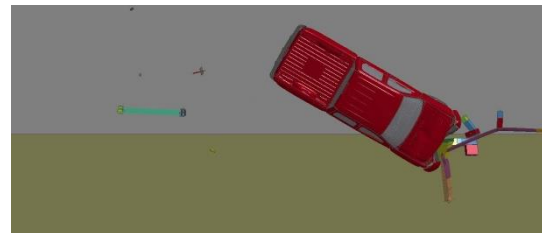
0.180 sec



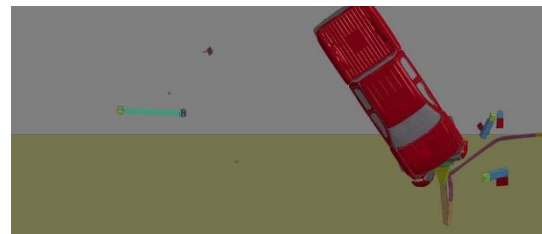
0.360 sec



0.540 sec



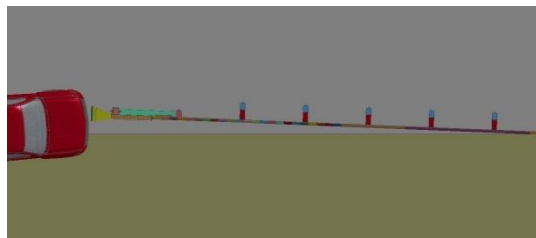
0.720 sec



0.900 sec

Simulation No. MASH-33-5deg-flared-2"

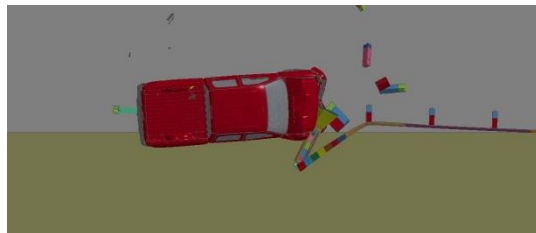
Figure 121. MASH 2009, Test No. 3-33 at 5 degrees, Overhead View



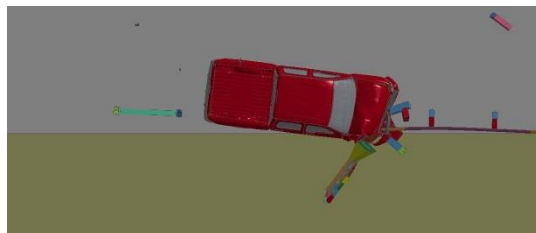
0.000 sec



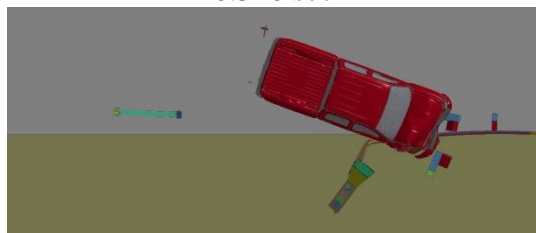
0.180 sec



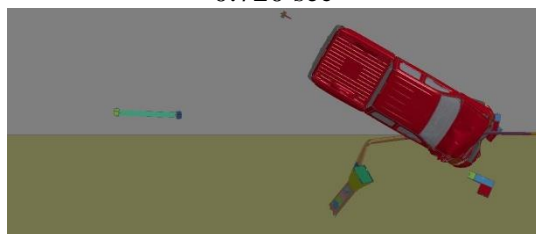
0.360 sec



0.540 sec

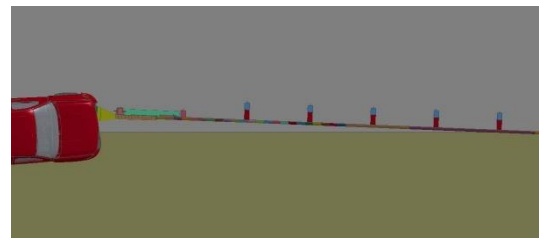


0.720 sec



0.900 sec

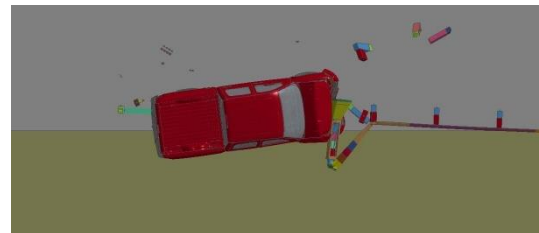
Simulation No. MASH-33-5deg-flared-4"



0.000 sec



0.180 sec



0.360 sec



0.540 sec



0.720 sec



0.900 sec

Simulation No. MASH-33-5deg-flared-6"

Figure 122. MASH 2009, Test No. 3-33 at 5 degrees, Overhead View

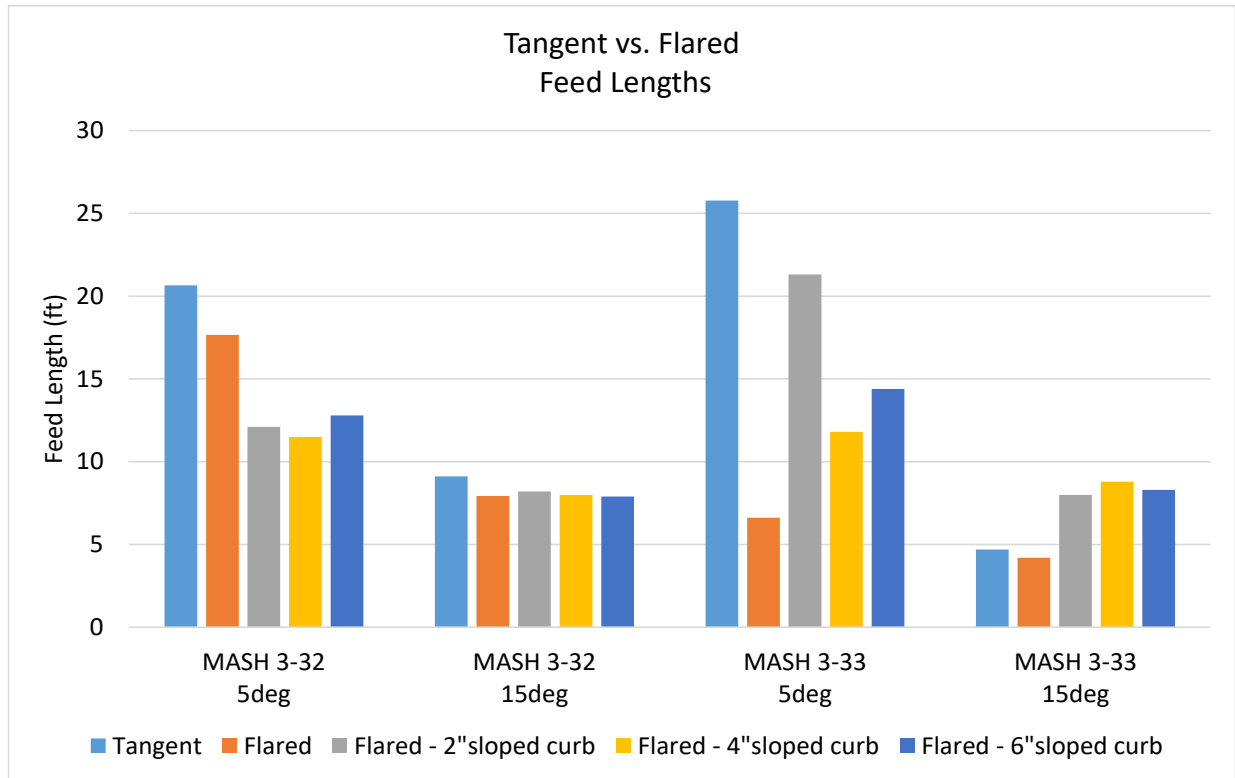


Figure 123. Flared End Terminal Simulations with Curbs, Feed Length

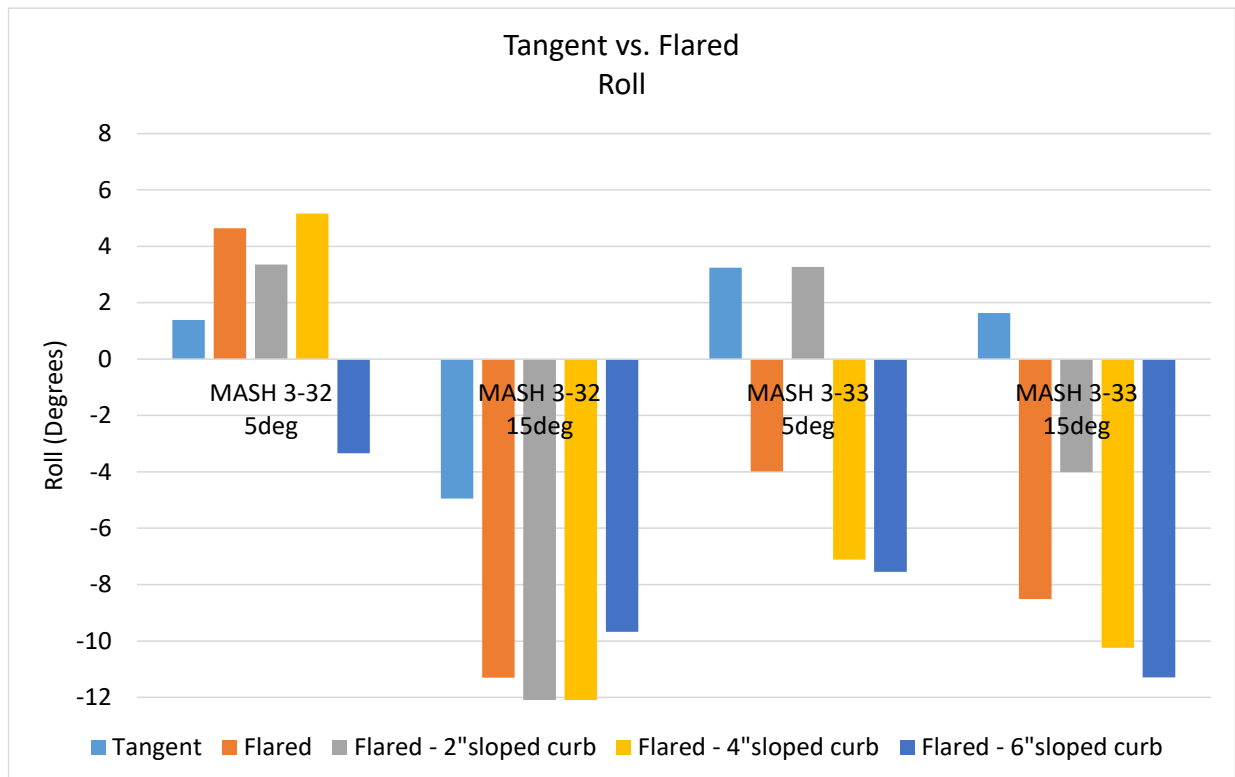


Figure 124. Flared End Terminal Simulations with Curbs, Vehicle Roll

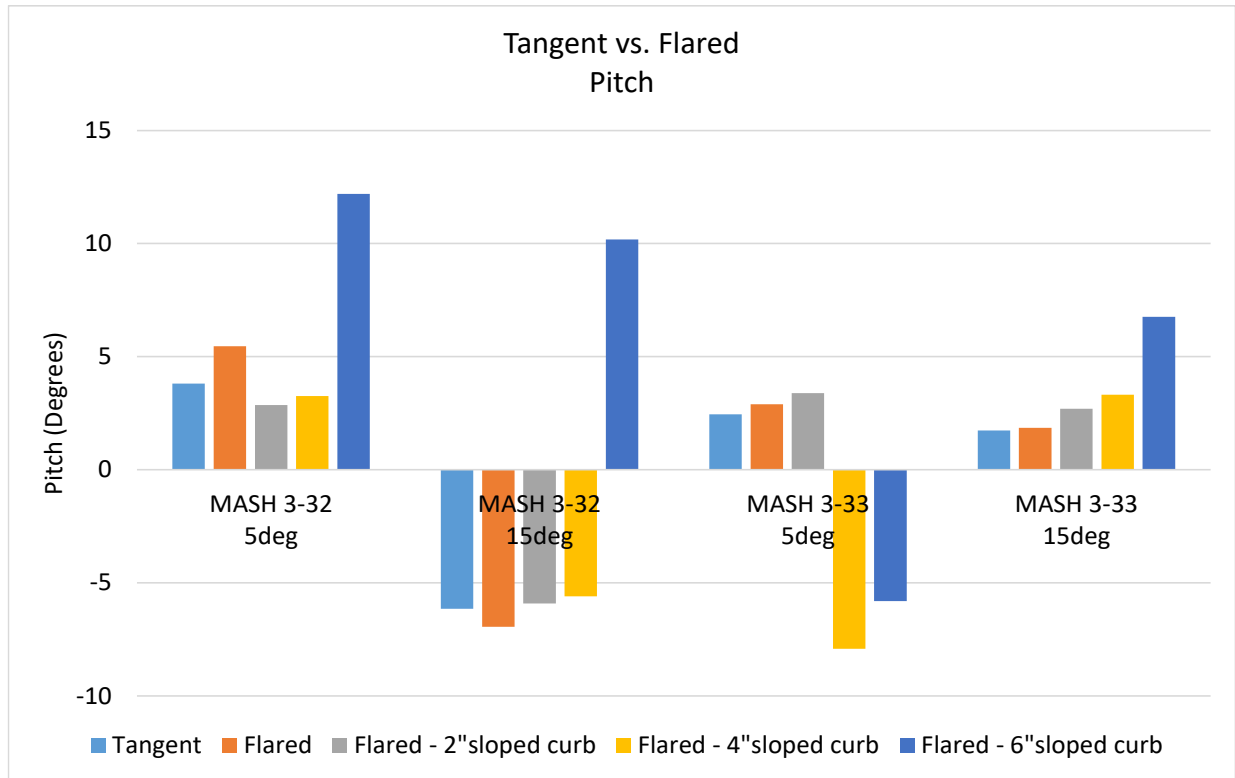


Figure 125. Flared End Terminal Simulations with Curbs, Vehicle Pitch

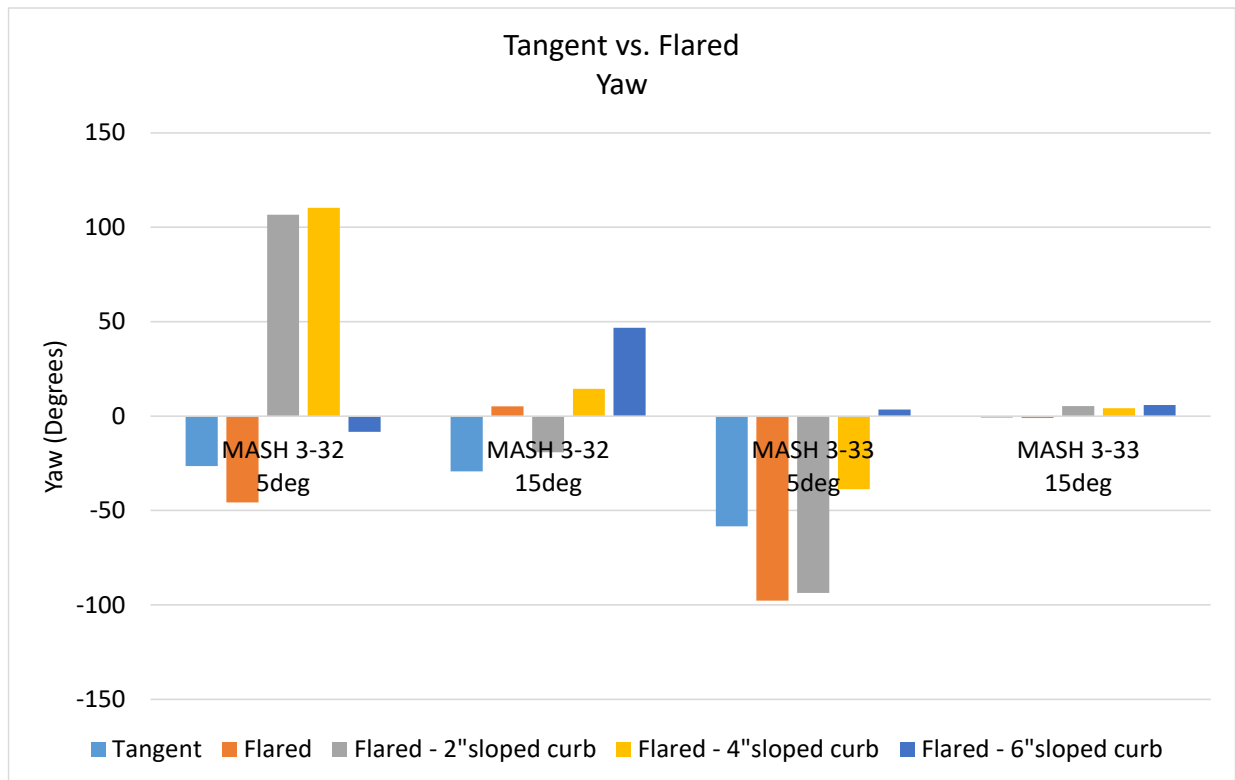


Figure 126. Flared End Terminal Simulations with Curbs, Vehicle Yaw

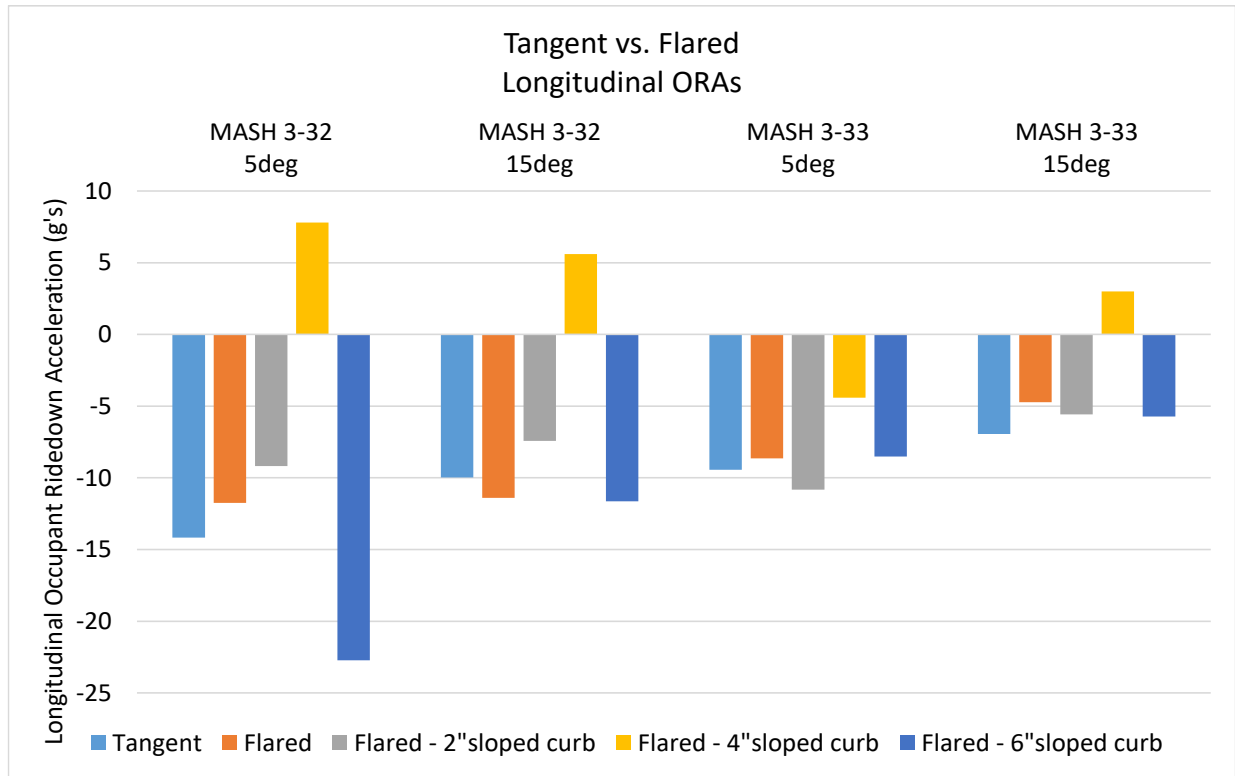


Figure 127. Flared End Terminal Simulations with Curbs, Longitudinal ORA

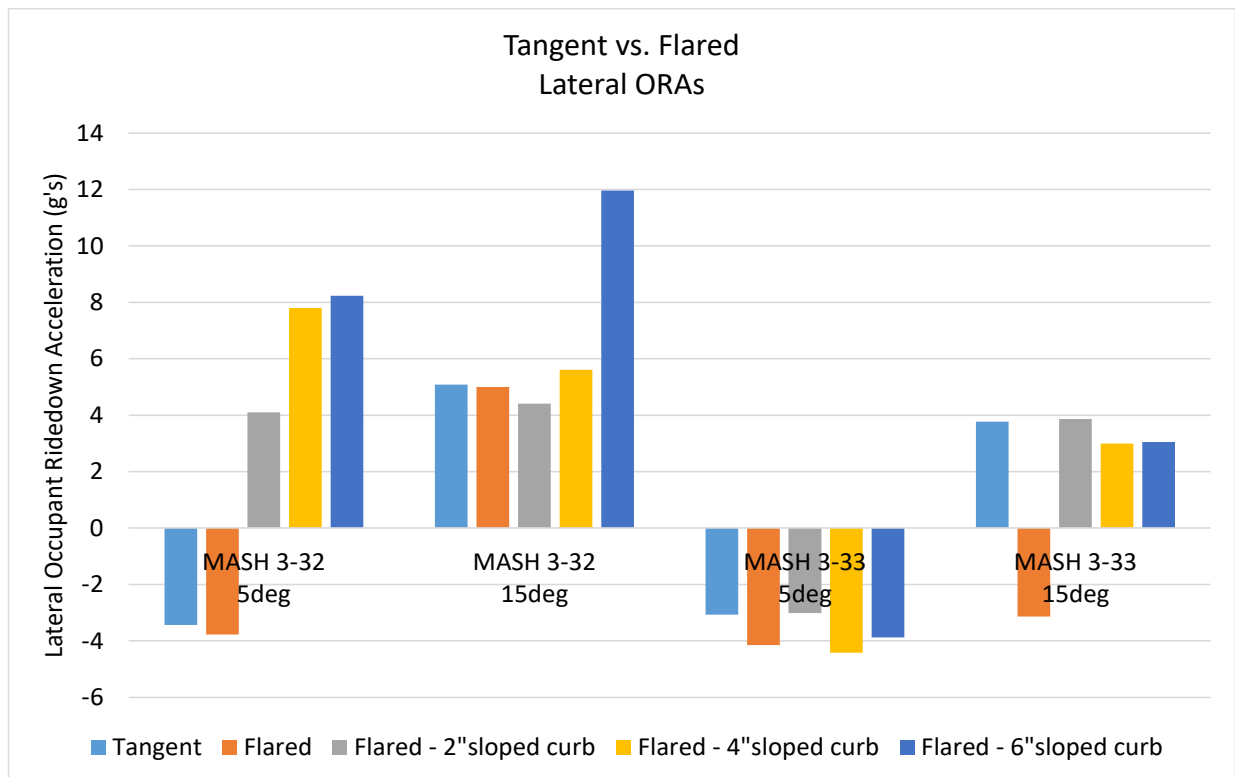


Figure 128. Flared End Terminal Simulations with Curbs, Lateral ORA

11 SUMMARY, CONCLUSIONS, AND RECOMMENDATIONS

Curb placement in advance of guardrail end terminals was investigated to determine if curbs significantly degraded terminal performance on high-speed roadways. In lieu of conducting several full-scale crash tests to evaluate end terminal systems with curbs, a computer simulation effort was conducted and the results were evaluated with MASH 2009 evaluation criteria. Only MASH 2009 test nos. 3-30 through 3-33 were evaluated, which involved impacts on the end of the end terminal instead of along the length of the terminal. Since several State DOTs install more than one type of end terminal system, a generic, tangent guardrail end terminal system that was representative of several compression-based systems (ET-2000, BEST, SKT, FLEAT, and ET-Plus) was evaluated.

The 175-ft (53.3-m) long MGS LS-DYNA finite element analysis model previously developed and validated at MwRSF was modified to incorporate the representative end terminal. Two variations of a 29-post, 175-ft (53.3-m) long model were created:

- 1) 27 $\frac{3}{4}$ -in. (706-mm) tall guardrail with posts with 8-in. (203-mm) deep blockouts representative of modified G4(1S) with the representative end terminal and
- 2) 31-in. (787-mm) tall guardrail with posts with 12-in. (305-mm) deep blockouts representative of MGS with the representative end terminal

The energy absorbing mechanism was not modeled for the generic end terminal system due to the variability between systems. Therefore, an average longitudinal force of 11.2 kips (50 kN), which was representative of the average forces produced by common energy-absorbing terminals, was applied on the impact head at the approximate location the rail would exit the impact head. Due to this modeling technique, very little compressive force was applied to the rail. Thus, buckling that often occurs in the rail (especially in NCHRP Report 350 or MASH 2009 test no. 3-30), was likely inaccurate. In addition, since the rail did not bend, deform, or exit the side of the impact head, the rail was sequentially deleted so that it did not penetrate the vehicle.

Several simulations were conducted on the tangent energy-absorbing end terminal attached to modified G4(1S) and MGS guardrail models with and without curbs with impacts on the end of the terminal (NCHRP Report 350 and MASH 2009 test nos. 3-30, 3-31, 3-32, and 3-33). The twelve baseline simulations were compared to several full-scale crash tests on compression-based terminals to ensure the end terminal model was representative of actual systems. While the performance of proprietary end terminals varies between systems, the end terminal model was representative of most of the full-scale crash test results.

The model was then evaluated with 108 simulations with various curb configurations. All simulations were conducted with the curb extending in advance of and along the entire length of the end terminal. The tangent end terminal model was evaluated with MASH 2009 test nos. 3-30, 3-31, 3-32, and 3-33 impact conditions with several curb configurations, including 2-in., 4-in., and 6-in. (51-mm, 102-mm, and 152-mm) tall wedge and vertical-shaped curbs with the toe laterally offset 0 in., 6 in. (152-mm), and 6 ft (1.8 m) away from the front face of the guardrail.

The tangent end terminal model was also flared at a 1:25 flare rate with a 2-ft (0.6-m) lateral offset and evaluated with and without curbs. Seven baseline simulations without curbs,

and twelve simulations with curbs were evaluated. The evaluated curb configurations were 2-in., 4-in., and 6-in. (51-mm, 102-mm, and 152-mm) tall wedge-shaped curbs with the toe laterally offset 0 in. away from the front face of the tangent guardrail.

Several conclusions were drawn. First, due to the small curb offsets, the vehicle interaction with the impact head was minimally affected by the curbs. However, larger lateral curb offsets may have more of an effect on the vehicle trajectory and interaction with the impact head. Second, the presence of curbs affected the small car impacts the most. The 4-in. (102-mm) and 6-in. (152-mm) tall vertical curbs affected vehicle yaw in the small car impacts, and the tires had a more difficult time traversing the curb, especially when the tires were non-tracking. The sloped curbs minimally affected vehicle yaw. Third, the flare affected the performance of the vehicle and end terminal the most in MASH 2009 test nos. 3-32 and 3-33 angled impacts. Finally, the vehicle and terminal performance was most similar to the baseline simulations with 2-in. (51-mm) tall curbs than 4-in. (102-mm) and 6-in. (152-mm) tall curbs.

Due to computer simulation limitations, improvements are recommended for future similar studies. First, model one specific end terminal, rather than a representative terminal, and validate the mode. Second, calibrate post-to-rail bolt release and tearing that may occur as the bolt releases under end-on terminal impacts. Third, conduct a curb traversal study at shallow angles with the current MASH 2009 vehicles and calibrate the vehicle steering and suspension models. Finally, improve the contact definition between the impact head and vehicle models.

It is recommended that full-scale crash testing be conducted on tangent and flared end terminals in conjunction with 4-in. (102-mm) tall or shorter sloped curbs, especially with MASH 2009 test nos. 3-30 and 3-32, to further evaluate the effects of curbs on end terminal performance. Additionally, further research may be required to evaluate impacts along the length of the end terminal. As noted previously, the height of the guardrail was relative to the top of the curb to keep breakaway features at the groundline, whereas previous testing on the length-of-need of W-beam guardrail systems has been conducted with a rail height relative to the roadway surface, or toe of the curb, at small lateral curb offsets. Therefore, further consideration should be given to the rail height and/or the location of the breakaway features relative to the groundline.

12 REFERENCES

1. Federal Highway Administration, "Roadside Terminals" Resource Chart, October 2012. http://safety.fhwa.dot.gov/roadway_dept/policy_guide/road_hardware/resource_charts/road_sideterminals.pdf
2. Federal Highway Administration, "Median Terminals" Resource Chart, September 2012. http://safety.fhwa.dot.gov/roadway_dept/policy_guide/road_hardware/resource_charts/medianterminals.pdf
3. Ross, H.E., Sicking, D.L., Zimmer, R.A., and Michie, J.D., *Recommended Procedures for the Safety Performance Evaluation of Highway Features*, National Cooperative Highway Research Program (NCHRP) Report 350, Transportation Research Board, Washington, D.C., 1993.
4. *Manual for Assessing Safety Hardware (MASH)*, American Association of State Highway and Transportation Officials (AASHTO), Washington, D.C., 2009.
5. *A Policy on Geometric Design of Highways and Streets 2004*, Fifth Edition, American Association of State Highway and Transportation Officials (AASHTO), Washington, D.C., 2004.
6. Polivka, K.A., Faller, R.K., Sicking, D.L., Rohde, J.R., Reid, J.D., and Holloway, J.C., *Guardrail and Guardrail Terminals Installed Over Curbs*, Research Report No. TRP-03-83-99, Midwest Roadside Safety Facility, University of Nebraska-Lincoln, Lincoln, Nebraska, March 21, 2000.
7. Polivka, K.A., Faller, R.K., Sicking, D.L., Rohde, J.R., Reid, J.D., and Holloway, J.C., *Guardrail and Guardrail Terminals Installed Over Curbs – Phase II*, Research Report No. TRP-03-105-00, Midwest Roadside Safety Facility, University of Nebraska-Lincoln, Lincoln, Nebraska, November 5, 2001.
8. Bullard, D.L. and Menges, W.L., *NCHRP Report 350 Test 3-11 on the G4(2W) Strong Post W-Beam Guardrail with 100 mm High Asphaltic Curb*, Report No. FHWA-RD-00, Federal Highway Administration, Washington, D.C., June, 2000.
9. Plaxico, C.A., Ray, M.H., Wier, J.A., Orengo, F., Tiso, P., McGee, H., Council, F., and Eccles, K., *Recommended Guidelines for Curb and Curb-Barrier Installations*, NCHRP Report 537, Transportation Research Board, Washington, D.C., 2005.
10. *Roadside Design Guide*, Fourth Edition, American Association of State Highway and Transportation Officials (AASHTO), Washington, D.C., 2011.
11. Polivka, K.A., Faller, R.K., Sicking, D.L., Reid, J.D., Rohde, J.R., Holloway, J.C., Bielenberg, R.W., and Kuipers, B.D., *Development of the Midwest Guardrail System (MGS) for Standard and Reduced Post Spacing and in Combination with Curbs*, Research Report No. TRP-03-139-04, Midwest Roadside Safety Facility, University of Nebraska-Lincoln, Lincoln, Nebraska, September 1, 2004.

12. Faller, R.K., Polivka, K.A., Kuipers, B.D., Bielenberg, R.W., Reid, J.D., Rohde, J.R., and Sicking, D.L., *Midwest Guardrail System for Standard and Special Applications*, Paper No. 04-4778, Transportation Research Record No. 1890, Transportation Research Board, Washington D.C., January 2004.
13. Zhu, L., *Critical Offset of the Midwest Guardrail System Behind a Curb*, Thesis, University of Nebraska-Lincoln, Lincoln, Nebraska, June 2008.
14. Zhu, L., Faller, R.K., Reid, J.D., Sicking, D.L., Bielenberg, R.W., Lechtenberg, K.A., and Benner, C.D., *Performance Limits for 152-mm (6-in.) High Curbs Placed in Advance of the MGS using MASH-08 Vehicles Part I: Vehicle-Curb Testing and LS-DYNA Analysis*, Research Report No. TRP-03-205-09, Midwest Roadside Safety Facility, University of Nebraska-Lincoln, Lincoln, Nebraska, May 6, 2009.
15. Thiele, J.C., Lechtenberg, K.A., Reid, J.D., Faller, R.K., Sicking, D.L., and Bielenberg, R.W., *Performance Limits for 6-in. (152-mm) High Curbs Placed in Advance of the MGS Using MASH Vehicles Part II: Full-Scale Crash Testing*, Research Report No. TRP-03-221-09, Midwest Roadside Safety Facility, University of Nebraska-Lincoln, Lincoln, Nebraska, October 30, 2009.
16. Thiele, J.C., Reid, J.D., Lechtenberg, K.A., Faller, R.K., Sicking, D.L., and Bielenberg, R.W., *Performance Limits for 6-in. (152-mm) High Curbs Placed in Advance of the MGS Using MASH Vehicles Part III: Full-Scale Crash Testing (TL-2)*, Research Report No. TRP-03-237-10, Midwest Roadside Safety Facility, University of Nebraska-Lincoln, Lincoln, Nebraska, November 24, 2010.
17. Parks, D.M., Stoughton, R.L., Stoker, J.R., and Nordlin, E.F., *Vehicular Tests of a 6 Inch High Curbed Gore with and without a Sand Barrel Crash Cushion*, Final Report to the California Department of Transportation, Report No. CA-TL-79-10, California Department of Transportation, Sacramento, CA, May 1979.
18. *Manual for Assessing Safety Hardware (MASH)*, American Association of State Highway and Transportation Officials (AASHTO), Washington, D.C., 2016.
19. Mongiardini, M., Faller, R.K., Reid, J.D., Sicking, D.L., Stolle, C.S., and Lechtenberg, K.A., *Downstream Anchoring Requirements for the Midwest Guardrail System*, Research Report No. TRP-03-279-13, Midwest Roadside Safety Facility, University of Nebraska-Lincoln, Lincoln, Nebraska, October 28, 2013.
20. Coon, B.A., and Reid, J.D., *Reconstruction Techniques for Energy-Absorbing Guardrail End Terminals*, Accident analysis and Prevention, Volume 38, 2006, pp. 1-13.
21. Coon, B.A., *Development of Crash Reconstruction Procedures for Roadside Safety Appurtenances*, Dissertation, University of Nebraska-Lincoln, Lincoln, Nebraska, 2003.
22. Pfeifer, B.G., Rohde, J.R., Sicking, D.L., *NCHRP Report 350 Compliance testing of the BEST System, Final Report to Federal Highway Administration – HNG – 1*, Research

Report No. TRP-03-63-96, Midwest Roadside Safety Facility, University of Nebraska-Lincoln, December 4, 1996.

23. Sillan, Seppo I., Federal Highway Administration. *Eligibility Letter No. HNG-14/CC-37 for the BEST as an NCHRP Report 350 test level 3 (TL-3) w-beam guardrail terminal*. To Brian Pfeifer, Midwest Roadside Safety Facility, November 20, 1996.
24. Jacoby, Carol H., Federal Highway Administration. *Eligibility Letter No. HSA-10/CC12J for alternative breakaway steel post system for use with currently-accepted versions of ET-2000*. To Hayes E. Ross, Jr., Texas Transportation Institute, June 24, 2002.
25. Poston, Jerry L., Federal Highway Administration. *Eligibility Letter No. HNG-14/CC-12c for the ET-2000 guardrail*. To Don H. Johnson, Syro Steel, Inc., August 22, 1995.
26. Home, Dwight A., Federal Highway Administration. *Eligibility Letter No. HNG-14/cc-12e for the use of 2 3810-mm long w-beam panels as an alternative to the single 7625 mm panel for use with the ET-2000 guardrail terminal*. To Hayes E. Ross, Jr., Texas Transportation Institute, September 22, 1998.
27. Ferren, J., *Full-Scale Crash Evaluations of the ET Plus End Terminal with 4-inch Wide Guide Channel Installed with a Rail height of 27³/₄ Inches*, Final Report to Trinity Highway Products, Southwest Research Institute (SwRI) Project No. 18.20887, SwRI Document Number 18.20887.03.100.FR0, January 23, 2015, Issue 1.
28. Ferren, J., *Full-Scale Crash Evaluations of the ET Plus End Terminal with 4-inch Wide Guide Channel Installed with a Rail height of 31 Inches*, Final Report to Trinity Highway Products, Southwest Research Institute (SwRI) Project No. 18.20887, SwRI Document Number 18.20887.05.100.FRO, February 17, 2015, Issue 1.
29. Baxter, J.R., Federal Highway Administration. *Eligibility Letter No. HSA-10/CC-94 for a modified version of ET-Plus guardrail terminal named the ET-Plus 31*. To Steve L. Brown, Trinity Highway Safety Products Division, September 2, 2005.
30. Home, Dwight A., Federal Highway Administration. *Eligibility Letter No. HMHS-CC12G for a modified extruder head for use with any of the previously-accepted terminal designs which used the ET-2000 extruder head*. To Hayes E. Ross, Jr., Texas Transportation Institute, January 18, 2000.
31. Home, Dwight A., Federal Highway Administration. *Eligibility Letter No. HNG-14/CC-46 for Flared Energy Absorbing Terminal (FLEAT)*. To Kaddo Kothmann, Road Systems, Inc., April 2, 1998.
32. Home, Dwight A., Federal Highway Administration. *Eligibility Letter No. HMHS-CC61 for a steel breakaway post as an alternative to the weakened timber posts that are currently used in your SKT-350 and FLEAT-350 w-beam guardrail end terminals*. To Kaddo Kothmann, Road Systems, Inc., August 27, 1999.

33. Baxter, John R., Federal Highway Administration. *Eligibility Letter No. HAS-10/cc-88 for modified versions of SKT, SKT-LITE, and FLEAT*. To Kaddo Kothmann, Road Systems, Inc., March 8, 2005.
34. Nicol, David A., Federal Highway Administration. *Eligibility Letter No. HSSD/CC-88B for the SKT and FLEAT with 2 Breakaway Posts*. To John Durkos, Road Systems, Inc., September 17, 2008.
35. Home, Dwight A., Federal Highway Administration. *Eligibility Letter No. HNG-14/CC-40 for a new w-beam guardrail terminal named the Sequential Kinking Terminal (SKT)*. To Kaddo Kothmann, Road Systems, Inc., April 2, 1997.
36. Hallquist, J.O., *LS-DYNA Keyword User's Manual*, LS-DYNA R7.1, Livermore Software Technology Corporation, Livermore, California, 2014.
37. Weiland, N.A., Reid, J.D., Faller, R.K., Bielenberg, R.W., and Lechtenberg, K.A., *Increased Span Length for the MGS Long-Span Guardrail System*, Research Report No. TRP-03-310-14, Midwest Roadside Safety Facility, University of Nebraska-Lincoln, Lincoln, Nebraska, December 17, 2014.
38. Julin, R.D., Reid, J.D., Faller, R.K., and Mongiardini, M., *Determination of the Maximum MGS Mounting Height – Phase II Detailed Analysis with LS-DYNA*, Research Report No. TRP-03-274-12, Midwest Roadside Safety Facility, University of Nebraska-Lincoln, December 5, 2012.
39. National Crash Analysis Center, *2010 Toyota Yaris FE Model*, Retrieved from <http://www.ncac.gwu.edu/vml/archive/ncac/vehicle/yaris-v1m.pdf>, Accessed June 1, 2013.
40. Pajouh, M.A., Bielenberg, R.W., Schmidt, J.D., Lingenfelter, J., Faller, R.K., and Reid, J.D., *Placement of Breakaway Light Poles Located Directly Behind Barrier*, Draft Report to the Illinois Tollway, MwRSF Research Report No. TRP-03-361-17, Midwest Roadside Safety Facility, University of Nebraska-Lincoln, Lincoln, Nebraska, May 19, 2017.
41. National Crash Analysis Center, *2007 Chevrolet Silverado Finite Element Model Validation Coarse Mesh*, Obtained: March 2012.
42. Home, Dwight A., Federal Highway Administration. *Eligibility Letter No. HMHS-CC12F for hinged breakaway (HBA) steel post as an alternative to the breakaway wood posts currently used in the ET-2000 w-beam guardrail terminal*. To Rodney A. Boyd, Trinity Industries, Inc., September 2, 1999.

END OF DOCUMENT